

OPHIOLITES FROM THE EGYPTIAN SHIELD:
A CASE FOR A POSSIBLE INTER-ARC BASIN ORIGIN

A. Y. Abdel Aal¹, E. S. Farahat¹, G. Hoinkes² & M. M. El Mahalawi¹

¹Department of Geology
Minia University, El-Minia 61111, Egypt
²Institute of Mineralogy and Petrology
University of Graz, Universitätsplatz 2, A-8010 Graz, Austria

The pyroxene and whole-rock chemistry of the ophiolitic metavolcanics of Wadi Um Seleimat (WUS) and Muweilih (MU) areas in the central Eastern Desert of Egypt are presented. WUS ophiolite suite seems to be intact where it comprises (from bottom to top): serpentinites, pyroxenites, metagabbros, massive diabases and pillowed metavolcanics. MU metavolcanics, about 10 km to the southeast of WUS area, consists predominantly of metabasaltic-metadiabasic pillowed and massive lava flows together with the corresponding pyroclastics. These metavolcanics, together with their associated metagabbros and serpentinites, can be considered as a part of a dismembered ophiolite sequence.

The mineral assemblage in WUS rocks is: albite, chlorite, epidote, titanite, calcite and quartz, which indicates a low greenschist facies (230–320°C) metamorphism. The mineral assemblage of MU metavolcanics includes: albite, actinolite, hornblende, epidote, chlorite, titanite, calcite, quartz and ilmenite that reflects a transitional greenschist-amphibolite facies metamorphism. Few samples of WUS contain plentiful clinopyroxene phenocrysts in plagioclase-free glassy groundmass. These features are typical of rocks of boninitic affinity.

Whole-rock and pyroxene chemistry demonstrate that the metavolcanics of both areas are mainly andesitic basalts with tholeiitic affinity. The boninitic affinity of some samples from WUS area is shown on TiO_2 - $SiO_2/100$ - Na_2O diagram of pyroxenes (Fig. 1). On the other hand, clinopyroxenes from metavolcanics associated with the boninitic rocks plot mostly in the island-arc tholeiites and mid-ocean ridge basalt fields. Clinopyroxenes from Muweilih area plot in island-arc tholeiitic-MORB overlap area.

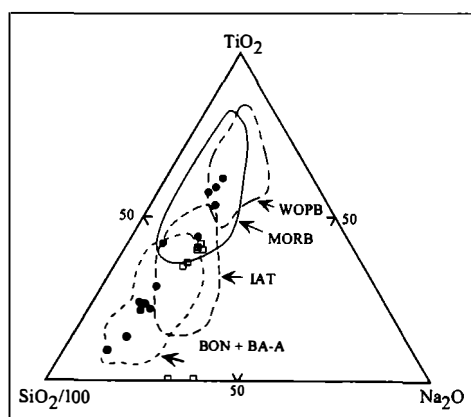


Fig. 1
 TiO_2 - $SiO_2/100$ - Na_2O diagram of pyroxenes [1].
MORB: mid-ocean ridge basalts; WOPB: within ocean plate basalts; IAT: island-arc tholeiites;
BON+BA-A: boninites+basaltic andesites and andesites from inter oceanic fore-arc regions.
Closed circles: Wadi Um Seleimat; Open squares: Muweilih.

The studied boninitic samples are classified as intermediate-Ti boninites [2]. On the TiO_2 -Zr diagram (Fig. 2) WUS rocks fall in volcanic-arc field and the area shared between MORB and volcanic-arc basalts, with high affinity to the latter. On the other hand, MU metavolcanics plot mostly in the volcanic-arc MORB overlap area, which may refer to their back-arc basin affinity. In agreement with most of the above discussed discrimination diagrams, WUS metavolcanic MORB normalized patterns (Fig. 3) are generally similar to those of the immature island-arc tholeiites, with relative low HFSE and high LILE than those of MORB. In contrast, MU metavolcanics have MORB-normalized patterns with HFSE value close to unity and relative enrichment in LILE (Fig. 3). These features may imply a transitional MORB-island-arc (i.e. back-arc basin) affinity of these rocks.

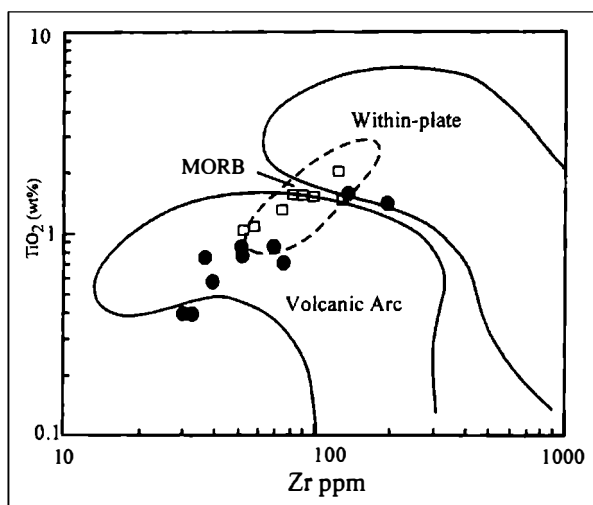


Fig. 2
 TiO_2 vs. Zr discrimination diagram [3].
Symbols as in Fig. 1.

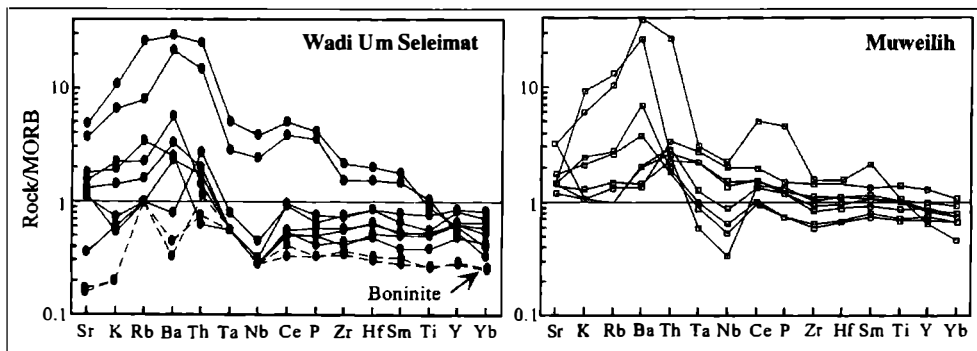


Fig. 3
MORB-normalized incompatible element spidergrams [3].

As modern boninites are found only in supra-subduction zone settings, it is inferred that ancient boninites also formed above a subduction zone. In the case of WUS metavolcanics, the previous geochemical studies [4] recognized their supra-subduction, i.e. fore-arc environment. However, the available data in the present study do not support such a model for the following reasons: a) the boninites overlie the arc-tholeiites; b) the absence of the sheeted dykes, which indicates incomplete extension; c) the thin volcanic section of this ophiolite and d) the little pyroclastics associated. These criteria may represent primary features of ophiolite formation in an incipient or rifted island-arc setting where arc volcanics are separated by thinner marginal basin crust [5].

Consequently, WUS tholeiites-boninite sequence appears to reflect the transgression from arc-style to (incipient) back-arc style volcanism. If the present interpretation is correct, MU metavolcanics, which lie about 10 km to southeast of WUS ophiolite sequence and display a back-arc geochemical characteristic, may represent a more advanced stage of this inter-arc basin while those of WUS represent their embryonic stage. The association of WUS and MU metavolcanics with ophiolitic mélange, which comprises ophiolitic dismembers of serpentines and metagabbros within the island-arc metavolcanics and volcanoclastic metasediments [6] are compatible with the above suggestion.

References

- [1] BECCALUVA, L., MACCIOTA, G., PICCARDO, G. B. & ZEDA, O. (1989): Clinopyroxene composition of ophiolitic basalts as petrogenetic indicator. - *Chemical Geology*, 77, 165-182.
- [2] BÉDARD, J. H. (1999): Petrogenesis of boninites from the Betts Cove ophiolite, Newfoundland, Canada: identification of subduction source components. - *Journal of Petrology*, 40, 1853-1889.
- [3] PEARCE, J. A. (1982): Trace element characteristic of lavas from destructive plate boundaries. - In: R. S. Thorpe (Editor), *Andesites*. Wiley, New York, pp. 525-548.
- [4] ABU EL ELA, F. F. (1990): Supra-subduction zone ophiolite of Qift-Qusseir road, Eastern Desert, Egypt. - *Bulletin Faculty of Science, Assiut University*, 19, 51-70.
- [5] SHERVAIS, J. W. & KIMBROUGH, D. L. (1985): Geochemical evidence of the tectonic setting of the coast Range ophiolite: a composite island-arc- oceanic crust terrain in Western California. - *Geology*, 13, 35-38.
- [6] AZZAZ, S. A., SABET, A. H., HASSAN, G.A. & EMAM, M. F. (1997): Ophiolites and the associated mélange of the Abu Mereiwa area along the Qift-Quseir Road, Eastern Desert, Egypt. - *Bulletin Faculty of Science, Assiut University*, 26, 141-163.

DIE ROLLE DER GEOLOGIE BEI NEUEN BERGBAUPROJEKTEN

G. Anthes

Technisches Büro für Geologie - *GEOsolutions*
Weißenbach 255, A-5351 Strobl, Austria

Die Neuanlage von obertägigen und/oder untertägigen Bergbauten steht heute in enger Beziehung zu wirtschaftlichen, rechtlichen, raumordnerischen und gesellschaftlichen Belangen. Daher muss die Gewinnungstätigkeit von mineralischen Rohstoffen nachhaltig und effizient geplant und durchgeführt werden. Für die Auswahl der geeignetsten Lagerstätte, der bestmöglichen Ausnutzung der Lagerstättenvorräte (Lagerstättenschutz) und einer optimalen Qualitätssteuerung kommt daher der Geologie eine besondere Rolle bei der Planung von neuen Bergbauprojekten zu.

Die genaue Kenntnis der geologisch-lagerstättenkundlichen Verhältnisse im Rohstoffvorkommen mit einem hohen Grad der geologischen Gewissheit setzt ein detailliertes Explorations- und Prospektionsprogramm voraus, dass auf die speziellen geologischen Bedingungen im Prospektionsgebiet abgestimmt sein muss. Dazu stehen dem Geowissenschaftler eine Vielzahl von modernen, mineralogischen, petrographischen, geochemischen, strukturgeologischen und geophysikalischen Untersuchungsmethoden zur Verfügung, die sinnvoll aufeinander abgestimmt und eingesetzt werden müssen, um effizient das Prospektionsziel – die hinreichend genaue Kenntnis über Lage, Erstreckung, Aufbau, Inhalt, Struktur und Qualitätsverteilung der Lagerstätte – erreichen zu können.

Diese geologisch-lagerstättenkundlichen Daten bilden die Grundlage für die gesamte Bergbauplanung, insbesondere für die Konzeptionierung der Geometrie, Gewinnungs-, Förder- und Maschinentechnik sowie der Sicherheit des Abbaus. Insbesondere bei hochwertigen und seltenen mineralischen Rohstoffen stellt eine optimale Qualitätssteuerung sowohl aus betriebswirtschaftlichen als auch volkswirtschaftlichen (Lagerstätteneffizienz) Gründen eine wesentliche Voraussetzung für einen effizienten Abbaubetrieb dar. Die Anforderungen an die Qualitätssteuerung hängen aber nicht nur von Produktanforderungen, sondern im wesentlichen auch von der Komplexität der Lagerstätte ab. Allgemein kann gesagt werden, dass eine nicht-optimale Qualitätssteuerung durch fehlende oder ungenügende geologische Kenntnis der Lagerstätte jedenfalls eine Verringerung der Produktqualität und somit Erlöseinbußen zur Folge hat. Weiters kann eine Erhöhung des Anteils nicht verwertbaren Materials (und damit erhöhtes Haldenvolumen) bzw. eine Verringerung der Vorräte (Verlust hochwertiger Qualität durch unbeabsichtigte Vermengung mit geringwertigem Material) daraus resultieren.

Im Rahmen der Wirtschaftlichkeitsberechnungen, der Wertschöpfungseffekte (öffentliches Interesse) und der Einreichplanungen für die behördlichen Genehmigungsverfahren des geplanten Bergbauprojektes – insbesondere bei Umweltverträglichkeitsprüfungen – kommt der Geologie ebenfalls eine bedeutende Rolle zu. Dazu zählen Studien zur regionalen und über-regionalen bis hin zu internationalen Verbreitung und Verfügbarkeit von mineralischen Rohstoffen, der Ersetzbarkeit und Güte des Rohstoffes sowie geologisch-hydrologisch-geotechnischer und gebirgsmechanischer Bewertungen des geplanten Abbauvorhabens.

Die genaue Kenntnis der allgemein verfügbaren mineralischen Ressourcen, des/der prospektierten Vorkommen(s) sowie Güte und Qualitätsverteilung der mineralischen Rohstoffe in der Lagerstätte bilden einen wichtigen Grundstein für einen langfristigen, effizienten, umweltverträglichen und wirtschaftlichen Bergbau.

**POTENTIAL SOURCE MINERALS OF RADON ANOMALIES -
HUNGARIAN CASE STUDIES**

A. Barabás¹, D. Breitner¹, Cs. Szabó¹, J. Nagy-Balogh¹, K. Gál-Sólymos¹ & Zs. Molnár²

¹Department of Petrology and Geochemistry

Eötvös University, Budapest, Hungary

²Institute of Nuclear Techniques

University of Technology and Economics, Budapest, Hungary

Radon, a radioactive noble gas, has three isotopes found in natural environments, which originate from decay series of uranium or thorium. The ^{222}Rn radioisotope, having a half life of 3.8 days, enter the atmosphere of ground-level bedrooms and living rooms of houses and may cause, in a long term scale, serious health problem as snipped into lung then attacking the tissues by emitting alpha particles. In Hungary, due to extended measurement of indoor radon level has been carrying out by the RAD Lauder Lab (Budapest), now several villages and towns are known characterized with elevated radon activity concentration. Three of these settlements and an additional one have been taken under a serious study in order to determine the potential sources of radon entering the houses. For this reason, detailed sedimentological, petrographical and geochemical study was performed on different materials (e.g. granite, soils) collected from the settlements chosen.

The areas studied were as follows: villages of Sukoró (S) in the Velence Mountains, Nézsa (N) at the foot of one of the Mesozoic blocks on the left bank of the Danube (Cserhát Mountains), Sajóhídvég (SH) (along Sajó River, North East Hungary), and Tápiószentmárton in the Great Hungarian Plain (T). All of them represent significantly different geological environments such as Paleozoic (carboniferous) granite (S), Mesozoic limestones and dolomites surrounded and partly covered by Oligocene and young sediments (N) and alluvial fan of River Sajó (SH), which consists mostly of sand, loess, silt and gravel, and in the case of locality T, loess and running sand cover the surface.

We have collected samples from both the surface (S, N, SH, T) and from shallow drills (N, SH). The samples in all cases were sieved and subsequently sorted and subjected to a wide range of examinations as follows: heavy mineralogy, gamma-spectrometry, trace element analysis (by instrument of neutron activation and optical emission spectrometry), electron microprobe and Roentgen diffraction analysis. Furthermore, at the N locality outdoor radon measurements were carried out in soil gas and in groundwater.

Neutron activation analysis showed no elevated amounts of radioactive elements (basically U and Th) in the bulk samples such as granite and granite rubble (up to 5.37 ppm U, 23.26 ppm Th), different kinds of soils (up to 3.2 ppm U, 12.8 ppm Th) and loess (up to 2.4 ppm U, 9.5 ppm Th) compared to the Clarke values of these rock types.

Electron microprobe analysis show in micrometer scale, potential source minerals such as monazite, xenotime, allanite, zircon and zirkelite, which contain the parental elements (U and Th) of radon. Among these minerals the monazite occurs most frequently and believed to be the most important radon emitter in the rocks and soils studied. Our petrographical and geochemical results suggest that monazites could have formed by near-surface alteration from allanite (Fig. 1). This indicates that these physical and chemical processes, which produce monazites may act

recently, too. However, minerals found at the T locality show no alterations which can be related to the low radon activity concentration at that location.

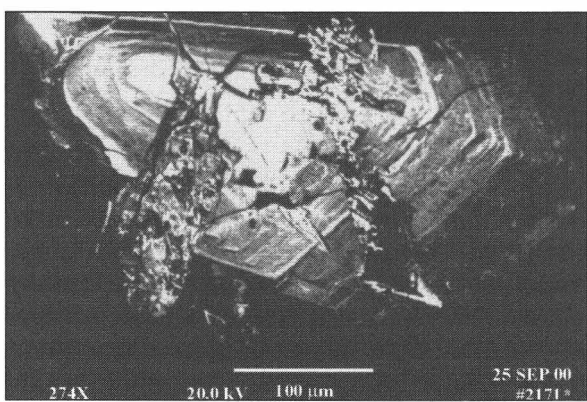


Fig 1

Fractured and altered zoned allanite from granite contain newly formed monazite and limonitic clay. Back-scattered electron image.

BISHERIGE ERGEBNISSE VON CELEBRATION 2000 UND ALP 2002 IM OSTALPENRAUM

M. Behm¹, CELEBRATION 2000 und ALP 2002 Working Groups

¹Institut für Geodäsie und Geophysik
Technische Universität Wien, Gusshausstrasse 27-29, A-1040 Wien, Austria

Die vorliegenden Datensätze erlauben sowohl 3D-Auswertungen als auch Inversionen und Modellierungen entlang von bestimmten Linien. Letzterer Ansatz wird derzeit vor allem von den internationalen Projektpartnern verfolgt, während im Vortrag auf die Ergebnisse der 3D-Betrachtungen eingegangen wird. Das Arbeitsgebiet beinhaltet die Ostalpen, die Dinariden und deren Übergang in das Pannonischen Becken, den östlichsten Teil der Molasse sowie den Süden der Böhmischem Masse. Prinzipiell zielt die Auswertung darauf ab, die Wellengeschwindigkeiten der Kruste durch tomographische Verfahren zu bestimmen. Getrennt davon werden ausgeprägte seismische Diskontinuitäten wie z.B. die Krusten-Mantel-Grenze durch flächenhafte Delayzeitmodelle beschrieben. Liegen beide Ergebnisse vor, können die Delayzeiten in Tiefen umgerechnet werden.

Das 3D-Modell der P-Wellengeschwindigkeiten ist als Tiefen-Geschwindigkeitsfunktion an Gridpunkten im 20 km - Abstand gegeben. Parallel dazu laufen analoge Untersuchungen der S-Wellen-Geschwindigkeiten. Es wird keine simultane 3D-Inversion angewandt, sondern durch CMP-Sortierung auf 1D-Probleme an den Gridpunkten übergegangen. Stapelungen mit speziellem Signalprocessing erhöhen den Offset der beobachtbaren Wellen, sodass zumeist Ein-drifttiefen bis über 20 km Tiefe erzielt werden. Gleichzeitig wird das so erhaltene Bild stark geglättet. Neben geophysikalischen/geologischen Interpretationen für große Bereiche kann dieses Modell als Startmodell für detaillierte lokale Inversionen, für die Abbildung von Grenzflächen und als Referenzmodell für spezielle Untersuchungen (z.B. Anisotropie) herangezogen werden.

Eine Delayzeitmodellierung der obersten Schichten bringt Korrekturwerte für die tomographische Inversion und zeigt eine hohe Korrelation mit den bekannten Sedimentbecken. Das selbe Verfahren wird auch für die Mohorovicic-Diskontinuität angewandt und zeigt qualitative Übereinstimmung mit bisherigen Erkenntnissen. Bei dieser Inversionsmethode werden auch Geschwindigkeiten der Grenzfläche bestimmt, wobei sich für die Krusten-Mantelgrenze eine Zone geringerer Geschwindigkeit im östlichen Alpenvorland abzeichnet. Verglichen mit der Behandlung der Kruste ist die Interpretationen der Welleneinsätze jedoch ungleich schwieriger. Stapelungen analog zur Behandlung der Kruste helfen die Ergebnisse zu verifizieren.

DIE HOCHDRUCKGESTEINE AM PIZ MUNDIN IM UNTERENGADINER FENSTER

R. J. Bertle & F. Koller

Institut für Geologische Wissenschaften
Universität Wien, Geozentrum, Althanstrasse 14, A-1090 Wien, Austria

Das Arbeitsgebiet liegt mitten im zentralem Bereich des Unterengadiner Fensters (UEF) rund um den Piz Mundin. Das UEF wird von Hangend gegen das Liegend aus Süd-, Mittel- und Nord-penninischen Einheiten aufgebaut. Das Hauptschichtglied bildet dabei verschiedene Bündner-schieferarten, die in 2 Großgruppen zusammengefaßt werden können: Bunte und Graue Bündner-schiefer, wobei letztere vor allem in den tieferen Deckeneinheiten dominieren. Der Rahmen des UEF gehört den oberostalpinen Ötztal- und Silvrettakristallinmassen mit deren Sedimentbedeckung (Engadiner Dolomiten) an.

Die Schichtfolge im Arbeitsgebiet beinhaltet neben Gesteinen der ozeanischen Kruste mit Serpentiniten, neu gefundenen Gabbros und Basalten eine bunte Schichtfolge von Sedimentgesteinen, die bisher wenig bekannt und untersucht war. Die ältesten Sedimentgesteine des Penninikums am Piz Mundin – das Neokom – bestehen aus Kalkschiefern, die gegen das Hangend in die Tristelformation übergehen. Die Tristelformation (Barrême und? Apt) stellt eine Turbiditsequenz dar, die aus Kalkbreccien mit detritärem Eintrag und Phylliten aufgebaut wird. Sie wird mit einem kontinuierlichen Übergang von der Gaultformation (Apt bis Alb) abgelöst, die durch einen mehrere m mächtigen sandigen Phyllithorizont (als "Fuorcla d'Alp Formation bezeichnet) abgeschlossen wird. Darüber folgt dann eine turbiditische Abfolge, die momentan noch als "Bunte Bündnerschiefer" bezeichnet wird und altersmäßig die gesamte Oberkreide umfassen dürfte. Ob Tertiäranteile vorhanden sind, kann derzeit nicht entschieden werden.

Die Vulkanitabfolgen des Piz Mundins sind durch das Auftreten von Diabasen, Basalt-Sills, Pillowlaven und Pillowbreccien gekennzeichnet. In ihnen kann eine metamorphe Paragenese einer niedrigtemperierten Blauschieferfazies mit akmitisch-jadeitischem Alkalipyroxen, stark zonierte Glaukophan oder Ferroglaukophan, Aragonit und Stilpnometan neben Pumpellyit, Chlorit und Epidot definiert werden. Für das Penninikum der Ostalpen konnte damit erstmalig erhaltener Hochdruck-metamorpher Aragonit nachgewiesen werden. Diese blauschieferfazielle Metamorphose zeigt sich in den umliegenden Sedimenten durch das Auftreten des seltenen Minerals Mg-Carpolith (BOUSQUET ET AL., 2002). Feld- und Dünnschliffuntersuchungen zeigen, daß das Auftreten von Mg-Carpolith an die Gesteinschemie der Neokomformation gebunden ist und damit in den anderen Formationen kein Carpolith mehr gefunden werden kann. An Hand der vorhandenen Paragenesen konnte BOUSQUET (1998) Druck-/Temp-peak-Bedingungen von P_{max} 12 bis 14 kbar und T_{max} von 375°C ableiten. Die Drucke dürften auf Grund der neu gefundenen metamorphen Pyroxenparagenesen mit 10–20 Mol.% Jadeit + 40–60 Mol.% Akmit in Ophikarbonatgestein, mit 12–20 Mol.% Jadeit + 45–55 Mol.% Akmit in Metabasalten und 25–40 Mol.% Jadeit + 50–60 Mol.% Akmit in Metasedimenten noch etwas höher anzusetzen sein.

Die Pyroxene werden sehr häufig von Glaukophan überwachsen und definieren damit in diesen Paragenesen den P-Peak. Grundsätzlich sind die Metamorphosetemperaturen durch das Auftreten Carpholit mit 375°C limitiert, da kein Chloritoid (= Abbauprodukt von Carpholit) gefunden werden konnte (BOUSQUET, 1998).

Fluid Inclusions-Untersuchungen an Kluftquarzkristallen zeigen Drucke bis 4.25 kbar bei angenommenen 200°C für die Einschlußbildung. Der rekonstruierte P-T-Pfad zeigt eine erste isothermale Dekompression bei ca. 375°C von ca. 15 kbar auf ca. 10 kbar an und von dort weg eine Exhumation entlang der Aragonit-Calcit-Isograde bis ca. 4 kbar bei 180°C, erst dann erfolgt die Exhumation entlang der 1 bis 0.95 g/cm³-Isochore des reinen Wassersystems. Die Metamorphose dürfte ihren P-Höhepunkt um 35 Ma gehabt haben – wie erste Rb-Sr-Datierungen von BERTLE (2000) zeigten. Das Ar-Ar-System ergibt ein etwas höheres Alter, das möglicherweise auf Ar-Überschuß hinweist.

Das gefundene Strukturinventar innerhalb der Bündnerschieferabfolgen des Piz Mundins ist äußerst vielfältig. Es konnten im Arbeitsgebiet mindestens 4 unterschiedliche Faltungsphasen auskariert werden (N-S, E-W Hauptfaltungsachsen, sowie eine spätere E-W streichende Crenulation; daneben top nach N Überschiebungen, stellenweise auch gegen S, und zusätzlich eine sprödtektonische Deformation. Die spröden Deformationen konnten bis ins Würm, vermutlich sogar bis ins Holozän nachgewiesen werden. In einzelnen Aufschlüssen konnte eine bis rezent andauernde Aktivität der Engadiner Linie nachgewiesen werden. Reine fluviatile Sande, die als Seebildung zu interpretieren sind, zeigen dabei steile gegen S abschiebende Versätze von über 10 cm an. Es sind dies Verschiebungsrichtungen wie sie aus geophysikalischen (HITZ, 1996) und strukturellen Untersuchungen im westlichen Bereich der Engadiner Linie (FROITZHEIM ET AL., 1996) erwartet wurden.

Reference

- BERTLE, R. J. (2000): Zur Geologie und Geochronologie um Alp Trida (Samnaun/Schweiz) einschließlich ingenieurgeologischer Fragen der Gebirgsauflösung und des Permafrosts. - Unpubl. Msc-Thesis. Univ. Wien, 395 S.
- BOUSQUET, R. (1998): L'exhumation des roches métamorphiques de haute pression – basse température: de l'étude de terrain à la modélisation numérique. Exemple de la fenêtre de l'Engadine et du domaine valaisan dans les Alpes Centrales. - Orsay N° D'Ordre: 5422. Diss. Université de Paris XI – Orsay.
- BOUSQUET, R., GOFFÉ, B., VIDAL, O., OBERHÄNSLI, R. & PATRIAT, M. (2002): The tectono-metamorphic history of the Valaisan domain from the Western to the Central Alps: new constraints on the evolution of the Alps. - Geol. Soc. America Bull., 114/2, S. 207-225.
- FROITZHEIM, N., SCHMID, S. M. & FREY, M. (1996): Mesozoic paleogeography and timing of eclogite facies metamorphism in the Alps: A working hypothesis. - Eclog. Geol. Helv., 89, 81-110.
- HITZ, L. (1996): The deep structure of the Engadine Window: Evidence from deep seismic data. - Eclog. Geol. Helv., 89, 657-675.

Die Untersuchungen wurden durch das FWF-Projekt 15278 "Bündnerschieferakkretion in den westlichen Ostalpen" finanziell unterstützt.

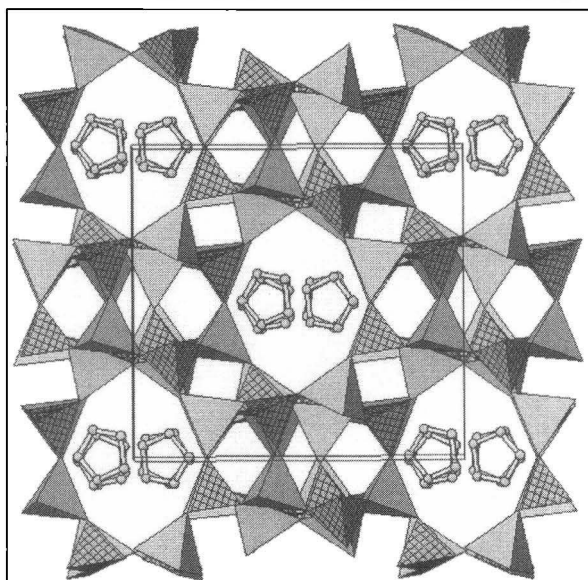
**MICROPOROUS SYNTHETIC METALLOPHOSPHATES: ZEOLITE-ANALOGUE
STRUCTURES AND NOVEL OCTAHEDRAL-TETRAHEDRAL FRAMEWORKS**

A. Bieniok, W. Lottermoser & G. Amthauer

Institut für Mineralogie
Universität Salzburg, Hellbrunnerstrasse 34, A-5020 Salzburg, Austria

Zeolite minerals and their synthetic analogues are useful in many industrial applications because of their great variety of interesting properties. Beside ion exchange capacity for water softening or humidity adsorption for drying processes, the catalytic activity of slightly modified zeolites combined with their shape selectivity is very important for further utilizations. Therefore not only chemical modification of known zeolites is a worthwhile research area but also the intensive search for new microporous materials with enhanced catalytic activity and novel framework structures. Microporous metallophosphates are a promising class of materials which show similar properties like zeolites together with high catalytic activity of the incorporated transition elements.

Hydrothermal and solvothermal synthesis procedures in teflon-lined steel-autoclaves under autogenous pressure and temperatures ranging from 160°C to 200°C are appropriate for the crystallization of microporous metallophosphates. We have prepared iron-aluminophosphate laumontite (FAPO-LAU) and iron-aluminophosphate sodalite (FAPO-SOD), two zeolite analogues with tetrahedral framework structures of alternating $[PO_4]^{3-}$ - and $[MeO_4]^{1/2-}$ -tetrahedra. Microprobe analyses and crystal structure analyses (MoK α , CCD detector) showed that



in the case of FAPO-LAU 32.4 % of the tetrahedral metal sites are occupied by Fe^{2+} -ions, in the case of FAPO-SOD the Fe^{2+} -substitution is 34.1 %.

Fig. 1
Polyhedral representation of the crystal structure of FeAPO-LAU (view along cell axis c). $[PO_4]$ and $[MeO_4]$ are the dark and light shaded tetrahedra. Inside the channels reside $C_3H_3N_2^-$ molecules.

At higher temperatures a second type of micro-porous metallophosphate crystallizes from our synthesis experiments - octahedral-tetrahedral frame-work structures consisting of an assembly of different shaped polyhedra, which have been firstly described in 1994 by MEYER & HAUSHALTER [1]. We have synthesized and characterized an ironalumino- $\text{NH}_4[\text{FeAl}_2\text{P}_3\text{O}_{12}(\text{H}_2\text{O})_2]$ and an irongallophosphate $\text{NH}_4[\text{FeGa}_2\text{P}_3\text{O}_{12}(\text{H}_2\text{O})_2]$ with microporous frame-works of 8-ring channels along [1 0 -1] and strongly elongated channels along [0 0 1]. Confirmed by Mössbauer spectroscopy and structural investigations we find Fe^{2+} in distorted octahedral coordination, Al^{3+} or Ga^{3+} in distorted trigonal bipyramids and P^{5+} in tetrahedral environment.

We have described here different microporous phosphate structures with iron incorporated into the framework either in tetrahedral or in octahedral coordination. The results demonstrate very well the remarkably structural variety of microporous metallophosphates compared to alumino-silicate zeolite structures.

Acknowledgement

The project is supported by the austrian Fonds zur Förderung der wissenschaftlichen Forschung (FWF) under P13663-GEO. We thank U. Brendel for performing the synthesis experiments.

References

- [1] MEYER, L. M. & HAUSHALTER, R. (1994): The first octahedral-trigonal bipyramidal-tetrahedral framework oxide: hydrothermal synthesis and structure of $\text{K}[\text{Ni}(\text{H}_2\text{O})_2\text{Al}_2(\text{PO}_4)_3]$. - Chemistry of Materials 6(4), 349-350.

TRANSALP UND ALP 2002: SEISMISCHE TOMOGRAPHIE IN DEN OSTALPEN

F. Bleibinhaus¹, TRANSALP und ALP 2002 Working Groups

¹Institut für Geodäsie und Geophysik
Technische Universität Wien, Gusshausstrasse 27-29, A-1040 Wien, Austria

Auf einem Profil zwischen München und Venedig wurden im Rahmen des TRANSALP-Projekts in den Jahren 1998/99 reflexions- und refraktionsseismische Messungen zur Erforschung der Struktur der Kruste und des oberen Mantels durchgeführt. Dabei wurden vibro- und sprengseismische Signale u.a. von bis zu 110 kurzperiodischen 3K-Stationen kontinuierlich aufgezeichnet. Für die Messkampagne ALP 2002 wurden drei Jahre später knapp 50 Stationspunkte wiederbesetzt (ALP 12), um den Anschluss dieses Datensatzes an TRANSALP zu gewährleisten. So können Ergebnisse von TRANSALP als Randbedingung für ALP 2002 verwendet und Teile der Daten einer gemeinsamen Auswertung zugeführt werden.

Laufzeiten von Ersteinsätzen und Weitwinkelreflexionen der TRANSALP-Daten wurden mit einem tomographischen 3D-Verfahren invertiert. Durch die Verwendung von über 30 Vibroseisktionen, die teilweise bis in 80 km Entfernung korrelierbares Signal zeigen, ergibt sich ein hochauflösendes dreidimensionales Bild der Geschwindigkeitsstruktur der oberen Kruste. Die simultane Inversion von sprengseismischen Refraktionen und Moho-Reflexionen (PMP) ermöglicht eine zweidimensionale Auflösung der Unterkruste und Moho, welche allerdings deutlich geringer ist als in der Oberkruste.

Die obere Kruste zeigt bemerkenswert starke Variationen der Geschwindigkeiten, von 2 km/s in den Vorlandbecken über 3–4 km/s in bestimmten Regionen in den Dolomiten bis zu 6 km/s und mehr im Nördlichen Kalkalpin (NCA). Beobachtungen von shear wave splitting und azimutabhängige Untersuchungen von Ersteinsatzlaufzeiten im Tauernfenster weisen außerdem auf eine Anisotropie von 10 % in den oberen 2–3 km mit einer E-W orientierten schnellen Achse hin, was durch Lateralbewegungen (escape tectonics) erklärt werden kann. Diese Anisotropie erklärt auch Laufzeitdifferenzen zwischen TRANSALP und dem älteren E-W gerichteten Alpen-längsprofil, welche sich im südlichen Zillertal senkrecht kreuzen.

Die europäische Unterkruste zeichnet sich gegenüber der adriatischen durch relativ geringe Geschwindigkeiten aus. Die europäische Moho ist ab einer Tiefe von 40 km in den NCA bis zu knapp 55 km etwas südlich des Hauptkamms durch Weitwinkelreflexionen belegt. Weiter südlich scheint sie ihren reflektiven Charakter zu verlieren. Die wenigen PMP-Beobachtungen von der adriatischen Moho weisen auf eine nordfallende Diskontinuität in etwa 40 km Tiefe hin. Im Einklang mit Ergebnissen anderer Teilprojekte von TRANSALP kann dieses Bild im Rahmen einer Subduktion penninischer ozeanischer Kruste nach Süden erklärt werden.

Ein vom Inntal nach Seinfallender und von der Steilwinkelseismik bis in die Unterkruste belegter Reflektor, der als tektonische Rampe interpretiert wird, lässt sich auch in den Geschwindigkeiten bis in die mittlere Kruste verfolgen.

Mit dem tomographischen TRANSALP-Modell wurden inzwischen erste Simulationen für Teile der ALP 2002-Daten gerechnet. Zwei profilnahe Schüsse zeigen in den Ersteinsätzen ebenso wie in den Reflexionen von der europäischen Moho gute Übereinstimmung, während die adriatischen PMP-Beobachtungen Differenzen aufweisen. Ob dies an Unzulänglichkeiten des Modells oder an lateralen Variationen liegt, wird noch zu klären sein.

ZIRKON MIT URANINITEINSCHLÜSSEN VON ARONDU,
BASHA RIVER, BALTIstan, PAKISTAN

F. Brandstätter & G. Niedermayr

Mineralogisch-Petrographische Abteilung
Naturhistorisches Museum, Burgring 7, A-1010 Wien, Austria

Einleitung

Im Jahr 2002 erwarb das Naturhistorische Museum in Wien eine Turmalinstufe aus Pakistan mit der Fundortangabe "Chogo Lungma Glacier, Arondu, Basha River, Baltistan". Die mit einem 7 cm langen schwarzen Turmalinkristall besetzte Stufe kommt aus einem der in dieser Region (nordöstlich von Gilgit) häufig vorkommenden Pegmatite. Nähere Fundumstände, insbesondere Art und Weise des Nebengesteins, waren nicht zu eruieren. Vermutlich stammt die untersuchte Probe aber aus einem jener Pegmatite, die im Gefolge junger, synorogener Prozesse gebildeten Granite entstanden sind (vgl. [1]).

Der in Längsrichtung (parallel zur c-Achse) eigentümlich ausgehöhlte Turmalin wird größtenteils von Albit und etwas Muskovit überwachsen. Jüngste Bildungen sind bräunlich durchscheinender nadeliger Turmalin, feinschuppiger Hellglimmer und Zirkon. Die bis 2 mm großen, prismatisch entwickelten Zirkone sitzen meist auf dem großen Turmalinkristall auf und werden teils von Albit überwachsen. Die Zirkone sind hellgrau gefärbt, mit feinstem Uraninit durchstäubt und zeigen nur die Formen {110} und {101}.

Die Besonderheit der Probe liegt darin, daß (i) Zirkon hier eines der jüngsten Minerale der Pegmatitparagenese ist, (ii) die Pegmatite selber aufgrund geologischer Überlegungen und aufgrund vorliegender radiometrischer Altersdaten aus den Nebengesteinen (und anderen Pegmatitmineralen) weltweit zu den jüngsten Pegmatiten zählen [2] und (iii) die Uraniniteinschlüsse im Zirkon die Möglichkeit bieten, mittels Mikrosondenanalyse chemische Alter zu bestimmen.

Experimentelles

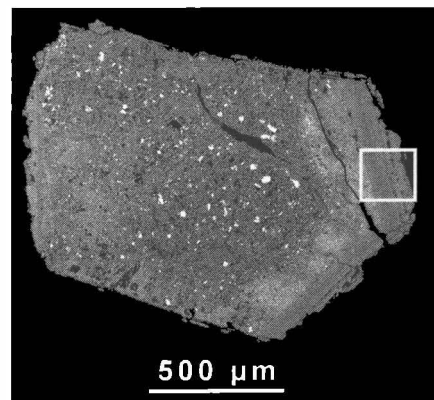
Im Rahmen dieser Studie wurden sechzehn Zirkonkörner mit Durchmesessern von in etwa 0.5–2.0 mm auf einem Glasträger montiert und anschließend ein poliertes Dünnschliffpräparat hergestellt. Mittels analytischem Rasterelektronenmikroskop (JEOL-JSM-6400) wurden für jedes einzelne Korn Zonarbau und Verteilung der Uraniniteinschlüsse dokumentiert. Zusätzlich wurde ein mit dem REM kombiniertes KL-System (OXFORD MonoCL 2) dazu verwendet, bei ausgewählten Zonarbereichen einiger Zirkone die Kathodolumineszenz zu untersuchen. Die chemische Zusammensetzung der Uraninite wurde mittels einer ARL-SEMQ Mikrosonde (15 kV, 20 nA Strahlstrom) bestimmt.

Ergebnisse

Die untersuchten Zirkone sind zonal aufgebaut, wobei meist deutlich zwischen einem Kernbereich und einem Hüllbereich unterschieden werden kann (Abb.1).

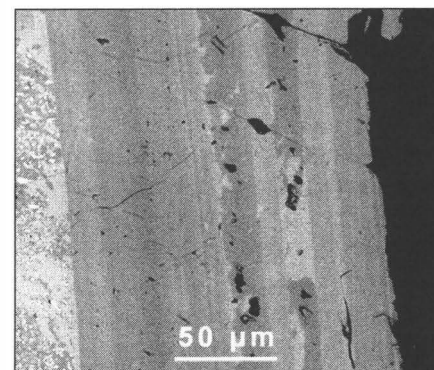
Der Kernbereich enthält zahlreiche xenomorphe Uraniniteinschlüsse mit Durchmessern von < 10 µm - > 50 µm. Zwischen dem Kern- und Hüllbereich ist des öfteren eine Zone zu beobachten, die mit feinsten Uraninitkristallen (Durchmesser < 0.1 µm – 1 µm) angereichert ist. Der äußere Hüllbereich (Abb. 2) ist frei von Uraninit-einschlüssen und zeigt im RückstreuElektronenbild eine ausgeprägte Hell-Dunkel-Zonierung, die hauptsächlich durch unterschiedliche Urangehalte bedingt ist.

Abb. 1
Zirkon von Arondu, Basha River, Baltistan, Pakistan mit Einschlüssen von Uraninit (weiß) im Kernbereich (dunkelgrau) des Kristalls. REM-Aufnahme RückstreuElektronen.



Alle Uraninite in den Zirkonkernen haben signifikante Thoriumgehalte (ca. 7.9–19.1 Gew. % ThO₂), wobei verschiedene Körner meist verschiedene Gehalte aufweisen. Der Bleigehalt der analysierten Uraninite lag stets unter der Nachweisgrenze der Mikrosonde und kann als < 0.1 Gew.% PbO angegeben werden.

Abb. 2
Detail der zonierten Hülle des Zirkons von Abb. 1 (weißer Rahmen). REM-Aufnahme , RückstreuElektronen.



Aus den jeweiligen Gehalten an UO₂, ThO₂ und der Obergrenze von 0.1 Gew. PbO wurden nach der Methode von [3] chemische Alter gerechnet. Die ermittelten Uraninitalter liegen im Bereich von 7.8–8.8 Mio. Jahren. In erster Näherung kann somit für die Uraninite ein chemisches Alter von < 10 Mio. Jahren angegeben werden.

Unter der Voraussetzung, daß (i) das chemische Alter des Uraninit dem Bildungsalter des Zirkons entspricht und (ii) Zirkon zwar ein spätgebildetes – aber primäres – Pegmatitmineral darstellt, kann auch für den Pegmatit ein Entstehungsalter von < 10 Mio. Jahren abgeschätzt werden. Dies steht in guter Übereinstimmung mit Angaben von [2], die für die Pegmatite von Stak Nala, nahe Gilgit, ein Intrusionsalter von > 5 Mio. Jahre postulieren.

Literatur

- [1] BENDER F. K. & RAZA , H. A. (Ed.) (1995): Geology of Pakistan. Berlin - Stuttgart: Gebr. Bornträger, 414 S.
- [2] LAURS, B. M. ET AL. (1998): Geological setting and petrogenesis of symmetrically zoned miarolitic granitic pegmatites at Stak Nala, Nanga Parbat - Haramosh Massif, Northern Pakistan. - Canadian Mineralogist 36, 1-47.
- [3] PARSLAW, G. R. ET AL. (1985): Chemical ages and mobility of U and Th in anatectites of the Cree Lake zone, Saskatchewan. - Canadian Mineralogist, 23, 543-551.

PHOSPHORUS-RICH GARNETS FROM LEUCOCRATE IGNEOUS ROCKS
(PŘIBYSLAVICE, MOLDANUBIKUM, CZECH REPUBLIC)

K. Breiter¹ & F. Koller²

¹Czech Geological Survey

Geologická 6, CZ-15200 Praha 5, Czech Republic

²Department of Geological Sciences

University of Vienna, Geocenter, Althanstraße 14, A-1090 Vienna, Austria

In the frame of a systematic study of P-rich granitoids we found in orthogneisses, granites and aplite-pegmatites from an area close to the village of Přibyslavice (central-eastern Bohemia) garnets with substantial amount of phosphorus. The contents of P in the garnet locally exceed 1 wt.% of P_2O_5 . Based on this observation we start a detail investigation on this unusual garnet occurrence.

The Přibyslavice orthogneiss-granite-pegmatite complex outcrops over an area of ~3 km², located ~5 km SSE of the town of Čáslav in the NE edge of the Moldanibicum [1]. A muscovite-tourmaline bearing orthogneiss body is enclosed in two-mica and biotite paragneisses with sillimanite and garnet. The orthogneiss show the same distinct foliation as the metamorphic country rocks. The central part of the orthogneiss body was intruded by a small stock of a Variscan muscovite granite, by several large dykes of garnet-bearing biotite-tourmaline aplite-pegmatites and by a thin dyke of a more evolved muscovite-tourmaline pegmatite.

All investigated rocks from Přibyslavice are leucocratic (< 1 wt.% $Fe_2O_{3\text{tot}}$), peraluminous (A/CNK 1.08 to 1.50), and rich in P (0.5–1.5 wt.% P_2O_5), B (300–500 ppm), Rb (300–700 ppm), poor in F and Li. The granite itself is strongly enriched in Sn (200–500 ppm), Nb, and Ta.

The Přibyslavice orthogneiss-granite-pegmatite complex had attracted mineralogists for a long time, mainly related to the occurrence of phosphate rich lenses with a large number of primary magmatic to late hydrothermal or supergene phosphate minerals [1] and to the occurrence of large crystals of Mn-rich garnets [2].

Several distinct types of garnets were recognised in the investigated rocks:

1. garnet crystals in lenses and veinlets of leucosome within the orthogneiss close to the granite and aplite-pegmatite intrusions: They are pure Mn-rich almandine crystals with a size of 2–3 mm and free of inclusions of other minerals. Normally they are strongly zoned with Mn+Ca-rich cores and Fe+Mg+P-rich rims. Content of spessartine reach about 30 % in the core and 20 % in the rims, together with about 0.1 wt.% P_2O_5 in the core and 0.2 wt.% P_2O_5 in rims. The growing of these garnets can be probably related to peak of regional Variscan metamorphism.

2. individual garnet crystals and garnet-quartz nodules in the muscovite-tourmaline orthogneiss near the contact to the aplite-pegmatite bodies: The size of the individual crystals is 5–10 mm. The nodules are generally rounded to irregular formed, 1–3 cm in diameter and without any crystal planes on the surface. Both nodules and crystals contain limited areas with graphic garnet-quartz intergrowth. Contents of spessartine varies between 15–20 % with a slight enrichment in the core. P contents are more enriched in the cores (0.5–0.6 wt.% P_2O_5) than in the rims (~0.3 wt.% P_2O_5). 97

3. garnet-quartz nodules and garnet crystals within the aplite-pegmatite bodies: This is the well known occurrence of garnet for mineral collections and reported in older publications [1, 2]. The homogeneous crystals of garnet are up to 1 cm large, the garnet-quartz nodules reach diameter up to 10 cm. The nodules have often a radial texture and/or are limited by combination of crystals plains. Graphic garnet-quartz intergrowths are common. Individual crystals are scarce within the pegmatitic facies, but common in transition zone between pegmatitic and aplitic facies. Nodules occur only in the aplitic facies. Most of the crystals and nodules are located within thin local shear zones crosscutting the aplite. The shear zones are characterized by new grown muscovite. The garnets are zoned with spessartine contents about 20–25 % in the core and 15–20 % in the rims. The contents of P_2O_5 reach up to 1 wt. % in core and 0.2–0.3 % in the rims.

4. garnet-quartz nodules in the muscovite granite. These irregular nodules, 1–5 cm in diameter, contain often more quartz (up to 60–70 vol.%) than garnet and have never crystal planes on the surface. Garnet occur in a cemented matrix of individual quartz grains. The nodules are homogeneous in the Mn-content (30 % spessartine), phosphorus is slightly enriched in the core (0.4 wt. % P_2O_5) in comparison to the rims (0.3 wt. % P_2O_5).

According to the trace element contents, all garnet types are enriched in HREE (10–60 ppm Yb, 1–10 ppm Lu, 40–150 ppm Y), whereas the LREE are very low (< 1 ppm La and Ce). Contents of scandium can be used as genetical indicator: metamorphic garnets (type1) contain only 40 ppm Sc, whereas all the other garnet types contain 100–200 ppm Sc.

Garnets of the types 2-4 are related to the post-metamorphic intrusion of granite and aplite-pegmatites. Graphic intergrowth of garnet and quartz was studied in detail in pegmatites in the Alps [3] and were interpreted as a product of magmatic crystallisation. In contrast in Přibyslavice, where the most garnet nodules with graphic intergrown occur within local shear zones or deformation plains, the growth of garnet is related to fluids activity. The garnet nodules in aplite-pegmatites contain about 50 % of quartz, but inclusions of other minerals (tourmaline, apatite) are very rare. This mean, that all alumino-silicates have been replaced by garnet, but quartz itself was a stable phase during the reaction. Phosphorus, primarily bound in feldspars, was incorporated into the newly formed garnet mainly caused by the lack of Ca to form apatite. The source of Fe can be found in the replaced micas and tourmaline, but Mn should be supplied by the fluids. The incorporation of phosphorus into tetrahedral position of the garnet lattice needs a compensation. One part of P is compensated with Al in the tetrahedral position (berlinite substitution), another part with Na in M^{2+} site. Further P shows a well defined positive correlation with Ti (about 0.1 % TiO_2 in P-rich domains). This means that the whole substitution roles are more complex and need additional investigations.

References

- [1] POVONDRA, P. ET AL. (1987): Přibyslavice peraluminous granite. - Acta Univ. Carol. Geol., 1987, No.3, 183-283.
- [2] NOVÁČEK, R. (1931): Garnets of czechoslovak pegmatites. - Věst. Král. Čes. Spol. Nauk., Tř. mat.-přírodnověd., 38, 1-55. Praha (in Czech).
- [3] ZHANG, CH. ET AL. (2001): Garnet-quartz intergrowths in granitic pegmatites from Bergell and Adamello, Italy. - Schweiz. Mineral. Petrogr. Mitt. 81, 89-113.

PETROGENETIC SIGNIFICANCE OF APATITE IN THE GRANITIC ROCKS
OF THE WESTERN CARPATHIANS

I. Broska¹, C. T. Williams² & J. Leichmann³

¹Geological Institute of the Slovak Academy of Science
Dúbravská cesta 9, 842 26 Bratislava, Slovak Republic

²Department of Mineralogy
The Natural History Museum, Cromwell Road, London SW7 5BD, UK
³Department of Geology and Paleontology
The Masaryk University, Kotlářská 2, 611 37 Brno, Czech Republic

Apatite as an ubiquitous accessory mineral phase in igneous rocks is essential to understanding phase equilibria of systems concerning phosphorus. The geochemical behaviour of P in granites, coupled with compositional variations in apatite, discriminate between the different genetic suites of Variscan granitic rocks in the West-Carpathian orogenic belt. Meso-Variscan granites, mostly of S-type affinity, show a good correlation between SiO₂ and P₂O₅, with decreasing amounts of P in the poorly and moderately fractionated granites, and increasing P contents in the most evolved and late differentiation products. The aluminium saturation index (ASI) correlates negatively with bulk P contents in I-type granites, and positively with P in S-type granites. [1] demonstrated that the incorporation of P into feldspars involves the coupled substitution of Al³⁺ + P⁵⁺ for 2 Si⁴⁺. This exchange is known as the berilinite substitution, where berilinite, AlPO₄, is isostructural with quartz or the Si₂O₄ framework component of feldspars. Relatively high P contents have been recorded in alkali feldspars (Af) from many different peraluminous granitic suites, and [1] reported about 60 localities where the P contents in Af, including potassium feldspar (Kfs) and sodic plagioclase (Pl), ranged from 0.1 to 0.8 wt. %. The P content of alkali feldspar (mainly Kfs) is usually very low (typically < 0.05 wt. % P₂O₅), or not detected in the slightly differentiated granites.

In the West-Carpathian late Variscan I/S-type granitoids, P is hosted mainly in the early-magmatic apatite, but is present also in the magmatic K-feldspar (up to 0.15 wt % of P₂O₅) that formed from the residual melts. In the post-orogenic S-type granites, the bulk of the P occurs in alkali feldspar (~0.3 wt. % P₂O₅), with a minor proportion present in primary early-magmatic apatite. These observations are consistent with the solubility of apatite in melt increasing with increasing temperature, decreasing polymerization of the melt, and decreasing silica concentration [2]. Clusters of small secondary apatite grains with a distinctive composition are distributed in alkali feldspar grains of the post-orogenic S-type granites. This apatite is considered to have formed post-magmatically from P released from P-rich alkali feldspar during decreasing temperature by reaction with a fluid-rich volatiles (including F and B), and alkali and alkali earth metals. A-type granites have the lowest bulk P contents. Consequently, phosphate minerals are relatively rare in this granite type, and the alkali feldspar has negligible P₂O₅ contents.

Apatite from the West-Carpathian granitoids is present in two forms: a colourless variety and a dark pigmented variety (black or dusky apatite). No significant compositional differences have been observed between these two apatite varieties (carbon was not analysed by electron microprobe). However, dark apatite has been interpreted as apatite that assimilated carbon from the black shales and now indicates the existence of a former reduction regime in the melt [3]. Sr contents in apatite correlate with the bulk Sr concentration of the host rocks: correlation coefficient ~0.8 for the primary apatites of orogenic granitic rocks, a correlation that has been observed for other localities (e.g. [4] and references therein). Other minor elements in apatite correlate less well with bulk rock composition, but the apatite composition also strongly depends on the physico-chemical conditions of the melt. The Mn content in apatite increases with the peraluminous character of the melt and with decreasing fO_2 . Thus, apatite from the S-type granites has significantly higher Mn contents than apatite from the I-type granites. However, apatite from A-type granites is enriched in Fe and HREE, reflecting the higher bulk Fe and HREE content of this granite type. Apatite from specialized S-type granites is enriched in Y and HREE. In general, the Cl and S content of apatite is higher in the basic members of the I-type granitic rocks.

Trace levels of the REE were determined by solution ICPMS on separated grains from two samples (T-18; S-type granitoid and T-22; I-type granitoid; [5]. A comparison of the abundances and normalised patterns of the REE in apatite from these two different granite types, with REE in apatites from the Lachland Fold Belt (a classical region for the division of the S- and I- granite typology [6], show no significant differences. For the S-type granite, both groups indicate a higher content of LREE, their fractionation, pronounced negative Eu-anomaly and a relatively flat HREE pattern. In contrast, the I-type granite has lower LREE, and a less pronounced Eu-negative anomaly, even no anomaly (T-22). The low oxygen fugacity and the high peraluminosity of the S-type granitoids melts enhance the Eu^{2+}/Eu^{3+} ratios while this ratio is lower in oxidised, metaluminous I-type melts [6]. Thus, a higher Eu^{2+}/Eu^{3+} indicates a lower content of Eu^{3+} in the melt, and consequently a lower concentration of Eu in apatite since the crystal structure of apatite shows a strong preference for Eu^{3+} . A strong negative Eu-anomaly (i.e. a lower Eu^{2+}/Eu^{3+} ratio) indicates a higher Eu^{3+} content in the relatively oxidised melt leading to an overall increase in Eu content in the apatite. This observation is in accordance with the knowledge that West-Carpathian S-type granitoids have lower content of water compared with the I-type [7].

Differences in fluorine concentrations in the melt and in the volatile phase were calculated after [8]. Differences in F composition were found between the cores and the rims of the apatites and also between the different kind of granitoid suites (I- and S-type). For the S-type samples, the concentration of fluorine in the cores of apatite grains is higher than in the rims; however, little difference is seen in apatite core-rim F values for the I-type granite. This phenomenon can be explained by the fact that the volatile phases tend to decrease in quantity with the progression of the crystallisation (degassation). Comparison of the two granite types show that the S type granite melts were 10 % richer in fluorine than the I type melts. These results are comparable to those obtained by [6]. This difference in F distribution could be explained by the fact, that I-type melts contained more water than the S-type melts, and thus lower concentration of halogens, including F.

References

- [1] LONDON, D. (1992): Phosphorus in S-type magmas: the P₂O₅ content of feldspars from peraluminous granites, pegmatites and rhyolites. - *Am. Mineral.* 77, 126-145.
- [2] LONDON, D., WOLF, M. B., MORGAN, G. B. & GARRIDO M. G. (1999): Experimental silicate-phosphate equilibria in peraluminous granitic magmas, with a case study of the Alburquerque batholith at Tres Arroyos, Badajoz, Spain. - *Jour. of Petrology*, 40, 215-240.
- [3] BROSKA, I., DIKOV, J. P., ČELKOVA, A. & MOKHOV, A. V. (1992): Dusky apatite from the Variscan granitoids of the Western Carpathians. - *Geol. Carpath.* 43, 195-198.
- [4] BELOUSOVA, E. A., WALTERS, S., GRIFFIN, W. L. & O'REILLY, S. Y. (2001): Trace-element signatures of apatites in granitoids from the Mt Isa Inlier, northwestern Queensland. - *Australian Jour. of Earth Sci.*, 48, 603-619.
- [5] BROSKA, I. & UHER, P. (1998): Apatite in I-, S- and A-type granites, Slovakia; distribution and petrological significance. - *Acta Univ. Carolinae Geol.*, 42, 20-22.
- [6] SHA, L.-K. & CHAPPELL, B. W. (1999): Apatite chemical composition, determined by electron microprobe and laser-ablation inductively coupled plasma mass spectrometry, as a probe into granite petrogenesis. - *Geochimica et Cosmochimica Acta*, 63, 3861-3881.
- [7] PETRIK, I. & BROSKA, I. (1993): Petrology of two granite types from the Tribeč Mountains, Western Carpathians: an example of allanite (+magnetite) versus monazite dichotomy. - *Geol. Journal, Manchester*, 29, 59-78.
- [8] PICCOLI, P. & CANDELA, P. (1994): Apatite in felsic rocks: a model for the estimation of initial halogen concentrations in the Bishop Tuff (Long Valley) and Tuolumne Intrusive Suite (Sierra Nevada Batholith) magmas. - *American Journal of Science*, 294, 92-135.

EINE NEUE GENERATION REFRAKTIONSSEISMISCHER UNTERSUCHUNGEN
DER LITHOSPÄHRE IN ZENTRALEUROPA UND DEN OSTALPEN

E. Brückl¹ & ALP 2002 Working Group

¹Institut für Geodäsie und Geophysik
Technische Universität Wien, Gusshausstrasse 27-29, A-1040 Wien, Austria

Im Jahr 1997 begann mit dem Projekt POLONAISE'97 in Polen eine neue Generation refraktionsseismischer Untersuchungen der Lithosphäre. Drei Jahre später folgte das Projekt CELEBRATION 2000, das gemeinsam mit POLONAISE'97 in einem 600 km breiten Streifen von der Ostsee über Zentraleuropa in den Ostalpenraum und das Pannonische Becken reichte. Im Jahr 2002 wurde mit dem Projekt ALP 2002 dieser Streifen über die Ostalpen bis zu den Dinariden und die Adria fortgesetzt. Durch das Projekt Sudetes 2003 wurde 2003 das Messprogramm verriegelt in der Tschechischen Republik und Polen verdichtet.

Charakteristikum dieser neuen Generation refraktionsseismischer Untersuchungen ist die große Anzahl (etwa 1000) seismischer Stationen eines neuen Typs, die flächenhafte Anordnung der Profile und die Registrierung der seismischen Schüsse auf allen gleichzeitig ausgelegten Linien. Bei allen vier Programmen wurden zusammen etwa an 4000 Stationen seismische Aufnehmer ausgelegt und über 300 Schüsse abgetan. Die gewählte Messanordnung wird neben der traditionellen Linienauswertung auch die Erstellung von 3D Modellen ermöglichen. Möglich wurden diese Untersuchungen nur durch eine breite internationale Kooperation von über 10 Ländern, wobei die Initiierung auf einer Kooperation zwischen der Universität von Texas in El Paso und der Polnischen Akademie der Wissenschaften beruht.

Für das Projekt ALP 2002 hat Österreich die Koordination übernommen. Die Datenerfassung wurde von 1. - 6. Juli 2002 durchgeführt, wobei 996 seismische Stationen entlang von 13 Profilen mit einer Gesamtlänge von 4312 km ausgelegt waren und 32 seismische Sprengungen mit einer durchschnittlichen Ladung von 300 kg abgetan wurden. Gemeinsam mit den Daten der dritten Auslage von CELEBRATION 2000 liegt damit ein seismischer Datensatz vor, dessen Auswertung wesentliche Fragen der Lithosphärenforschung im Ostalpenraum klären sollte.

**ULTRAHIGH-PRESSURE METAMORPHISM:
TRACING CONTINENTAL CRUST INTO THE MANTLE**

C. Chopin

Laboratoire de Géologie
UMR 8538 du CNRS, Ecole normale supérieure, 24 rue Lhomond, F-75005 Paris, France

More and more evidence is being discovered in Phanerozoic collision belts of the burial of crustal rocks to previously unsuspected (and ever increasing) depths, presently on the order of 150 to 200 km, and of exhumation from such depths. This extends by almost one order of magnitude the depth classically ascribed to the metamorphic cycling of continental crust, and demonstrates its possible subduction. The pieces of evidence for this new, ultrahigh-pressure (UHP) metamorphism exclusively occur in the form of relics of high-pressure minerals that escaped back transformation during decompression. The main UHP mineral indicators are the high-pressure polymorphs of silica and carbon, coesite and microdiamond, respectively; the latter often demonstrably precipitated from a metamorphic fluid and is completely unrelated to kimberlitic diamond or any shock event. Recent discoveries of pyroxene exsolutions in garnet and of coesite exsolutions in titanite suggest a precursor garnet or titanite containing six-fold coordinated silicon, therefore still higher pressures than implied by diamond stability, on the order of 6 GPa. The UHP rocks raise a formidable geological problem: that of the mechanisms responsible for their burial and, more pressingly, for their exhumation from the relevant depths. The petrological record indicates that large tracts of UHP rocks were buried to conditions of low T/P ratio, consistent with a subduction-zone context. Decompression occurred in most instances under continuous cooling, implying continuous heat loss to the footwall and hangingwall of the rising body. This rise along the subduction channel – an obvious mechanical discontinuity and weak zone – may be driven by buoyancy up to mid-crustal levels as a result of the lesser density of the acidic crustal rocks (even if completely reequilibrated at depth) after delamination from the lower crust, in a convergent setting. Chronological studies suggest that the rates involved are typical plate velocities (1 to 2 cm/y), especially during early stages of exhumation, and bear no relation to normal erosion rates.

Important observations are that: i) as a result of strain partitioning and fluid channelling, significant volumes of subducted crust may remain unreacted (i.e. metastable) even at conditions as high as 700°C and 3 GPa – with implications as to geophysical modelling; ii) subducted continental crust shows no isotopic or geochemical evidence of interaction with mantle material.

An unknown proportion of subducted continental crust must have escaped exhumation and effectively recycled into the mantle, with geochemical implications still to be explored, bearing in mind the above inefficiency of mixing. The repeated occurrence of UHP metamorphism, hence of continental subduction, through time and space since at least the late Proterozoic shows that it must be considered a common process, inherent to continental collision. Evidence of older, Precambrian UHP metamorphism is to be sought in high-pressure granulite-facies terranes.

RETROGRADE GOLD ENRICHMENT IN SKARNS:
EXAMPLES FROM ROMANIAN DEPOSITS

C. L. Ciobanu & N. J. Cook

Geological Survey of Norway
NO-7491 Trondheim, Norway

The mineralogy and association of gold in three skarn deposits Băișoara, Băița Bihor, Ocna de Fier) of Late Cretaceous age in Romania is described. None of these have been exploited primarily for Au, but they nevertheless provide insights into Au enrichment mechanisms in skarns. Associations of exotic trace elements, including a common-to-all Au-Bi-Te signature, are abundant throughout parts of the orebodies with intense retrograde overprinting. Moreover, Au is always seen associated with a range of shock-induced and brecciation textures recording episodes of transient overpressure at the time of Au deposition. Skarn systems typically evolve through prograde and subsequent retrograde stages. The latter are recognisable by their strong overprinting character onto earlier skarn assemblages [1] and gold can be associated with either stage. In skarns, as well as in porphyry deposits, initial temperatures of ~700°C are reported. Therefore, the role played by Cu-Fe sulphides in assisting Au-enrichment can be of particular importance because of their potential to act as precious metal carriers [2]. Prograde, high-temperature bornite_{ss} played such a role in both Ocna de Fier and Băița Bihor [3]. Here, however, we discuss only Au enrichment induced during retrograde stages. In skarns, devolatilisation reactions that cause sudden changes in the volatile budget of fluids can either enhance or retard flow. If such reactions are coupled with abrupt changes in porosity/permeability at the skarn front, sudden spurts of devolatilisation can cause back-flow fluxes and brecciation assisted by peaks of transient overpressure [4]. The latter are particularly critical since they cause destabilisation of Au-carrying volatile species in the fluids. If this happens at critical points when fluids cross $f\text{S}_2/f\text{O}_2$ buffers and at temperatures above the melting point of Bi, than Bi-melts are valuable scavengers for Au [5]. Bi-tellurides and selenides are commonly found together with Au [6], due to incorporation within Bi_{melt}. The compositions of Bi-Te-Se-Au_{melt} in the resulting associations reflect the reducing/oxidizing character of fluids [7].

The Bi_{melt} scavenger for Au seen in Au-Bi-Te-Se associations

Tellurides of bismuth are widespread in all deposits, where they occur in patches and trails that cross cut ores marked by overprinting. The retrograde stage in Fe skarn at Băișoara is initiated by strong sulphidation. In samples from deep in Mașca Mine and in distal Zn-Pb skarn at Valea Lita, 3 km NW of Mașca, gold and Bi-tellurides are observed in early stages of Mt replacement. In Cu-Mo skarn at Băița Bihor, Bi-tellurides are identified in Cp ores in forsterite-Di₉₀₋₆₀Hd₁₀₋₄₀ skarn buffered by Po/Mt. Bi-tellurides and small Au blebs follow trails and halos of fluid inclusions within Cp or in the silicate mass. In the Cu-Fe core from Simon Iuda orebody, Ocna de Fier, clusters of retrograde As-apatite (turneaureite), pierce the forsterite-bearing Bn-Cp-Mt ore.

A range of Bi- and Bi-Ag tellurides and selenides [8] is associated with apatite emplacement. They form swarms that include blebs of Au and Bi. Both REE-phosphates and uraninite are associated with emplacement of apatite. Abundant minute grains of Au, cervelleite and a range of Bi-minerals [9] is seen within bands of Di_{90} skarn, at the margin of Mt-Cp ore. In the same deposit, Au is also associated with occurrence of Bi-minerals in Mt ores from the Fe zone (e.g. Ocna Turcească orebody). Native In is an additional unusual mineral in Au-enriched ores. Magnetite ores from distal Fe zone (Paulus Mine) are crosscut by trails of gold and Bi-tellurides, the assemblages also include maldonite. There is little variation in speciation of the assemblages in the above skarns. Hedleyite, joséite-A, -B and tsumoite are dominant.

Gold extraction during devolatilisation reactions

In two skarns, Au is seen in assemblages that are strongly affected by sudden devolatilisation reactions. These can be caused by formation of volatile-rich phases, as in Băița Bihor. In samples with Cu-Fe sulphides in forsterite skarn (deeper part of Antoniu), an unusual fluorite-rich overprint is seen associated with Au deposition. Strong brecciation of the assemblage is caused by formation of fluorite along dilational cracks, as well as bleaching-induced rims and chaotic zonation in forsterite. 'Fronts' of secondary minerals, all associated with fluorite formation, corrode bornite margins. Abundant Au, as patches and filaments, occur in pressure shadows of forsterite grains that underwent bleaching and brecciation. A second type of sudden devolatilisation is represented by erratic decarbonation that accompanied cessation of infiltration at the end of the prograde stage. This caused back-flow and brecciation (carbofracturing) in the Fe zone from both distal and proximal skarn at Ocna de Fier. Minute Au grains occur as inclusions in Mt and garnet displaying shock-induced textures and affected by subsequent brecciation. Gold is associated with emplacement of calcite-quartz clusters, or enclosed within overgrowths onto abraded and rounded Mt. In the Fe zone, Au and scheelite are products of carbofracturing (e.g. Ocna Turcească, Paulus), occurring as dusty inclusions in Fe-oxides, or along cracks extending into the enclosing carbonate-silica matrix.

Discussion

Despite the fact that all skarns include forsterite, it is only in Băița Bihor and Ocna de Fier that Au-enrichment occurred during formation of high-volatile associations, subsequent to forsterite formation. Only in Ocna de Fier was the Bi_{melt} scavenger for Au activated at this stage. The association of apatite, uraninite and REE-phosphates with Au forces comparison with that typical for Fe-oxide-Cu-Au deposits. In Băița Bihor, the Bi_{melt} scavenger for Au is activated only by sulphidation, as shown by changes in silicates at the Po/Py buffer. Still stronger sulphidation is seen in replacement of Mt by Po at Băișoara, where the abundance of Bi-tellurides is greatest. In contrast, at Ocna de Fier, the Bi_{melt} scavenger for Au is activated during carbofracturing by $f\text{O}_2$ fluctuation at the Hm-Mt buffer. Prograde sulphidation at the Fe and Zn-Pb zone boundary does not impact on Au enrichment; instead, carbofracturing in the Fe zone is responsible. Despite similarities, we conclude that the relative importance of different Au enrichment mechanisms depends on individual paths of fluid evolution in each deposit. There is a marked contrast between Băișoara, where the importance of Bi_{melt} scavenger during sulphidation is greatest, and Ocna de Fier, where devolatilisation played the greater role. At Băița Bihor, retrograde Au extraction is minor, most Au being incorporated with Bi in prograde bornite.

References

- [1] EINAUDI, M. T. ET AL. (1981): Skarn deposits. - Econ. Geol. 75th anniv. vol., 317-391.
- [2] KESLER, S. E. ET AL. (2002): Gold in porphyry copper deposits: its abundance and fate. - Ore Geol. Rev., 21, 103-124.
- [3] CIOBANU, C. L. ET AL. (2003): Gold enrichment in deposits of the Banatitic Magmatic and Metallogenetic Belt, southeastern Europe. - Extended abstract, SGA Biennial Symposium, Athens, Greece, August 2003.
- [4] DIPPLE, G. M. & GERDES, M. L. (1998): Reaction-infiltration feedback and hydrodynamics at the skarn front. - MAC Short Course, 26, 71-97.
- [5] DOUGLAS, N. ET AL. (2000): The liquid bismuth collector model: an alternative gold deposition mechanism. - AGC Abstract volume, 59, 135.
- [6] AFIFI, A. M. ET AL. (1988): Phase relations among tellurides, sulfides, and oxides: I. Thermochemical data and calculated equilibria. - Econ. Geol., 83, 377-394.
- [7] CIOBANU, C. L. & COOK, N. J. (2002): Tellurides, selenides (and Bi-sulphosalts) in gold deposits. 11th IAGOD Symposium – Geocongress. - CD vol. of extended abstracts, Geol. Surv. Namibia.
- [8] COOK, N. J. & CIOBANU, C. L. 2001. Paragenesis of Cu-Fe ores from Ocna de Fier-Dogenecea (Romania), typifying fluid plume mineralisation in a proximal skarn setting. – Mineral. Mag., 65, 351-372.
- [9] COOK, N. J. & CIOBANU, C. L. (2003): Cervelleite, Ag_4TeS , from three localities in Romania, substitution of Cu, and the occurrence of the associated phase, $\text{Ag}_2\text{Cu}_2\text{TeS}$. - Neues Jahrb. Mineral. Monatsh., 321-336.

MODELS AND EVIDENCE FOR THE PETROGENESIS OF S-TYPE GRANITIC MAGMAS

J. D. Clemens

School of Earth Sciences and Geography
CEESR, Kingston University, Penrhyn Rd., Kingston-upon-Thames, Surrey, KT1 2EE, UK

Despite a perception that it represents a perverse divergence, it is perfectly possible to believe in the existence S- and I-type granites (and the implications for the nature of their protoliths) [1], and to disbelieve in the applicability of the restite-unmixing model [2] for chemical variation in granitic magmas. The major advance represented by the White and Chappell S-I classification was the recognition that highly contrasting parental materials must be involved in the genesis of granitic magmas. The restite-unmixing model is commonly seen as a companion to the S-I classification, but it is really a separate issue. This model implies that the compositions of granites ‘image’ those of their source rocks in a simple way. However, there are other, equally valid models that can explain the data, and none of them represents a unique solution [3]. The most cogent explanation for the high-grade metasedimentary enclaves in most S-type granites is that they represent mid-crustal xenoliths; restitic enclaves are either rare or absent [4]. Inherited zircons in S-type rocks are certainly restitic. However, the occurrence of a substantial restitic zircon population does not imply an equally substantial restitic component in the rest of the rock. Zircon and zirconium behaviour are controlled by disequilibrium and kinetics, and Zr contents of granitic rocks can rarely be used to infer magma temperatures.

The evidence is overwhelming that the dark, microgranular enclaves that occur in both S-and I-type granites are igneous in origin [5]. They represent globules of quenched, more mafic magma mingled and modified by chemical exchange with the host granitic magma. However, magma mixing does not appear to have been a significant process affecting the chemical evolution of the host magmas at emplacement level. Likewise, multi-component mixing models erected for some granitic rock suites [6] are mathematically non-unique and, in some cases, violate constraints from isotopic studies. S- and I-type magmas commonly retain their distinct identities. This suggests limited mixing of source rocks, limited magma mixing and limited wall-rock assimilation. Though granite varieties intermediate between S- and I-types certainly exist, they are probably relatively minor in volume.

Crystal fractionation probably plays the major role in the differentiation of very many granitic magmas, including most S-types, especially those emplaced at high crustal levels or in the volcanic environment [3]. Minor mechanisms include magma mixing, wall-rock assimilation and restite unmixing. Isotopic variations within plutons and within granite suites could be caused by source heterogeneities, magma mixing, assimilation and even by isotopic disequilibrium [7]. However, source heterogeneity, coupled with the inefficiency of magma mixing is probably the major cause of observed heterogeneity.

Normal geothermal gradients are seldom sufficient to provide the necessary heat for partial melting of the crust; crustal thickening likewise fails to provide sufficient energy [8]. Generally, the mantle must be an important contributor to the thermal budget. This might be provided through mantle upwelling and crustal thinning, and possibly through the intra- and underplating of mafic magmas. In this context, it is noteworthy that upper crustal extension seems to have been common in regions undergoing granitic magmatism. Migmatites probably provide poor analogues of granite source regions because they are mostly formed by fluid-present reactions. In contrast, most granitic magmas are formed by fluid-absent reactions [9]. Where we do see rare evidence for arrested fluid-absent partial melting, the melt fraction is invariably concentrated into small shear zones, veinlets and small dykes. Thus, it seems likely that dyking is important in transporting granitic magma, on a variety of scales and at many crustal levels [10, 11]. However, one major missing link in the chain is the mechanism by which melt fractions, in small-scale segregations distributed over a wide area, can be gathered and focused to efficiently feed much wider-spaced major magma conduits. Answers may lie in the geometry of the melting zones and in the tendency of younger propagating fractures to curve toward and merge with older ones [12]. Self-organization almost certainly plays a role.

References

- [1] CHAPPELL, B. W. & WHITE, A. J. R. (1974): Two contrasting granite types. - *Pacific Geology*, 8, 173-174.
- [2] CHAPPELL, B. W. ET AL. (1987): The importance of residual source material (restite) in granite petrogenesis. - *Journal of Petrology*, 28, 1111-1138.
- [3] WALL, V. J. ET AL. (1987): Models for granitoid evolution and source compositions. - *Journal of Geology*, 95, 731-750.
- [4] CLEMENS, J. D. (2003): S-type granitic magmas – petrogenetic issues, models and evidence. - *Earth Science Reviews*, 61, 1-18.
- [5] VERNON, R. H. (1984): Microgranitoid enclaves in granites-globules of hybrid magma quenched in a plutonic environment. - *Nature*, 309, 438-439.
- [6] COLLINS, W. J. (1996): Lachlan Fold Belt granitoids: products of three-component mixing. - *Transactions of the Royal Society of Edinburgh: Earth Sciences*, 87, 171-179.
- [7] HARRIS, N. ET AL. (2000): From sediment to granite: timescales of anatexis in the upper crust. - *Chemical Geology*, 162, 155-167.
- [8] ENGLAND, P. C. & THOMPSON, A. B. (1986): Some thermal and tectonic models for crustal melting in continental collision zones. - *Geological Society Special Publication*, 19, 83-94.
- [9] CLEMENS, J. D. & WATKINS, J. M. (2001): The fluid regime of high-temperature metamorphism during granitoid magma genesis. - *Contributions to Mineralogy and Petrology*, 140, 600-606.
- [10] CLEMENS, J. D. & MAWER, C. K. (1992): Granitic magma transport by fracture propagation. - *Tectonophysics*, 204, 339-360.
- [11] CLEMENS, J. D. ET AL. (1997): Ascent mechanisms of granitic magmas: causes and consequences. - in: *Deformation-enhanced Fluid Transport in the Earth's Crust and Mantle*, M. Holness, Editor, Chapman & Hall, London, p. 144-171.
- [12] ITO, G. ET AL. (1997): Magma transport in oceanic lithosphere through interacting dikes. - *Eos*, 78, F694.

**GOLD DEPOSITS CONTAINING TELLURIDES AND SELENIDES –
PROBLEMS AND OPPORTUNITIES**

N. J. Cook & C. L. Ciobanu

Geological Survey of Norway
NO-7491 Trondheim, Norway

Tellurium- and/or selenium-bearing deposits of Au (\pm Ag) are both economically important and worthy of scientific attention, inasmuch as the mechanisms leading to their formation are incompletely understood. The huge importance of such studies is underlined by the fact that the majority of the world's Au resources are provided by super-large and giant deposits of porphyry and epithermal type (each containing 100 to $>$ 1000 t. Au [1]). All or parts of these deposits are commonly enriched in Se and Te.

Problems

Generalized characteristics and origin of Au-rich Cu-porphyry and epithermal Au deposits have been the subjects of numerous papers [1, 2 etc.]. The relative significance of S, Se and Te within large-scale porphyry-epithermal systems, the influence of these elements on the behaviour of Au and the concentration mechanisms thereof, are nevertheless poorly constrained. Although attempts have been made [e.g. 3, 4], the lack of a comprehensive, internally consistent thermodynamic database for many Se- and Te-bearing systems is a major factor precluding routine modelling. The limited level of current understanding is also due to the uneven treatment of trace mineralogy in the various deposit types within the magmatic-hydrothermal spectrum. For example, whereas ore mineralogical data are seldom reported for world-class porphyry or epithermal Au deposits, gold skarns worldwide are almost always described with attention to the trace minerals that accompany Au [5].

The conventional view is that Te- or Se-enriched deposits are a distinct style of mineralisation, formed at $<$ 250°C. Observations [6-8] of porphyry, skarn and epithermal deposits in the Late Cretaceous Banatitic Magmatic & Metallogenetic Belt, BMMB [9], SE Europe, have revealed that tellurides and selenides are not restricted to late-stage, low temperature mineralisation. A strong link between Au and Bi is widely reported from the skarns, with widespread participation of Bi-tellurides and maldonite in Au-bearing assemblages. We report a comparable Bi-Te mineralogy from all Au-enriched parts of porphyry Cu deposits. The speciation of Bi-tellurides in each association is dependant on the reduced or oxidised type of porphyry system. Furthermore, zones of Au-enrichment at upper levels in epithermal massive sulphide ores in the same belt have similar trace mineral associations as seen in the porphyry ores, irrespective of HS or LS character. Formation of these Au-Te-Bi associations is directly related to retrograde stages in skarn, secondary boiling in porphyry, or boiling at the upper parts because of fluid mixing in epithermal ores. In all, the fluids cross the main buffers in fO_2/fS_2 space.

Such observations are supported by experimental data [3, 4]. Consensus suggests that mixing of magma-derived fluids with meteoric waters may result in substantial changes in overall fluid character reflected in the distinct alteration styles, but does not change the Au-Bi-Te speciation. Instead, the trace minerals associated with Au in porphyry and epithermal deposits are primarily constrained by the reduced or oxidised type of hydrothermal system; itself dependant upon the intrusion (I or S type).

The above observations, in which formation of Bi-telluride assemblages have been modelled for a diverse range of deposits across a large metallogenic belt, are in sharp contrast to studies of Au-telluride rich vein provinces. In such cases, the Au-Te mineralogy remains unchanged with respect to the type of magmatic intrusion. For example, Au-telluride assemblages in the upper part of vein-epithermal systems in the Neogene Golden Quadrilateral, South Apuseni Mts. (SAM), Romania [10], are very similar to those from the Emperor Au-telluride deposit, Fiji [e.g. 11]. This is despite the fact that magmatism in the two provinces differs markedly: calc-alkaline (SAM), and alkaline (Fiji). Our study [10], in one deposit of the SAM, Larga, has corroborated evidence for significant roles for Te, Se (and Bi), and shown that Bi-telluride speciation is responsive to physical-chemical zonation across a hydrothermal system. In the Larga deposit, we note that Au is associated with Bi-tellurides rather than Au-tellurides at deeper levels. We therefore raise the question as to whether Au-telluride associations seen in magmatic-hydrothermal systems are less dependent on their magmatic parentage than the Au-Bi-telluride associations in the porphyry or epithermal deposits.

In comparison with porphyry or epithermal systems, skarns are intrinsically characterised by a greater interaction with their environment. In all BMMB skarns, the Bi-Te association reflects the overall reducing character of the retrograde fluids, despite the oxidised skarn type they represent. In any other skarn, the Bi-Te associations will reflect the changes induced by fluid-rock interaction during the development of that skarn, depending on the time of extraction from the fluids. Such studies can be extended to cover other Te- and Se-bearing systems. Comparative studies of orogenic (mesothermal) and metamorphosed deposits in Precambrian terranes (e.g. Fennoscandian, Ukrainian Shields) have demonstrated the value of the approach, showing that the same basic principles apply also in these types of Au-deposits.

Opportunities

With these ideas in mind, Project 486 of the International Geological Correlation Programme (IGCP) is designed to provide data that may help tackle the following:

- * Can we determine spatial and temporal zonal relationships between tellurides - (\pm selenides) and Au in porphyry/skarn and epithermal ores ?
- * Are Au-Te (\pm Se) ores a distinct type ? - or can they be formed in a variety of different deposits by a convergence of processes ?
- * Development of a quantitative thermodynamic database (from analytical and experimental data) to model the roles played by Te and Se in Au acquisition, transport and deposition.

References

- [1] KERRICH, R. ET AL. (2000): The geodynamics of world-class gold deposits; characteristics, space-time distribution, and origins. - Rev. in Econ. Geol., 13, 501-551.
- [2] SILLITOE, R. H. (2000): Gold-rich porphyry deposits: Descriptive and genetic models and their role in exploration and discovery. - Rev. in Econ. Geol., 13, 315-345.
- [3] AFIFI, A. M. ET AL. (1988): Phase relations among tellurides, sulfides, and oxides: II. Application to telluride-bearing ore deposits. - Econ. Geol., 83, 395-404.
- [4] SIMON, G. ET AL. (1997): Phase relations among selenides, tellurides, and oxides; II, Applications to selenide-bearing ore deposits. - Econ. Geol., 92, 468-484.
- [5] MEINERT, L. D. (2000): Gold in skarns related to epizonal intrusions. - Rev. in Econ. Geol., 13, 347-375.
- [6] COOK, N. J. & CIOBANU, C. L. (2001): Paragenesis of Cu-Fe ores from Ocna de Fier-Dogenecea (Romania), typifying fluid plume mineralisation in a proximal skarn setting. - Mineral. Mag., 65, 351-372.
- [7] COOK, N. J. ET AL. (2002): Trace mineralogy of the Upper Cretaceous Banatitic Magmatic & Metallogenic Belt, SE Europe. - 11th IAGOD Symp.-Geocongress. CD vol. of ext. Abstr, Geol. Surv. Namibia.
- [8] CIOBANU, C. L. ET AL. (2003): Gold enrichment in deposits of the Banatitic Magmatic and Metallogenetic Belt, southeastern Europe. - Extended abstract, SGA Biennial Symposium, Athens, Greece, August 2003.
- [9] CIOBANU, C. L. ET AL. (2002): Regional setting and geochronology of the Late Cretaceous Banatitic Magmatic and Metallogenetic Belt. - Mineralium Deposita, 37, 541-567.
- [10] COOK, N. J. & CIOBANU, C. L. (2003, in press): Bismuth tellurides and sulphosalts from the Larga hydrothermal system, Metaliferi Mts., Romania: Paragenesis and genetic significance. - Mineral. Mag.
- [11] PALS, D. W. ET AL. (2003): Invisible Gold and Tellurium in Arsenic-Rich Pyrite from the Emperor Gold Deposit, Fiji: Implications for Gold Distribution and Deposition. - Econ. Geol., 98, 479-493.

DETrital Cr-SPINELS IN CULM SEDIMENTS AND THEIR TECTONIC SIGNIFICANCE

R. Čopjaková & P. Sulovský

Institute of Geological Sciences
Masaryk University, Kotlářská 2, 611 37 Brno, Czech Republic

Detrital Cr-spinel is one of important minerals in heavy mineral assemblages. The chemical composition of the spinels provides specific information about the types of their source rocks in different tectonic settings. Cr-spinel $(\text{Mg}, \text{Fe}^{2+})(\text{Cr}, \text{Al}, \text{Fe}^{3+})\text{O}_4$ is a ubiquitous accessory mineral in basalts and peridotites. The spinel composition reflects the magma chemistry, degree of partial melting and fractional crystallization (Cr and Mg partitioning into the solid, Al partitioning into the melt), temperature, $f\text{O}_2$ (ratio of Fe^{2+} to Fe^{3+}) [1]. The Mg# in volcanic spinels reflects the cooling rate.

Detrital Cr-spinels were found in the heavy mineral assemblages of graywackes from Drahany Culm. Spinels show significant variations in most important compositional parameters such as Mg# ($\text{Mg}/(\text{Mg}+\text{Fe}^{2+})$), Cr# ($\text{Cr}/(\text{Cr}+\text{Al})$), TiO_2 and $\text{Fe}^{2+}/\text{Fe}^{3+}$. These variations suggest multiple sources of spinels.

The detrital Cr-spinels are mostly homogenous with the exception of some grains from the Myslejovice Formation that show typical features of spinels from metamorphic rocks. These spinels have increased contents of ZnO (3.3–6.1 wt.%), very low Mg#, high Cr# and usually form symplectites with Cr-chlorite-kämmererite (Cr_2O_3 2–19 wt.%). Such spinels are typically present in Moldanubian metamorphic rocks such as eclogites.

In order to distinguish between volcanic and peridotitic spinels we used the TiO_2 content in conjunction with $\text{Fe}^{2+}/\text{Fe}^{3+}$ ratio [2]. High TiO_2 and low $\text{Fe}^{2+}/\text{Fe}^{3+}$ volcanic spinels dominate the population in the Protivanov Formation. The proportion of volcanic spinels decreases toward the younger part of Culm sediments. This trend correlates very well with the decreasing amount of the volcanic pebbles in the conglomerates from older to younger Culm sediments.

We distinguished some types of volcanic spinels with the use of classification diagrams of authors [3, 4]. High Al_2O_3 (> 25 wt.%) with Mg# 0.5–0.7 and Cr# 0.3–0.5 compositions plot well within the field of MORB or MORB-type back-arc spinels. Spinels with 1623 wt.% Al_2O_3 , $\text{TiO}_2 < 1$ wt.%, Cr# 0.5–0.7 and Mg# 0.3–0.7 may come from subduction-related back-arc basalts or continental tholeiites. It is not possible to distinguish these spinels from spinels of other tectonic settings on the basis of Mg# and Cr#. Spinels with high TiO_2 (>1.5 wt.%), low Al_2O_3 (above 18 wt.%), Mg# 0.47 and Cr# 0.60 fit well into the field of intraplate spinels, especially from ocean island basalts. Only one spinel with low Al_2O_3 (9 wt.%) and high Cr# 0.8 is close to the spinels from arc basalts and andesites.

The proportion of peridotite spinels with low TiO_2 and high $\text{Fe}^{2+}/\text{Fe}^{3+}$ increases toward the younger part of Culm sediments. A large part of peridotitic Cr-spinels has Cr# between 0.4–0.55 and Mg# 0.5–0.62. The comparison with data on spinels from ultramafic rocks [5] indicates that the compositional range of the detrital spinels closely matches that of spinels from ocean-floor peridotites with affinity to more Al-poor harzburgites.

The origin of many detrital spinels can be seen in the Letovice-Rehberg ophiolite, which represents a remnant of the Rheic ocean situated between Brunovistulicum and Moldanubicum. Letovice and Rehberg complexes exhibit complete ophiolite sequence [6]. Both complexes consist of serpentinites (former harzburgites), ultramafic cumulates, metagabbro bodies, the interlayered amphibolites and metagabbros (interpreted as a gabbro/dyke complex), amphibolites (represent former basalts and tuffs) and the alternation of amphibolites and gneisses (paragneisses represent the primary sedimentary cover). Spinels with chemical composition close to the spinels from MORB and BABB basalts came probably from upper part of ophiolite. The lower part of ophiolite (harzburgites) we can consider as source rock of "peridotite" spinels.

Some authors [7] regard as source region of volcanic and magmatic pebbles an island arc, denuded in lower Carboniferous. Our study of detrital spinels and their tectonic settings does not confirm the material coming from an island arc.

This research work was supported by Grant GACR (Grant No. 205/99/0567) and Grant FRVŠ of the Czech Republic (Grant No. 576/2003).

References

- [1] YONG, I. L. (1999): Geotectonic significance of detrital chromian spinel: a review. - *Geosci. J.*, 3, 1, 23-29.
- [2] LENAZ, D. & KAMENETSKY, V. S. (2000): Melt inclusions in detrital spinel from the SE Alps (Italy-Slovenia): a new approach to provenance studies of sedimentary basins. - *Contrib. Mineral. Petrol.*, 139, 748-758.
- [3] KEPEZHINSKAS, P. K., TAYLOR, R. N. & TANAKA, H. (1993): Geochemistry of plutonic spinels from the North Kamchatka Arc – Comparisons with spinels from other tectonic settings. - *Mineral. Mag.*, 57, 389, 575-590.
- [4] KAMENETSKY, V. S., CRAWFORD, A. J. & MEFFRE, S. (2001): Factors controlling chemistry of magmatic spinel: an empirical study of associated olivine, Cr-spinel and melt inclusions from primitive rocks. - *J. Petrol.* 42, 655-671.
- [5] BARNES, S. J. & ROEDER, P. L. (2001): The Range of Spinel Compositions in Terrestrial Mafic and Ultramafic Rocks. - *J. Petrol.*, 42, 2279-2302.
- [6] HÖCK V., MONTAG O. & LEICHMANN J. (1997): Ophiolite remnants at the eastern margin of the Bohemian Massif and their bearing on the tectonic evolution. - *Mineral. Petrol.*, Austria : Springer Verlag, 60, s. 267-287.
- [7] TOMÁŠKOVÁ, A. & PŘICHYSTAL, A. (1995): Valouny vulkanitu z kulmských slepenců: pravděpodobná geotektonická pozice a možné zdrojové oblasti vulkanitu. - *Geol. Výzk. Mor. Slez.* v r. 1994, 75-77.

**LOW-TEMPERATURE HEAT CAPACITY OF ILVAITE FROM SERIPHOS (GREECE):
A TEST CASE FOR THE QUANTUM DESIGN® MICROCALORIMETER**

E. Dachs, Ch. Bertoldi & G. Amthauer

Institut für Mineralogie
Universität Salzburg, Hellbrunnerstrasse 34, A-5020 Salzburg, Austria

The heat capacity of natural ilvaite from Seriphos (Greece) was measured between 5 and 300 K with the Quantum Design® microcalorimeter (QDM), newly established at the Department of Mineralogy, Salzburg University (financed by FWF project P15880-NO3, which is gratefully acknowledged). This device allows the measurement on milligram-sized samples and is based on a relaxation-time calorimetric method [1]. Ilvaite from Seriphos was chosen, because low-temperature heat capacities have already been obtained for this substance by adiabatic and differential scanning calorimetry [2, 3] and a sound sample characterisation is available [3]. The natural ilvaite used has a composition close to the end-member formula [3]: $\text{Ca}_{0.992}(\text{Fe}^{2+})_{1.935}\text{Fe}^{3+}_{0.968}\text{Mg}_{0.022}\text{Mn}_{0.018}\text{Al}_{0.053})[\text{Si}_{2.003}\text{O}_7\text{O(OH)}_{0.998}]$. Its unit cell parameters are [3]: $a_0 = 13.011(2)$ Å, $b_0 = 8.801(2)$ Å, $c_0 = 5.851(1)$ Å, $\beta = 90.05(1)$ °. For the QDM-measurement, a 4 x 4 mm-shaped 0.3 mm thick ilvaite plate weighing 17.73 mg was placed on the sample platform of the microcalorimeter and heat capacities were collected at 40 setpoints linearly spaced between 5 and 300 K (Figure 1, dots; each setpoint represents the mean of three separate measurements). A complete measurement lasts around 20 hours compared to several weeks required in adiabatic calorimetry. The amount of sample material for the adiabatic technique is in the order of grams, general a severe limitation for applying this method to synthetic samples. The agreement between QDM- and adiabatic heat capacities is satisfactory (Figure 1). Below 100 K the QDM-data are somewhat higher (maximal 4 % around 50 K), above 100 K at maximum 2 % lower than the adiabatic data reported by [2].

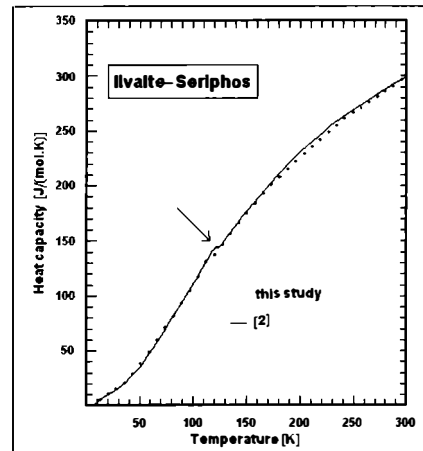


Figure 1

Low-temperature heat capacity of ilvaite from Seriphos, obtained by the Quantum Design® microcalorimeter on a 17.73 mg sample (dots, this study), compared to adiabatic calorimetry data using 408.794 g sample material (line, [2]). Arrow indicates an antiferromagnetic phase transition occurring around 120 K.

A close-up of the heat capacities is shown in Figure 2 for the temperature region 0–40 K and around 120 K, where an antiferromagnetic phase transition is known to occur. Worth mentioning is that our QDM-data show this transition at a 7 K lower temperature (113 K) compared to 120 K from adiabatic calorimetry [2]. The reason for this discrepancy is unclear but may be related to slightly different $\text{Fe}^{2+}/\text{Fe}^{3+}$ -ratios in the samples investigated.

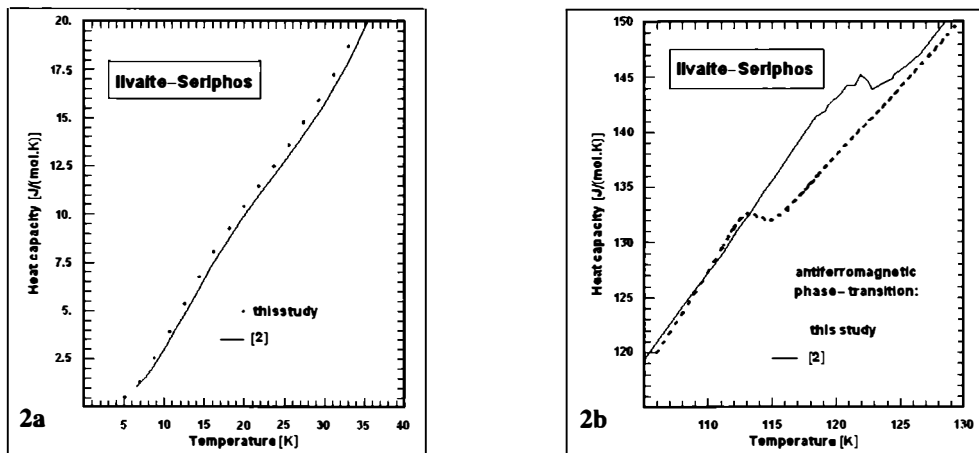


Figure 2

Close-up of ilvaite heat capacities versus temperature. a) temperature region 0–40 K: the concave curvature visible in both data sets is attributed to a minimum in the magnetic susceptibility in this temperature interval by [2]. The QDM-data are at maximum 4 % higher than the adiabatic data. b) temperature region 105–130 K: the QDM-measurements on our ilvaite sample, collected in 0.33 K intervals, indicate that the antiferromagnetic phase transition occurs around 113 K, whereas the adiabatic data show this transition at 120 K.

Numerically integrating our QDM-data yields a standard entropy for ilvaite from Seriphos of 291.7 [J/(mol.K)], which agrees within error with 292.3 ± 0.6 [J/(mol.K)] calculated by [2].

Further measurements with QDM on single-crystals and powders of various substances, whose low-temperature heat capacities are known from adiabatic calorimetry, will be undertaken to further test the reliability of this technique. QDM will then be used to measure low-temperature heat capacities of various synthetic samples and to determine standard entropies for a number of important rock-forming mineral end-members from these data.

References

- [1] BACHMANN, R. ET AL. (1972): Heat capacity measurements on small samples at low temperatures. - Review of Scientific Instruments 43/2: 205–214.
- [2] ROBIE, R. ET AL. (1988): Thermophysical properties of Ilvaite $\text{CaFe}^{2+}_2\text{Fe}^{3+}\text{Si}_2\text{O}_5\text{O(OH)}$; heat capacity from 7 to 920 K and thermal expansion between 298 and 856 K. - Phys. Chem. Minerals 15, 390–397.
- [3] BERTOLDI, CH. ET AL. (2002): The heat capacity of ilvaite. - Beih. Eur. J. Mineral. 14,(2002):19.

**THE PETROLOGICAL EVOLUTION OF HIGH-GRADE METAPELITES
FROM THE SAUWALD, SOUTHERN BOHEMIAN MASSIF**

I. Deibl, P. Tropper & P. W. Mirwald

Institute of Mineralogy and Petrography
University of Innsbruck, Innrain 52, A-6020 Innsbruck, Austria

The Sauwald area is located at the southern rim of the Bohemian Massif in Upper Austria and contains S-type granites and migmatites (meta- and diatexites) with some inlayers of high-grade metapelitic paragneisses. These rocks formed during the post-collisional high T/low P stage of the Variscan orogeny (~320–330 Ma). Metapelitic samples from two localities near Kößldorf and Pyret were investigated. They contain the mineral assemblage garnet + cordierite + spinel + sillimanite + K-feldspar + plagioclase + quartz + biotite + muscovite + magnetite + graphite. The peak metamorphic assemblage is: garnet + cordierite + spinel + sillimanite + plagioclase + quartz and occurs either as inclusion assemblage in garnet or in the matrix. The absence of muscovite and the presence of K-feldspar porphyroblasts and sillimanite needles, suggests that the dehydration of muscovite took place already. The biotites show textures indicating partial melting (e.g. biotite-quartz myrmekites) but the absence of orthopyroxene indicates that the P-T conditions did not exceed the thermal limit (e.g. dehydration breakdown) of the biotite stability field.

Garnet exhibits a slight chemical zoning with increasing Fe contents towards the rims. Cordierite shows no obvious chemical zoning in Fe and Mg, but shows a slight increase in the Na content from the core to the rims from 0.029 to 0.043 Na a.p.f.u. Within plagioclase analyses, three groups can be distinguished: plagioclase inclusions in garnet show An-contents of 35–65, plagioclase porphyroblasts in the matrix show An-contents of 10–45 and albite rims around the matrix porphyroblasts show An-contents of 0–15. Also, two groups of sillimanite can be distinguished. The texturally older, coarse grained sillimanite needles contain >1 wt.% FeO, while the younger, finer grained needles show smaller FeO contents of <1 wt.%. Spinel occurs either as green, brown-green or brown grains. The green spinel grains are the only ones, that contain sillimanite inclusions. The chemical composition of these grains shows differences in the ZnO and Cr₂O₃ contents, which increase from the green to the brown spinel. Relict old biotite grains from the matrix show high TiO₂ contents of up to 6.74 wt.% TiO₂. Mineral chemical and textural data indicate the following stages of mineral growth: peak assemblage garnet + cordierite + spinel (green) + sillimanite + plagioclase (An_{35–65}) + quartz. This peak assemblage continuously changes mineral compositions and thus subsequently the post-peak assemblages: garnet + cordierite + spinel (brown-green and brown) ± sillimanite + plagioclase (An_{10–45} and An_{0–15}) + quartz forms. The last stage of mineral growth is indicated by the growth of muscovite.

The P-T conditions of the assemblage garnet + cordierite + spinel + sillimanite + quartz were calculated by using (1.) the garnet – cordierite – spinel – sillimanite – quartz thermobarometry as calibrated by [1], who considered equilibria among the assemblages garnet – spinel – sillimanite – quartz , cordierite – spinel – sillimanite – quartz and garnet – cordierite – sillimanite – quartz for thermobarometric calculations. This yields pressures ranging from 2.9–5.3 kbar and temperatures of 752°C–764°C for calculations in the systems FAS and FASH. (2.) We also used the inverse equilibrium approach by [2] and obtained pressures of 2.8–3.9 kbar and temperatures of 645–814°C. These data are in good agreement with the P-T results of [3] which yielded P-T conditions of 780°C and 3.8 kbar. Our observed phase relations indicate heating along a clockwise P-T path into the stability field of the assemblage garnet + cordierite + spinel.

During the retrograde portion of the P-T path, the Fe# in garnet increases due to the backreactions of the melt such as: garnet + K-feldspar + melt \leftrightarrow cordierite + biotite and garnet + sillimanite + melt \leftrightarrow cordierite + biotite. These reactions are indicated by resorbed garnets and newly grown cordierite and biotite at the rims of some garnets. Based on the absence of retrograde muscovite, it can also be deduced that the rocks were cooled below 3.8 kbar [4].

References

- [1] NICHOLS, G. ET AL. (1992): Contrib. Mineral. Petrol., 111, 362-377.
- [2] GORDON, T. M. (1992): Geochim. Cosmochim. Acta, 56, 1793-1800.
- [3] KNOP, E. ET AL. (2000): Beih. Eur. J. Mineral., 1, 98.
- [4] SPEAR, F. S. ET AL. (1999): Contrib. Mineral. Petrol. 134, 17-32.

**THERMOBAROMETRY INVOLVING CORDIERITE IN HIGH-GRADE METAPELITES
FROM THE SAUWALD, SOUTHERN BOHEMIAN MASSIF**

I. Deibl¹, P. Tropper¹, R. Kaindl² & P. W. Mirwald¹

¹Institute of Mineralogy and Petrography

University of Innsbruck, Innrain 52, A-6020 Innsbruck, Austria

²Institute of Mineralogy and Petrology

University of Graz, Universitätsplatz 2, A-8010 Graz, Austria

The Sauwald area is located in the southern rim of the Bohemian Massif and contains migmatites and high-grade metapelitic and granitic gneisses. These rocks were metamorphosed during the post-collisional high T/low P stage of the Variscan metamorphic event (~330 Ma). The metapelitic samples were taken from two localities near Kößldorf and Pyret in Upper Austria. The investigated samples contain the mineral assemblage garnet + cordierite + spinel + sillimanite + K-feldspar + quartz + biotite + muscovite + magnetite + graphite. The peak metamorphic assemblage is: garnet + cordierite + spinel + sillimanite + K-feldspar + quartz.

The P-T conditions of the assemblage garnet + cordierite + spinel + sillimanite + quartz were calculated with the thermobarometry of [1] and this yields pressures ranging from 2.9–5.3 kbar and temperatures of 752–764°C for calculations in the systems FAS and FASH. (2.) Application of the inverse equilibrium approach by [2] yields pressures of 2.8–3.9 kbar and temperatures 645–814°C. Latter calculations were performed with dry cordierite and thus only provide limiting P-T estimates. Thermobarometric calculations involving THERMOCALC [3] yield P-T results ranging from 768°C/4.5 kbars ($a_{H_2O} = 1.0$) to 764°C/3.8 kbars ($a_{H_2O} = 0.5$) to 723°C/2.9 kbar ($a_{CO_2} = 1.0$). These results show that informations about the fluid-content of the cordierites is necessary. Current investigations with microraman spectroscopy at the Institute of Mineralogy and Petrology at the University of Graz yields clear evidence for considerable H₂O and CO₂ contents in the core and the rim of cordierite porphyroblasts, thus indicating that calculations involving high $a_{(H_2O)}$ might not yield correct P-T estimates.

An important part of the evaluation of the P-T- $a_{(H_2O)}$ conditions of these high-grade metapelites is the application of additional thermobarometric techniques involving cordierite. In recent years, an extensive evaluation of cordierite as a petrogenetic indicator in high-grade metapelites was performed [4, 5]. These studies focused on the incorporation of sodium in cordierite as a function of temperature, pressure and $a_{(H_2O)}$. [6] and [5] found an inverse correlation between the sodium content and temperature, allowing a potential application of this relation as a thermometer. Their study also showed that the incorporation of sodium into cordierite is virtually pressure-independent. [5] and [7] showed that the sodium content of cordierite is also a monitor of the presence of fluid or melt in metapelitic rocks. Therefore, the sodium content of cordierites may also serve as a monitor for $a_{(H_2O)}$ in the rocks.

Our data indicate temperatures of ca. 650–700°C for the cordierite cores in the presence of a fluid phase in an $a_{(H_2O)}$ range of 0.5 to 1.0. The Na content of cordierite in the presence of melt would indicate temperatures exceeding 850°C! The frequently observed assemblage cordierite + garnet in migmatites can also be used as a geobarometer based on the divariant reaction - (Mg, Fe)-cordierite \leftrightarrow (Mg, Fe)-garnet + aluminiumsilicate + quartz + H₂O (MIRWALD & KNOP, 1995). Using the Mg# of the garnet and cordierite cores yields pressures of ca. 4 kbar for temperatures of 750°C. These data provide important independent P-T estimates in addition to thermobarometric estimates based on multi-equilibrium methods and are in good agreement with the P-T results of [8] which yielded P-T conditions of 780°C and 3.8 kbar.

References

- [1] NICHOLS, G. ET AL. (1992): Contrib. Mineral. Petrol., 111, 362-377.
- [2] GORDON, T. M. (1992): Geochim. Cosmochim. Acta, 56, 1793-1800.
- [3] HOLLAND, T. J. B. & POWELL, R. (1998): J. Metam. Geol. 16: 309-343.
- [4] MIRWALD, P. W. & KNOP, E. (1995): Geol. Paläont. Mitt. Univ. Innsbruck, 20, 153-164.
- [5] KNOP, E. & MIRWALD, P. W. (2000): J. Conf. Abs. 5: 58.
- [6] MIRWALD, P. W. (1986): Fortschr. Mineral., 64, Beiheft 1, 113.
- [7] SCHEIKL, M. & MIRWALD, P. W. (2000): J. Conf. Abs. 5: 58.
- [8] KNOP, E. ET AL. (2000). Beih. Eur. J. Mineral., 1, 98.

**NEW ASPECTS ON THE MECHANISM OF SILICATE WEATHERING –
IMPACT OF POLYSILICIC ACIDS AND HYDROXYALUMINOSILICATE COLLOIDS**

M. Dietzel¹, F. Gérard², J. Jaffrain², O. Nestroy¹, H. Weber³, A. Möller⁴ & J. Hillebrecht⁴

¹Institut für Technische Geologie und Angewandte Mineralogie
Technische Universität Graz, Rechbauerstrasse 12, A-8010 Graz, Austria

²Institut National de la Recherche Agronomique (INRA)
Centre de Nancy, Unité Biogéochimie des Ecosystèmes Forestiers, 54280 Champenoux, France

³Institut für Organische Chemie
Technische Universität Graz, Stremayrgasse 16, A-8010 Graz, Austria

⁴Geowissenschaftliches Zentrum Göttingen
Universität Göttingen, Goldschmidtstrasse 1, D-37077 Göttingen, Germany

The availability of both silica and aluminium in natural systems is mainly controlled by the dissolution and neoformation silicates. At a primary stage dissolved silica and aluminium are liberated into the solution by weathering of minerals and rocks. The concentration of free Al³⁺ and Si(OH)₄[°] may be reduced by precipitation of new solid phases as well as by adsorption at solid surfaces or by the formation of dissolved complexes and colloids. Although, dissolved polysilicic acids as well as hydroxyaluminosilicates complexes and colloids (HAS) may affect the mechanisms of silicate weathering [1] and are assumed to be a precursor of aluminosilicates in natural environments [2, 3], the boundary conditions of their formation as well as the stability and the occurrence in nature are still a matter of debate [4, 5].

In analogy to the structures of silicates various linked Al- and Si-components occur in aqueous solutions as dissolved molecules, complexes, and colloids (e.g. polysilicic acids, HAS, Al13). Dissolution experiments by [6] confirmed that upon dissolution of silicate minerals monosilicic as well as polysilicic acids are liberated into the solution. Such polysilicic acids are thermodynamically stable only in alkaline solutions, but can survive up to several months in acid solutions. Considering this new aspect the occurrence and formation of polymeric silica complexes and colloids are experimentally studied and their occurrence is verified in natural environments. Experiments were carried out at 20°C and at constant pH values between 3.5 and 4.5 by the interaction of dissolved aluminium ions with monosilicic and polysilicic acid. As the experiments proceed various fractions of the solution were separated by ultrafiltration (0.5 to 300 kDalton). The concentrations of Si and Al as well as the polymerisation degrees of Si were analysed in the filtrated and unfiltrated solutions by ICP-OES and β-silicomolybdate reaction rate method, respectively [see 6]. Precipitates and colloids were characterized by photon correlation spectroscopy, atomic force microscopy, X-ray diffraction, infrared, and ²⁷Al-NMR spectroscopy.

The results show that the reaction of Al(H₂O)₆³⁺ with polysilicic acid can lead to the formation of a significant amount of HAS at rather low pH even in solutions which are undersaturated with respect to amorphous Al(OH)₃ and proto-imogolite (Al₂O₃SiOH(OH)₃), potential precipitates with respective high solubility products.

This implies a decrease of “free” dissolved Si and Al of 50 up to 80 mol%. Colloidal HAS ($0.5 < \text{Si}/\text{Al} < 2$) appear as spherical particles with typical size dimensions of 0.1 or 0.8 μm and survive several months. The destruction of polymeric silica molecules is inhibited within the HAS structure and polymerized silica reduces the substitution of Al within the Si-O-tetrahedron. Following the experimental results, linked silica tetrahedrons released by the dissolution of silicates can be fixed within dissolved polymers and HAS. Nevertheless, the occurrence of polysilicic acid and colloidal HAS have to be verified in natural systems. For this purpose soil samples from acidic soils were collected in France and Austria which are suitable for the existence of polysilicic acids and HAS. The respective soil solutions were separated by drainage centrifugation and 0.45 μm filtration and were subsequently analysed by the above methods.

The soil solutions comprise pH values between 3 and 5. Several solutions contain significant concentrations of dissolved polymeric silica. The proportion of silica fixed within such polymeric structures versus total dissolved silica reaches 30 mol% of Si. Subsequent ultrafiltration of the 0.45 μm filtrated soil solutions reduces the concentration of the dissolved aluminium and silica. Thus, linked silica molecules occur within such acidic solutions.

It is verified from experiments and analyses of soil solutions that dissolved and colloidal polymeric silica appear at high proportions of total dissolved silica in acidic waters. Such components are thermodynamically not stable but can survive for several months, especially in the presence of aluminium ions. The polymeric silica is primary liberated from silicates by weathering. Nevertheless, the polymerisation degree of the liberated silica mostly does not represent the structure of the solids. This is caused by incongruent dissolution behaviours and low dissolution rates of silicates which provide a formation of a boundary layer at solid-liquid interface. The chemical composition and structure of such layers are different from that of the primary crystalline silicate and significantly affect the solid-liquid interaction. Thus, aspect of dissolved and colloidal polymeric silica has to be carefully considered for analyses and geochemical modelling in acidic soil and interstitial solutions with respect to both the mechanisms of the silicate weathering and the aluminium and silica speciation.

References

- [1] WEISSBART, E. J. & RIMSTIDT, J. D. (2000): Wollastonite: Incongruent dissolution and leached layer formation. - *Geochim. Cosmochim. Acta*, 64, 4007-4016.
- [2] LOU, G. & HUANG, P. M. (1988): Hydroxy-aluminosilicate interlayers in montmorillonite: implications for acidic environments. - *Nature*, 335, 625-627.
- [3] XU, S. & HARSH, B. (1993): Labile and nonlabile aqueous silica in acid solutions: relation to the colloidal fraction. - *Soil Sci. Soc. Am. J.*, 57, 1271-1277.
- [4] GERARD, F. ET AL. (2002): Process controlling silica concentration in leaching and capillary soil solutions of an acidic brown forest soil (Rhone, France). - *Geoderma*, 107, 47-76.
- [5] DOUCET, F. J. ET AL. (2001): The formation of hydroxyaluminosilicates of geochemical and biological significance. - *Geochim. Cosmochim. Acta*, 65, 2461-2467.
- [6] DIETZEL, M. (2000): Dissolution of silicates and the stability of polysilicic acid. - *Geochim. Cosmochim. Acta*, 64, 3275-3281.

**NEUE IMPULSE IN DER ANGEWANDTEN MINERALOGIE:
MINERALOGISCHE ENTWICKLUNGSPOTENTIALE IN
ENERGIEWANDLUNG UND ENERGIESPEICHERUNG**

H. Dittrich

Zentrum für Sonnenenergie- und Wasserstoff-Forschung
Helmholtzstrasse 8, D-89081 Ulm, Germany

Der tägliche, selbstverständliche Umgang mit PC oder Mobiltelefon erfolgt häufig ohne tieferen Einblick in Komplexität der Systeme und Funktionsweise der Systemkomponenten, welche überwiegend auf Energiebereitstellung und Energiewandlungsprozessen und somit auf spezifische Eigenschaften der, in den Bauteilen verwendeten Materialien beruhen. Anhand verschiedener Beispiele aus aktueller Forschung und Entwicklung soll gezeigt werden, wie grundlegendes mineralogisches Wissen und Verständnis in der Entwicklung und Optimierung von Systemkomponenten eine wichtige Rolle spielen können.

Die physikalischen Prozesse der Energiewandlung werden bestimmt durch die Struktur-Eigenschaft-Korrelation der aktiven Materialien. So ist z. B. in der Photovoltaik die Wandlungseffizienz an Bandabstand, Absorptionskoeffizienten, p-/n-Dotierung und Leitfähigkeit des Halbleitermaterials gebunden. Als wirtschaftlichere Alternative zu den geläufigen Si-Solarzellen wurden und werden Chalkopyrit-Dünnschicht-Solarzellen im Materialsystem Cu-(In,Ga)-(S,Se) entwickelt [1], bzw. befinden sich bereits auf dem Markt (Fa. Siemens, Fa. Würth-Solar). Eine der möglichen Struktur-Eigenschaft-Korrelationen, welche Stöchiometrie, polykristallines Gefüge und elektrische Eigenschaft in CIGS-Dünnschicht-Solarzellen miteinander verknüpft, wurde mit Hilfe der Texturmessung der klassischen Röntgenpulverdiffraktometrie untersucht [2, 3]. Beispielhaft zeigt sich die Bedeutung der mineralogischen Analysenmethodik in technischen Materialentwicklungen.

Ein weiterer Impuls bezieht sich auf das große Reservoir von anorganischen Verbindungen der speziellen Mineralogie. Eine systematische Suche nach neuen Photovoltaik-Materialien unter den sulfidischen Erzmineralen zeigte, daß die Gruppe der Sulfosalz-Minerale eine wichtige Rolle in zukünftigen Dünnschichtsolarzellen-Systemen spielen kann [4, 5]. Bei der Entwicklung geeigneter Dünnschicht-Depositionsverfahren der Sulfosalze liefern die Entstehungsbedingungen der vulkanisch-exhalativen Lagerstätten dieser Minerale wertvolle Hinweise auf geeignete Parameterfenster.

Auch auf dem Gebiet der SOFC-Brennstoffzellen spielen Verbindungen der Perowskit-Familie eine bedeutende Rolle. Wichtig für die Funktion der Elektroden bei Temperaturen zwischen 700° und 900°C sind die thermodynamischen Stabilitätsbereiche, welche zum großen Teil von Mineralogen untersucht wurden [6]. Sauerstoffionen-leitende Eigenschaften bestimmen die Effizienz der Energiewandlung. Ein geeignetes Modell zur Simulation von Ionenleitung in kristallinen und amorphen Festkörpern wird in der Mineralogie entwickelt [7].

Ein bedeutendes Gebiet der aktuellen Materialforschung ist die elektrochemische Energiespeicherung. Als Beispiel sei hier die Sekundär-Batterie (Akku) erwähnt. Das Funktionsprinzip besteht in einer reversiblen Ionen-Ein- und -Auslagerung an den Elektroden der Batterie (Rocking-Chair-Prinzip) unter externem Elektronenfluß, entsprechend den beteiligten Redox-Reaktionen. Auch in diesen Anwendungen finden sich überwiegend mineralische Verbindungen wieder:

	Li-Ionenbatterien	Ni-Metallhydrid
Kathodenmaterialien	Spinelle	Theophrastit
	Li-Mn-Oxide (Birnessit...)	Takovit
	Triphylin	
Anodenmaterialien	Graphit	AB ₅ -Legierungen

Die zu optimierenden Materialeigenschaften der Elektrodenmaterialien beziehen sich auf Kapazität, Leitfähigkeit und Stabilität der Elektroden. Optimale elektrochemische Eigenschaften sind oftmals gekoppelt an das Vorliegen stark gestörter Kristallstrukturen. Auch hier spielen klassische strukturelle Charakterisierungsmethoden der Mineralogie eine wichtige Rolle. Als Beispiele seien hier die quantitative Erfassung von Schichtstapelfehler des Theophrastits [8] sowie die qualitative Erfassung teilweise Li-interkaliert Graphit-Strukturen [9] mittels der DIFFaX-Simulation erwähnt.

Es zeigt sich, daß ein weiter Bereich der aktuellen industriellen Materialforschung und -entwicklung auf mineralogischen Materialsystemen und Analysenmethoden beruhen. Unter der Voraussetzung der Einarbeitung in relevante physikalisch-technische Aspekte der Anwendungen, kann der Mineraloge eine wichtige Position auf diesen Gebieten besetzen.

Literatur

- [1] DITTRICH, H. ET AL. (1988): Thin Film Solar Cells Based on Cu(Ga,In)Se₂ Chalcopyrite Semiconductors. - Proc. Euroforum Renew. Energies, Saarbrücken, Vol. 3, (Stepens & Assoc., Bedford, 1988), 202.
- [2] DITTRICH, H. ET AL. (1991): Epitaxial Effects and Diffusion in Polycrystalline Chalcopyrite Thin Films. - Proc. 10th EC Photov. Solar Energy Conf., Lisboa, (Kluwer, Dordrecht, 1991), 917.
- [3] DITTRICH, H. ET AL. (1991): Analysis of Growth Structures of Polykristalline Chalcogenide Thin Films by X-ray Diffraction. - in "Polycrystalline Semiconductors II: Proc. 2nd Int. Conf. Polycryst. Semicond.", POLYSE, Schwäbisch Hall, 1990", Springer Proc. Phys. 54, J.H. Werner and H.P. Strunk (eds.), Springer, Berlin, 432.
- [4] DITTRICH, H. ET AL. (1994): New Photovoltaic Materials from Systematic Mineralogy. - Proc. 12th European PV Solar Energy Conf., Amsterdam 1994, H.S. Stephens & Ass., 587.
- [5] DITTRICH, H. ET AL. (1996): Photovoltaic Effects in Natural Sulfosalt Minerals. - Proc. 10th Int. Conf. on Ternary and Multinary Comp., Stuttgart, in Cryst. Res. Technol. Berlin 31 Spec. Issue 1, 833.
- [6] MAJEWSKI, P., EPPLER, L., ROZUMEK, M., SCHLUCKWERDER, H. & ALDINGER, F. (2000): J. Mater. Res., 15(5), P1161.
- [7] ADAMS, ST. ET AL. (2002): Pathway models for fast ion conductors by combination of bond valence and reverse Monte Carlo methods. - Solid State Ionics, 154-155, 151-159.
- [8] TESSIER, C. ET AL. (1999): The Structure of Ni(OH)₂: From the Ideal Material to the Electrochemically Active One. - Jour. Electrochem. Soc., 146 (6), 2059-2067.
- [9] DITTRICH, H. ET AL. (2000): Stacking Fault Analysis in Layered Materials. - Proceedings E-MRS Straßburg, Spring Meeting 2000, J. Inorg. Mat. 3, 1137-1142.

**ORIGIN OF THE DOLOMITE MINERALIZATION FROM A PEGMATITE DIKE
AT HORNI BORY, MOLDANUBICUM, CZECH REPUBLIC**

Z. Dolniček¹, K. Malý² & J. Dvořák³

¹Department of Geology

Palacký University, tř. Svobody 26, 771 46 Olomouc, Czech Republic

²Muzeum Vysočiny

Masarykovo nám, 55, 586 01 Jihlava, Czech Republic

³Krásněves 20, 594 44, Czech Republic

In the quarry near Horní Bory (50 km NW from Brno) samples of a typically hydrothermal assemblage occur as youngest fill of a pegmatite dike. Granulite and migmatitized paragneiss in this area belong to the Stráček Moldanubicum and are crosscut by numerous dikes of primitive pegmatites (Q, Kfs, Plg, Bt, Ms, ± Crd, Sch, Ap) [1].

The hydrothermal mineralization overgrows crystals of smoky quartz, muscovite and biotite in the pegmatite vugs. It is formed especially by coarse grained Fe-dolomite, less common are prismatic crystals of quartz and pyrite cubes, only accessory is siderite. The crystallization succession is as follows: quartz-dolomite-siderite-pyrite. The mineralization was studied using fluid inclusion and stable isotope techniques with the aim to better understand its genesis.

Fluid inclusions

Primary, primary-secondary and secondary fluid inclusions (FI) within dolomite have been studied by means of optical microthermometry. Secondary FI have low homogenization temperatures up to 52°C and low salinity from 0 to 3 wt. % NaCl equiv.

Two types of primary and primary-secondary FI can be distinguished. The first one are two-phase L+V inclusions containing aqueous solution, which have homogenization temperatures in the range 136–167°C. The low eutectic temperatures (-70 to -52°C) and brown coloration of the frozen FI indicate that Ca and Na chlorides are present. As the last solid phases in these FI melts either ice (melting temperature, Tm, between -7.4 and -14.0°C corresponding to bulk salinity 11–17.8 wt.% NaCl equiv.) or hydrohalite (Tm in the range -17 to +1.6°C indicating salinity 24–26.3 wt.% NaCl equiv.). The distribution of the measured data in the Th-salinity plot shows the presence of two separated pulses of fluid with the same temperatures but different salinities. Within both groups simple cooling of the fluid as the most probably depositional mechanism during crystallization of dolomite could be recognized.

The second type of fluid inclusions coexists with aqueous FI and this type is filled with vapour only. During cooling sometimes a small solid white phase nucleates on the wall of these FI; during the next deeper cooling a liquid phase condenses. The liquid did not freeze even at -196°C. Homogenization of the liquid phase to vapour was observed at temperatures -97.5 to -99.1°C. The solid phase (CO₂?, H₂S?) sublimated in a wide temperature interval from -94 to -60°C. Most probably, the vapour inclusions contain CH₄-N₂ fluids with predominant methane and a small admixture of the above mentioned gases.

The presence of cogenetic FI with different compositions allows direct determination of the real temperature and pressure on the basis of thermometric data only. Using the method of intersecting isochores, a pressure as high as 100–115 bar was found. Thus, the so called "pressure correction" to the Th values of aqueous FI reach in this case only about 5°C.

Stable isotopes

A pyrite sample showed the $\delta^{34}\text{S}$ value of +5.4 ‰ CDT. This value probably corresponds to average reduced sulphur derived from host metasedimentary and igneous rocks.

Fe-dolomite has $\delta^{13}\text{C}$ = -6.2 ‰ PDB and $\delta^{18}\text{O}$ = +13.4 ‰ SMOW. The calculated $\delta^{13}\text{C}$ value for the parent fluid (using trapping temperatures derived from FI) varies between -7.4 and -8.8 ‰ PDB, indicating the presence of the "deep" carbon or carbon of the homogenized Earth's crust. Calculated $\delta^{18}\text{O}$ of the parent solution is between -1.2 and +1.2 ‰ SMOW, which are typical values for marine water.

Conclusions

The dolomite mineralization from Horní Bory originated in a dynamic hydrothermal system with contribution of three types of fluids. The parent solutions were saline brines rich in Ca and Na chlorides. Fluid inclusion microthermometry indicates formation temperature between 141 and 173°C and very low pressure ranging from 100 to 115 bar. Near-zero oxygen isotopic composition of the parent fluid precludes a magmatic or metamorphic origin of the fluid but is easily comparable with sedimentary brines. Sulphur and carbon either may be leached from host rocks or were provided by the fluids. Based on our data, the genetic link to the fading pegmatite process seems to be not realistic. However, mineral composition, chemical composition of the minerals, isotopic composition of C, S, O, temperature, pressure, and fluid composition and salinities of the studied mineralization are very similar to the parameters of post-Variscan dolomites from epithermal polymetallic veins occurring within Moravicum (Svatka Dome) and Culm of the Nízký Jeseník Mts. [2, 3]. All these occurrences, partly hosted also by crystalline complexes, support an idea of large-scale migration of post-Variscan sedimentary brines through the Bohemian massif [4].

References

- [1] ŠPINAR, P. (1995): The relationship between pegmatites and Alpine-type veins in the quarry near Horní Bory. - Vlastivědný sborník Vysočiny, odd. věd přírodních, 12, 3-18. (in Czech).
- [2] DOLNÍČEK, Z. & MALÝ, K. (in print): Mineralogy and genesis of the epithermal veins from the quarry in Dolní Loučky near Tišnov. - Acta Mus. Moraviae, Sci. geol., 88. (in Czech).
- [3] SLOBODNÍK, M. & DOLNÍČEK, Z. (2001): Fundamental features of fluids of hydrothermal mineralization near Hrabětka, Nízký Jeseník Upland. - Geol. Výzk. Mor. Slez. v r. 2000, 8, 52-54. (in Czech).
- [4] SLOBODNIK, M., MUCHEZ, PH. & DOLNÍČEK, Z., ZÁK, L. (1999): Regional occurrence of saline, mineralising fluids at the eastern border of the Bohemian Massif. - In: Stanley C. J. et al. (eds.): Mineral deposits: Processes to Processing, 901-904. A. A. Balkema. Rotterdam.

THE PALEOGENE RECORD OF THE RHENODANUBIAN FLYSCH:
TECTONIC AND CLIMATIC IMPLICATIONS

H. Egger

Geologische Bundesanstalt
Rasumofskygasse 23, A-1031 Wien, Austria

The Paleocene to lowermost Eocene formations of the Rhenodanubian Flysch were deposited in an abyssal environment, at the continental rise to the south of the European Plate. The pattern of paleocurrents indicates a number of small distributary systems for the turbiditic material, which entered the basin from the north and was deflected to the east and to the west. Heavy mineral assemblages in the turbidites suggest the erosion of medium-grade metasediments in the Danian and the progressive erosion of underlying metamorphic magmatic rocks in the Thanetian and Ypresian.

The most obvious sedimentary event is the breakdown in turbidite sedimentation during the late Danian to the early Thanetian. Remarkably, this death of turbidites is associated with high values of chlorite in the clay mineral assemblages of interturbidite shales, indicating increased mechanical erosion of the adjoining land areas. Tectonic uplift of these areas and associated block faulting and tilting is assumed to be responsible for this increase in erosion as well as for the synchronous cutting off of the basin from the source area of the turbidites. This tectonic activity is related to the onset of the collision of the European and the Adriatic Plates. A second major event documented in the Paleogene record is the change from a predominantly siliciclastic system to a carbonaceous system in the upper Thanetian. Associated with the global negative carbon isotope excursion (CIE) in the upper part of calcareous nannoplankton zone NP9 is a strong three-fold increase in the rate of hemipelagic sedimentation. This indicates enhanced continental run-off, which probably was the result of the establishment of a monsoonal climate. This is supported by the composition of clay mineral assemblages, which display a slight increase in kaolinite. The top of the enhanced kaolinite input is poorly constrained because of a very high input of smectite due to volcanic activity in sub-zone NP10a. This igneous activity is assigned to the opening of the Northern Atlantic Ocean and has no geodynamic relevance for the Rheno-danubian Basin.

**ARE YOU HUNTING PRE-VARISCAN ROCKS SOMEWHERE BETWEEN
SWITZERLAND AND BAVARIA ?
TRY AUSTRIA'S TAUERN WINDOW !**

R. Eichhorn¹, U. Teipel² & G. Loth²

¹Bayerisches Staatsministerium für Landesentwicklung und Umweltfragen
Rosenkavalierplatz 2, D-81925 Munich, Germany

²Bayerisches Geologisches Landesamt
Heßstrasse 128, D-80797 Munich, Germany

Until the 90's, the pre-Variscan evolution of the Tauern Window and its geotectonic setting have been a mystery due to missing or unreliable geochronological data. Concepts and models had to rely on petrological, geochemical and field data, only. Geotectonic and palaeogeographic conclusions were reduced to mere guesswork.

In recent years, the data situation improved significantly. Intense geochronological work led to the identification of Neoproterozoic to Ordovician relics of oceanic crust and subduction-related rocks in basement areas of all four Alpine domains (i.e. the Southalpine, Austroalpine, Penninic and External domains). A tentative reconstruction of the palaeogeographic situation before the Variscan orogeny puts these relics in a position at the northern Gondwana active margin [1]. High-quality zircon age data revealed a complex evolution at least in one of the four domains, the 'Habach terrane' [2] of the Penninic Tauern Window. SHRIMP data indicate geological events at 2.64–2.06 Ga, at ~830, 551–507, 496–482 and 422–414 Ma [3, 4]: The provenance region of the Archaean (2.64–2.06 Ga) zircons is assumed to be a terrane of Gondwana affinity, most probably the West African craton. The Habach terrane was formerly interpreted as a bottom-to-top sequence with the oldest at the bottom (Stubach Group), overlain by the Habach Group, consisting of the Basisschieferfolge, the Eruptivgesteinsfolge und the youngest unit, the Habach-phyllitsequenz. Nowadays, the "bottom-to-top" sequence is radically re-interpreted as a lateral and +/- coeval emplacement of all the units in an active continental margin with ensialic back arc development:

Radiometric and isotopic data revealed a subduction-induced magmatism in the Cambrian, between 551 and 507 Ma. Back-arc diorites and arc basalts were intruded by ultramafic sills and subsequently by small patches of mantle-dominated granitoids. Fore-arc (shales; Habach-phyllitsequence) and back-arc (greywackes, cherts; Basisschieferfolge) basin sediments as well as arc (Eruptivgesteinsfolge) and back-arc (Stubach Group) magmatites were not only nappe-stacked by the Caledonian compressional regime closing the presumably narrow oceanic back-arc basin and squeezing mafic to ultramafic cumulates out of high-level magma chambers (496–482 Ma). It also induced uplift and erosion of deeply rooted crystalline complexes and triggered development of a successor basin filled with predominantly clastic greywacke-arkosic sediments (also Basisschieferfolge).

The Habach terrane is seen as the 'missing link' between similar units of the more westerly positioned External domain (e.g. Aar, Aiguilles Rouges) and the Austroalpine domain to the east (Oetztal, Silvretta).

New U-Pb SHRIMP data from zircons of metamigmatites from the Bayerischer Wald (Germany) reveals a complex evolution of this section of the Moldanubian Zone exposed in the western Bohemian Massif [5]. In fact, geochronological data and geotectonic implications from the Bayerischer Wald are quite similar to the evolution of the Habach terrane (Tauern Window): Inherited zircon cores indicate a Palaeoproterozoic-Archaean (2.70, 2.02 Ga) source region, presumably of Gondwana affinity (West African craton), and document Cadomian magmatism (640 to 560 Ma). Magmatism at 555–549 Ma in the south-western part of the Bayerischer Wald probably took place at an active continental margin with ensialic back-arc development. Magmatism and anatexis at 480–486 Ma and 491–457 Ma, respectively, are documented in the north-eastern parts of the Bayerischer Wald and point to an active continental margin setting, possibly with some lateral variation (accretion/collision) in the Lower Ordovician.

A tentative palaeogeographic reconstruction puts the "Bayerischer Wald" in a close relationship with the Habach terrane (Tauern Window), as the "eastern" prolongation of terranes of the northern Gondwana margin.

References

- [1] VON RAUMER, J. F. (1998): The Paleozoic evolution in the Alps: from Gondwana to Pangea. - *Geologische Rundschau*, 87, 407-435.
- [2] FRISCH, W. & NEUBAUER, F. (1989): Pre-Alpine terranes and tectonic zoning in the Eastern Alps. - *Geological Society of America Special Paper*, 230, 91-100.
- [3] EICHHORN, R., HÖLL, R., LOTH, G. & KENNEDY, A. (1999): Implications of U-Pb SHRIMP zircon data on the age of the Felbertal tungsten deposit (Tauern Window, Austria). - *International Journal of Earth Sciences*, 88, 496-512.
- [4] EICHHORN, R., LOTH, G. & KENNEDY, A. (2001): Unravelling the pre-Variscan evolution of the Habach terrane (Tauern Window, Austria) by U-Pb SHRIMP zircon data. - *Contributions to Mineralogy and Petrology*, 142, 147-162.
- [5] TEIPEL, U., EICHHORN, R., ROHRMÜLLER, J., LOTH, G., HÖLL, R. & KENNEDY, A. (2003): U-Pb SHRIMP and Nd isotopic data from the western Bohemian Massif (Bayerischer Wald, Germany): Implications for Upper Vendian and Lower Ordovician magmatism. - *International Journal of Earth Sciences*, submitted.

**ZUR LITHOLOGIE UND GEOLOGISCHEN POSITION VON PREBICHLFORMATION UND
GRAUWACKENZONE ZWISCHEN DACHSTEINGRUPPE UND RADSTÄDTER TAUERN**

Ch. Exner

Institut für Geologische Wissenschaften
Universität Wien, Althanstrasse 14, A-1090 Wien, Austria

Vorgestellt wird eine neue geologische Manuskriptkarte 1:25.000 und eine Tafel von handgezeichneten N-S Parallelprofilen im Gebiet des Kartenblattes "Radstadt" (ÖK. 126). Die geologische Feldaufnahme hat der Verfasser in den Sommermonaten 2000 bis 2002 vorgenommen. Sie soll zugleich anschließen an das geologische Kartenblatt "Schladming" (ÖK. 127) und an die prächtige neue geologische Sonderkarte der Dachsteinregion von G. W. MANDL [1]. Die klastischen Schichten unter dem Salinar des Haselgebirges wurden bereits von F. NEUBAUER [2] für den Sockel der Nördlichen Kalkalpen nicht nur in der namensgebenden Steiermark, sondern auch für die westlichen Bundesländer dem Begriff Prebichlformation zugeordnet. Die alpidische Epimetamorphose: Neukristallisation von Chloritoid, Albit, Hellglimmer und Chlorit mit niedrigthermaler Anchimetamorphose im höheren Teil (hier: Plattenserie) wurde bereits vor Jahrzehnten besonders von Salzburger und Innsbrucker Kollegen im Raum der westlich anschließenden Kartenblätter ÖK. 124 und 125 erforscht [3]. Sie haben geklärt, dass die Rotliegendsedimente des Perms im Zuge der alpidischen Metamorphose die rote primäre Sedimentfarbe verlieren und zu grünen und grauen Gesteinen umgewandelt sind, was sich nun auch im vorliegenden Gebiet auf Blatt "Radstadt" gut nachweisen lässt. Schließlich hat H. MOSTLER [4] die stratigraphische Interpretation der Prebichlformation von wahrscheinlichem Oberkarbon bis zum oberpermischen Haselgebirge für den Raum des einstigen Mitterberger Kupferbergbaues gegeben. Dessen Prinzip gilt im wesentlichen auch für die Kartierungsergebnisse des Verfassers: Grobklastische Wildbachsedimente und Ablagerung vulkanischer Tuffe im unteren (Wexlerserie) Bereich, dann eine interpermische Breccienbildung im mittleren (Filzmoosserie) und abschließend eine sehr mächtige Sandsteinentwicklung mit reichlicher Beimengung fein aufbereitenden vulkanoklastischen Materials eines fernen Lieferungsgebietes im oberen (Plattenserie) Bereich der Prebichlformation. Erst darüber folgt das oberpermische Salinar.

Die Prebichlformation ist im Gebiet des Kartenblattes "Radstadt" trotz der dichten Vegetationsbedeckung vorzüglich durch ein enges Netz von Forstwegen und künstlichen Einbauten (Skigebiet und Sommertouristik) aufgeschlossen. Die Liegengrenze der Filzmoosserie folgt der morphotektonischen alten Talfurche in E-W Richtung: Terrassenlandschaft über den Mandlingtälern (Mühlebner und Hachau) – Flache Wasserscheide des Übermooses bei Filzmoos – Längstal des Fritzaches (bis N Eben im Pongau). Mit geringen Abweichungen streichen die Gesteine der Prebichlformation E-W und fallen mittelsteil nach N und erreichen im NW-Sektor der Plattenserie söhlige Lagerung.

Wenn auch einige lokale tektonische Komplikationen gefunden wurden (tektonische Schuppenbildung mit vertikalen Schicht-Wiederholungen und lokale Bildung von Querfalten), scheint doch weithin eine stratigraphische, schwach diskordante Auflagerung der Prebichlformation über der komplizierter zusammengesetzten altpaläozoischen Grauwackenzone zu bestehen.

Nach derzeitiger Vermutung des Verfassers dürfte die Wexlerserie mit ihren anscheinend monometamorphen vulkanischen Tuffen weiter nach S ins Ennstal reichen, als im ersten Kartierungsbericht [5] angenommen wurde. Das diesbezüglich interessanteste Gestein ist der recht feste, Roßbrand-Bänderquarzit, der eventuell einen vulkanischen Metatuffit darstellt. Er baut die harte und N-fallende Felsplatte über dem weichen altpaläozoischen Schwarzphyllit der tief und steil eingeschnittenen Mandlingschlucht auf.

Die geologische Kartierung des Verfassers der letzten Jahre wurde in Zusammenarbeit des Wiener geologischen Universitätsinstitutes mit der Geologischen Bundesanstalt ermöglicht. Sie erbrachte in einer anderen, bereits computergestützten farbigen Manuskriptkarte der geologischen Umgebung von Wagrain [6] die Bestätigung der von HEISSEL, W. [7] gefundenen, innerhalb der altpaläozoischen Grauwackenzone isoliert vorkommenden Ginauscholle als Rest der einst transgressiv auflagernden Prebichlformation. Die Gesteine sind dieselben. Es handelt sich um einen tektonisch eingezwickten Sedimentkeil.

Literatur

- [1] MANDL, G. W. (1998): Geologische Karte der Dachsteinregion mit Profiltafel. Maßstab 1:50.000. - Verlag Geologische Bundesanstalt und Umweltbundesamt Wien.
- [2] NEUBAUER, F. (1993): In: von Raumer, J. F. und Neubauer, F. (Eds.): Pre-Mesozoic Geology in the Alps, 677 Seiten, Springer-Verlag, Berlin.
- [3] SCHRAMM, J. M. (1980): Bemerkungen zum Metamorphosegeschehen in klastischen Sedimentgesteinen im Salzburger Abschnitt der Grauwackenzone und der Nördlichen Kalkalpen. - Mitt. österr. geol. Ges., 71/72, 379-384.
- [4] MOSTLER, H. (1972): Zur Gliederung der Permoskyth-Schichtfolge im Raum zwischen Wörgl und Hochfilzen (Tirol). - Verh. Geol. B.-A., Jg. 1972, 155-162.
- [5] EXNER, CH. (2001): Bericht 2000 über geologische Aufnahmen in Prebichlformation und Grauwackenzone auf den Blättern 125 Bischofshofen und 126 Radstadt. - Jb. Geol. B.-A., 143, Heft 3 (im Druck).
- [6] EXNER, CH. (2002): Geologische Karte der Umgebung von Wagrain im Maßstabe 1:25.000. - Archiv der Geologischen Bundesanstalt in Wien.
- [7] HEISSEL, W. (1949): Bericht (1948) über Aufnahmen auf Blatt St. Johann im Pongau (5050). - Verh. Geol. B.-A., Jg. 1949, 59-61.

METAMORPHISM OF KOLET UM KHARIT METAVOLCANICS, SOUTH EASTERN DESERT, EGYPT: A CASE OF TRANSITIONAL GREENSCHIST-AMPHIBOLITE FACIES

E. S. Farahat

Department of Geology
Minia University, El-Minia 61111, Egypt

The late Precambrian metavolcanics of Kolet Um Kharit (KUKh) at southern Eastern Desert of Egypt comprise mainly massive mafic lavas of tholeiitic nature. These rocks are thought to be of ensialic back-arc basin or rifted margin tectonic environments. The petrographical and mineral-chemical investigation of the mineral assemblages of KUKh metavolcanics (hornblende + actinolite + albite + epidote \pm chlorite \pm biotite \pm titanite + ilmenite + magnetite \pm calcite \pm quartz \pm K-feldspare) indicates monometamorphic conditions under transitional greenschist-amphibolite facies conditions. Amphiboles vary in composition from actinolite to magnesio-hornblende. Feldspars are represented by albite ($An_{0.9}$) and rarely oligoclase. Amphibole, amphibole-plagioclase geothermobarometry (Table 1) and thermometry-oxygen-barometry of ilmenite-magnetite intergrowths (Fig. 1) reveal metamorphic conditions of about 480–510°C, 5–7 kbar and $\log fO_2$ of -18 to -21.

Table 1
Estimated P-T conditions.

	Temperature (°C)	Pressure (kbar)
[1]	~ 490-510	
[2]	~ 480-510	~ 6-7
[3]		5.03-6.84
[4]		5.3-7.31
[5]	--	5.4-7.18

Textural and chemical relationships in coexisting actinolite and hornblende, which is characteristic feature of transitional greenschist-amphibolite facies metamorphic rocks, have been examined in detail. Actinolite and hornblende coexist in a well-developed epitaxial intergrowth. The two amphiboles form porphyroblasts that are patchwork of the two phases. A different texture shows porphyroblasts with actinolite cores totally rimmed by hornblende. Coexisting actinolite and hornblende are characterized by sharp optical and chemical boundaries. Sharpness of the interfaces between the two phases, together with the P-T estimates (Fig. 2), is consistent with the presence of a miscibility gap (solvus) between actinolite and hornblende.

The compositional variations of Fe-Ti oxides with metamorphism are also discussed. Fe-Ti oxides are represented by ilmenite and magnetite. The good preservation of ilmenite reflects a very low CO_2 activity. Ilmenite from the investigated metavolcanics has anomalously high Mn-content (1.7–2.26 wt.% MnO) and depleted in Mg. It is free from hematite exsolution bodies (Hm is < 8 mol%) suggesting relatively reducing condition during metamorphism. The Mn-distribution coefficient for coexisting magnetite-ilmenite pairs ($KD = Mn^{mt}/Mn^{ilm} < 0.1$) proves that the calculated T- fO_2 solutions represent the last episode of re-equilibration of the oxides.

The metamorphic re-equilibration temperature (540–580°C) obtained for the coexisting Fe-Ti oxides (Fig. 1) are relatively higher than those derived from the silicate assemblages (480–510°C). This might be attributed to the fact that the investigated Fe-Ti oxides contain significant amounts of Mg, Mn, Cr, and Al. Therefore, the estimated temperatures obtained from the silicate assemblages are considered to be more reliable.

FARAHAT [8] described transitional greenschist-amphibolite facies mineral assemblages from other metavolcanic occurrences in the Egyptian Shield. Accordingly, major parts of metavolcanics in the Egyptian Shield might have undergone a similar P-T evolution.

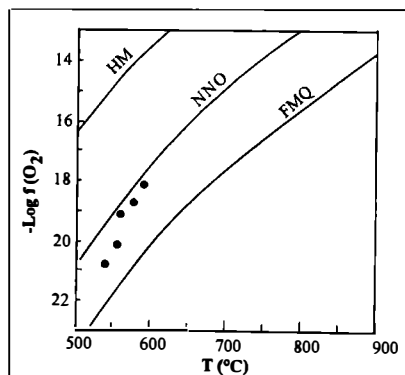


Fig. 1

Log fO₂ vs. T°C calculated using co-existing Fe-Ti oxide pairs. The curved lines give various buffers (HM = hematite-magnetite, NNO = nickel-nickel oxide; FMQ = fayalite-magnetite-quartz).

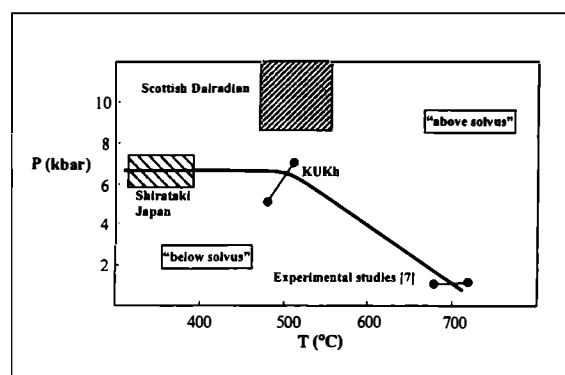


Fig. 2

Schematic P-T slope (heavy line) for the crest of solvus in Ca-amphiboles [6], combining P-T data of KUKh metavolcanics with those of other natural metabasites sequences and the experimental data [7].

References

- [1] SPEAR, F. S. (1980): NaSi↔CaAl exchange equilibria between plagioclase and amphibole, an empirical model. - Contributions to Mineralogy and Petrology, 72, 33-41.
- [2] PLYUSNINA, L. P. (1982): Geothermometry and geobarometry of plagioclase-hornblende bearing assemblages. - Contributions to Mineralogy and Petrology, 80, 140-146.
- [3] HAMMARSTROM, J. M. & ZEN, E. (1986): Aluminium in hornblende: an empirical igneous geobarometer. - American Mineralogist, 71, 1297-1313.
- [4] HOLLISTER, L. S., GRISSMO, G. C., PETERS, E. K., STOWELL, H. H. & SISSON, V. B. (1987): Confirmation of the empirical correlation of Al in hornblende with pressure of solidification of calc-alkaline plutons. - American Mineralogist, 72, 231-239.
- [5] SCHMIDT, M. W. (1992): Amphibole composition in tonalite as a function of pressure: an experimental calibration of the Al-in hornblende barometer. - Contributions to Mineralogy and Petrology, 110, 304-310.
- [6] BEGIN, N. J. & CARMICHEAL, D. M. (1992): Textural and compositional relationships of Ca-amphiboles in metabasites of the Cap Smith Belt, Northern Quebec: Implication for a miscibility gap at medium pressure. - Journal of Petrology, 33, 1317-1343.
- [7] OBA, T. & YAGI, K. (1987): Phase relations on the actinolite-pargasite join. - Journal of Petrology, 28, 23-36.
- [8] FARAHAT, E. S. (2001): Comparative petrological studies of some pillowed lavas in the Eastern Desert, Egypt. - Ph.D. Thesis, Minia University, Minia, Egypt, 241 p.

**DIE SULFIDMINERALISATIONEN VON ARZBERG (STEIERMARK):
ERGEBNISSE PETROGRAPHISCHER, MINERALCHEMISCHER
UND GEOCHEMISCHER UNTERSUCHUNGEN**

M. M. Feichter^{1, 2} & A. Mogessie¹

¹Institut für Mineralogie und Petrologie
Universität Graz, Universitätsplatz 2, A-8010 Graz, Austria
²Rotekreuzstrasse 7, D-30627 Hannover, Germany

Das Revier Arzberg-Haufenreith liegt im oberostalpinen Deckenkomplex des Grazer Paläozoikums. Von etwa 1200 bis 1927 wurde sporadisch untertägiger Bergbau auf Ag-hältige Bleierze betrieben. Die Metallanomalien (Pb, Zn, Ba und Ag) beschränken sich auf niedrig- bis mittelgradig metamorphe, vorrangig mergelige Paraserien obersilurisch bis mitteldevonischen Alters ("Arzbergformation") der Schöckeldecke. Zwei sulfidische Mineralisationstypen werden unterschieden: (1) Geringmächtige, feinkörnige, stratiforme Vererzungen (Bleiglanz+Magnetkies+Pyrit), die lateral in Barytmineralisationen übergehen. Das konkordante Auftreten der Mineralisationen innerhalb der Wirtsgesteine spricht für eine synsedimentäre Metallanlieferung und -fällung in beckenförmigen Erzfallen [1]. Die stratiforme Mineralisation zeigt charakteristische Merkmale für "Stockwerk"-, bzw. "feeder"-Systeme aus SEDEX-, bzw. VMS-Lagerstätten. (2) Ein grobkörniger, epigenetischer Mineralisationstyp (Bleiglanz+Kupferkies+Pyrit), der an diskordante Quarz-Karbonat-Dehnungsgänge in tuffitischen Chlorit-Biotitschiefern gebunden ist.

Stratiforme magnetkiesreiche Vererzungen – in Paragenese mit Pyrit, bzw. Bleiglanz – sind lediglich im Süden des Stollensystems aufgeschlossen. Im Norden treten dagegen fast ausschließlich reine Bleiglanzmineralisationen auf. Zinkblende und Kupferkies sind als Nebengemenge bevorzugt in den magnetkiesreichen Paragenesen vertreten. Als Akzessorien kommen Ag-führende Phasen (Freibergerit, Pyrargyrit, Ag-Au-Hg Legierungen), Cobaltit [CoAsS], Ullmannit [NiSbS] und Breithauptit [NiSb] ausnahmslos in enger Assoziation mit Bleiglanz vor. Der beprobte Lagerstättenebereich liegt im mittelsteil nach Norden einfallenden Nordschenkel einer großräumigen E-W streichenden Antiklinale. Daher kann der kontinuierliche Übergang von S nach N mit einer räumlichen Zonierung einer stratigraphisch liegenden, proximalen Magnetkiesfüllung zu einer hangenden, distalen Bleiglanz-Mineralisation interpretiert werden. Intensive Deformation wie Isoklinalverfaltung und multiple Abschiebungen unterschiedlichster Größenordnungen erschweren die Rekonstruktion des ursprünglichen Ablagerungsraumes und der Mineralsukzession.

Die stratiformen Sulfidvererzungen lassen sich mineralogisch und geochemisch in vier Paragenesestypen unterteilen, vom Typ I im Norden bis zum Typ IV im Süden des Untersuchungsgebietes. Diese Typen unterscheiden sich zusätzlich in Paragenese und Mineralchemie der Gangartminerale. Die magnetkiesdominierten Vererzungen sind an chloritreiche Paragenesen gebunden, während die bleiglanzreichen Typen in karbonatischen Nebengesteinen liegen, in denen als Besonderheit Stilpnomelan auftritt.

Kupferkies führt reproduzierbar hohe Ag-Gehalte (bis 7000 ppm in Paragenese III), während die Ag-Konzentrationen im Bleiglanz meist unterhalb der Nachweisgrenze der Mikrosonde liegen (< 500 ppm). Bis zu 700 ppm Co und Ni wurden in Magnetkies gemessen. Pyrit ist Co-dominierend (bis zu 8700 ppm Co, max. 2000 ppm Ni). Der Fe-Gehalt von Zinkblende schwankt in der Sulfidvererzung von 5 bis etwa 8 Gew.%. Die Zinkblenden der Barytmineralisation sind mit Fe-Gehalten < 1 Gew.% deutlich Fe-ärmer.

Die Fahlerze sind als Freibergite zu klassifizieren (Ag-Gehalte > 20 Gew.%, As < 1 Gew.%). Der durchschnittliche Ag-Gehalt liegt in der Typ I Mineralisation bei 27 Gew.% und steigt in den Typen II und III deutlich über 30 Gew.% an. In Berührungsparagenese mit diesen Ag-reichen Fahlerzvarietäten stehen wenige µm große Erzphasen mit Ag > 43 Gew.%, die sich optisch und chemisch von Freibergerit und Pyrargyrit abheben und wahrscheinlich eine eigenständige, homogene, fahlerzhähnliche Mineralphase repräsentieren.

Im Rahmen der vorliegenden Arbeit wurden erstmals Ag-Au-Hg Legierungen aus Arzberg dokumentiert. Sie sind bevorzugt an Rissfüllungen ausgeheilter Pyrite der Vererzungstypen I und II gebunden und mit Ag-Gehalten zwischen 66 und 84 Mol% sowie Au-Gehalten zwischen 17 und 32 Mol% als goldführendes Silber anzusprechen. Der Hg-Gehalt liegt zwischen 0 und 6 Mol%.

Die Chemismen von Karbonat und Chlorit unterliegen, bezogen auf ihre räumliche Entfernung zum Vererzungshorizont, starken Schwankungen. So beobachtet man eine Verschiebung von sehr Fe-reichen Varietäten (Siderit, Ankerit und Daphnit) im unmittelbaren Vererzungsbereich über Mg-reichere Ankerite im Alterationsbereich bis hin zu Calcit und Rhipidolith im hydrothermal unbeeinflussten Nebengestein. Die Begleitminerale der diskordanten Quarz-Karbonat-Gänge sind chemisch nahezu äquivalent ihren unmittelbaren Umgebungsgesteinen (tuffitische Chloritschiefer).

Hellglimmer sind ausnahmslos phengitisch ($3.4 < \text{Si}/[^{41}\text{Al}] < 4.8$) und reich an Ba (bis 7.7 Gew.% BaO). Stilpnomelan ist Fe-reich ($0.83 < X_{\text{Fe}} < 0.93$), liegt in enger Assoziation mit Siderit und Magnetit vor und führt außergewöhnlich hohe BaO-Konzentrationen (1.9–2.7 Gew.%). Feldspäte sind in die Alkalifeldspatreihe Orthoklas-Albit einzuordnen; die maximale Celsiankomponente in Kalifeldspat liegt bei knapp 3.8 Mol%, die Anorthitkomponente in Albit ist mit max. 0.3 Mol% sehr gering. Die Turmaline sind als Mischglieder der Schörl-Dravitreihe mit deutlicher Fe-Vormacht einzustufen [2].

Die Sulfidvererzungen in Arzberg sind Pb-dominiert (max. 36 %) sowie arm an Cu (< 0.2 %), Zn (< 1.5 %) und As (< 150 ppm). Au (< 620 ppb) und Ag (< 340 ppm) sind in den Paragenesestypen I bis III angereichert. Die Untergliederung in die Paragenesestypen I bis IV ist typisch für eine lateral und vertikal zonierte sedimentgebundene Sulfidlagerstätte mit $\text{Cu} \rightarrow \text{Zn} \rightarrow \text{Pb} (+\text{Ag}, \text{Au}) \rightarrow \text{Ba}$.

Pb-Isotopenmessungen ergeben ein $^{207}\text{Pb}-^{206}\text{Pb}$ Modellalter von 460 Mio. Jahren, und deuten somit auf altes kontinentales Krustenblei als Metallquelle hin. Die Schwefelisotope der konkordanten Sulfiderze weisen positive Werte zwischen +3 und +6 ‰ [PDB] auf. Pyrite aus den tuffitischen Nebengesteinen haben sehr leichten Schwefel (-9 ‰). Die S-Isotopie von Baryt (+16.9 ‰) stimmt gut mit unter- bis mitteldevonischem Meerwasser (+18 ‰) überein.

Quarz und Karbonat zeichnen sich durch vergleichbar schwere Sauerstoffisotopenverhältnisse von +18 bis +20 ‰ [SMOW] aus. Homogene Sauerstoff-Isotopendaten von Quarzen der verschiedenen Vererzungstypen, sowie Fraktionierungen zwischen Quarz, Chlorit und Magnetit deuten auf Äquilibrierung mit metamorphen Fluiden bei 400–500°C hin.

Temperaturabschätzungen mittels Chloritthermometrie ergeben 320 bis 360°C, und mittels Siderit-Ankerit-Paaren 350 bis 580°C für die metamorphe Überprägung von Mineralisation und Nebengesteinen. Die Phengitkomponente in Hellglimmern weist auf Minimaldrucke von 3.0–5.5 kbar hin, während das Zinkblendebarometer (Zinkblende in Paragenese mit Pyrit und Magnetkies) unrealistisch hohe Drucke liefert.

Das Projekt P12180-TEC wurde vom Fonds zur Förderung der wissenschaftlichen Forschung (FWF) unterstützt.

Literatur

- [1] WEBER, L. (1980): Die Blei-Zinkerzlagerstätten des Grazer Paläozoikums und ihr geologischer Rahmen. - Archiv für Lagerstättensforschung der Geologischen Bundesanstalt, 12, 289 Seiten.
- [2] FEICHTER, M. M., MOGESSIE, A., THALHAMMER O. A. R. & WEBER, L. (1998): Die Pb-Zn Lagerstätte Arzberg/Steiermark. - Mitteilungen der Österreichischen Mineralogischen Gesellschaft, 143, 271-272.

ZUR MINERALOGIE DES MAGNETIT-VORKOMMENS
WOLLANIG BEI VILLACH, KÄRNTEN

A. Ferenczi & M. A. Götzinger

Institut für Mineralogie und Kristallographie
Universität Wien, Geozentrum, Althanstrasse 14, A-1090 Wien, Austria

Obwohl die Magnetitvererzung Wollanig WNW Villach seit langer Zeit bekannt und Spuren bergmännischer Tätigkeit zu sehen sind (Pingen, Halden, Einbauten), liegen nur wenige Daten vor. Die geologischen Verhältnisse des Gebietes wurden von PLÖCHINGER (1953, 1980) und ANDERLE (1977) dargestellt.

Die Magnetitvererzung liegt an der SW-Flanke des Wollanig in ca. 800 m SH im (mittelostalpinen) Alt-kristallin. Dieses wird hier durch Zweiglimmer-Schiefergneise (Disthen, Staurolith) mit eingelagerten Amphiboliten und Marmoren gebildet. Die geologische Entwicklung ist durch einen sauren Magmatismus kaledonischen Alters (409 ± 32 Ma [3]) und einer mittelgradigen bis hochgradigen variszischen Metamorphose, gefolgt von einer schwachen, alpinen Diaphtorese (84 ± 3 Ma [3]) charakterisiert. Die Gesteine sind von mehreren kleinen Pegmatitkörpern durchschlagen. Diese sind auffällig mineralarm (K-Feldspat, Albit, Quarz, wenig Muskovit, Turmalin, Apatit, stellenweise Granat). Die Magnetit-Mineralisation steht mit Granat-amphiboliten in Zusammenhang. Nach [2] sind die Amphibolite (sowie Hornblendeschifer und Kalksilikatgesteine) an die Grenze zwischen Marmoren und Glimmergesteinen gebunden.

Im Bereich des Magnetitvorkommens treten gemäß eigener Begehung folgende Gesteine auf:

- 1) Amphibolite und Granatamphibolite mit Übergängen zu Granat-Biotit-Schiefern
- 2) Magnetit-Amphibolite (\pm Epidot)
- 3) Magnetit-Klinopyroxen-Epidot-Gesteine
- 4) Magnetit-Epidot-Andradit-Gesteine
- 5) Magnetit-Quarz-(\pm Epidot, Andradit)-Gesteine

Die Gesteine 2 bis 4 dürften das Bergbauinteresse geweckt haben, denn sie enthalten etwa 20 bis 40 Vol.% Magnetit.

1) Amphibolite und Granatamphibolite mit Übergängen zu Granat-Biotit-Schiefern

Diese relativ feinkörnigen Amphibolite (Korngr. um 1 mm) zeigen einerseits Schollen von Meta-Eklogiten und andererseits Übergänge zu Granat-Biotit-Schiefern. In diesen weisen die ca. 3 mm großen Granate sehr deutlichen Zonarbau auf (Angaben in Mol.%):

Kernbereich: Alm 71, Spess 2, Gross 15, Andr 12

Rand: Alm 60, Spess 13, Gross 15, Andr 12

Ilmenite haben ca. 2 Mol.% Pyrophanit-Komponente; Klinopyroxene sind teilweise in Amphibole umgewandelt.

2) Magnetit-Amphibolite (\pm Epidot)

Diese Gesteine sind deutlich kornvergröbert (4 bis 8 mm). Magnetit (reliktisch) enthält Entmischungslamellen von Hämatit-Ilmenit. Titanomagnetite zeigen schwankende Ti-Gehalte (bis

20 Gew.%) und konstanten Mn-Gehalt (2.5 Gew.%). Reine Magnetite sind selten. Ilmenite weisen schwankende Pyrophanit-Komponenten auf (2 bis 15 Mol.%).

Epidote besitzen fallweise Allanit-Kerne. Es gibt Übergänge zum Gestein 3.

3) Magnetit-Klinopyroxen-Epidot-Gesteine

Mit 2 bis 4 mm Korngröße der genannten Minerale zeigt der Klinopyroxen diopsidischer Zusammensetzung allerdings Auflösungsscheinungen zu einem sehr feinkörnigen Mineralgemenge. Teilweise gibt es Amphibol-Neusprossung, aber vor allem Epidot (ohne Allanit). In geringer Menge gibt es Titanomagnetit (bis 12 Gew.% Ti und 0.5 bis 1 Gew.% Mn). Dieser ist älter als der reine Magnetit, der hier mengenmäßig deutlich überwiegt.

4) Magnetit-Epidot-Andradit-Gesteine (\pm Calcit, Quarz)

In diesem "Kalksilikat"-Gestein (Korngröße 2 bis 10 mm) sind Neusprossungen auffällig: Der Magnetit ist \pm Ti-frei, enthält jedoch bis 15 Gew.% Mn. Um den Magnetit bildete sich häufig Epidot, der wieder an Granat grenzt. Es ist praktisch reiner Andradit mit einer Gitterkonstante von $12.016 \pm 0.003 \text{ \AA}$. Calcit, Plagioklas (Ab91), geringe Mengen Quarz und gelegentlich zerstzter Klinopyroxen runden das Bild ab. Dieses Gestein bildet den Übergang von 3 zu 5.

5) Magnetit-Quarz-(\pm Epidot, Andradit)-Gesteine

Mit einer Korngröße bis 15 mm (vor allem Magnetit) ist dieses Gestein das grobkörnigste und im Gelände besonders auffällig (schwarz-weiß). Nahezu reiner Magnetit (0.8 Gew.% Mn und 0.4 Gew.% Ti) bildet ovale, ellipsoidische Körner in der weißen Quarz-Matrix. In Schlieren und Bändern bzw. Lagen treten Andradit und Epidot auf (Gestein 4).

Auffällig in allen Gesteinen ist eine durchgehende, feinkörnige Apatit-Führung, wobei in 1 und 5 geringere Mengen zu finden sind, deutliche Anreicherungen hingegen in 2 bis 4. Es handelt sich um rundlichen, kurzprismatischen, flächenreichen Apatit. Dieser enthält häufig (reinen) Magnetit als tropfenförmige Einschlüsse und umgekehrt findet sich tropfenförmiger Apatit im Magnetit als Einschluß. Titanit kommt als Neusprossung nach Ti-reichem Magnetit und zersetzen Klinopyroxen vor.

Die Entstehung dieses Vorkommens ist noch unklar. Leider lassen die nunmehr schon sehr schlechten Aufschlußverhältnisse keine klaren Beobachtungen und Schlüsse zu. Einen möglichen Einfluß könnten die in dem Bereich häufigen Pegmatite gehabt haben: Temperaturerhöhung, Quarz-Zufuhr und das Fluidangebot. Mineralinhalt und der zonare Aufbau der Gesteine mit Übergangszonen vom Amphibolit bis zum Magnetit-Quarz-Gestein erwecken den Eindruck eines Reaktions-Skarnes. Mineralneusprossungen von Amphibol und Epidot liefern den Hinweis auf erhöhte Fluidaktivitäten.

Literatur

- [1] ANDERLE, N. (1977): Geologische Karte der Republik Österreich, Blatt 200 Arnoldstein, 1:50.000. - Geologische Bundesanstalt Wien.
- [2] PLÖCHINGER, B. (1953): Erläuterung zur geologischen Neuaufnahme des Draukristallinabschnittes westlich von Villach. - In: Küpper, H., Exner, Ch., Grubinger, H.: Skizzen zum Antlitz der Erde, Kober-Festband, Verlag Brüder Hollinek, Wien, 422 S., 193-206.
- [3] PLÖCHINGER, B. (1980): Das Altkristallin nordwestlich von Villach und im Klagenfurter Becken. - In: Der Geologische Aufbau Österreichs, R. Oberhauser (Red.), S 371-373, Geol. B.-A. Wien, Springer Wien.

CHARACTERIZATION OF REACTION TEXTURES IN SKARN NEAR REŠICE,
MOLDANUBICUM, WESTERN MORAVIA

J. Filip¹ & S. Houzar²

¹Institute of Geological Sciences
Masaryk University, Kotlářská 2, 611 37 Brno, Czech Republic

²Department of Mineralogy and Petrography
Moravian Museum, Zelný trh 6, 659 37 Brno, Czech Republic

The well-exposed skarn at Rešice near Moravský Krumlov (western Moravia) is situated in the Gföhl Unit within the Moldanubicum of Western Moravia. The skarn body ca 50 m thick with ENE-WSW direction, dips 60–70° to SSE. It forms lenses, divided into number of large blocks by near N-S trending faults, enclosed in felsic fine-grained Gföhl gneiss and partly in migmatized biotite paragneiss accompanied by granulites, serpentinites, eclogites, amphibolites, and rare by marbles. The contact with the host rocks is tectonic, some small boudins are enclosed in surrounding gneiss. The Rešice skarn underwent of complex metamorphic evolution [1], high-pressure regional metamorphism at T up to 850°C and P > 1.4 GPa (eclogite to granulite facies conditions) was followed by decompression and Variscan metamorphism under amphibolite facies. In the skarn body, iron calcic skarn predominates over magnesium- and very rare REE-skarn. The most frequent petrographic type is banded clinopyroxene (Hd₅₅₋₆₀) – garnet (Adr₂₅Alm₁₈-Grs₅₅Py₂) skarn gradating into either massive garnetite or clinopyroxene rocks. Scarce Cpx ± Grt ± Pl skarn, amphibole + Cpx skarn, Mg-skarn and very rare skarn with biotite and REE-mineralisations (allanite and secondary REE-fluorcarbonates) spatially associated with massive magnetite layer [2], also compose this skarn body, as well as many pegmatite dikes of different composition and origin. Feldspars-bearing calc-silicate rocks, skarnoids, and hornfelses are characteristic rocks near marginal skarn along the contact with Gföhl gneiss. Within this skarn iron-rich Grt and Cpx represent the oldest mineral association [1] whereas amphibole-bearing mineral assemblages are clearly younger. Many grains of garnet contain clouds of inclusions of minute minerals, for example sphene, clinopyroxene, and zircon.

Primary (pre-metamorphic) origin of skarn remains ambiguous: a hypothesis that it have been originally metasomatic Mg-(Ca-) skarn is more possible [3].

The Rešice skarn displays unique textures, which illustrate mainly the metamorphic multistage overprint. The following reaction textures in various skarn types have been distinguished:

- (i) Oriented Mg-hercynite ($X_{Fe} 65$) intergrowths within magnetite grains.
- (ii) Pyroxene – magnetite – ilmenite symplectite.
- (iii) Coronal textures around garnets – Grt \rightarrow Pl \rightarrow Mag \rightarrow Cpx \rightarrow Qtz.
- (iv) Amphibole ($X_{Fe} 80$) coronas around garnet ($X_{Fe} 90$) in pyroxene skarn ($X_{Fe} 55$).
- (v) Clinopyroxene ($X_{Fe} 55$) - plagioclase (An_{10-20}) ± potassium feldspar symplectites after garnets.

- (vi) Fine clinopyroxene-amphibole ± zoisite symplectites between magnetite and garnet.
- (vii) Poikiloblastic intergrowths of amphibole ($X_{Fe} \approx 55$) and plagioclase (An_{25}).

Well-developed transformation textures enable to understand the reaction mechanisms, diffusion processes and kinetics of the reactions. We assume that these textures can be rigorously explained only as the products of reaction in an open system (influx of Na and K and increased oxygen activity). Limited infiltration of external aqueous fluids significantly contributes to preservation of these textures during younger metamorphism of amphibolite facies. Only spatially restricted infiltration of H_2O (+ boron)-rich fluids in last stage of metamorphism exists and produces some amphibole-bearing skarns and alpine-like veins with amphibole, epidote and ferroaxinite [2]. In analogous skarns in Gföhl and various units of the Moldanubicum no similar reaction textures have been described. Only in the magnetite skarn of Kottaun (Moldanubicum, Lower Austria) Cpx-Mag symplectites (our (ii) type) was found which are considered to be pseudomorphs after ilvaite [4].

The research work was supported Research Project MKOCEZ 00F402.

References

- [1] PERTOLD, Z., PERTOLDOVÁ, J. & PUDILOVÁ, M. (1997): Metamorphic history of skarns in the Gföhl unit, Moldanubicum, Bohemian Massif, and implications for their origin. - Acta Universitatis Carolinae -geologica, 41, 3-4, 157-166.
- [2] FILIP, J., HOUZAR, S. & SULOVSKÝ, P. (2002): Allanite and its alteration products from pegmatite and skarn near Rešice, Western Moravia, Czech Republic. - Acta Musei Moraviae, Sci. geol., 87, 87-101. (in Czech with English summary).
- [3] NEMEC, D. (1991): Regional typization of the iron skarns of the Bohemian-Moravian Heights (Českomoravská vrchovina). - Acta Musei Moraviae, Sci. nat., 76, 51-82.
- [4] GÖTZINGER, A. M. (1981): Mineralogische Untersuchungen des Magnetitvorkommens Kottaun bei Geras, niederösterreichisches Moldanubikum. Ein Beitrag zur Genese von Skarnen. - Sitzungsber. Österr. Akad. Wiss., Mathem.-naturw. Kl., Abt. I, 190/4, 45-78.

**A RECORD OF DEVONIAN HIGH-GRADE METAMORPHISM
IN THE CENTRAL HOHE TAUERN ?**

F. Finger & A. Bankhammer

Institut für Mineralogie
Universität Salzburg, Hellbrunnerstrasse 34, A-5020 Salzburg, Austria

We have studied muscovite gneisses which occur as intercalations within the amphibolites of the Zwölferzug formation, between the Felbertal and the Stubachtal. Such rocks have been mapped as "Muskowitaugengneis" by [1] and [2], while [3] introduced the name muscovite-plagioclase gneisses. Based on zircon typology investigations, [3] considered the gneisses as the metamorphosed products of highly fractionated granitoids. [4] presented concordant SHRIMP zircon ages of 374 ± 10 Ma for one sample, described as a high- to medium-K, I-type granodiorite. They interpreted the dated rock as a potentially subduction related, early-Variscan I-type granitoid. On the other hand, it seems clear that the rocks must have experienced a strong, probably Variscan, high-grade metamorphic overprint, like their amphibolitic host rocks. [1] described a pre-Alpine metamorphic paragenesis with plagioclase, K-feldspar, garnet and coarse muscovite. Relics of garnets, although mostly totally transformed into chlorite, could often be observed also in our samples.

We have analysed twenty samples of these gneisses by XRF methods. Major element compositions are intermediate to felsic (SiO_2 60–70 wt.%, $\text{Fe}_2\text{O}_{3\text{tot}}$ 5–7 wt.%, MgO 2–3 wt.%) and broadly granodioritic (K_2O 1–3 wt.%, Na_2O around 3 wt.%). However, when compared to other Variscan I-type granodiorites (e.g. [5, 6, 7]), the CaO contents are remarkably low (often below 1 wt.%). Furthermore, the gneisses have unusually high A/CNK ratios (often > 1.8 !). Clearly, the rocks do not show a typical granitoid major element composition, and are either no magmatic rocks at all (metasediments ?), or were affected by severe chemical alteration. If the latter was the case, then the major phase of chemical alteration must have occurred prior to the Alpine orogeny, because the preserved pre-Alpine mineral paragenesis with many big muscovites is already indicative of a strongly peraluminous rock composition.

The trace element spectrum of the rocks is characterised by high Cr (100–200 ppm) and high Ni contents (30–60 ppm), low Rb (< 50–100 ppm) at moderate Sr contents (100–200 ppm), and high Ba (500–1000 ppm). These trace element patterns would rather fit to a paragneiss than a felsic granitic rock (see e.g. [8]). LREE concentrations are 30–100 times enriched relative to chondrite, the HREE and Y are less enriched (Y_N 10–20). Nb varies between 10 and 15 ppm, Zr between 150 and 200 ppm.

Interestingly, several of the gneisses contain big accessory monazite. A pre-Alpine generation of monazite shows secondary coronas consisting of apatite, allanite and epidote [9], a younger generation of small monazites grew during the Alpine metamorphic overprint. Chemical dating by means of the electron microprobe yielded a weighted average age of 373 ± 15 Ma (95 % CL) for the older monazite generation (Fig. 1).

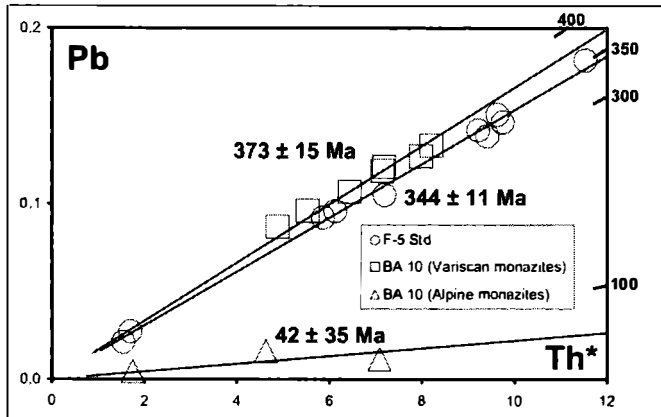


Fig. 1

Total Pb vs. Th* isochron diagram after [12] using the values listed in Tab. 1. Time scale shown is based on the position of zero-intercept isochrons. Drawn isochrons refer to the calculated weighted average ages for the two monazite age groups in sample BA 10 and the monazite standard F5 (recommended age 341 ± 2 Ma).

	La_2O_3	Nd_2O_3	Y_2O_3	Th	U	Pb	Th*	Age
1	12,63	10,87	0,60	4,306	0,100	0,016	4,627	78 ± 117
2	14,42	11,24	0,67	1,454	0,093	0,005	1,751	59 ± 155
3	12,26	10,53	1,11	6,587	0,156	0,012	7,084	37 ± 38
4	13,07	12,84	0,04	2,953	0,789	0,096	5,530	390 ± 49
5	12,94	12,91	0,02	3,304	0,959	0,107	6,431	373 ± 42
6	12,78	12,33	0,04	4,163	1,171	0,127	7,978	358 ± 34
7	12,86	12,61	0,01	4,058	0,957	0,121	7,181	378 ± 37
8	12,99	12,68	0,05	4,403	1,165	0,133	8,203	365 ± 33
9	12,99	13,10	0,02	3,826	1,018	0,119	7,148	373 ± 38
10	13,53	13,23	0,05	2,673	0,675	0,087	4,879	400 ± 55

Tab. 1

Chemical characteristics (wt.%) and Th-U-Pb model ages of monazites from sample BA 10. Errors on the age are 2σ . Th* values calculated after [12]. Note the extremely low Y_2O_3 contents of the Variscan monazites and the systematically higher Y contents and Th/U ratios (low U) of the Alpine monazites (analyses 1-3).

This age is practically identical to the zircon age published by [4] for another sample of this gneiss unit. However, since their yttrium contents were always extremely low (Tab. 1), we believe that the c. 370 Ma old monazite relics grew in paragenesis with garnet and, therefore, probably date an early Variscan high-grade metamorphic event. Alternatively, if the monazites are magmatic and their host rock granitic with a c. 370 Ma intrusion age, then this granite should have had an unusual mineralogy involving considerable amounts of magmatic or restitic garnet. Zircons separated from the same sample (BA 10) are rounded and do not look like granite-zircons. They may eventually be detrital in origin. However, zircons from granulitic rocks often show such morphological features as well [10]. Therefore, it is also at issue whether the zircon age published by [4] perhaps dates an early-Variscan, high-grade, possibly even granulite-facies metamorphic event in the Zwölferzug.

Likewise it should be checked, if some of the Devonian/Early Carboniferous zircon ages recently reported from basement units of the central Hohe Tauern [11] could not be interpreted as metamorphic ages as well. Furthermore, we need to investigate, if there is evidence of a (second?) phase of Variscan metamorphism in the Zwölferzug formation or other parts of the Stubach complex posterior to 370 Ma, i.e. in the Carboniferous, as may be indicated by c. 320 Ma K-Ar ages of amphiboles [1].

References

- [1] PESTAL, G. (1983): Ph.D. thesis, Vienna University, 117 pages.
- [2] FRANK, W. ET AL. (1987): Geologische Karte der Republik Österreich, Blatt 152, Geol. B.-A. Wien.
- [3] LOTH, G. & HÖLL, R. (1994): In: Seltmann et al. (eds) Metallogenesis of Collisional Orogens, Prague, 357-363.
- [4] EICHHORN, R. ET AL. (2001): Contrib. Mineral. Petrol. 139, 418-435.
- [5] FRASL, G. & FINGER, F. (1988): Schweiz. Mineral. Petrogr. Mitt. 68, 433-439.
- [6] FINGER, F. ET AL. (1993): in Neubauer F. & von Raumer J.: Springer Verlag, p. 375-391.
- [7] JANOUŠEK, V. ET AL. (2000): J. Petrol. 41, 511-543.
- [8] LINNER, M. (1996): Miner. Petrol. 58, 215-234.
- [9] FINGER, F. ET AL. (1998): American Mineralogist 83, 248-258.
- [10] HOPPE, G. (1966): Berichte deutsch. Ges. geol. Wiss., B, Miner. Lagerstättenf. 11, 47-81.
- [11] KEBEDE, T. KLÖTZLI, U. S. & PESTAL G. (2003): Mitt. Österr. Mineral. Ges. 148.
- [12] SUZUKI ET AL. (1991): Sediment. Geol. 75, 141-147.

**GENETISCHE PROBLEME DER GEBÄNDERTEN EISENERZLAGERSTÄTTEN:
EIN BEISPIEL AUS DER TSCHECHISCHEN REPUBLIK**

B. Fojt

Institut für Geowissenschaften
Masaryk-Universität, Kotlářská 2, CZ-61137 Brno, Czech Republic

Die gebänderten Eisenformationen gehören zu den größten Lagerstätten der Welt. Auch in dem Gebiet der Tschechischen Republik sind diese Erzvorkommen verbreitet, allerdings in viel kleinerem Maßstab. Die gebänderte/geschichtete Assoziation einiger kleiner Erz-Lokalitäten, die bis 1865 abgebaut wurden, befinden sich im Gebiet des Jesenky Gebirges (Altvatergebirges). 12 Erzlager sind in den Biotit/Chlorit-Gneisen der Desná-Einheit (Desná-Gewölbe) eingelagert. Das Alter der prograden Metamorphose der Gneise im Rahmen der Amphibolit-Fazies [1] wurde mit 570–650 Ma errechnet [4]. Diese führte an manchen Stellen nicht nur zu einer Rekristallisation des Gestein- und Erzgefüges, sondern auch zu einem partialen begrenzten Schmelzprozeß und der Neuentstehung granodioritähnlicher Matrix. Vor 340 bis 300 Ma [5] wurden die Gesteine durch eine retrograde Metamorphose, die Grünschieferfazies erreichte, überprägt. Auch in der "höheren devonischen Etage" gibt es mehr als 20 kleine stratiforme (gebänderte) Eisenerz-lagerstätten, deren geologische, mineralogische, texturelle und chemische Daten den SEDEX - Lagerstätten vom Lahn-Dill-Typus entsprechen.

Die oben erwähnten präkambrischen linsenförmigen Erz-Körper bilden zwei subparallele Streifen in der Nachbarschaft der Amphibolit-Ausläufer des Sobotín-Amphibolit-Massivs und sind mehr als 10 km lang. Die Mächtigkeit einzelner Lager variiert von 0.3 bis 3.6 m. Die Eisengehalte bewegen sich von 24 bis zu 52 Gew.%. Die gebänderte Textur des Erzes besteht hauptsächlich aus granoblastischen Individuen von Magnetit und Quarz. Sehr selten findet man massive Magnetit-Texturen. Als Nebenbestandminerale sind Chlorit/Biotit oder Amphibol, Apatit, weniger schon Calcit, Epidot, Albit, sehr selten auch Ilmenit vorhanden. Getrennt von den Magnetit-Streifen befinden sich an einigen Lokalitäten Granat-Aggregate und Pyrit-Bänder.

Eine historische Übersicht der genetischen Ansichten kann in drei Gruppen zusammengefaßt werden: 1) die ältesten [3] hielten die Magnetit-Anhäufungen für magmatogene Segregate der Metabasite 2) in der zweiten Hälfte des vergangenen Jahrhunderts haben die Forscher [8] diese Erze zu den sedimentären, oder sedimentär-exhalativen (BIF) Lagerstätten gezählt 3) zuletzt haben die Autoren [6, 7] mehrmals die Idee des sogenannten "Filter-Pressing-Prozesses" der Basite bei der Entstehung der Magnetite geäußert. Die Quarz-Aggregate wurden bei dieser Deutung als jüngere (metamorphogene) Silizifizierungs-Phase und die Granat-Assoziation als vulkano-sedimentäre Gondite betrachtet. Wesentlich dabei ist die neuere Diskussion und Ergänzung dieser Meinung [3].

Wichtige Aspekte zur Lösung der genetischen Aspekte:

- a) Beziehung zwischen Erz und Quarz: Beide Komponenten des gebänderten Erzgefüges und die Nebengesteine (Gneise) zeigen die gleichen Rekristallisationserscheinungen. Die räumliche Koexistenz beider Mineralien in den Erzlagern, obwohl nicht in der Form von Magnetit und Quarz, entspricht dem ursprünglichen protolithischen Bild - vergleichbar mit den jüngeren devonischen Eisenerzlagerstätten des Altvatergebirges.
- b) Beziehungen zwischen Erz, Granat- und Pyrit-Aggregaten: Almandin-Spessartite und Pyrite im Hangenden der vererzten Zonen haben ihren Platz außerhalb der Magnetit-Bänder – wieder ganz ähnlich wie bei einigen Eisenerzlagerstätten im silesischen Devon. Die Spurengehalte von Nickel und Kobalt der Pyrite und Magnetite zeigen im Diagramm Ni/Co denselben Trend mit fast ähnlichen Regressions-Gleichungen und Regressionsfaktoren. Die Isotopen-Zusammensetzung des Pyritschwefels weist auf einen Schwefel biogen-sedimentären Ursprungs ($\delta^{34}\text{S} = 10$ bis -35 ‰ CDT) hin.
- c) Pauschalchemismus der Erze und Nachbargesteine: Die Ergebnisse der Erzanalysen im Diagramm von KLEIN & BEUKES [2] unterstreichen einen engen Zusammenhang mit der proterozoischen "iron formation". Der Chemismus der Gneise aus der unmittelbaren Umgebung der Erz-Lager weist auf einen Grauwacken-Protolithen hin. Die erhöhte magnetische Suszeptibilität ist wahrscheinlich mit dem vulkano-pyroblastischen Anteil der ursprünglichen Fels-Matrix verbunden.
- d) Chemismus der Mineralien des Erzgefüges: Es gibt keine Unterschiede zwischen den Chloriten und Biotiten der Gneise und der Erz-Bänder. Beide sind typische Mg>Fe Glieder. In den Gneisen sind nur untergeordnet akzessorische Amphibole (Aktinolithe) vertreten. In dem Erz treten alterierend Amphibole ($X_{\text{Mg}} = 0.74\text{--}0.91$) und Biotite auf. Die Apatite im Gestein und Erz sind Fluor-Apatite (bis 3.8 % F). Die Menge des Apatits im Erz ist an manchen Stellen einiger Lokalitäten ziemlich hoch (bis 12 % in einigen Proben). Ilmenit ist im Gneis mehr vertreten, als im Erz. Die Gehalte der Pyrophanit-Komponente in den Ilmeniten variieren sehr deutlich – auch an einer und derselben Lokation.

Es ist somit eindeutig, daß die Erze und Nebengesteine von derselben Metamorphose überprägt wurden. Bei der mehrphasigen metamorphen Differentiation, Rekristallisation und Mobilisation haben sich die Mineralbestandteile des Erzgefüges geändert – wahrscheinlich auch konform mit dem Gesteinsmilieu.

Alle weiter oben angeführten Argumente sprechen für eine vulkanosedimentäre Genese der Vererzung während des Proterozoikums und können im Sinne von [9] als "Meta-Exhaliten" bezeichnet werden.

Literatur

- [1] FEDIUKOVÁ, E., FIŠERA, M., CHÁB, J., KOPEČNÝ, V., OPLETAL, M. & RYBKA, R. (1985): Garnets of the predevonian rocks in the eastern part of the Hrubý Jeseník Mts (North Moravia, Czechoslovakia). - Acta Univ. Carol., 3, 197-234. Praha.
- [2] KLEIN, C. & BEUKES, N. J. (1993): Proterozoic iron-formations. - In: Condé, K. C., ed.: Proterozoic crustal evolution, 10, 383-418. Elsevier, Amsterdam.

- [3] KRETSCHMER, F. (1911): Das metamorphe Diorit- und Gabbromassiv in der Umgebung von Zöptau (Mähren). - Jahrbuch Geol. Reichsanst., 61, 53-179. Wien.
- [4] KRÖNER, A., ŠTIPSKA, P., SCHULMANN, K. & JÄCKEL, P. (2000): Variscan evolution of the northeastern margin of the Bohemian Massif, Czech Republic. - Journ. Geol. Soc., spec. publ., 179, 175-197. London.
- [5] MALUSKI, H., RAJLICH, P. & SOUČEK, J. (1995): Pre-Variscan, Variscan and Early-Alpine thermo-tectonic history of the north-eastern Bohemian Massif: An $^{40}\text{Ar}/^{39}\text{Ar}$ study. - Geol. Rundschau, 84, 345-358. Stuttgart.
- [6] MÜCKE, A. & FARHAD, F. (2001): Whole-rock compositions of Precambrian iron formations and Phanerozoic ooidal ironstones: Comparative considerations and mineralogical differentiation of subtypes. - In: Piestrzyński et al., eds.: Mineral deposits at the Beginning of the 21st Century., 971-974. Kraków.
- [7] MÜCKE, A. & LOSOS, Z. (2000): Polymetamorphic overprinted and silicified magnetite ores from the Desná gneisses (Silesicum, Czech Republic). - Acta Mus. Moraviae, Sci. Geol., 85, 47-80. Brno.
- [8] POUBA, Z. (1970): Pre-Cambrian banded magnetite ores of the Desná Dome. - Sbor. Geol. věd, LG, 12, 7-64. Praha.
- [9] SPRY, P. G., PETER, J. M. & SLACK, J. F. (1997): Meta-Exhalites as Exploration Guides to Ore. - Geological Survey of Canada, Contribution no. 1997162.

**PRECAMBRIAN GOLD EXPLORATION:
NEW PARADIGMS, SOUND SCIENCE AND GEOPOLITICAL CONSTRAINTS**

B. Foster

Exploration Consultants Limited
Henley on Thames, UK

Precambrian shield areas of the world are extremely important sources of gold, copper and zinc (volcanic-hosted massive sulphide deposits), chrome, nickel +/- PGE's (orthomagmatic deposits), and iron (sedimentary deposits). Most of the deposits yielding these metals were developed during the intrusive and volcano-sedimentary activities and subsequent orogenic events that contributed to crustal growth and stabilization of the cratonic. Foremost amongst these is gold, the search for which led to (and is still leading to) opening up of some of the most inaccessible parts of the world. With its relatively low exploration costs and often low capitalization requirements, especially where exploited by open pit methods, gold remains a key focus for exploration in these ancient geological terranes. Add to this the high gold price of mid-2003, which is probably sustainable for at least the coming year or two, and it is very likely that the cratonic regions of the world are likely to experience even greater levels of exploration activity in the near future.

Historically and today the major gold-yielding cratons of Archaean age have proved to be: the Superior and Slave of Canada; the Sao Francisco and Amazonian of Brazil; the Kola-Karelian of Fennoscandia; the West African craton extending from Mauritania east and south, under cover sequences, to Niger and Sierra Leone; the Kalahari (Zimbabwe and Kaapvaal) of Southern Africa; the Tanzania craton; the Dharwar of southern India; and the Yilgarn craton of western Australia. An early Proterozoic example of an accretionary orogen that has, since c. 2.0 Ga, behaved as a stable block is the Birimian terrane underlying much of Côte d'Ivoire, western Ghana, southern Niger, and western Mali. The latter is an important host to significant gold deposits including Ashanti/Obuasi, Prestea, Sadiola, and Morila.

Gold deposits exploited in these cratonic regions are dominated by fault- and shear-zone-hosted mesothermal deposits generated during compressional tectonism, but also include possible porphyry-style deposits (e.g. Boddington in the Yilgarn craton) and gold-rich volcanic-hosted massive sulphide deposits (e.g. Horne and Bousquet in the Superior craton). The giant deposits of the Witwatersrand Basin are also of early Precambrian age, with the host sediments deposited c. 2.9–2.7 Ga in an active orogenic foreland environment. The origin of the gold in the Witwatersrand conglomerate units is still hotly debated but there is considerable evidence of widespread migration of aqueous and hydrocarbon fluids throughout the West and Central Rand sequences, indicating an important role for hydrothermal processes.

Increasingly, late Precambrian terranes are also being recognized as targets for gold exploration, the Pan-African terranes of Central and Northern Africa being potentially important examples. Significant gold discoveries in the Hoggar Block of southern Algeria, in particular, highlight exploration opportunities in what is probably the largest consolidated accretionary arc terrane in the world, extending 3,500 km from the eastern margin of the West African Craton to the Red Sea, where gold deposits in eastern Sudan and Egypt have also been exploited.

Within the past decade explorationists have targeted the Pan-African terranes of Central Africa in the search for potentially giant iron oxide-copper-gold (IOCG) deposits, reportedly with some degree of success. No doubt, it is timely and appropriate to consider the potential for the discovery of such deposit-types in early- and mid-Proterozoic terranes and perhaps extending as far back as the late-Archaean.

The abundance, grade-tonnage profiles, and economics of deposits in various cratons and geographic regions differ considerably and a full understanding of the underlying reasons for these variations is critical to the development of future exploration strategies. The Superior, Kalahari, and Yilgarn cratons appear to be particularly well-endowed both with major gold deposits -

Deposit	Craton	Gold resource (t)
Kalgoorlie	Yilgarn	1389
Ashanti	Birimian (Ghana)	710
Fazenda Brazileiro	Sao Francisco	600
Hemlo	Superior	597
Morro Velho	Sao Francisco	480
Kerr Addison	Superior	324
Campbell	Slave	311
Bulyanhulu	Tanzania	310
Lamaque-Sigma	Superior	258
Giant-Lolor	Slave	225
Prestea	Birimian (Ghana)	219
Barnat - Canada - East	Superior	165
Con - Rycon - Negus	Slave	164
Norseman	Yilgarn	150
Cam and Motor	Kalahari (Zimbabwe)	146
Pamour - Hainor	Superior	145
Ankerite - Aurnor - Delnrite	Superior	143
Sheba - Fairview	Kalahari (Kaapvaal)	126
Globe and Phoenix	Kalahari (Zimbabwe)	120
Sons of Gwalia	Yilgarn	105
Boddington	Yilgarn	104
Mt. Charlotte	Yilgarn	103

(Table 1) and with a spectrum of small- to medium-sized deposits that suggest geologically favourable conditions for gold metallogenesis and thus ostensibly offer greater opportunities for brownsite and greenfields exploration.

Table 1
Larger craton-hosted mesothermal gold deposits.

However, in addition to a scientifically sound knowledge of the metallogenic potential of a cratonic terrane, today's exploration strategies have also to be underpinned by an appreciation of all pertinent political, legal, and fiscal factors ("sovereign risk") and (critically) by an awareness of dollars likely to be expended for each ounce of gold discovered and produced. It has also to be recognized that the metallogenic "favourability" of a terrane based on past discoveries and mining activities (the empirical approach) may be influenced by historical decisions whether or not to explore that are no longer pertinent today. Equally, major companies are now commonly looking to "purchase" gold via direct buy-ins to discoveries and also via company takeovers or mergers, the latter having been a common phenomenon in the gold sector within the past five years.

These factors are briefly reviewed in the context of the major cratons to provide a framework to justify future exploration decisions.

**BAUMATERIALKARTIERUNG DER GOTISCHEN KAPELLE,
BURGRUINE KROPFSBERG, TIROL**

C. Franzen, M. Unterwurzacher, A. Diekamp & P. W. Mirwald

Institut für Mineralogie und Petrographie
Universität Innsbruck, Innrain 52, A-6020 Innsbruck, Austria

Die Aufnahme von Baumaterial ist eine notwendige Grundlage für Restaurierungsarbeiten und stellt einen wichtigen Teilbereich der wissenschaftlichen Dokumentationsuntersuchungen dar. Die Ruine Kropfsberg bei Reith im Alpbachtal befindet sich auf der östlichen Seite des Ausganges des Zillertales auf einem Härtling im Inntal, der aus Schwazer Dolomit aufgebaut ist. Die Burgenanlage stammt zu wesentlichen Teilen aus dem 13. Jahrhundert und wurde bis ins 17. Jahrhundert ausgebaut. Der innere Teil des Komplexes wird von einer Ringmauer umgeben. Reste eines Palasbereiches sowie einer gotische Kapelle sind erhalten. Die Erhaltung der Ruine stellt vielfältige denkmalpflegerische Anforderungen. Nach einer früheren Maßnahme am Palaskomplex [1] wurde nun mit einer Gesteinskartierung die Erhaltungskampagne auf die Kapelle ausgedehnt.

Kartierungsunterlagen bildeten orthographische entzerrte Fotos in digitaler Form, die es erlauben, die Ergebnisse der Geländeaufnahme auf den Rechner zu übertragen. Die untersuchten Mauerwerke enthalten zahlreiche verschiedene Gesteinstypen (Alpiner Buntsandstein, drei Karbonate (Kalke und Dolomite), quartärer Quelltuff, Gneis, Amphibolit sowie zwei Ziegelarten). Die Gesteinspalette spiegelt einen guten Teil der regionalen Geologie wider. Die Baugesteine wurden aus dem fluviatilen Geröll gesammelt oder lokal gebrochen. Die Geröllsteine, die insbesondere in der Ringmauer Verwendung fanden, stammen aus den quartären Alluvionen des Inn. Ausgewählte Putz- und Fugenmörtel wurden hinsichtlich Struktur und Zusammensetzung untersucht. Die Ergebnisse aus der Gesteinsaufnahme sowie der Mörteluntersuchungen dienen zur Korrelation mit den bauhistorischen Befunden und bilden eine Entscheidungshilfe im weiteren Umgang mit der historischen Bausubstanz. So belegen erste Ergebnisse an verschiedenen Stellen einen klaren Zusammenhang zwischen der Verwendung von bestimmtem Baumaterial zu einzelnen Bauphasen.

Insgesamt kann gesagt werden, dass die unterschiedlichen Bauzeiten sich in verschiedenen Mauerwerkstechniken und in der Materialverwendung widerspiegeln. Zum Beispiel kann der dunkelrote Buntsandstein als Werkstein insbesondere im unteren Teil der Ringmauer, die sonst zum größten Teil als Rollsteinmauerwerk ausgeführt ist, angetroffen werden. Quelltuff wurde überwiegend als Architekturmateriale für die Gliederungselemente in den gotischen Bruchsteinmauerwerksteilen verwendet.

[1] HAUSER, W. & MIRWALD, P. W. (1996), Material- und Bauhistorische Analyse als Grundlage zur Entwicklung des Konservierungskonzeptes (Burgruine Kropfsberg/Tirol. - Restauratorenblätter Bd. 17, 20 Jahre Stein-konservierung 1976-1996, Bilanz und Perspektiven, S.73-78.

BULK MODULI AND PHASE TRANSITIONS OF CARBIDONITRIDOSILICATES
AND OXONITRIDOSILICATES AT HIGH PRESSURES UP TO 36 GPa

A. Friedrich¹, K. Knorr², A. Lieb³, H. A. Höppe³, B. Winkler¹, W. Schnick³ & M. Hanfland⁴

¹Institut für Mineralogie, Abteilung Kristallographie

Johann Wolfgang Goethe-Univ., Senckenberganlage 30, D-60054 Frankfurt a. M., Germany

²Institut für Geowissenschaften

Christian-Albrechts-Universität, Olsenhausenstrasse 40, D-24098 Kiel, Germany

³Department Chemie

Ludwig-Maximilians-Universität, Butenandtstrasse 5-13/D, D-81377 München, Germany

⁴European Synchrotron Radiation Facility (ESRF)

B.P. 220, F-38043 Grenoble, France

A new exciting field in material science was opened by the systematic investigation of nitridosilicates [1-3]. Nitridosilicates and oxonitridosilicates can be formally derived from oxosilicates by a total or partial exchange of nitrogen for oxygen. All of them are synthesised by high-temperature reactions and mainly form condensed three-dimensional networks. The exceptional thermal and chemical stability combined with high performance mechanical properties (hardness and strength) make these compounds very interesting for the materials science community. The replacement of oxygen by the more covalently behaving nitrogen extends the structural possibilities significantly. New structural features appear which are not known in oxosilicate chemistry. For example, nitridosilicates with star-like units $[N^{[4]}(SiN_3^{[2]})_4]$ of four SiN_4 -tetrahedra, which share a common corner, were recently found for the first time [4-6]. A further extension of the nitridosilicates can be found by a formal exchange of the central nitrogen of the $[N^{[4]}(SiN_3^{[2]})_4]$ unit by carbon in carbidonitridosilicates [7]. Nitridosilicates allow a long range of cation- and anion-substitution mechanisms leading to a variation of their physical properties. We have begun to study the influence of substitution effects on the properties of these materials by *in situ* high-pressure X-ray diffraction as well as ab initio computations.

In situ high-pressure powder diffraction experiments up to pressures of 36 GPa were performed at beamline ID09 of the ESRF. The samples were loaded into diamond anvil cells using liquid neon as a pressure-transmitting medium. Pressures were determined by means of the laser-induced ruby fluorescence method. Full powder diffraction rings were recorded on a MAR345 image plate system using a wavelength of 0.4138 Å. The images were processed and integrated with FIT2D [8]. LeBail refinements were carried out with GSAS [9].

Carbidonitridosilicates: $Ln^{III}2[Si_4N_6C]$ ($Ln = Ho, Er$)

In the $Ln_2[Si_4N_6C]$ compounds [7], the carbon atom is negatively polarised. It connects four Si tetrahedra-centres to form a star-like unit $[C^{[4]}(SiN_3^{[2]})_4]$. $Ho_2[Si_4N_6C]$ [$P2_1/c$, $a = 5.931(1)$, $b = 9.900(1)$, $c = 11.877(3)$ Å, $\beta = 119.69(1)^\circ$, $V = 605.74(5)$ Å³] and isotropic $Er_2[Si_4N_6C]$ [$V = 602.70(5)$ Å³] were both investigated up to pressures of 36 and 21 GPa, respectively.

Both compounds show a similar compressional behaviour. Hence, the substitution of lanthanides, such as Ho and Er, seems to have no significant influence on the high-pressure properties. A third-order Birch-Murnaghan equation of state was fitted to the P-V data of $\text{Ho}_2[\text{Si}_4\text{N}_6\text{C}]$ between 0.0001 and 36 GPa. The values obtained for the isothermal bulk modulus and its pressure derivative are $B_0 = 159(3)$ GPa and $B' = 5.6(2)$. The bulk modulus is higher if compared to the computed bulk moduli of other nitridosilicates, such as $\text{SrSiAl}_2\text{O}_3\text{N}_2$ with $B_0 = 131.9(3)$ GPa, and $\text{Ce}_4[\text{Si}_4\text{O}_4\text{N}_6]\text{O}$ with $B_0 = 131(2)$ GPa and $B' = 5.0(2)$ [10]. The more covalent character of the Si-C bond compared with the Si-N bond might have an influence on the improved hardness and structural high-pressure stability of these compounds. The axial compressibilities show anisotropic behaviour with the b axis being most compressible. Quantum-mechanical DFT-based computations of the high-pressure properties of $\text{Y}_2[\text{Si}_4\text{N}_6\text{C}]$ are on-going and will be compared to the experimental results, allowing a further evaluation of the influence of lanthanide substitution.

Oxonitridosilicates (Sions):

With $\text{Ce}_4[\text{Si}_4\text{O}_4\text{N}_6]\text{O}$ (space group $P2_13$) a novel layer structure type was found [11]. The topology of the layer is hyperbolically corrugated, which can explain the unprecedented cubic symmetry for a layer silicate. The layer is built up by three-membered rings of corner-sharing SiON_3 tetrahedra, cross-linked through additional SiON_3 tetrahedra. While such small rings are not favoured in oxosilicates due to the electrostatic repulsion of SiO_4 tetrahedra, they are frequently found in less ionic nitridosilicates. Quantum-mechanical DFT-based computations at high pressures revealed a bulk modulus of $B_0 = 131(2)$ GPa for $\text{Ce}_4[\text{Si}_4\text{O}_4\text{N}_6]\text{O}$ [10]. However, when calculating the elastic constants of $\text{Ce}_4[\text{Si}_4\text{O}_4\text{N}_6]\text{O}$ by imposing finite strains, very large errors for the bulk modulus [$B_0 = 155(23)$ GPa] indicated structural instabilities and a possible phase transition at high pressures up to 18 GPa. Our experiments up to 28 GPa confirmed the proposed instability of this structure type. We detected a first-order phase transition occurring in a range between 8 and 10 GPa. This phase transition is reversible and shows a slight hysteresis. The space group symmetry is reduced to $P2_12_12_1$ following a group-subgroup relationship, which indicates a displacive structural mechanism.

The authors gratefully acknowledge financial support from the Deutsche Forschungsgemeinschaft (DFG) through a Research Fellowship (WI 1232/17-1) within the project SPP-1136. Thanks are due to the ESRF for synchrotron beam time.

Literature

- [1] SCHNICK, W. & HUPPERTZ, H. (1997): Nitridosilicates - a Significant Extension of Silicate Chemistry. - *Chem. Eur. J.*, 3, 679-683.
- [2] SCHNICK, W., HUPPERTZ, H. & LAUTERBACH, R. (1999): High-Temperature Syntheses of Novel Nitrido- and Oxonitridosilicates and Sialons Using RF Furnaces. - *J. Mater. Chem.*, 9, 289-296.
- [3] SCHNICK, W. (2001): Nitridosilicates, Oxonitridosilicates (Sions), and Oxonitridoaluminosilicates (Sialons) – New Materials with Promising Properties. - *Int. J. Inorg. Mater.*, 3, 1267.

- [4] HUPPERTZ, H. & SCHNICK, W. (1996): BaYbSi₄N₇ - überraschende strukturelle Möglichkeiten in Nitridosilicaten. - *Angew. Chem.*, 108, 2115; *Angew. Chem. Int. Ed. Engl.*, 35, 1983.
- [5] HUPPERTZ, H. & SCHNICK, W. (1997): Synthese, Kristallstruktur und Eigenschaften der Nitridosilicate SrYbSi₄N₇ und BaYbSi₄N₇. - *Z. Anorg. Allg. Chem.*, 623, 212.
- [6] HUPPERTZ, H. & SCHNICK, W. (1997): Eu₂Si₅N₈ and EuYbSi₄N₇ - The First Nitridosilicates with a divalent Rare Earth. - *Acta Crystallogr. Sect. C*, 53, 1751.
- [7] HÖPPE, H. A., KOTZYBA, G., PÖTTGEN, R. & SCHNICK, W. (2001): High-temperature synthesis, crystal structure, optical properties, and magnetism of the carbidonitridosilicates Ho₂[Si₄N₆C] and Tb₂[Si₄N₆C]. - *J. Mater. Chem.*, 11, 3300-3306.
- [8] HAMMERSLEY, A. (1998): FIT2D, Version 10.27, Reference Manual, ESRF, Grenoble, France.
- [9] LARSON, A. C. & VON DREELE, R. B. (1994): Los Alamos National Laboratory Report LAUR, 86-748.
- [10] WINKLER, B., HYTHA, M., HANTSCH, U. & MILMAN, V. (2001): Theoretical study of the structures and properties of SrSiAl₂O₃N₂ and Ce₄[Si₄O₄N₆]O. - *Chemical Physics Letters*, 343, 622-626.
- [11] IRRAN, E., KÖLLISCH, K., LEONI, S., NESPER, R., HENRY, P. F., WELLER, M. T. & SCHNICK, W. (2000): Ce₄[Si₄O₄N₆]O – a Hyperbolically Layered Oxonitridosilicate Oxide with an Ordered Distribution of Oxygen and Nitrogen. - *Chem. Eur. J.*, 6, 2714-2720.

P-T METAMORPHIC PATH OF GARNET-KYANITE-BEARING SCHISTS:
CHEPELARE FORMATION, CENTRAL RHODOPE, BULGARIA

M. Georgieva^{1,2}, A. Mogessie², C. Hauzenberger², A. Proyer² & Z. Cherneva¹

¹Geological Institute

Bulgarian Academy of Sciences, Acad. G. Bontchev Str., bl. 24, 1113 Sofia, Bulgaria

²Institute of Mineralogy and Petrology

University of Graz, Universitätsplatz 2, A-8010 Graz, Austria

In the tectonic evolution of the Rhodope massif two successive compressional and extensional events which occurred during the Alpine time are distinguished. Both stages resulted from the collision between Eurasian and African plates in early Cretaceous time. During the compressional stage, the rocks have been subjected to regional metamorphism and a system of large-scale south verging thrusts emerged. The extensional stage began with tectonic erosion of the anomalous thickened crust and continued with the formation of detachment fault system. The latter has been connected with a development of granitic and migmatitic domes and imposed graben depressions filled with sediments of Palaeogene age. The Late Cretaceous-Tertiary extensional system in the Central Rhodopes area consists of two plates: an upper plate (Asenitsa unit) that has been affected by amphibolite facies metamorphism (550°C / 13 kbar); and a lower plate (Arda unit) that has been affected by migmatization (620–680°C / 4–8 kbar). The Arda unit migmatites were exhumed during the Oligocene (35–34 Ma) and formed the core of the Central Rhodopian Dome [1].

This work presents new petrologic data and preliminarily P-T estimations on garnet-kyanite-bearing schists from Chepelare formation, Central Rhodope.

Chepelare formation crops out in the N periphery of the Central Rhodopian Dome (CRD), in the vicinity of the town of Chepelare. It consists of medium- to coarse grained biotite gneisses, banded two mica gneisses with garnet porphyroblasts, micaschists with garnet and kyanite porphyroblasts, amphibolites, fine-grained aplitic gneisses, and fine- to coarse-grained marbles in an irregular alternation. According to the latest tectonic subdivision of the CRD, it occupies the uppermost levels of Arda 1 tectonic unit.

Within the Chepelare formation garnet-kyanite schists form layers and lenses with irregular form and shapes with thickness up to 900 m [2]. Matrix mineral assemblage consists of Grt, Ky, Bt, Qtz, Pl ± Phen, Sil, Chl and accessory zircon, apatite, ilmenite, pyrite, graphite, rutile. Garnet and kyanite have variable proportions and form large porphyroblasts.

The analysed garnet porphyroblasts (3–4 mm) are almandine type (X_{Fe} 0.58–0.60, X_{Mg} 0.28–0.30, X_{Ca} 0.11–0.12, X_{Mn} 0–0.01). Garnets are found as largely unzoned grains only with variably developed Mn-enriched rim as resorption during retrogression or around large inclusions. Grain boundaries are corroded and grain shapes are elongated to the foliation. Inclusions of St, Ky, Pl, Bt, Chl and Qtz, are found near the garnet rim. Accessory rutile, ilmenite, ± zircon, xenotime, pyrite, apatite, allanite are widespread within the garnet.

Kyanite elongated to the foliation grains, includes rounded Qtz. Si content in phengites range from 6.54 to 6.59. Staurolite was found only as inclusion in Grt, in association with Pl, Bt, Qtz, Rt and Ilm. Its absence in matrix assemblage suggests temperatures higher than St-stability field - 700°C [3].

Thermobarometric calculations have been performed using PET and TWQ software. Different calibrations of Grt-Bt and Grt-St geothermometers and GASP and GRAIL geobarometers were used. Reequilibration of garnet rim and diffusion changes in some of the inclusions made the exact determination of peak metamorphic conditions difficult. Preliminary geothermometric and geobarometric results characterise changing metamorphic conditions: from 600–650°C / 7–8 kbar for garnet inclusions assemblage to 700–750°C / 9–10 kbar for the matrix. These results are consistent with the presence of Ky inclusions in garnet, consumption of staurolite and complete homogenisation of garnet composition.

Because of strong retrogression of the rock, it is possible that some P-T to be underestimated, taking in mind that recently mineralogical evidence for UHP from garnet-kyanite-bearing schists have been reported - maximum P of 6.8 GPa [4].

The first author thanks the Austrian Exchange Service for the scholarship to do research at the University of Graz for one academic year 2002/2003.

References

- [1] IVANOV, Z. ET AL. (2000): ABCD-GEODE workshop, Borovets, Guide to excursion (B), 6-17.
- [2] KOSTOV, I. ET AL. (1962): Dysten deposit in the vicinity of village of Chepelare, Smolian district. - Trav. Geol. Bulg., ser. Geoch. Miner. et Petr., 3, 69-92. (in Bulgarian).
- [3] SPEAR, F. (1993): Metamorphic phase equilibria and pressure-temperature-time paths. - Mineralogical Society of America, Washington DC.
- [4] KOSTOPOULOS, D. ET AL. (2003): First evidence of UHP metamorphism in the Central Rhodope massif of southern Bulgaria. - Geophysical Research Abstracts, Vol. 5, 08327.

**CHARAKTERISIERUNG DER POLIERSUSPENSION PP 503 HX
(KUNSTSTOFFGLASFERTIGUNG) UND DAS ALTERUNGSVERHALTEN VON IM
PROZESSKREISLAUF SICH BEFINDLICHEN SUSPENSIONEN DER
GRUNDZUSAMMENSETZUNG PP 503 HX**

M. Habäck^{1,2}, G. Amthauer¹ & A. Kaufmann²

¹Institut für Mineralogie

Universität Salzburg, Hellbrunnerstrasse 34, A-5020 Salzburg, Austria

²Rodenstock GmbH, Abteilung FP-F

Bahnhofstrasse 45, D-94209 Regen, Germany

Die Firma Rodenstock GmbH ist national und international in der Brillenherstellung, von Kunststoffgläsern und auch Silikatgläsern tätig.

In der Flächenbearbeitung von Brillengläsern sind die Hauptarbeitsgänge Schleifen und Polieren. Beim Schleifen wird die geforderte geometrische Form erzeugt. Eine geschliffene Glasoberfläche besteht aus muschelförmigen Kratern und aus Rissen, die in die Tiefe gehen, da der Abtrennvorgang vorwiegend durch Bruch- und Splittervorgänge erfolgt. Durch das nachfolgende Polieren werden die muschelförmigen Krater und die Tiefenrisse entfernt. Das Ergebnis des Polierprozesses soll eine Oberfläche höchster Präzision und Sauberkeit sein, die frei von Ablagerungen und Fremdpartikel ist.

In der Brillenglasfertigung wird zum Polieren von Kunststoffgläsern eine Suspension eingesetzt, die aus Al₂O₃-Feststoffpartikeln besteht, welche in einer Mischung aus Wasser, Aluminiumnitrat, organischen Komponenten und Entschäumer homogen verteilt sind. Für die Untersuchung wurde das Poliermittel PP 503 HX (Loh Opticservice) ausgewählt.

In dieser Arbeit wurden durch Anwendung verschiedener Messmethoden die Poliersuspension im ursprünglichen Zustand (Neuansatz) charakterisiert. Ausgehend von diesen Ergebnissen wurde der Alterungsprozess (Eintrag von Kunststoffabrieb) und die damit verbundenen chemischen und physikalischen Veränderungen gegenüber einem Neuansatz beschrieben.

Die Anwendung der Röntgenbeugungsanalyse lieferte keinen Hinweis auf die Alterung, da mit "harten" Polierkörnern (Al₂O₃) ein "weiches" Material poliert wird. Es erfolgt kein Verschleiß der Polierkörner. Beim Polieren von Silikatgläsern erfolgt ein Abrieb des Polierkorns, da ein "hartes" Material mit einem "weichen" Polierkorn (CeO₂) bearbeitet wird [1]. Der Poliermechanismus wird durch tribochemische Reaktionen hervorgerufen.

Bei der Ermittlung des Zetapotentials zeigte sich, dass verschiedene Partikelarten bei den sich im Prozesskreislauf befindlichen Suspensionen auftreten, verursacht durch den Kunststoffeintrag.

Die Neigung der Poliersuspensionen zur Bildung von Agglomeraten konnte mit Hilfe der Elektronenmikroskopie beobachtet und durch die Methodik der Streumessung an Teilchenkollektiven (Korngrößenanalyse) bewiesen werden. Die Viskositätsmessungen, mit Hilfe eines Rotationsviskosimeters, zeigten bei einer Temperatur von 12°C (Prozessrelevanz) ein Absinken der Viskosität bei den Suspensionen, die sich im Prozesskreislauf befinden (zusätzlicher Eintrag von Kunststoffpartikeln).

Diese charakterisierten Veränderungen korrelieren mit dem Polierabtrag und den Oberflächen-sauberkeiten.

Literatur

- [1] KALLER, A. (1991): On the polishing of glass, particularly the precision polishing of optical surfaces. - Glas-technische Berichte 64 Nr. 9 (1991), 241-252.

**IR-SPEKTROSKOPISCHE UNTERSUCHUNGEN VON OH-DEFEKten IN
EISENHALTIGEN (^{IV}Fe²⁺) SPINELLPHASEN**

M. M. Halmer, E. Libowitzky & A. Beran

Institut für Mineralogie und Kristallographie
Universität Wien, Geozentrum, Althanstrasse 14, A-1090 Wien, Austria

Vorausgegangene experimentelle Untersuchungen haben gezeigt, dass Mg-Silikat-Spinellphasen, die bevorzugt in der Übergangszone des Erdmantels auftreten, beachtliche Mengen an Wasser (<2.7 Gew.%) in Form von OH-Gruppen enthalten. Unsere Probenauswahl beinhaltet natürliche Spinellphasen aus unterschiedlichen geologischen Milieus (z.B. MgAl-Spinell, Franklinit, Gahnit), aber auch synthetische Spinelle (z.B. nicht-stöchiometrische Verneuil-MgAl-Spinelle). Die IR-Spektroskopie ist eine höchst empfindliche Methode, mit der geringste Spuren von an Sauerstoff gebundenem Wasserstoff in "trockenen" Mineralphasen gemessen werden können. Das Ziel der Studie ist, die Anwesenheit von OH-Defekten in Spinellen von natürlichen Paragenesen zu erkunden und Modelle über den strukturellen Einbau von Wasserstoff zu entwickeln. Mit IR-spektroskopischen Messungen an synthetischen Phasen wurden bereits positive Ergebnisse bezüglich des Wassergehalts in Spinellen erzielt. Diese nicht-stöchiometrischen Verneuil-MgAl-Spinelle sind durch zwei starke Banden mit unterschiedlichen Bandenintensitäten charakterisiert, die bei 3355 und 3540 cm⁻¹ liegen und eine zusätzliche Schulter bei 3500 cm⁻¹ aufweisen. Die Wassergehalte für die synthetischen Spinelle liegen zwischen 7 und 270 Gew.ppm. Die Werte wurden mit Hilfe der Kalibrierung von LIBOWITZKY & ROSSMAN [2] ermittelt. Natürlich vorkommende Franklinit- (ZnFe₂O₄) und Gahnitkristalle (ZnAl₂O₄) zeigen breite Absorptionen mit zwei Maxima in einem Wellenzahlbereich von 5500–3400 cm⁻¹. Diese Spektren erinnern an jene der synthetischen OH-haltigen Verneuil-MgAl-Spinelle, die eine geringe Menge Eisen enthalten. Nach SKOGBY & HÅLENIUS [1] können die zwei breiten Absorptionen den d-d Übergängen von ^{IV}Fe²⁺ zugeschrieben werden. Im Wellenzahlbereich mit geringeren Absorptionen (3600–3100 cm⁻¹) sind nur undeutlich OH-Banden zu erkennen, da diese von den Absorptionsbanden des Fe²⁺ stark überlagert bzw. teilweise verdeckt werden. Jedoch kann die Anwesenheit dieser schwachen Banden bei 3540 und 3500 cm⁻¹, die zuvor eindeutig OH-Banden im eisenhaltigen Verneuil-Spinellkristall zugeschrieben wurden, als ein Hinweis für die Existenz von OH-Defekten in natürlichem Franklinit interpretiert werden.

Diese Arbeit wurde teilweise von der EU mit dem "Human Potential Program" HPRN-CT-2000-0056 unterstützt.

Literatur

- [1] SKOGBY, H. & HÅLENIUS, U. (2003): An FTIR study of tetrahedrally coordinated ferrous iron in the spinel-hercynite solid solution. - American Mineralogist, (in press).
- [2] LIBOWITZKY, E. & ROSSMAN, G. R. (1997): An IR absorption calibration for water in minerals. - American Mineralogist, 82: 1111-1115.

**NITRILOTRIACETATO ZIRCONATES OF ALKYL AND POLYALKYL AMINES:
STRUCTURAL AND PHYSICAL PROPERTIES**

E. Haussühl^{1,2}, S. Haussühl³ & E. Tillmanns¹

¹Institut für Mineralogie und Kristallographie

Universität Wien, Althanstrasse 14, A-1090 Vienna, Austria

²Institut für Mineralogie, Abteilung Kristallographie

Johann Wolfgang Goethe-Universität, Senckenberganlage 30, D-60054 Frankfurt a. M., Germany

³Institut für Kristallographie

Zülpicherstrasse 49B, D-50674 Köln, Germany

A large percentage (> 40%) of the nitrilotriacetato zirconates $X_m(Zr[N(CH_2COO)_3]_2)_n \cdot yH_2O$ possesses an acentric structure within the so far investigated inorganic cations X. Therefore, we expected a considerable number of the zirconates formed by organic cations like amines to exhibit polar structures, too. Such crystals might be candidates for pyroelectric, piezoelectric and non-linear optical applications. The syntheses were successfully carried out employing the method of LARSON & ADAMS [1] with the alkyl monoamine cations $(C_rH_{2r+1}NH_3)^+$ for $r = 1$ to 8 and alkyl diamine cations $(C_rH_{2r}(NH_3)_2)^{2+}$ for $r = 2$ to 12. The structural properties of most of these species have already been reported as NCS in Z. Kristallogr. during the last years. Large single crystals of these compounds having optical quality could be grown from aqueous solutions by standard methods (controlled lowering of temperature or controlled evaporation). In the cases of larger r values the nitrilotriacetato zirconates possess plastic properties which impede the measurement of physical properties.

The following general results were obtained from the study of about 80 phases with different cations:

1. The nitrilotriacetato zirconates of the amines so far investigated crystallize exclusively in orthorhombic and monoclinic space groups.
2. The salts of the monoamines exhibit a rather high percentage of acentric structures (about 60 %), whereas the salts of the symmetric diamines form centrosymmetric structures, so far without exception.
3. The maximum pyroelectric and piezoelectric effects are in most cases considerably stronger than those found in tourmaline or α -quartz, respectively.
4. Despite a heavy anisotropy of expansion and elastic stiffnesses the volume thermal expansion and the mean elastic stiffness $C = (c_{11} + c_{22} + c_{33} + c_{44} + c_{55} + c_{66} + c_{12} + c_{13} + c_{23})/9$ differ only slightly within these nitrilotriacetato zirconates. However, the salts of the diamines show distinct smaller values of α and larger values of C. An analogous behaviour is observed with the temperature dependence of the elastic properties.

These common properties stem from the similarity of the structural arrangement of the anionic layers.

Literature

[1] LARSEN, E. M. & ADAMS, A. C. (1967): Potassium bis (Nitrilotriacetato) Zirconate (IV). - Inorg. Synth. 10. 7-8.

The authors are gratefully indebted to the Austrian Fonds zur Förderung der wissenschaftlichen Forschung FWF (P14125-GEO) and the International Centre for Diffraction Data for financial support of this work (Grant 90-03 ET).

**DIE KONTROVERSE DISKUSSION DES ORDNUNGSVERHALTENS
VON Fe^{2+} UND MG IN OLIVINEN**

R. Heinemann¹, H. Kroll¹, A. Kirfel² & B. Barbier²

¹Institut für Mineralogie
Corrensstrasse 24, D-48149 Münster, Germany

²Mineralogisch-Petrologisches Institut
Popelsdorfer Schloß, D-53115 Bonn, Germany

‘In-situ’-Neutronenbeugungsexperimente an natürlichen Olivin-Einkristallen (Fa12) [1, 2] und synthetischen Olivin-Pulvern (Fa50) [3] zeigen oberhalb $\sim 900^\circ\text{C}$ (Fa12) bzw. $\sim 600^\circ\text{C}$ (Fa50) einen starken Anstieg der Fe,Mg-Ordnung bei steigendem Fe^{2+} -Gehalt auf dem M2-Platz. Dies steht im Widerspruch zu allen zuvor veröffentlichten Ergebnissen, die mit Röntgen-Methoden gewonnen wurden, und auch zu neuesten Ergebnissen, die mit Mössbauer-Spektroskopie an synthetischen, ins Gleichgewicht getemperten und abgeschreckten Fa50-Pulvern [4] erhalten wurden. Bei diesen war mit steigender Temperatur ein stetiger, leichter Anstieg der Fe-Mg-Ordnung mit steigendem Fe^{2+} -Gehalt auf dem M1-Platz zu beobachten.

Um diesen Widerspruch zu klären, haben wir Röntgeneinkristallmessungen an natürlichen Olivinen (Fa25 und Fa48) durchgeführt. Dazu wurden in Bonn ‘in-situ’ Datensätze bis $\sin\theta/\lambda = 0.7$ ($1/\text{\AA}$) zwischen RT und 900°C gemessen, in Münster wurden Kristalle bei Temperaturen zwischen 525°C und 700°C ins Gleichgewicht getempert, abgeschreckt und anschließend Datensätze bis $\sin\theta/\lambda = 1.1$ ($1/\text{\AA}$) bei RT gemessen. Die Sauerstoff-Fugazitäten wurden durch CO/CO_2 - bzw. Fe/FeO -Puffer kontrolliert.

Die bei den ‘in-situ’-Messungen bestimmten Gitterkonstanten, ebenso wie die bei den Strukturverfeinerungen bestimmten Temperaturkoeffizienten und interatomaren Abstände (M-O) verlaufen stetig. Im Gegensatz zu [1, 2, 3] erfolgt bei hohen Temperaturen kein ‘cross-over’ der thermischen Parameter und M-O-Abstände. Die verfeinerten Besetzungszahlen zeigen, daß mit

steigender Temperatur der Fe-Mg-Ordnungsgrad unter Anreicherung des Fe^{2+} auf dem M1-Platz stetig ansteigt. Eine Umkehrung der Richtung des Fe,Mg-Platzwechsels, d. h. Bevorzugung von Fe^{2+} auf M2, die beim Olivin Fa48 nach [3] bei ca. 600°C erfolgen soll, ist nicht zu erkennen.

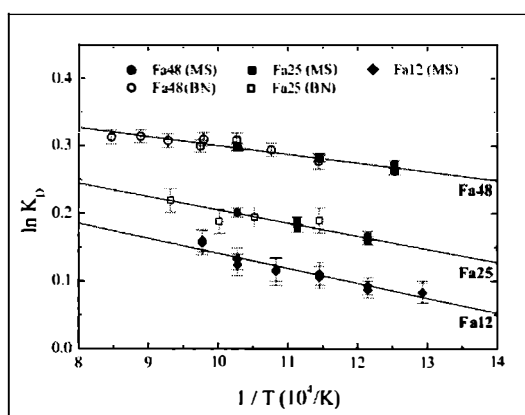


Fig. 1
Die $\ln K_D$ -Geraden der Olivine mit Fa12, Fa25 und Fa48.

Die $\ln K_D$ -Geraden der Olivine mit Fa12 [5], Fa25 und Fa48 verlaufen nahezu parallel. Die aus den ‘in-situ’ Messungen und aus den RT-Messungen an abgeschreckten Proben berechneten $\ln K_D$ -Werte stimmen innerhalb ihrer Fehlergrenzen überein, d. h. die an unterschiedlich behandelten Kristallen auf zwei unterschiedlichen Einkristalldiffraktometern von zwei verschiedenen Operatoren gemessenen Daten führen zu gleichen Ergebnissen. Zudem zeigt dies, daß Olivinkristalle ohne ‘resetting’ von mindestens 700°C abgeschreckt werden können, was von [1, 2, 3] infrage gestellt worden ist.

Literatur

- [1] ARTIOLI, G. ET AL. (1995): High-temperature Fe-Mg cation partitioning in olivine: In-situ single-crystal neutron diffraction study. - Am. Min. 80, 197-200.
- [2] RINALDI, R. ET AL. (2000): Octahedral cation ordering in olivine at high temperature. I: in situ neutron single-crystal diffraction studies on natural mantle olivines (Fa12 and Fa10). - Phys Chem Miner 27, 623-629.
- [3] REDFERN, S. A. T. ET AL. (2000): Octahedral cation ordering in olivine at high temperature. II: an in situ neutron powder diffraction study on synthetic $MgFeSiO_4$ (Fa50). - Phys Chem Miner 27, 630-637.
- [4] MOROZOV, M. ET AL. (2001): Mössbauer effect study of the Mg^{2+} , Fe^{2+} -distribution in synthetic olivine (fa50 fo50). - Beihefte zum E. J. M. 13, 127.
- [5] HEINEMANN, R. ET AL. (1999): Temperature dependence of Fe,Mg partitioning in Acapulco olivine. - Am. Min. 84, 1400-1405.

FIRST EVIDENCE OF VOLCANISM ON THE ANAFI ISLAND

E. Hejl & J. Leichmann

Institute for Geology and Paleontology
University of Salzburg, Hellbrunnerstrasse 34, A-5020 Salzburg, Austria

Anafi Island is situated approximately 20 km west from the island of Thira, which belongs to the archipelago of Santorini. Its geographical position suggests that Anafi could belong to the present-day Hellenic volcanic arc. However, no volcanic activity was reported from the island yet. REINECKE et al. [1] described four major tectono-stratigraphic units. They are from the base to the top:

- 1) Palaeogene flysch
- 2) Series of greenschists
- 3) High temperature metamorphites and associated granites
- 4) Theologos formation – continental sediments of Plio- to Pleistocene age [2]

We found several geological phenomena, indicating that the Anafi Island was affected by volcanic and hydrothermal activity in Neogene and/or Quaternary times. They are: (i) Dikes and sills of rhyolites, (ii) hydrothermal veins and hydraulic fractured rocks, (iii) penetrative hydrothermal alteration of country rock.

Dikes of Rhyolite (i) with a thickness of up to 2 m intruded the units 2, 3 and 4. In addition to the dikes, rhyolite sills with a thickness of up to 1 m occur in the basal part of the Theologos formation (unit 4). Within the fine-grained sediments of the latter, the rhyolite intrusions have caused contact metamorphic rims. The evidence of volcanic activity is restricted on the basal members of Theologos formation. We suppose therefore that the volcanism was contemporaneous with the opening of the basin.

The rhyolites are porphyritic rocks with corroded quartz phenocryst, up to 5 mm large. The feldspar phenocrysts are replaced by a mixture of clay mineral close to nacrite, and Ba-rich muscovite. The matrix consists of clay minerals, chemically identical with those from phenocryst, but much finer-grained, and quartz. The matrix is locally strongly carbonatized, thus the rock can be mistaken with marble being common on the island. Some veins contain large xenoliths of country rocks within the fine-grained matrix. Apart from massive rhyolites we found layers of black volcanic glass at the base of Theologos fm., spatially close related to rhyolite veins. The siliciclastic sediments of the basal Theologos fm. contain an important portion of reworked volcanic material.

Hydrothermal carbonate veins (ii) are very common, mainly in the rocks of the third tectonic unit. They are several hundred meters long and up to 30 cm thick. In association with these veins, hydraulic fractured breccias appear rarely. These breccias form irregular domains several tens of meters in diameter. The matrix between the rock fragments is mainly carbonate. Some carbonate veins are associated with faults, which are manifested by several meters high and up to 500 m long scarps.

The rhyolites as well as carbonate veins are accompanied by several hundred meters thick alteration zones (iii). The original feldspar of felsic rocks is strongly kaolinised, the mafic rock are limonitised. Carbonatisation is very common too. The alteration affects all four main tectonic units.

Because the volcanic and hydrothermal activity affects even the Plio-Pleistocene rocks of the Theologos fm., we suppose that this volcanic activity is closely connected with the magmatism in the present-day Hellenic arc. The volcanic activity of Anafi Island was short-living only. The volcanism was probably initiated by an extensional event contemporaneous with the formation of the Theologos sedimentary basin. Syn- and postsedimentary folding of the Theologos fm. indicates rapid quenching of the extensional regime, which was followed by compression and extinction of volcanic activity.

Literature

- [1] REINECKE, E., ALTHERR, R., HARTUNG, B., HATZIPANAGIOTOU, K., KREUZER, H., HARRE, W., KLEIN, H., KELLER, J., GEENEN, E. & BÖGER, H. (1982): Remnants of a Late Cretaceous High Temperature Belt on the Island of Anáfi (Cyclades, Greece). - N. Jb. Miner. Abh., 145,2,157-182.
- [2] VORWERK, W., (1979): Das Neogen im Nordwestteil der Insel Anaphi (Kykladen) Griechenland. Unpubl. - Diplomarbeit. Math. naturwiss. Fakultät, Universität Kiel. 83 p.

**Pd-BISMUTHOTELLURIDES AND OTHER TELLURIDES FROM SOME
CU-NI-PGE DEPOSITS, EASTERN DESERT, EGYPT**

H. M. Helmy

Minia University
Minia, Egypt

Pd-bismuthotellurides and other tellurides are described from three Cu-Ni-PGE deposits from the Eastern Desert of Egypt. These deposits – Abu Swayl, Genina Gharbia and Gabbro Akarem – are hosted in Late Precambrian Mafic-ultramafic rocks and have different geologic history. Abu Swayel deposit occurs in conformable, lenslike mafic-ultramafic rocks in metasediments. The mineralization and the enclosing rocks have been metamorphosed to amphibolite facies (550–650°C and 4–5 kbar) and syn-metamorphically sheared. The amphibolite facies metamorphism and the associated fluid regimes resulted in remobilization and transport of Cu-rich sulfides (50 % by volume chalcopyrite) and PGE and in the development of hydrosilicates. Tellurides are represented by michenerite (PdBiTe), merenskyite (PdTe_2), Pd-Bi melonite ($(\text{NiPdBi})\text{Te}_2$), melonite (NiTe_2), hessite (AgTe_2), altaite (PbTe) and joseite. They occur as inclusions in mobilized sulfides and along cracks in metamorphic silicates; garnet and plagioclase.

The Genina Gharbia and Gabbro Akarem Cu-Ni-PGE deposits are hosted in concentrically zoned (Alaskan-type) complexes. Genina Gharbia Cu-Ni-PGE ore forms either disseminations in peridotite or massive patches in hornblende-pyroxenite in vicinity to metasediments. The host rocks are not metamorphosed, important petrographic features are the dominance of hornblende, biotite and Cl-bearing apatite and alteration of plagioclase to epidote. The disseminated and net-work sulfide ore are dominated by pyrrhotite, pentlandite, chalcopyrite and minor pyrite. Accessory sulfides comprise cobaltite, molybdenite and valleriite. Sulfide textures and host rock petrography suggest a prolonged late-magmatic hydrothermal event. The tellurides comprise michenerite, merenskyite, palladian bismuthian melonite, altaite, hessite, a bismuthotelluride (BiTe) and native tellurium. These tellurides are present mainly at the contact between sulfides and silicates.

The Gabbro Akarem concentrically zoned complex is not metamorphosed. The Cu-Ni-PGE deposit is hosted in dunite pipes where net-textured and massive sulfides are found in association with Al-Mg-rich spinel and Cr-magnetite. Tellurides are represented by michenerite, merenskyite, Pd-Bi melonite and hessite. They occur mainly as inclusions in net-textured sulfides. The role of late-and post-magmatic hydrothermal processes is limited as indicated by typical magmatic textures of sulfides also the silicate mineral assemblage.

The different geologic history of the different deposits enables to examine the role played by late-magmatic and post-magmatic metamorphic fluids in the diversity of telluride mineralogy. The high tellurium activities, as indicated by various tellurides, at Abu Swayel and Genina Gharbia are attributed to the participation of hydrothermal solutions generated during amphibolite facies metamorphism and late-magmatic hydrothermal fluids, respectively. The limited role played by hydrothermal fluids in the Gabbro Akarem deposit is responsible for the low Te activity. It is suggested that the hydrothermal fluids introduced by late- and post-magmatic processes largely control tellurium activity in Cu-Ni-PGE deposits hosted in mafic-ultramafic rocks. Involvement of a sedimentary component either early, during magma contamination or later, during metamorphism highly increases the tellurium activity.

LANGZEITVERHALTEN VON RESTSTOFFEN DER MÜLLVERBRENNUNGSANLAGEN

S. Heuss-Aßbichler

Department für Geo- und Umweltwissenschaften
Universität München, Theresienstrasse 41/III, D-80333 München, Germany

In den Industrieländern fällt jährlich Siedlungsmüll in der Größenordnung von 450 kg pro Kopf an. Bisher wurde ein Großteil dieser Reststoffe unbehandelt deponiert. Eines der umweltpolitischen Ziele der EU ist das Aufkommen von Reststoffen zu vermeiden und Wertstoffe konsequent zurückzugewinnen. Die Verwertung der anfallenden Abfälle kann stofflich oder energetisch erfolgen. Nach den gesetzlichen Vorgaben darf in Deutschland ab 2005 kein Reststoff mehr unbehandelt deponiert werden. Kriterium ist der gesamte organische Kohlenstoffgehalt im Abfall. Neben der mechanisch-biologischen Behandlung können diese Vorgaben nur durch thermische Behandlung der Reststoffe erreicht werden. Das anfallende Müllvolumen wird in Müllverbrennungsanlagen MVA um etwa 90 Prozent verringert. Die Entsorgung bzw. Weiterverwertung der anfallenden Reststoffe soll ohne Umweltbelastung erfolgen. Durch MultibARRIERensysteme in den Deponien soll eine wirksame und auch dauerhafte Sperrung gegen Schadstoffemission erreicht werden; langfristig ist das Ziel eine "nachsorgearme Deponie". Das bedeutet, dass im Zeitabschnitt nach der Ablagerungsphase bzw. der endgültigen Stilllegung eines Deponieabschnitts bis hin zur Entlassung aus der Nachsorge die Umsetzungsreaktionen abgeschlossen sein sollen, so dass zu keiner Zeit eine Beeinträchtigung des Allgemeinwohls erfolgen kann.

Entgegen den ersten Erwartungen verhalten sich die anfallenden MVA-Reststoffe nicht inert. Verschiedene Untersuchungen haben gezeigt, dass diese Materialien sehr reaktiv sein können. Noch während der Ablagerungsphase ist durch den Ablauf verschiedener exothermer Reaktionen mit einer Erwärmung des Materials zu rechnen [1]. Ebenso können verschiedene, zum Teil ökotoxische Elemente ausgewaschen werden. Ein weiterer Aspekt ist die langfristige Emission von Wasserstoffgas [2]. In Hinblick auf die Deponiesicherheit ist daher neben dem Charakterisieren der Reststoffe und dem Erfassen der Auslaugungsprozesse in der Deponie das Langzeitverhalten der MV-Reststoffe von großer Umweltrelevanz.

Säurepuffersysteme der sekundär gebildeten Karbonate sollen maßgebend das Langzeitverhalten von MV-Schlacken bestimmen. Generell wird eine Mobilisation von Schwermetallen bei einer Abnahme des pH-Wertes auf Werte < pH 7 erwartet. Bisher werden zur Beurteilung der Materialien Elutionsverfahren wie DEV-S4-Test oder pHstat-Versuche bei pH 4 herangezogen. Untersuchungen in MV-Schlacke-Monodeponien haben jedoch gezeigt, dass die Karbonatbildung durch Reaktion von Portlandit mit CO₂ und damit der Aufbau der Karbonatpufferkapazität viel langsamer erfolgt als bisher prognostiziert wurde. Damit findet auch die erwartete Fixierung von Schwermetallen in den karbonatischen Phasen nur begrenzt statt. Der Vergleich der 24-Stunden-Tests mit den Ergebnissen aus Lysimeterversuchen über mehreren Monate zeigte, dass die Gesamtverfügbarkeit der Schwermetalle durch verschiedene Faktoren, wie die Korngröße der Materialien oder die Bindungsart der Schwermetalle im Primärmaterial beeinflusst wird [3].

Durch Korrosionsprozesse von metastabilen Phasen, z.B. MVA-Schmelzprodukte, oder Zersetzung von kristallinen Phasen in MV-Schlacke kann langfristig der Anteil der Schwermetalle im Sickerwasser ansteigen. Die Bildung von Speichermineralen wie CSH-Phasen, Ettringit, Ellesit oder Me/Me-Hydroxosalze ist ebenfalls nur zu einem geringen Anteil festzustellen. Zudem fällt es auf, dass der pH-Wert der Sickerwässer (pH 7 bis 10) relativ niedrig ist. Dennoch sind die Sickerwässer dieser Monodeponien nur geringfügig belastet.

Eine alternative Methode, um Langzeitreaktionen in einer Deponie abschätzen zu können, ist die Untersuchung von Reaktionsabläufen in salzreichen Systemen. Mit den hierdurch induzierten, erhöhten Korrosionsprozessen, verbunden mit erhöhter Löslichkeit der verschiedenen Spezies, sind Rückschlüsse auf die Freisetzungsmechanismen und -faktoren in den MV-Reststoffen möglich. Solche Systeme sind durch die gemeinsame Lagerung von chlorreichen Rauchgasreinigungsrückständen RGR gemeinsam mit MVA-Schlacke gegeben. Drei verschiedene Phänomene sind zu nennen [4]:

- 1) Die erhöhten Salzgehalte in den Reststoffen werden nicht sofort aus dem Material herauswaschen. Vielmehr werden durch kontinuierliche Lösungsprozesse, Transport entlang der Korngrenzen der porösen Materialien und Ausfällungsprozesse Salze und Schwermetalle aus den Reststoffen herausgelöst und in den Porenräumen aufkonzentriert. Die Inkrustationen tragen dazu bei, dass die – reaktiven – Phasen nicht mehr unmittelbar mit dem Sickerwasser in Kontakt kommen. Die niedrigen pH-Werte der Sickerwässer im Vergleich zu den hohen pH-Werten der eluierten Deponiematerialien dokumentieren diesen Tatbestand. Nach dem Erreichen eines Schwellenwertes ist jedoch mit einer massiven Mobilisation der Schwermetalle zu rechnen, wodurch die je nach Elutionsverfahren zu erwartenden Werte weit überschritten werden können.
- 2) Bei diesen salzreichen Lösungen kann eine Durchlässigkeitssdiskontinuität innerhalb der Deponie eine verstärkte Ausfällung der Salze begünstigen und zur Ausbildung eines Salzhorizontes führen. Hierdurch können leichtlösliche Schwermetalle innerhalb der Deponie gebunden werden.
- 3) Ein besonders wirksamer Mechanismus zum Fixieren von Schwermetallen und Salzen ist die Zugabe von Aluminium- oder Eisenhydroxiden. Durch Adsorptionsprozesse kann rasch und effektiv der Anteil ökotoxischer Elemente, wie z.B. Blei, herabgesetzt werden.

Mit Kurzzeittests wie Elutionsreaktionen oder Auslaugungsreaktionen durch Lysimeter kann das Langzeitverhalten der MV-Reststoffe nicht ausreichend beschrieben werden. Modellierungen können diese Prozesse bisher ebenfalls nur unbefriedigend beschreiben, da hier die Adsorptionsprozesse oder Bindungen von Schwermetallen in Salzen oder amorphen Phasen nur unzureichend wiedergegeben werden. Im Hinblick auf die Deponiesicherheit sind andere Verfahren zu entwickeln, mit denen sich das Langzeitverhalten der Rohstoffe erfassen lässt.

- [1] KLEIN, R., BAUMANN, T., NESTLE, N. & NIESSNER, R. (2003): Numerische Simulation der Temperaturentwicklung in Monodeponien aus Rückständen der Hausmüllverbrennung, - Müll und Abfall 35.
- [2] MAGEL, G., UNZEITIG, H., HEUSS-ABBICHLER, S., FEHR, K. T. & GERTHNER, F. (2002): Wasserstoffproduktion auf einer Deponie für MV-Rückstände. - Müll und Abfall 06/2002, 338-343.
- [3] HIRSCHMANN, G. (1999): Langzeitverhalten von Schlacken aus der thermischen Behandlung von Siedlungsabfällen - Fortschritt-Berichte VDI, Reihe 15, Umwelttechnik, Nr. 220, VDI Verlag.
- [4] HEUSS-ABBICHLER, S. & SPIEGEL, W. (2001): The use of additiva for long-term stabilization of boiler ashes and gas cleaning residues of municipal solid waste incinerator. - In: Eight International Waste-Management and Landfill Symposium, eds. T. H. Christensen, R. Cossu & R. Stegmann, Vol. I, Sardinia, 657-666.

**100 YEARS AFTER PIERRE TERMIER'S DISCOVERY OF THE TAUERN WINDOW:
WHAT LESSON SHOULD WE LEARN ?**

V. Höck & C. Tomek

Institute of Geology and Paleontology
University of Salzburg, Hellbrunnerstrasse 34, A-5020 Salzburg, Austria

The discovery of the Tauern window by Pierre Termier during his short stay at the International Geological Congress (Vienna 1903) field trip was a milestone in the geological study of the Eastern Alps. Termier's discovery came as a consequence of a new "nappe hypothesis" wave, introduced by M. Bertrand, H. Schardt, M. Lugeon and others in the Central and Western Alps. Termier's paper, the Tauern core of the Eastern Alps was widely regarded as the oldest (Paleozoic). This theory was unfortunately lastly published just in 1903 by Carl Diener in "Bau und Bild der Alpen" in the large publication "Geologie von Österreich" edited by Eduard Suess. But Termier's "veni, vidi, vici" was not that simple like nearly all the textbooks inform us. We will deal with this history in more detail in the following.

Termier probably came to the IGC pre-excursion led by Franz Becke in the Zillertal in July 1903 already prepared for the revolution. He was in close contact with other proponents of the nappe theory, mainly with Maurice Lugeon. And it was just Lugeon in 1902, who – without any visit(!) – destroyed Victor Uhlig's theory about the geological evolution of the West Carpathians and completely reinterpreted the structural history of the Tatra Mts. Victor Uhlig was at that time a leading person of the Austrian geology and follower of Eduard Suess as a professor of geology at the Vienna University. Moreover, Lugeon's paper about the West Carpathians was full of basic mistakes. Lugeon did not read carefully Uhlig's papers and overlooked the Eocene (Lutetian) transgression on the nappe edifice that he regarded as a post-Eocene one, similar to the Swiss Alps. After this, Lugeon, in summer 1903, also visited the IGC pre-excursion in the West Carpathians. His discussions with Uhlig were very sharp. Lugeon, therefore, discredited the new theory by this incredible mistake. Many of the followers of the new nappe thinking were, moreover, self confident and ready to fight. So this was the situation just before the Congress in summer 1903.

Termier came to the Zillertal excursion to find proves for the nappe theory. He saw immediately that the "Kalkphyllites" regarded as Paleozoic are in fact identical to the French "schistes lustres," known to him as being Mesozoic or Cenozoic in his French Alps. Moreover, he saw the arching structure of the Hohe Tauern and deduced that these, in fact, are the lowermost nappes of the whole edifice. He discussed the matter with Franz Becke, who helped him a lot in understanding the petrography of Tauern rocks. Termier informed already the Congress participants about his observations and similarly Lugeon made it about the Carpathians. Both presented also basic information about the nappe evolution of the Western and Central Alps. Later, Termier informed in November 1903 the French Geological Society about his new interpretations and all was published in April 1904.

The main recognition of the Tauern window as a tectonically lowermost structure of the Eastern Alps was correct and started an extremely fruitful era of the Alpine research in Austria. But the publication was full of mistakes in geological details. Only one field trip and the study of literature in German (!) were not adequate to the complicated problems. Termier unfortunately visited also the Semmering area during other field trip and his parallelization of the Semmering unit with Permo-Carboniferous "Zone de Vanois" of the Western Alps in the same article was highly incorrect. This story was immediately sarcastically commented by W. Hammer. Diener answered to Termier by a new paper published in Stuttgart and Franz Kossmat criticized heavily the "trainneau écraseur" hypothesis of Termier that the Southern Alps after the overcome of the Tauern are now presented as a part of the Northern Limestone Alps. Kossmat and Hammer were completely right. Would it be today, the Lugeon's paper about the Carpathians and the Termier's paper about the Eastern Alps would be by reviewers regarded most likely as not suitable for publication.

However, Eduard Suess and with him also Victor Uhlig decided during 1905–1907 to accept the new theory. It was an incredible testimony about the psychic and mental spirit of more than 75 years old Suess. The nappe theory and Tauern window are already part of his third volume of the "Antlitz der Erde". Also Uhlig was not bitter more than two years after the hard controversy with Lugeon. He visited critical locations of the new theory in Switzerland, discussed with proponents and accepted. Suess and Uhlig both developed the basic division of the nappes in the Alps. Their "Ostalpine" and Lepontine (today Penninic) nappes division is widely accepted until today. The influence of both on the young generation of Austrian geologists was enormous. Eduard Suess's son Franz Eduard Suess and students of Uhlig like L. Kober and F. Trauth were convinced proponents of a new theory. The fights between old and new, however, lasted for another 40 years. W. Hammer remained unconvinced. All the time he criticized the technical impossibility of the new theory. Otto Ampferer and he proposed different mechanism for the nappe edifice structure. Their "Verschluckung Theorie" was never widely accepted by Alpine geologists.

Leopold Kober and his student Alexander Tollmann were uncritical fans of the Termier's genius. They followed his theory until seventies and eighties of last century. In the meantime, however, it was found that the situation with the Tauern window is not that simple. Ronald Oxburgh's (1968) discovery of young – Neogene – metamorphic age of the Tauern rocks changed the situation completely. Plate tectonics later in 1968 confirmed that Ampferer and Hammer were right and that "trainneau écraseur" concept of Lugeon and Termier were wrong. Jane Selverstone – student of Clarke Burchfiel at MIT - later applied her teacher's theory of extensional nappes to Tauern in 1985 and a new – non compressional concept - started.

So what is the lesson from this history? One must be prepared for new discoveries as Termier and Lugeon were. One must be courageous enough, self confident and lucky and stay in the right moment at the right place. One must publish quickly regardless of small details. (These were nearly all wrong by both). How similar is this history with nearly contemporaneous Alfred Wegener story about continental drift. How similar with Joe Tuzo Wilson discovery of the plate tectonics and hot spot theory in early sixties of last century.

THE AGE OF THE KONRADSHEIM LIMESTONES (GRESTEN UNIT, AUSTRIA)

V. Höck¹, A. Ślączka², A. Gasiński² & M. B. Bąk²

¹Institute of Geology and Paleontology

University of Salzburg, Hellbrunnerstrasse 34, A-5020 Salzburg, Austria

²Institute of Geological Sciences

Jagiellonian University, Oleandry 2a, 30-063 Kraków, Poland

The Gresten unit is one of the units situated in front of the Northern Calcareous Alps (NCA) [1]. The most characteristic lithofacies are the Gresten Beds, with arkoses, sandstones and shales, intercalated by coal in the lower part (Hettangian), and calcareous deposits in the upper part (Sinemurian-Toarcian). The Gresten facies in the foreland of the NCA is known only from the Gresten unit and from several boreholes at the basement of the Molasse Zone in the eastern part of Lower Austria [2]. However, similar deposits are developed also within the western part of the Pieniny Klippen Belt and in the Apuseni Mts [3].

The Gresten Beds of the Gresten Unit are covered by Aalenian spotted marls, the Posidonia Marls (Bajocian - Callovian) and radiolarites (Oxfordian). The Malmian and Neocomian sediments are represented mainly by siliceous Aptychus limestones and spotted marls similar to the deposits from the NCA. In the vicinity of the village Konradsheim and in the Pechgraben area the Konradsheim Limestones were also included into the Malmian sediments. The Konradsheim limestones are developed usually as thick to very thick self- and matrix supported conglomerates and sedimentary breccias, usually displaying a gradation. The clasts are represented generally by fragments of limestones, up to tens of centimetres in diameter. The Malmian age of the Konradsheim Limestones in the Konradsheim area (NÖ) was established [4] on the basis of a macrofauna and in the Pechgraben area (OÖ) it was based on the occurrence of Tithonian Aptychus and Ammonites in the conglomerates [5]. In general, the Malmian age of the Konradsheim Limestones is accepted [1]; however, Schnabel [6] mentioned the occurrence of Cretaceous foraminifera in shales connected with the Konradsheim Limestones near Konradsheim.

The present study was carried out in two areas: on the Castle hill in the Konradsheim village and in the Pechgraben area. Near Konradsheim several samples were collected from the intercalations of greenish marls between the Konradsheim conglomerates layers, exposed on the lower bend of the road to the church. In the Pechgraben area two exposures were sampled. Several samples were taken from marly limestones and marls intercalated with the Konradsheim conglomerate layers, exposed in an abandoned quarry. The quarry is situated in the area Hohenberg, along the road from Stangl to Kohlgraben. Other samples were collected from the area of Arthofer from the big exposure on road bend near Dichlberger, where a complex of conglomeratic Konradsheim Limestones lay above the folded Scheibbsbach Beds. Samples were collected from conglomerates and marly shales.

Biostratigraphical investigations of pelitic intercalations within the Konradsheim Limestones, both, from the Konradsheim and Pechgraben area, that contain foraminifera assemblages with *Caudammina (Hormosina) ovulum* (Grzybowski), explicitly show that those limestones are of Cretaceous age, not older than Barremian [7]. The age of a part of the Konradsheim Limestones, younger than previously accepted is also supported by the occurrence of the Radiolaria assemblages of Early Cretaceous age in clasts from conglomerates in the Arthofer area. The co-occurrence of *Pseudoaulophacus (?) florealis*, *Triactoma luciae*, *Pseudoeucyrtthis (?) fusus*, *Sethocapsa leiostraca*, *Podobursa triacantha* and *Parvingula mashitaensis* indicate an age not older as Early Valanginian. The Radiolaria assemblage represents a low-latitude Tethyan microfauna. The age of rounded, redeposited clasts that contain the Radiolaria is older than the age of the host rocks. A similar co-existence of Malmian and younger pebbles were also described from conglomerates of the Gresten Unit near Scheibbs [8]. Our results imply that the monomictic conglomerates build up mainly of calcareous pebbles, described as the Konradsheim Limestones, could be deposited during different periods of Late Jurassic and Cretaceous.

The sedimentary structures of the conglomerates from Konradsheim Limestones show that they could represent deposits of high concentration turbidity currents and debris flows, that infilled submarine channels. The additional occurrence of the Konradsheim Limestones as blocks within marly deposits imply that, in some cases, they can also represent resedimented bodies (olistolithes). The provenience of material is open for discussion, however, a source area for a part of the radiolarian limestones was probably connected with the Tethyan realm. The observed similarity between conglomerates of the Konradsheim Limestones from the Gresten Klippen and a part of a sedimentary breccia, built mainly from limestones clasts, from the Gruber quarry in the northeastern part of the Tauern Window (Grossarl valley) implies a possibility of a connection between both conglomerates.

References

- [1] OBERHAUSER, R. (ed.), (1980): Der Geologische Aufbau Österreichs. - Springer-Verlag, Wien, New York, 695p.
- [2] JANOSCHEK, W. R. & MATURA, A. (1980): Outline of the Geology of Austria. - Abhandlungen der Geologischen Bundesanstalt, 34, 7-98.
- [3] JANOVICI, V. ET AL. (1976): Geologia Muntilor Apuseni. - Editura Academiei Republica Socialiste Romania, Bucuresti, 631p.
- [4] TRAUTH, F. (1950): Die fazielle Ausbildung und Gliederung des Oberjura in den nördlichen Ostalpen. - Verh. Geol. B. A. 1948, 145-218.
- [5] WIDDER, R. W. (1988): Zur Stratigraphie, Fazies und Tektonik der Grestener Klippenzone zwischen Maria Neustift und Pechgraben - O.Ö. - Mitteilungen der Gesellschaft Geol. Bergbaustudenten. 34/35, 79-133.
- [6] SCHNABEL, W. (1970): Zur Geologie des Kalkalpennordrandes in der Umgebung von Waidhofen/Ybbs, Niederösterreich. - Mitteilungen der Gesellschaft Geol. Bergbaustudenten., 19, 131-188.
- [7] GRADSTEIN, F. M. ET AL. (1994): Cenozoic biostratigraphy of the North Sea and Labrador Shelf. - Micro-paleontology 40. Supplement, 1-152.
- [8] FAUPL, P. & SCHNABEL, W. (1987) Ein Breccievorkommen bei Scheibbs (Niederösterreich). Zur Kenntnis palaeogener Grobklastika aus der Buntemergelserie. - Jahrbuch der Geologischen Bundesanstalt, 130, 153-161.

CELEBRATION 2000: P-WAVE VELOCITY MODELS OF THE BOHEMIAN MASSIF

P. Hrubcová & CELEBRATION 2000 Working Group

Geophysical Institute

Academy of Sciences of the Czech Republic, Bocni II/1401, 142 00, Czech Republic

The deep structure of the Bohemian Massif (BM), the largest stable outcrop of Variscan rocks in Central Europe, was studied along two refraction profiles, CEL09 that traverses the whole massif in the NW-SE direction, and CEL10 that extends along its eastern edge almost perpendicular to CEL09. Good quality recordings with clear first arrivals of crustal and upper mantle phases show an apparent velocity 5.9 km/s for the upper crust with a slightly higher gradient in the NW part of the BM and an apparent velocity 8.0 to 8.1 km/s for the uppermantle. The decrease of amplitudes of crustal phases, visible in some sections may be connected with a specific upper crustal structure (zero to negative velocity gradient zone). Pronounced Moho reflections in the central part of the BM suggest a well-defined Moho in that part and not so clear a Moho with a smaller velocity contrast in other parts of the BM.

For interpretation, the tomographic inversion routine of Hole [1] was used as an efficient tool to determine the seismic P-wave velocity distribution in the crust using first arrivals. Tomographic models were verified by forward ray tracing modelling based on a well-established algorithm developed by ČERVENÝ & PŠENČÍK [2], where, apart from first arrivals, also further phases were included. 2-D velocity models of first arrivals and reflected phases show a high P-wave velocity gradient zone reaching the depth of 5–7 km followed by a small gradient and a laterally homogeneous P-wave velocity distribution in the middle crust. Differences in velocity distribution in the lower crust delimit the central part of the BM (sharp Moho discontinuity) from other tectonic units within the BM (lower crust with high gradient transition zone). The position of the Moho discontinuity ranging from 32 km to 40 km and reflectors within the crust complement the P-wave velocity distribution. The presented models also show the contact of the BM with its neighbouring units – Carpathians, Paleozoic Platform, Vienna Basin and the Alps.

References

- [1] HOLE, J. A. (1992): Non-linear high-resolution three-dimensional seismic travel time tomography. - *J. Geophys. Res.* 97, 6553-6562.
- [2] ČERVENÝ, V. & PŠENČÍK, I. (1983): Program SEIS83, Numerical Modelling of Seismic Wave Fields in 2D Laterally Varying Layered Structures by the Ray Method. - Charles University, Prague.

**THERMODYNAMISCHE EIGENSCHAFTEN DER MISCHREIHE
HEDENBERGIT-PETEDUNNIT $\text{Ca}(\text{Fe},\text{Zn})\text{Si}_2\text{O}_6$**

A. L. Huber & K. T. Fehr

Department für Geo- und Umweltwissenschaften
Universität München, Theresienstrasse 41/III, D-80333 München, Germany

Eine Vielzahl gesteinsbildender Prozesse ist eng verknüpft mit dem Mischungsverhalten unterschiedlicher Klinopyroxene. Unabdingbare Voraussetzung für die Modellierung dieser petrogenetischen Prozesse ist eine exakte thermodynamische Charakterisierung von Klinopyroxen-Mischreihen.

Während Hedenbergit bei niederen Drucken stabil ist, beginnt das Stabilitätsfeld von Petedunnit hin zu hohen Drucken ab etwa 1.2 GPa. Synthesen der Reihe Hedenbergit-Petedunnit $\text{Ca}(\text{Fe},\text{Zn})\text{Si}_2\text{O}_6$ belegen ab etwa 1.2 GPa eine lückenlose Mischbarkeit [1]. Das thermodynamische Mischungsverhalten der homogenen Mischreihe Hedenbergit-Petedunnit $\text{Ca}(\text{Fe},\text{Zn})\text{Si}_2\text{O}_6$ wird durch die mittlere molare freie Mischungsenthalpie ΔG_m

$$\Delta G_m = \Delta G_{id} + \Delta G^e = RT \sum_i x_i \ln a_i$$

bestimmt. Kennzeichnende Größen der Mischkristallreihe sind die Aktivitäten ($a_i = x_i \gamma_i$), die anhand einer Zustandsgleichung zu ermitteln sind. Zur experimentellen Bestimmung der Aktivität von Hedenbergit in Petedunnit nutzt man die Zersetzung von Hedenbergit in Anwesenheit von Sauerstoff zu Andradit, Magnetit und Quarz:



Die Gleichgewichtskonstante dieser Reaktion ist eine Funktion der Sauerstofffugazität, die mittels EMK-Methoden (elektromotorische Kraft) gemessen wird. Ersetzt man in der Reaktion Hedenbergit durch Hedenbergit-Petedunnit-Mischkristalle, so reflektieren die Gleichgewichtskonstanten die chemischen Potentiale von Hedenbergit in Petedunnit. Dementsprechend können die Aktivitäten von Hedenbergit gemäß

$$4 F * \text{EMK} = 2/9 \ln a_{hd} \quad (\text{F: Faradaykonstante})$$

direkt aus den EMK-Experimenten ermittelt werden. Die Aktivität dieser Mischreihe ist temperaturabhängig (Abb. 1). Die Mischreihe weist kein Exzess-Mischungsvolumen auf [1]. Dies bedeutet, dass die Aktivitätskoeffizienten γ_i nicht vom Druck abhängen. Die Aktivität zeigt als Funktion der Zusammensetzung ein nicht lineares Verhalten (Abb. 1), woraus sich das nicht ideale Verhalten der Mischreihe Hedenbergit-Petedunnit ableitet. Die Nichtidealität impliziert die Existenz der mittleren freien molaren Exzess-Enthalpie ΔG^e .

$$\Delta G^e = x_{hd} \mu_{hd}^e + x_{pd} \mu_{pd}^e$$

Mit Hilfe von EMK-Methoden kann das chemische Exzess-Potential μ_{hd}^e von Hedenbergit bestimmt werden. Das chemische Exzess-Potential μ_{pd}^e von Petedunnit ist unbekannt. Die Aktivität von Petedunnit kann dennoch anhand des Redlich-Kister-Modells

$$\Delta G^e = x_1 x_2 (A_0 + A_1(x_2 - x_1) + A_2(x_2 - x_1)^2 + \dots)$$

sowie der Darkenfunktion

$$\begin{aligned}\Phi &= RT \ln \gamma_{hd} (1-x_{hd})^{-2} = \mu_e_{hd} (1-x_{hd})^{-2} \\ &= (A_0 + A_1(4x_{hd}-1) + A_2(2x_{hd}-1)(6x_{hd}-1) + \dots)\end{aligned}$$

ermittelt werden. Im Vergleich mit den Messdaten wird deutlich, dass die Mischreihe Hedenbergit-Petedunnit mit einem drei-Parameter-Redlich-Kister-Modell

$$\begin{aligned}\Delta G_m &= \Delta G^{id} + \Delta G^e \\ &= RT \sum_i x_i \ln x_i + x_1 x_2 (A_0 + A_1(x_2 - x_1) + A_2(x_2 - x_1)^2 \\ &= RT \sum_i x_i \ln a_i,\end{aligned}$$

mit A_0, A_1, A_2 in J/mol

$$\begin{aligned}A_0 &= -55737(2468) + 49.3(2.2)*T(K) & r^2 &= 0.9943 & sd &= 294 \\ A_1 &= -44566(4046) + 11.8(3.8)*T(K) & r^2 &= 0.7612 & sd &= 733 \\ A_2 &= -149688(10504) + 112.7(9.9)*T(K) & r^2 &= 0.9774 & sd &= 1903\end{aligned}$$

vollständig charakterisierbar ist (Abb. 1).

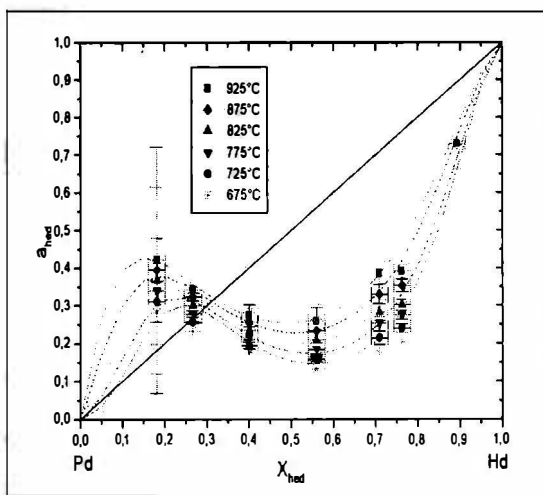


Abb. 1
Aktivität von Hedenbergit in der Mischreihe mit Petedunnit.

Im Gegensatz zur Mischkristallreihe Hedenbergit-Petedunnit ist die Reihe Hedenbergit-Diopsid mit zwei Redlich-Kister- bzw. Margulesparametern beschreibbar [2]. Die Existenz von drei Parametern des Redlich-Kister-Modells für die Reihe Hedenbergit-Petedunnit weist auf Nahordnungsphänomene in der Mischkristallstruktur hin. Dies ist umso bedeutender, da anhand von Raumtemperatur- [1] bzw. Tieftemperatur- ($T = 83$ K) Mößbauerspektroskopie, keine Hinweise auf eine Nahordnung in der Mischreihe Hedenbergit-Petedunnit nachgewiesen werden konnten.

Literatur

- [1] HUBER, A. L. ET. AL. (2002): Characterisation of synthetic hedenbergite ($\text{CaFeSi}_2\text{O}_6$)-petedunnite ($\text{CaZnSi}_2\text{O}_6$) solid solution series by X-ray powder diffraction and ^{57}Fe Moessbauer spectroscopy. - Physics and Chemistry of Minerals, subm.
- [2] MEYRE , C. ET AL. (1997): A ternary solid solution model for omphacite and its application to geothermo-barometry of eclogites from the Middle Adula nappe (Central Alps, Switzerland). - Journal of Metamorphic Geology, 15, 687-700.

**WHOLE-ROCK GEOCHEMISTRY OF FELSIC GRANULITES FROM THE GFÖHL UNIT
(MOLDANUBIAN ZONE, AUSTRIA AND CZECH REPUBLIC): PETROGENETIC IMPLICATIONS**

V. Janoušek & F. Finger

Institut für Mineralogie
Universität Salzburg, Hellbrunnerstrasse 34, A-5020 Salzburg, Austria

The presumed root of the Variscan orogen in the Bohemian Massif, the Moldanubian Zone, represents a tectonic assemblage of medium- to high-grade metamorphic rocks, intruded by numerous granitoid masses. Its uppermost, allochthonous Gföhl Unit consists of anatetic gneisses, HP-HT granulites (minimum P ~ 1.5 GPa, 950–1050°C), Grt/Spl peridotites, pyroxenites and eclogites [1-4]. The age of the HP granulite metamorphism is constrained at ~ 340 Ma [2 and references therein]. Among the granulites prevail leucocratic types with the assemblage Grt + Ky + Qtz + mesoperthite (former ternary feldspar); mafic-intermediate pyroxene-bearing types are subordinate.

The felsic granulites ($\text{SiO}_2 > 70\%$) are acidic ($\text{SiO}_2 = 74.5$, median), slightly peraluminous ($\text{A/CNK} \sim 1.1$), potassium- ($\text{K}_2\text{O}/\text{Na}_2\text{O} = 1.5$) and rather iron-rich ($\text{FeO}_t = 1.9$, mg# ~ 30). At given SiO_2 the CaO (1.0 %) is fairly high. No significant regional trends in the whole-rock geochemistry are apparent. The felsic granulites show variably low ΣREE , slight LREE enrichments ($\text{Ce}_N/\text{Yb}_N = 1.5\text{--}8.7$) and pronounced negative Eu anomalies ($\text{Eu}/\text{Eu}^* = 0.11\text{--}0.72$), deepening with increasing acidity. Compared to the average upper crust, Cs, U and Th are depleted, perhaps indicating some element mobility during the high-pressure metamorphism [5-6]. On the other hand, Rb and K as well as MREE and HREE (+Y) seem to be in the upper crustal range and much of the trace-element signature (e.g. variable depletions in Nb, Ti, Ba and Sr) can be explained in the terms of the protolith composition. High concentration ranges of these elements, resulting from closed-system evolution, are typical of many acid volcanic rocks [7]. Trends of rapidly falling Sr and Ba with rising Rb are also common in evolved granites crystallizing Kfs-dominated assemblages. The sharp drop in Zr, Y and P indicates crystallization of zircon and apatite, characteristic of fractionated I-type granite suites [8].

According to [6, 9-10] and our data, the felsic granulites contain radiogenic Sr ($^{87}\text{Sr}/^{86}\text{Sr}_{340} = 0.7106\text{--}0.7706$, median 0.7283) and unradiogenic Nd ($\epsilon^{340}\text{Nd} = -4.2$ to -7.5 , median -6.0). In the $^{87}\text{Sr}/^{86}\text{Sr}_{340} - \epsilon^{340}\text{Nd}$ plot the analyses from Austria and Czechia form subparallel, partly overlapping fields, with the former apparently shifted to lower (i.e. more negative) $\epsilon^{340}\text{Nd}$ values. These fields run diagonally from the less to more felsic rocks, the latter with considerably more radiogenic Sr-Nd isotopic compositions. Apparently, the whole-rock Rb-Sr system failed to equilibrate, on a large scale, in Variscan times. Likewise some zircons it may preserve memory of the igneous protolith age (?Silurian–Ordovician: see SHRIMP data of [2, 11]. In the Ab-Qz-Or ternary, the normative compositions of felsic granulites fall close to the low-pressure minimum. This further reinforces the argument for origin from upper crustal acid igneous rocks (rhyolites/fractionated granites) [5] subducted into the mantle during the Variscan collision [4].

The remarkable compositional uniformity of the felsic granulites requires an unusually siliceous and rather homogeneous metaigneous protolith, widely available in the pre-Variscan crust. As noted already by [6], the major- and trace-element chemistry together with the Sr-Nd isotopic compositions of the Gföhl gneisses match almost perfectly those of the felsic granulites. Subtle differences are in the U and Th (that are generally undepleted), also Nb, Sr, Zr and Hf tend to be slightly higher. The Gföhl gneisses, whose igneous protolith has been dated by SHRIMP at 482 ± 6 Ma [12], may in part represent retrogressed granulites [13].

For instance, analogous whole-rock geochemistry show orthogneisses and metarhyolites from the Fichtelgebirge, dated at 455–480 Ma [14 and references therein], i.e. falling within the spectrum of inherited ages observed in the granulites. The Sr isotopic system many of the Fichtelgebirge samples has been disturbed, but the Wunsiedel orthogneiss gave a whole-rock Rb-Sr age of 480 ± 4 Ma with $^{87}\text{Sr}/^{86}\text{Sr}_\text{i} = 0.7095$ [14] that compares well with the mean of the felsic granulites recalculated to 480 Ma (0.7086 ± 0.010 , 1s). Moreover, the $\epsilon^{480}\text{Nd}$ values for samples from Fichtelgebirge with $\text{SiO}_2 > 70\%$ (orthogneisses: -3.5 ± 0.4 , metarhyolites: -4.8 ± 1.1) are also matching the mean $\epsilon^{480}\text{Nd}$ (-4.9 ± 1.9) for the felsic Moldanubian granulites.

Taken together, the bulk of the South Bohemian granulites does not seem to represent HP melts separated in Variscan times from the unmelted residua (cf. [15-17]) but rather metamorphosed (even though in part anatetic) equivalents of an older igneous complex.

This work was financed by the FWF project 15133-GEO that is gratefully acknowledged.

References

- [1] CARSWELL, D. A. & O'BRIEN, P. J. (1993): Thermobarometry and geotectonic significance of high-pressure granulites: examples from the Moldanubian zone of the Bohemian Massif in Lower Austria. - *Journal of Petrology*, 34, 427-459.
- [2] KRÖNER, A. ET AL. (2000): Zircon ages for high pressure granulites from South Bohemia, Czech Republic, and their connection to Carboniferous high temperature processes. - *Contributions to Mineralogy and Petrology*, 138, 127-142.
- [3] COOKE, R. A. (2000): High-pressure/temperature metamorphism in the St. Leonhard Granulite Massif, Austria: evidence from intermediate pyroxene-bearing granulites. - *International Journal of Earth Sciences*, 89, 631-651.
- [4] O'BRIEN, P. J. & RÖTZLER, J. (2003): High-pressure granulites: formation, recovery of peak conditions and implications for tectonics. - *Journal of Metamorphic Geology*, 21, 3–20.
- [5] FIALA, J. ET AL. (1987): Moldanubian granulites and related rocks: petrology, geochemistry, and radioactivity. - *Rozpravy Československé akademie věd, řada matematických a přírodních věd*, 97, 1-102.
- [6] VELLMER, C. (1992): Stoffbestand und Petrogenese von Granuliten und granitischen Gesteinen der südlichen Böhmisches Masse in Niederösterreich. - PhD. thesis, Georg-August-Universität, Göttingen.
- [7] HILDRETH, W. (1979): The Bishop Tuff: evidence for the origin of compositional zonation in silicic magma chambers. - *Geological Society of America Special Paper* 180, 43-75.
- [8] CHAPPELL, B. W. & WHITE, A. J. R. (1992): I- and S-type granites in the Lachlan Fold Belt. - *Transactions of the Royal Society of Edinburgh, Earth Sciences*, 83, 1-26.

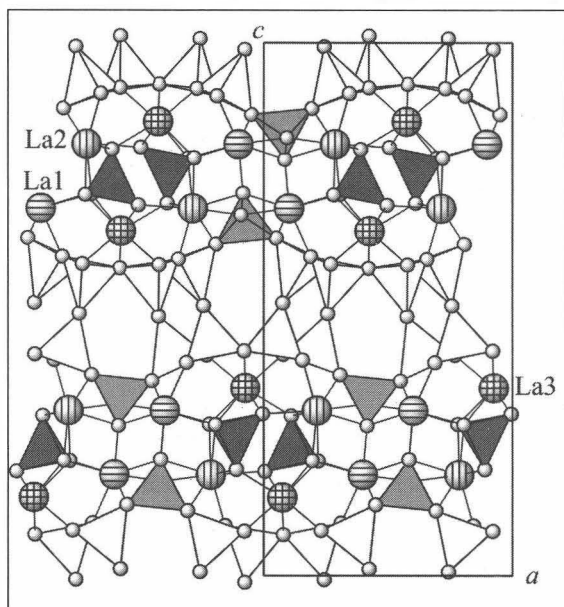
- [9] VALBRACHT, P. J. ET AL. (1994): Sr and Nd isotopic determinations in three Moldanubian granulite massifs in southern Bohemia. - *Journal of the Czech Geological Society*, 39, 114.
- [10] BECKER, H. ET AL. (1999): Geochemistry of glimmerite veins in peridotites from Lower Austria - implications for the origin of K-rich magmas in collision zones. - *Journal of Petrology*, 40, 315-338.
- [11] FRIEDL, G. ET AL. (2003): U-Pb SHRIMP dating and trace element investigations on multiple zoned zircons from a South-Bohemian granulite. - *Journal of the Czech Geological Society*, in print.
- [12] FRIEDL, G. ET AL. (1998): New SHRIMP-zircon ages for orthogneisses from the south-eastern part of the Bohemian Massif (Lower Austria). - *Acta Universitatis Carolinae, Geologica*, 42, 251-252.
- [13] COOKE, R. A. & O'BRIEN, P. J. (2001): Resolving the relationship between high P-T rocks and gneisses in collisional terranes: an example from the Gfohl gneiss-granulite association in the Moldanubian Zone, Austria. - *Lithos*, 58, 33-54.
- [14] SIEBEL, W. ET AL. (1997): Early Palaeozoic acid magmatism in the Saxothuringian belt: new insights from a geochemical and isotopic study of orthogneisses and metavolcanic rocks from the Fichtelgebirge, SE Germany. - *Journal of Petrology*, 38, 203-230.
- [15] VRANA, S. & JAKEŠ, P. (1982): Orthopyroxene and two-pyroxene granulites from a segment of charnockitic crust in southern Bohemia. - *Věstník Českého geologického ústavu*, 57, 129-143.
- [16] JAKEŠ, P. (1997): Melting in high-P region - case of Bohemian granulites. - *Acta Universitatis Carolinae, Geologica*, 41, 113-125.
- [17] KOTKOVA, J. & HARLEY, S. L. (1999): Formation and evolution of high-pressure leucogranulites: experimental constraints and unresolved issues. - *Physics and Chemistry of the Earth, Part A: Solid Earth and Geodesy*, 24, 299-304.

SYNTHETIC LAALSiO₅: A MIXED-ANION RARE EARTH ALUMOSILICATE

V. Kahlenberg & H. Krüger

Institut für Mineralogie und Petrographie
Universität Innsbruck, Innrain 52, A-6020 Innsbruck, Austria

The crystal structure of a new synthetic lanthanum alumosilicate with composition LaAlSiO₅ has been investigated using single crystal diffraction data collected at room conditions. LaAlSiO₅ crystallizes in the non-centrosymmetric orthorhombic space group $P2_12_12_1$ with twelve formula units per cell ($a = 11.0525(7)$ Å, $b = 5.2261(3)$ Å, $c = 23.7049(21)$ Å, $V = 1369.2(3)$ Å³, $R(|F|) = 0.023$ for 2875 independent observed reflections) and belongs to the group of mixed anion aluminosilicates. Basic building units are isolated [SiO₄] groups as well as tetrahedral double layers of composition [(Al,Si)₅O₁₁]. The two single layers comprising a single double layer are related by 2_1 screw axes running along [100]. Each of these two layers can be thought of as being built from the condensation of unbranched as well as open-branched *zweier* single chains running parallel [010]. Therefore, the whole anion can be classified as a hybrid *zweier* double layer. Stacking of the layers parallel to [001] results in the formation of a three-dimensional structure in which lanthanum cations and isolated SiO₄-groups are incorporated for charge compensation. The three crystallographically independent La-atoms are coordinated by 7–8 oxygen ligands. Concerning the connectedness of tetrahedra in the structure of LaAlSiO₅ one singular (Q⁰), one primary (Q¹) and four quaternary (Q⁴) groups can be distinguished (cf. Figure 1).



Bond valence calculations were performed to obtain the Al/Si distributions for the symmetrically independent T-sites. Four out of six tetrahedra show a strong preference for either Al or Si, whereas the remaining two tetrahedral centers show a Al:Si ratio close to 1:1. Using the silicate classification procedure introduced by Liebau the structural formula of the present compound can be written as $\text{La}_3\{\text{hB}, 2\text{x}^2\}[(\text{Al}, \text{Si})_5\text{O}_{11}][\text{SiO}_4]$.

Figure 1
Projection of the crystal structure of LaAlSiO₅ parallel [010]. White, medium and dark grey tetrahedra correspond to Q³, Q² and Q¹ units.

**AB-INITIO DETERMINATION OF $\text{Na}_2\text{Si}_3\text{O}_7$ FROM CONVENTIONAL
POWDER DIFFRACTION DATA**

V. Kahlenberg¹, B. Marler², J. C. Muñoz Acevedo³ & J. Patarin⁴

¹Institut für Mineralogie und Petrographie
Universität Innsbruck, Innrain 52, A-6020 Innsbruck, Austria

²Institut für Mineralogie
Ruhr-Universität Bochum, D-44780 Bochum, Germany

³Laboratorio de Cristalografía

Facultad de Ciencias Fisicas y Matemáticas, Univ. de Chile, Blanco Encalada 2008, Santiago, Chile

⁴Laboratoire de Matériaux Minéraux
ENSCMu., UPRES-A 7016, 3 rue Alfred Werner, F-68093 Mulhouse, France

The crystal structure of $\text{Na}_2\text{Si}_3\text{O}_7$ has been determined by direct methods using integrated intensities of conventional powder diffraction data and subsequently refined with the Rietveld technique. The title compound was prepared from $\text{Na}_2\text{Si}_3\text{O}_7 \cdot \text{H}_2\text{O}$ by careful thermal decomposition at 440°C. Sodium trisilicate adopts monoclinic symmetry, space group $P2_1/c$ with unit cell parameters $a = 7.1924(5)\text{\AA}$, $b = 10.6039(8)\text{\AA}$, $c = 9.8049(7)\text{\AA}$, $\beta = 120.2478(4)^\circ$, $V = 646.0(9)\text{\AA}^3$ and $Z = 4$. It belongs to the group interrupted framework silicates of four- and three-connected $[\text{SiO}_4]$ -tetrahedra with a ratio of $\text{Q}^3:\text{Q}^4 = 2:1$. There exist different possibilities to subdivide the interrupted framework structure of $\text{Na}_2\text{Si}_3\text{O}_7$ into tetrahedral layers which build up the whole network by corner sharing.

Figure 1 shows the connectivity between the Si-atoms of a single tetrahedral layer perpendicular to [001] in sodium trisilicate. Within the corrugated sheet, chains can be isolated which consist of four-membered (S4R) and six-membered (S6R) rings. At the interface between neighboring chains, S8R are formed. Each S4R consists of two Q3 and two Q4 groups, whereas a single S6R contains four Q3 and two Q4. A projection of $\text{Na}_2\text{Si}_3\text{O}_7$ parallel to [100] is given in Figure 2. As can be seen the framework contains channels running along a with pore openings formed by ten-membered rings. Charge balance within the structure is achieved by the incorporation of sodium atoms which are coordinated by 4 to 6 oxygen ligands. The Na2 atoms are located within the central regions of the tunnels mentioned above, whereas the Na1 ions occupy positions closer to the boundary of the channels. The porous character of the new phase is reflected in a framework density $\text{FD} = 18.6 \text{ T-atoms}/1000 \text{ \AA}^3$, a value which is comparable to those observed in zeolitic materials.

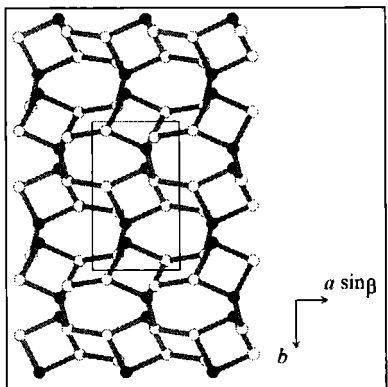


Fig. 1
Projection of a single tetrahedral layer parallel to [001]. O^4 - and O^3 -atoms are represented by black and white spheres, respectively.

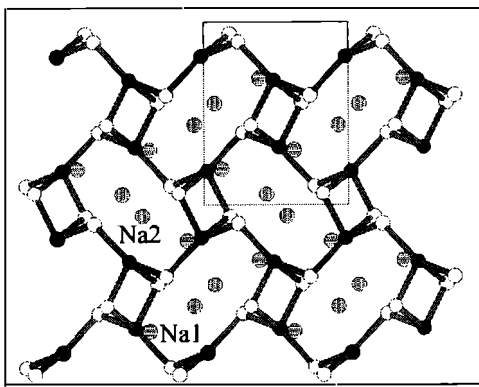


Fig. 2
Projection of the framework parallel to [100].

POLYTYPISM AND STRUCTURAL PHASE TRANSITIONS IN
SODIUM DISILICATE ($\text{Na}_2\text{Si}_2\text{O}_5$)

V. Kahlenberg¹, H. Krüger¹ & S. Rakic²

¹Institut für Mineralogie und Petrographie
Universität Innsbruck, Innrain 52, A-6020 Innsbruck, Austria

²Department of Physics
Faculty of Science, University of Novi Sad, 21000 Novi Sad, Serbia and Montenegro

Alkali disilicates have been studied frequently because of their complex polymorphism as well as for their interesting material scientific applications as ion exchangers in washing powders or sodium ion conductors. Melts with composition $(\text{Na}_{1-x}\text{K}_x)_2\text{Si}_2\text{O}_5$ have been used by geoscientists as models for silicate melt phases. At ambient pressure, as many as six different polymorphs of $\text{Na}_2\text{Si}_2\text{O}_5$ (phases α_{III} , α_{II} , α_{I} , β , γ , δ) are known to appear as a function of temperature and synthesis conditions ([1] and references cited in there). Furthermore, the structures of three high pressure phases, C-, κ -, and ϵ - $\text{Na}_2\text{Si}_2\text{O}_5$ have been described. In the course of an ongoing project on the crystal chemistry of the alkali disilicates we studied samples obtained from the devitrification of glasses. Synthesis conditions covered a pressure and temperature range up to 700°C and 3 Kbar. Structural studies were conducted using X-ray and neutron diffraction at room conditions and at elevated temperatures.

For the single layer silicate α - $\text{Na}_2\text{Si}_2\text{O}_5$ high temperature single crystal diffraction studies have been performed. The compound undergoes two reversible transitions at 678°C and 707°C. The transformations are involved with minor distortions of the SiO_4 -groups and rotations of the tetrahedra about the direction normal to the layer.

Another unsolved structural problem within the group of the known sodium disilicates was the crystal structure of γ - $\text{Na}_2\text{Si}_2\text{O}_5$, a metastable modification which can be obtained from the low temperature crystallization of glasses in the range between 500–580°C at ambient pressures. According to our studies the γ -phase shows a reversible phase transformation at about 563°C. The crystal structures of the LT- and the HT-modification have been determined from single crystal diffraction data. They belong to the rare group of interrupted framework silicates and exhibit low framework densities comparable to zeolite-type materials.

From the hydrothermal experiments single crystals of two new $\text{Na}_2\text{Si}_2\text{O}_5$ phases (C and κ) have been obtained and structurally characterized. Both compounds are based on identical tetrahedral single layers containing six-membered rings and can be considered as polytypes: differences between the structures can be attributed to different ways of stacking of adjacent sheets.

In summary one can say that even in comparatively simple binary systems like Na_2O - SiO_2 there are still a lot of open questions concerning the structural data and the phase relationships of the sodium silicates.

[1] KAHLENBERG, V. ET AL. (1999): The crystal structure of δ - $\text{Na}_2\text{Si}_2\text{O}_5$ - Journal of Solid State Chemistry, 146, 380-386.

**A COMBINED IN-SITU X-RAY AND MÖSSBAUER STUDY
OF THE $P2/n \leftrightarrow C2/c$ PHASE TRANSITION IN OMPHACITE $(Na,Ca)[Al,Mg,Fe^{2+}]Si_2O_6$**

**Katerinopoulou¹, G. Amthauer¹, A. Bieniok¹, M. Bernroider¹, E. Dachs¹,
R. Heinemann², A. H. Kroll², W. Lottermoser¹, G. Redhammer¹ & G. Tippelt¹**

¹Institut für Mineralogie
Universität Salzburg, Hellbrunnerstrasse 34, A-5020 Salzburg, Austria

²Institut für Mineralogie
Universität Münster, Corrensstrasse 24, D-48149 Münster, Germany

At intermediate compositions of the pyroxene solid solution jadeite $NaAlSi_2O_6$ - augite $Ca(Mg, Fe^{2+})Si_2O_6$ and at low temperatures an ordered phase with the space group $P2/n$ occurs, which is known as the mineral omphacite. In addition, natural omphacites may contain variable amounts of acmite $NaFe^{3+}Si_2O_6$. At temperatures around $860^{\circ}C$, the $P2/n$ omphacite undergoes a phase transition to the $C2/c$ space group which is caused by increasing cation disordering (see [1] and references therein). The space group $P2$ has also been described for the ordered omphacite [2]. In the $P2$ structure, there are four distinct M1 and four distinct M2 sites whereas in the $P2/n$ structure there are two distinct M1 and two distinct M2 sites. Structure refinements of the $P2/n$ omphacite show that Mg^{2+} and Al^{3+} are strictly ordered between the two kinds of M1 sites and that Na and Ca are partially ordered between the two kinds of M2 sites. Mg and Al alternate in successive M1 octahedra parallel to the c-axis. This ordering is mainly caused by the different ionic sizes and charges of Mg^{2+} and Al^{3+} as well as by their presence in approximately equal amounts. This ordering at the M1 sites is combined with an ordering at the M2 sites, i.e. Na^+ prefers the M2 sites close to Al^{3+} and Ca^{2+} the M2 sites close to Mg^{2+} in order to achieve local charge balance. An ideal formula for an ordered omphacite would be $(Na_{0.5}Ca_{0.5})[Mg_{0.5}Al_{0.5}]Si_2O_6$, i.e. $Jd_{50}Di_{50}$. In the present investigation a natural omphacite from the island of Syros, Greece is used [3]. Its structure and composition are determined by electron microprobe, scanning electron microscope, and single crystal X-ray diffraction. The transition temperature and the nature of the phase transition are determined by in-situ high temperature X-ray powder diffraction in treated and untreated samples under Argon and vacuum. In addition, heating experiments under controlled oxygen fugacities were performed with the same sample below and above phase transition temperature. The oxidation state and site distribution of iron in treated and untreated samples of both phases have been determined by Mössbauer spectroscopy. At present time, in-situ high temperature Mössbauer measurements are carried out.

Literature

- [1] CARPENTER, M. A. & BOFFA BALLARAN, T. (2001): In: EMU Notes in Mineralogy 3. Solid Solutions in Silicate and Oxide Systems. C. A. Geiger (ed.) 155-178.
- [2] CLARK J. R. & PAPIKE J. J. (1968): Amer.Min. 53: 840-868.
- [3] BRÖCKER, M. & ENDERS, M. (2001): Chemical Geology 175: 581-603.

SINGLE ZIRCON U-Pb GEOCHRONOLOGY OF PRE-VARISCAN AND VARISCAN
BASEMENT UNITS OF THE CENTRAL TAUERN WINDOW, EASTERN ALPS (AUSTRIA)

T. Kebede¹, U. S. Klötzli¹ & G. Pestal²

¹Laboratory for Geochronology - Department of Geological Sciences
Geo-Center, University of Vienna, Althanstrasse 14, A-1090 Vienna, Austria

²Geological Survey of Austria
Tongasse 10-12, A-1031 Vienna, Austria

Variscan and pre-Variscan basement units of the Tauern Window (TW) were strongly overprinted by Alpine orogeny; and, hence, delimiting the basement assemblages into their respective components remains to be challenging. In the last decade several geochronological investigations have been conducted on the TW basement units, however, distinction between the pre-Variscan and Variscan components of the basement rocks of the TW was not done unambiguously. Thus, here we present new single zircon U-Pb ages (all calculated at 2σ) derived from selected lithotectonic units (Basisamphibolit, Biotitporphyroblastenschiefer and equivalent lithologies, Zwölferzug, Habach Phyllite, and Zentralgneis) of the central TW basement sequence. These and published previous age data are combined to resolve outstanding problems such as the relation of Basisamphibolit to Zwölferzug, stratigraphic position and maximum sedimentation age of the Biotitporphyroblastenschiefer, and distinction of the lower and the upper magmatic sequences [UMS & LMS; 1, 2] of the Habach Formation.

Conventional U-Pb zircon geochronology of the different varieties of the Basisamphibolit, namely the coarse-grained garnetiferous metagabbro, banded amphibolite, and medium-grained amphibolite yielded 343 ± 1 Ma, 349 ± 1 Ma, and 352 ± 2 Ma concordia ages, respectively, which are considered as protolith formation ages distinct from that of the Zwölferzug garnet amphibolite ($486 +5/-4$ Ma; [3]). The Basisamphibolit and the Zwölferzug were equated together for several years [4]; however, apart from their different $\epsilon_{Nd}(t)$ values [3], which suggest distinct evolutionary history; the magmatic protolith ages of these rocks provide additional evidence that they are unrelated. Unlike the Basisamphibolit, which formed during Variscan tectonics (Lower Carboniferous), the Zwölferzug garnet amphibolite may have formed coeval with the LMS of the Habach Formation at the margin of Gondwana [cf. 5], and thus need to be disengaged and treated separately in reevaluation of the lithotectonic setup of the TW basement units.

Moreover, laser ablation inductively coupled plasma mass spectrometry (LA-ICP-MS) and conventional U-Pb detrital zircon dating of samples from the banded porphyroblastic biotite schist (Wager Alm, Amertal), porphyroblastic biotite schist (Lemperbach) and two-mica plagioclase gneiss (Brentling and Lemperbach) from the Biotitporphyroblastenschiefer yielded maximum sedimentation ages at 362 ± 5.7 Ma, 368 ± 17 Ma, and 368 ± 16 Ma, respectively. In addition, a banded garnetiferous leucocratic gneiss sample (Zwölferzug) also produced a maximum sedimentation age at 357.9 ± 9.7 Ma.

The banded garnetiferous leucocratic gneiss was believed to be a granitic orthogneiss emplaced into the Zwölferzug garnet amphibolite. However, the presence of abundant detrital zircon grains of which some produced older ages (496 ± 13 Ma, 550 ± 6 Ma, 587 ± 13 Ma) than that of the garnet amphibolite ($486 +5/-4$ Ma; [3]) strongly suggest a sedimentary origin of the unit. Furthermore, conventional U-Pb dating of a pinkish euhedral magmatic zircon population (derived from the abundant gabbroic clasts) and rounded detrital zircon grains from the meta-agglomerate (Habach Phyllite, Felberberg) yielded an upper intercept age at 536 ± 8 Ma and nearly concordant age at 506 ± 8.5 Ma, respectively. The 536 ± 8 Ma age is interpreted as a magmatic protolith age of a gabbroic source rock that is comparable to LMS of the Habach formation [e.g., 7]. Even though, the detrital zircons were well screened the 506 ± 8.5 Ma age can be tentatively considered as maximum sedimentation age for the meta-agglomerate of the Habach Phyllite, which was considered to be part of the sedimentary cover of the UMS [2].

Overall, the Upper Devonian maximum sedimentation ages obtained from the detrital zircons derived from samples of the Biotitporphyroblastenschiefer and Zwölferzug coupled with protolith ages of the Basisamphibolit, which has unconformable contact with the Biotitporphyroblastenschiefer [6], further constrain the maximum sedimentation age of these sediments to be Upper Devonian to Lower Carboniferous. Hence, the Basisamphibolit and the Biotitporphyroblastenschiefer form parts of the Variscan basement sequence of the central TW; but not Upper Proterozoic to Lower Paleozoic pre-Variscan basement as formerly contemplated. The LMS of the Habach Formation [488–547 Ma; 3, 7] and the Zwölferzug garnet amphibolite predate the opening of the Paleo-Tethys in the Early Silurian [e.g., 8], may constitute parts of the European Hun Terranes and also represent part of the pre-Variscan basement rocks in the TW. Conversely, the UMS of the Habach Formation constitutes part of the Variscan basements. Thus, distinction must also be made between the LMS and the UMS of the Habach Formation, which represent parts of the pre-Variscan and Variscan basements, respectively. The lithotectonic positions of the central TW basement units require reevaluation and reinterpretation in view of the new age data, which may have significant contribution to the geological history of the eastern Alps in general.

Reference

- [1] KRAIGER, H. (1988): Die Habachformation – ein Produkt ozeanischer und kontinentaler Kruste. - Mitt. Österr. Geol. Ges., 81, 47-64.
- [2] HÖCK, V. (1993): The Habach-Formation and the ‘Zentralgneis’ - a key in understanding the Paleozoic evolution of the Tauern Window (Eastern Alps). - In: Raumer, J. F. von, Neubauer, F. (eds) Pre-Mesozoic geology in the Alps. Springer, Berlin Heidelberg, pp 361-374.
- [3] QUADT, A. VON (1992): U-Pb zircon and Sm-Nd geochronology of mafic and ultramafic rocks from the central part of the Tauern Window (Eastern Alps). - Contribution Mineralogy Petrology, 110, 57-67.
- [4] FRASL, F. & FRANK, W. (1966): Zur Mineralogie und Geologie des Landes Salzburg und der Tauern. - Aufschluß, 15, 30-58.
- [5] RAUMER, J. F. VON ET AL. (2002): Organization of pre-Variscan basement areas at the north-Gondwana margin. - International Journal Earth Sciences, 91, 35-52.
- [6] PESTAL, G. (1983): Beitrag zur Kenntnis der Geologie in den mittleren Hohe Tauern in Bereich des Amer- und des Felbertales. - Ph.D. Thesis, Univ Wien.

- [7] EICHHORN, R. ET AL. (1999): Implications of U-Pb SHRIMP zircon data on the age and evolution of the Felbertal tungsten deposit (Tauern Window, Austria). - International Journal Earth Sciences, 88, 496-512.
- [8] STAMPFLI, G. M. & BOREL, G. D. (2002): A plate tectonic model for the Paleozoic and Mesozoic constrained by dynamic plate boundaries and restored synthetic oceanic isochrons. - Earth Planetary Science Letters, 196, 17-33.

This work is financially supported by FWF (Project No. 14228).

STABLE ISOTOPE STUDY ON TRAVERTINES FROM BUDAKALASZ
(BUDA MTS., HUNGARY)

S. Kele¹, O. Vaselli² & Cs. Szabó¹

¹Lithosphere Fluid Research Lab. - Department of Petrology and Geochemistry
Eötvös University, Budapest, Hungary

²Department of Earth Sciences
University of Florence, Florence, Italy

Travertines from the Pannonian Basin have been studied for almost one hundred years. However, principles, concepts and technical background in geology have been dramatically changed during the past decades. As a consequence, beside stratigraphic and microfacies descriptions, valuable information can be contributed to paleohydrological and paleoclimatological studies by using geochemical and stable isotope data obtained on travertines. The major goal of this work is to carry out a detailed C and O stable isotope study on Budakalász travertine (Buda Mts., Hungary) in agreement with previous microfacies analyses (KOVACS, 1995) to find out the origin of CO₂ in water from which travertine deposited.

The Pleistocene Budakalász travertine deposit lies on early Oligocene Hárshegy Sandstone and Kiscell Clay Formations. Early Pleistocene limnic clay and gravel terrace can be found under the limestone suggesting a former limnic and fluvial environment (SCHEUER ET AL., 1987). The travertine is covered by a few meters thick loess and overlain by a thin humus layer. The Ezüsthegy quarry is approximately 800 meters long and 15–20 meters high. Sixty travertine samples have been collected at three vertical sections of the travertine quarry. Microfacies and petrographic analyses have been performed on some samples. Selected travertines were analyzed for δ¹³C and δ¹⁸O using Finnigan 250 MAT Delta-S mass-spectrometer.

Based on petrographic and microfacies analyses, the Budakalász travertine samples of the three sections studied can be divided into two stratigraphic groups. The lower part of each section (approx. 15 meters thick) consists of massive travertine that represents smooth slope facies, and in the terrace pools, shrub facies (Fig. 1) as the result of bacterial activity. The whole lower part of the sections is characterized by values of δ¹³C(PDB) = 2.2 ‰ and δ¹⁸O(PDB) = -12.1 ‰. The upper part of the beds studied represents marsh pool facies, deposited from a small lake, and has values of δ¹³C(PDB) = 1.7 ‰ and δ¹⁸O(PDB) = -10 ‰. Between the lower and upper parts of the sections calcareous mud layers were observed inferring to terrestrial period and could have been a relatively long break in deposition. Based on the isotopic data, and using Pentecost's (1995) classification, the Budakalász travertine is thermogene fresh water limestone which formed presumably associated with late activity of the Miocene volcanism widely recognized around the studied area.

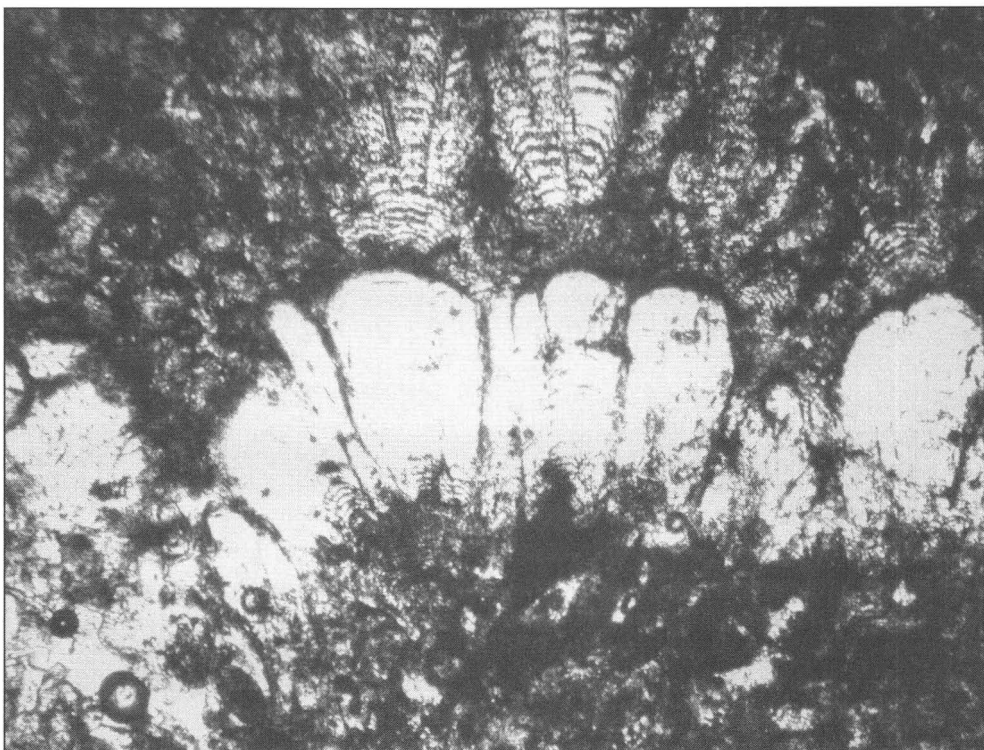


Fig. 1

Bacterial shrub-facies in travertine.

References

- KOVÁCS, A. (1995): M. Sc. thesis, Eötvös University, Budapest, Department of Applied and Environment Geology.
PENTECOST, A. (1994): Quaternary Science Review, 14, 1005-1028.
SCHEUER, GY., SCHWEITZER, F. & SZLABÓCZKY, P. (1987): Építőanyag, 39, 102-107.

**THE “BOZENER QUARZPORPHYR” (SOUTHERN ALPS, ITALY):
SINGLE ZIRCON U/PB AGE EVIDENCE FOR 10 MILLION YEARS OF MAGMATIC
ACTIVITY IN THE LOWER PERMIAN**

U. S. Klötzli¹, V. Mair² & G. M. Bargossi³

¹Laboratory for Geochronology - Department of Geological Sciences
Geo-Center, University of Vienna, Althanstrasse 14, A-1090 Vienna, Austria

²Amt für Geologie und Baustoffprüfung
Eggentalerstrasse 48, I-39053 Kardaun, Italy

³Department of Earth Sciences
University of Bologna, Piazza di Porta S. Donato, I-40126 Bologna, Italy

During the Permian the Southern Alps were affected by a prominent igneous activity that produced voluminous basic to acidic volcanic and plutonic rocks. The magmatism originated during a period of post-orogenic extension and transtensional faulting controlling magma ascent and emplacement.

The "Bozener Quarzporphyry", well known for its usage in road and house construction, forms part of the Atesina Volcanic District (AVD). Together with the Monte Luco volcanics, and the Cima d'Asta, Bressanone, Ivigna, Monte Croce and Monte Sabion intrusives, it constitutes a major part of the Permian magmatism in the central-eastern Southern Alps. The rocks represent a continuum of lithologies ranging from basaltic andesites to rhyolites, and from gabbros to monzo-granites, respectively, and where acidic varieties are more common. The metaluminous to slightly peraluminous rocks exhibit mineralogical, petrographical, and geochemical characteristics of a high-K calc-alkaline suite. Isotopic and geochemical evidence support a hybrid nature of both volcanic and plutonic rocks being derived by complex interactions between mantle melts and crustal material [1].

Published radiometric age determinations of different volcanic and plutonic rocks range between 297 Ma and 270 Ma (Rb/Sr and K/Ar biotite ages, U/Pb zircon ages, Th/Pb allanite ages [2, 3, 4]). For the Collio Basin single zircon U/Pb ages for the magmatic activity range between 283 ± 1 Ma and 281 ± 2 Ma [5]. A somewhat younger volcanic activity is recorded in the Monte Luco sequence, as suggested by palynostratigraphic "ages" (260 Ma – 255 Ma) determined on lacustrine sediments (Tregiovo Formation) intercalated with rhyolitic ignimbrites [6].

The volcanics of the AVD have not been dated directly previously. Therefore, a detailed single zircon U/Pb study was made in order to establish the absolute age and duration of the AVD igneous activity (reported errors are ± 2 sigma).

In concordance with field evidence the oldest volcanic activity of the AVD is recorded in the Formazione di Plazzoles: Ignimbritic rhyolites forming intercalations within the Ponte Gardena Conglomerate are dated at 284.9 ± 1.6 Ma. Rhyodacitic porphyries exhibit the same age (284.5 ± 1.7 Ma).

After a break of c. 5 Ma the volcanic activity continues with the extrusion of the Formazione di Monte Luco: a pyroclastic flow, interpreted as a surge product, is dated at 279.6 ± 1.5 Ma, whereas a rhyodacitic lava dome has an age of 278.4 ± 1.5 Ma. The overlying rhyodacitic ignimbrite, termed Ignimbrite di Gargazzone, shows at its base an age of 276.5 ± 1.1 Ma. A subvolcanic body found within these ignimbrites, the so called Subvulcanite di Terlano, is indistinguishable in age (276.1 ± 1.5 Ma). Rhyolitic ignimbrites of the Formazione di Nalles more to the SE of the Formazione di Gargazzone again show the same age as the latter two formations (276.7 ± 1.1 Ma). The next higher unit is called Ignimbrite di Gries. It is made up by rhyolitic ignimbrites which in some parts were deposited concordantly on the Formazione di Nalles but in other areas show an erosive contact to the Ignimbrite di Gargazzone. Its age is 276.9 ± 2.3 Ma. Also with an erosive contact to the Formazione di Nalles the rhyolitic lavas of the Lave di Andriano formation were extruded at 274.6 ± 2.1 Ma. This suggests that after the deposition of the Formazione di Nalles and Gargazzone and going hand in hand with erosional events there seems to be a hiatus in the volcanic activity of 1–2 Ma.

Somewhat problematic is the age of 277.0 ± 2.0 Ma found for the rhyolitic ignimbrites of the Ignimbrite di Vadena. According to the mapping results these deposits should be younger than the Ignimbrite di Gries. The volcanic activity terminates with the formation of the Ignimbrite di Predonico at 274.1 ± 1.4 Ma.

The following conclusions can be drawn from the age data: a) The very long volcanic activity suggested by the published age data [2, 3, 4] cannot be further substantiated. The new single zircon U/Pb age data suggest that the volcanism in the AVD lasted only c. 10 Ma. b) The activity was not continuous but was interrupted twice for some million years. c) Compared to the Collio Basin [5] the volcanism was more long lasting. d) The palynostratigraphic "ages" of the Tregiovo Basin [6] have to be corrected according to the age found for the Formazione di Monte Luco (c. 279 Ma). e) The determined ages fit well into the general age pattern found for the Permian magmatism in the Southern Alps.

References

- [1] ROTTURA, A., ET AL. (1998): Origin and significance of the Permian high-K calc-alkaline magmatism in the central-eastern Southern Alps, Italy. - *Lithos*, 45, 329–348.
- [2] BARTH, S. (1994): Calc-alkaline basic to silicic rock suites from the Late Hercynian Atesina - Cima d'Asta volcano-plutonic complex. - *Neues Jahrbuch für Mineralogie, Abhandlungen*, 168, 15–46.
- [3] ROTTURA, A., ET AL. (1997): Petrogenesis of the Monte Croce granitoids in the context of the Permian magmatism of the Southern Alps. - *European Journal of Mineralogy*, 9, 1293–1310.
- [4] CASSINIS, G. & NERI, C. (1999): Outline of the Permian stratigraphy in the Southern Alps. - In: *Field Trip Book, International field conference on "The continental Permian of the Southern Alps and Sardinia (Italy)"*, Brescia, Italy, 7–11.
- [5] SCHALTEGGER, U. & BRACK, P. (1999): Radiometric age constraints on the formation of the Collio Basin (Brescian Prealps). - In: *Field Trip Book, International field conference on "The continental Permian of the Southern Alps and Sardinia (Italy)"*, Brescia, Italy, 71.
- [6] BARTH, S. & MOHR, B. (1994): Palynostratigraphically determined age of the Tregiovo sedimentary complex in relation to radiometric emplacement ages of the Atesina volcanic complex (Permian, Southern Alps, Italy). - *Neues Jahrbuch für Geologie und Paläontologie, Abhandlungen*, 192/2, 273–292.

**REGOLITH MIXING RELATIONSHIPS ON THE SURFACE OF MARS:
INFLUENCE ON MINERALOGY AND GEOCHEMISTRY**

C. Kolb¹, R. Abart^{2,3} & R. Kaindl²

¹Space Research Institute

Austrian Academy of Sciences, A-8042 Graz, Austria

²Institute of Mineralogy and Petrology

University of Graz, A-8010 Graz, Austria

³Institute of Mineralogy and Petrography

University of Basel, CH-4056, Switzerland

Due to the cessation of active plate tectonics several billions years ago, the Martian sedimentary record represents a long term archive of the exogenic cycle. Meteoritic and aeolian gardening is an important physical process acting on this record. The fingerprint of chemical fractionations and mineralogical transformations may provide insight into the processes involved in primary material degradation and sediment formation and they may allow to reconstruct the environmental conditions on the ancient Martian surface. In this context the main target is to identify chemical trends or mineral phases that are diagnostic for specific processes and environments. Weathering under warm and wet conditions would have produced typical secondary mineralogical remnants such as clay minerals [1]. Hydrothermal activity and acid fog weathering would produce sulphates and chlorides [2], and biological activity could be the source of carbonates and iron oxides such as magnetite [3]. In particular the variation of element concentrations with depth may allow to reconstruct past changes in the contributions from different source materials [4, 5] and in soil formation processes, which involve volcanic aerosols and hydrothermal activity [2, 6].

Given that the evolution of the rate of meteoritic infall is known a depth profile of the Ni concentration in the Martian regolith may give insight into the evolution of the rate of soil formation during the geologic past. Pristine, cosmic material, which is continuously delivered to the Martian surface through meteoritic infall, contains considerable quantities of organic matter – the prerequisites for the evolution of life. Organic material has, however, not yet been detected on the surface of the planet. The lack of organic material on the Martian surface despite of the continuous meteoritic delivery is ascribed to the reactivity of the Martian soil [7]. This is obviously a result of intense atmosphere-surface interaction under strong UV solar-radiation and has important influence on future human space-flight and Exobiology in general - and possibly involves adsorbed superoxide [8]. Such radicals not only drive the degradation of organic matter, they may also contribute to oxidative weathering of primary minerals [9]. It is known from earlier missions, that iron and sulphur occur in high oxidation states in the Martian regolith, and provided, that this is not the case in the magmatic and meteoritic precursor materials, the Martian surface may act as an oxygen sink and in this respect may have a considerable effect on the evolution of the Martian atmosphere [10].

We present a study of regolith mixing relationships, in particular stressing the meteoritic contribution in the Martian soil by means of least squares (LS) analysis of chemical data from APXS-*Mars-Pathfinder* (*MPF*) [11] and XRF-*Viking* [12] measurements. Despite of other possible soil formation processes, the soil composition may be represented as a mixture of primitive cosmic material (CI-chondrite), the *MPF*-soil free rock (SFR) and physical weathering products of *MPF*-andesites (PWP). In our LS analysis 13 major elements were taken into account. The SFR and CI-chondrite compositions were taken from [11] and [13], respectively. Prior to LS analysis a CIPW normative calculation was done on the SFR chemistry. In analogy to Antarctic weathering scenarios, minerals with high susceptibility to physical disintegration were assigned to a fraction of detritus PWP according to their normative ratios in parent andesites. To account for the uncertainties inherent in analytical data from Mars, the individual element concentrations were weighted accordingly. The convergence of linear regression lines to a single point indicate the existence and the composition of a Global Dust Unit (GDU). GDU material appears to be intimately admixed to *MPF* surface soils and also to *Viking* deep soil samples. Some GDU material also appears to adhere to *MPF* rock samples. According to the inferred meteoritic contribution, 1.4 wt.% C is missing in the Martian soil. Similarly, 0.4 wt.% Ni should be present in surface soils. This is more than APXS X-ray mode data would suggest. Secondary fluorescence of Fe_{Kα} may have reduced the Ni_{Kα} radiation in the presence of abundant iron. Alternative in-situ analytical techniques, such as Laser-induced Plasma Spectroscopy (LIPS), may help to resolve this problem. APXS spots were targets of vis/NIR reflectance analysis during the Pathfinder mission. Consequently, the oxidation states of these samples can be determined by means of terrestrial analogue calibration. Three dimensional regression analysis of oxidation states suggests that the meteoritic fraction is main source material for oxidation processes. Based on terrestrial analogue calibration the product phases may comprise nanophased ferric oxides, which are thought to be present on the Martian surface [14].

References

- [1] WYATT, M. & H.Y. McSWEEN, JR. (2002): Spectral evidence for weathered basalt as an alternative to andesite in the northern lowlands of Mars. - *Nature*, 417, 263-266.
- [2] NEWSOM, H. E. & HAGERTY, J. J. (1999): Mixed hydrothermal fluids and the origin of the Martian soil. - *J. Geophys. Res.*, 104, 8717-8728.
- [3] THOMAS-KEPRTA, K. L. ET AL. (2002): Magnetofossils from Ancient Mars: a Robust Biosignature in the Martian Meteorite ALH 84001. - *Appl. Env. Micro.*, 68, 3663-3672.
- [4] FLYNN, G. J. & MCKAY, D. S. (1990): An Assessment of the Meteoritic Contribution to the Martian Soil. - *J. Geophys. Res.*, 95, 14,497-14,509.
- [5] KOLB, C. ET AL. (2003): The meteoritic component on the surface of Mars: Implications for organic and inorganic geochemistry. - 66th Annual Meteoritic Society Meeting, #5014.
- [6] WIENS, R. C. ET AL. (2002): Critical Issues in Martian Geochemistry Involving Minor and Trace Elements, and the Application of Laser-Induced Breakdown Spectroscopy (LIBS). - *LPSC*, XXXIII, #1348.
- [7] OYAMA, V. I. & BERDAHL, B. J. (1977): The Viking Gas Exchange Experiment Results From Chryse and Utopia Surface Samples. - *J. Geophys. Res.*, 82, 4669-4676.
- [8] YEN, A. S. ET AL. (2000): Evidence that the Reactivity of the Martian Soil is due to Superoxide Ions. - *Science*, 289, 1909-1912.

- [9] YEN, A. S. (2001): Composition and Color of Martian Soil from Oxidation of Meteoritic Material. - LPSC, XXXII, #1766.
- [10] LAMMER, H. ET AL. (2002): Loss of water from Mars: Implications for the oxidation of the soil. - submitted to Icarus.
- [11] WÄNKE, H. ET AL. (2001): Chemical Composition of Rocks and Soils at the Pathfinder Site. - Space Sci. Rev., 96, 317-330.
- [12] CLARK, B. C. ET AL. (1982): Chemical Composition of Martian Fines. - J. Geophys. Res., 87, 10,059-10,067.
- [13] WASSON, J. T. & KALLEMEYN G. W. (1988): Composition of Chondrites. - Phil. Trans. Roy. Soc., A325, 535-544.
- [14] MORRIS, R. V. ET AL. (2000): Mineralogy, composition, and alteration of Mars Pathfinder rocks and soils: Evidence from multispectral, elemental, and magnetic data on terrestrial analogue, SNC meteorite, and Pathfinder samples. - J. Geophys. Res., 105, 1757-1817.

SYNTHETIC MARS ANALOGUE MATERIALS

C. Kolb¹, R. Abart^{2, 3}, G. Ragg⁴, P. Ulmer⁵ & W. Lottermoser⁶

¹Space Research Institute

Austrian Academy of Sciences, A-8042 Graz, Austria

²Institute of Mineralogy and Petrology

University of Graz, A-8010 Graz, Austria

³Institute of Mineralogy and Petrography

University of Basel, CH-4056, Switzerland

⁴Institute of Mineralogy and Petrography

University of Innsbruck, A-6020 Innsbruck, Austria

⁵Institute of Mineralogy and Petrography

ETH-Zürich, CH-8092 Zürich, Switzerland

⁶Institute of Mineralogy

University of Salzburg, A-5020 Salzburg, Austria

For most planetary investigations only remotely sensed or robotic lander data are available. With the exception of meteorites, the Moon is the only celestial body, from which material was brought into terrestrial laboratories, up to now. For the correct identification of the extraterrestrial materials, comparisons with terrestrial analogue materials are absolutely necessary. From former Mars missions several well defined material properties of the Martian surface soil are known: bulk chemistry (*Viking, Mars Pathfinder*), vis/NIR reflectance spectra (*Mars Pathfinder, Phobos 2*, ground-based telescopes), grain size limits (*Mars Pathfinder*), specific surface (*Viking*), thermal emission spectra (TES on *Mars Global Surveyor*). Mössbauer spectroscopy – a part of *Beagle 2* (lander of ESA's Mars Express mission) – will provide useful data on oxidation states in addition to existent vis/NIR reflectance spectra [1]. From reflectance studies at the *Pathfinder* landing site [2] it was found that almost all iron in the Martian dust or soil occurs in oxidation state III ($\text{Fe}^{3+}/\text{Fe}^{2+} = 20-3$), which is in contrast to oxidation states of Martian andesites ($\text{Fe}^{3+}/\text{Fe}^{2+} = 3-0.7$). Obviously, oxidation occurred during soil formation. The mineralogy of the weathering products is hardly known. Studies of multispectral properties argue for hematite and nanophase goethite. Maghemite, akaganeite, schwertmannite, and nanophase lepidocrocite are also possible interpretations for Martian ferric weathering minerals [2]. Mg-sulphates, chlorides and clay minerals are additionally regarded as weathering phases [3, 4, 5].

The synthesis of analogue mixtures may give insight on formation processes of Martian surface materials. Provided that the condition of formation of the terrestrial analogue materials is known properly, this could lead to a better knowledge of the formation of these materials on other planets. In this context it is important that the co-genetic mineral-paragenesis is considered as an integrity.

Hence, the search for numerous planetary analogue sites on Earth is an important task in comparative planetology [6]. Further, appropriate analogue materials in planetary simulation experiments could reveal processes, which are not only important for the understanding of the planet of interest, but also for the solar system in general. To decide between natural and synthetic phase mixtures in analogue mineralogy, one has to take under consideration the aim of each experiment. The advantage of nature-sediments is the possibility of cheap delivery of large amounts of soil. The disadvantage is the uncertainty in characterising of natural soils (not useful e.g. in quantitative adsorption-experiments and other experiments with high or even unknown complexity) and the (recent) difference in soil-forming-processes between Earth and Mars. Synthetic mixtures may nicely complement natural materials. An advantage of synthetic materials is the possibility of fine-adjustment of their components and therefore the evaluation of their influence. The physico-chemical properties of the prepared material can fit as much as possible the observed data from space missions. The synthesis of analogue materials may be adjusted to the kind of experiments and the complexity of the desired information. To define and characterise analogue materials, several analytic techniques are necessary: chemical analysis (XRF), X-ray diffraction (XRD), diffuse reflectance vis-NIR-spectroscopy, FTIR-spectroscopy, Combustion Analysis, Mössbauer spectroscopy, grain size analysis, Scanning Electron Microscopy, nitrogen desorption and adsorption experiments (pore volume and specific surface area), etc.

We prepared synthetic mixtures of synthetic rock glass powder with - partly nanophasized - ferric oxides, sulphates, chlorides and clay minerals. The synthetic rock glass matches the chemical composition of Martian fines diminished by anticipated weathering phases. Additionally, the oxidation state of iron was adjusted to different levels by means of glass synthesis under controlled oven atmospheres. Comparisons with data from the Martian surface and other analogue materials will be shown. Especially, vis/NIR Reflectance and Mössbauer Spectroscopy results are considered.

References

- [1] KLINGELHÖFER, G. ET AL. (1996): Mineralogical analysis of Martian soil and rock by a miniaturized back-scattering Mössbauer spectrometer. - *Planet. Space Sci.*, 44, 11, 1277-1288.
- [2] MORRIS, R. V. ET AL. (2000): Mineralogy, composition, and alteration of Mars Pathfinder rocks and soils: Evidence from multispectral, elemental, and magnetic data on terrestrial analogue, SNC meteorite, and Pathfinder samples. - *J. Geophys. Res.*, 105, 1757-1817.
- [3] TOULMIN, P. ET AL. (1977): Geochemical and Mineralogical Interpretation of the Viking Inorganic Chemical Results. - *J. Geophys. Res.*, 82, 4625-4634.
- [4] MCSWEEN JR., H. Y. & KEIL, K. (2000): Mixing relationships in the Martian regolith and the composition of globally homogeneous dust. - *Geochim. Cosmochim. Acta*, 64, 2155-2166.
- [5] WYATT, M. & MCSWEEN JR., H. Y. (2002): Spectral evidence for weathered basalt as an alternative to andesite in the northern lowlands of Mars. - *Nature*, 417, 263-266.
- [6] KOLB, C. ET AL. (2001): Mineralogy of Mars Soil Analogue material. - IWF-137, 50 pp.

**THE CRYSTAL STRUCTURE OF AN APPARENTLY NEW
MAGNESIUM SILICATE MINERAL: A POLYTYPE OF CARLOSTURANITE ?**

U. Kolitsch¹, E. Belluso², A. Gula^{1,2} & G. Ferraris²

¹Institut für Mineralogie und Kristallographie

Universität Wien, Geozentrum, Althanstrasse 14, A-1090 Wien, Austria

²Dipartimento di Scienze Mineralogiche e Petrologiche

Università degli Studi di Torino, Via Valperga Caluso, 35, I-10125 Torino, Italia

Preliminary results will be presented on the crystal structure and physico-chemical properties of an apparently new magnesium silicate mineral which may be a polytype of carlosturanite, $M_{24}[T_{12}O_{28}(OH)_4](OH)_{30}\cdot H_2O$ (where M = Mg, Fe, Ti, Mn, and Cr; and T = Si and Al) [1-3]. Carlosturanite (CST) is a water- and Mg-rich, Si-poor, serpentinite-like, asbestosiform mineral, which is locally common in low-grade serpentinite rocks in the Italian Western Alps [4]. On the basis of chemical composition, XRPD and TEM data, a structure model of CST differing from that of lizardite only by substitution of rows of $[Si_2O_7]^{6-}$ by $[(OH)_6H_2O]^{6-}$ groups was proposed [2]. However, subsequent HRTEM images suggested possible variants of the proposed model [5].

The present studies used samples from two very close localities in the Po Valley, Cuneo, Piedmont, Italy. Fibrous samples intergrown with a not well identified layer silicate, from the first locality, were investigated by TEM, XRPD, SEM-EDS and EPMA, and results suggested a close relation to CST. Well-crystallised samples from the second locality provided brownish, transparent to translucent, lath-shaped crystals (platy on (100) and elongated along [010]) suitable for a single-crystal structure determination (Mo-K α radiation, CCD area detector, $2\theta_{max} = 60^\circ$, $R_{int} = 1.8\%$). These crystals are monoclinic, space group $C2/m$, with $a = 14.583(3)$, $b = 9.414(2)$, $c = 18.306(4)$ Å, $\beta = 102.09(3)^\circ$, $V = 2457.4(9)$ Å 3 , and $Z = 2$. By the transformation matrix (102/010/-100) an F-centred cell with $a = 36.46$, $b = 9.414$, $c = 14.583$ Å, $\beta = 100.93^\circ$ is obtained. This cell orientation suggests a close, polytypical relation (see below) to CST which has the unit cell $a = 36.70$, $b = 9.41$, $c = 7.291$ Å, $\beta = 101.1^\circ$, $V = 2470.8$ Å 3 , space group Cm [1, 2]. The structure has been solved and refined to $R1 = 3.0\%$ and $wR2_{all} = 9.4\%$ for 6643 'observed' reflections with $F_o > 4\sigma(F_o)$.

The structure refinement gave the formula $(Mg,Fe,Ti,Mn)_{24}(Si,Al)_{12}O_{32}(OH)_{32}$, which appears richer in octahedral cations than that given for CST. However, because only a TEM-based structure model is known for CST [2], and the determination of its correct chemical formula was hampered by intergrowths with serpentinite minerals and fibrous diopside, the chemical formula of CST may in fact be very close to that of the new mineral. The X-ray powder diffraction patterns of both species are very similar, especially if the probable influence of preferred orientation is considered.

The structure is characterised by two interpenetrating octahedral sheets composed of MgO_6 octahedra: one sheet parallel to (-201) and another, staggered sheet parallel to (001). At the intersection, both sheets are vacant and a [010] tunnel corresponding to an empty row of octahedra occurs. Thus, the octahedral sheets actually consist of two kinds of [010] strips: one is six-octahedra wide and parallel to (-201); the other is two-octahedra wide and parallel to (001). Silicate strips with a fixed width run along the b-axis. They are built from 6-membered rings linked along [010] via a single common O_{Si} atom. These silicate strips decorate the (-201) octahedral sheets in an alternating way (strips attached to the sheet bottom alternating with strips attached to the top; both 'bottom' and 'top' strips are linked to each other along [102] via two common O_{Si} ligands, thus resulting in 4-, 6- and 8-membered rings. The presence of silicate strips decorating octahedral sheets reveals some structural relations to the strip-like members of the 2:1 sheet silicates (ganophyllite/eggletonite, tamaite, minnesotaite, bannisterite, ajoite).

A refinement of the occupancies of all 8 Mg positions confirmed, along with polyhedral distortions of these positions, that most of these sites host variable but minor amounts of Fe and Ti (and very minor Mn), in agreement with the EPMA data.

It appears likely that the crystal structure of CST can be obtained from that of the apparent new polytype by shifting one TO layer of $b/2$. In this way, the periodicity of 14.583 Å is halved and the F-centred cell mentioned above becomes the C-centred cell reported for CST [1, 2]. Simulation of HRTEM images of both phases is in progress.

G. C. Piccoli and M. Ciriotti are thanked for kindly providing the studied samples. Financial support by the Austrian Science Foundation (FWF) (Grant P15220-N06) is gratefully acknowledged.

References

- [1] COMPAGNONI, ET AL. (1985): Carlostanite, a new asbestosiform rock-forming silicate from Val Varaita, Italy. - American Mineralogist, 70, 767-772.
- [2] MELLINI, ET AL. (1985): Carlostanite: HRTEM evidence of a polysomatic series including serpentine. - American Mineralogist, 70, 773-781.
- [3] MELLINI, M. & ZUSSMAN, J. (1986): Carlostanite (not 'picrolite') from Taberg, Sweden. - Mineralogical Magazine, 50, 675-679.
- [4] BELLUSO, E. & FERRARIS, G. (1991): New data on balangeroite and carlostanite from alpine serpentinites. - European Journal of Mineralogy, 3, 559-566.
- [5] FERRARIS, G. (1997): Polysomatism as a tool for correlating properties and structure. In S. Merlini (ed.): Modular aspects of minerals. EMU Notes in Mineralogy, 1, 275-295.

Cs₃ScSi₈O₁₉, A NEW MICROPOROUS SILICATE WITH EIGHT-MEMBERED RINGS

U. Kolitsch & E. Tillmanns

Institut für Mineralogie und Kristallographie
Universität Wien, Geozentrum, Althanstrasse 14, A-1090 Wien, Austria

During investigations of the system Sc₂O₃-Al₂O₃-TiO₂-SiO₂, which contains several important ceramic phases, a new microporous compound, Cs₃ScSi₈O₁₉, was synthesized as colourless, glassy plates from a CsF-MoO₃ flux. The crystal structure was determined from single-crystal X-ray diffraction data (Mo-K α radiation, CCD area detector, $2\theta_{\max} = 60^\circ$, $R_{\text{int}} = 1.3\%$). The compound is orthorhombic, space group *Pnma*, with $a = 11.286(2)$, $b = 7.033(1)$, $c = 26.714(5)$ Å, and $Z = 4$ ($R_1 = 2.6\%$ and $wR_2^{\text{all}} = 7.3\%$ for 3066 'observed' reflections with $F_o > 4\sigma(F_o)$).

The structure of Cs₃ScSi₈O₁₉ represents a novel, mixed octahedral-tetrahedral framework structure type. It is based on isolated, nearly regular ScO₆ octahedra [$d_{av}(\text{Sc}-\text{O}) = 2.112$ Å] sharing corners with SiO₄ tetrahedra to form an open framework with four-, six- and eight-membered rings; the latter are composed of SiO₄ tetrahedra only. Three non-equivalent Cs atoms occupy large voids in the framework, close to the puckered eight-membered rings. The voids are connected into channels running along several directions. One Cs position is split into four partially occupied and disordered sites. Determinations of the unit-cell parameters at 120 K suggest no phase transition, and an only very small volume shrinkage of ca. 0.4 %.

The structure is compared with that of the structurally related compound Cs₂TiSi₆O₁₅ [1, 2] and with other natural and synthetic microporous titano- and zircono-silicates, which recently have attracted considerable interest due to their microporous properties, e.g. [3]. Cs₃ScSi₈O₁₉ or derivatives may be important in the context of immobilisation of radioactive Cs waste, cationic conductivity or catalysis.

Financial support by the Austrian Science Foundation (FWF) (Grant P15220-N06) is gratefully acknowledged.

References

- [1] GREY ET AL. (1997): The crystal structure of Cs₂TiSi₆O₁₅. - *Journal of Solid State Chemistry*, 131, 38-42.
- [2] NYMAN ET AL. (2000): Integrated experimental and computational methods for structure determination and characterization of a new, highly stable cesium silicotitanate phase, Cs₂TiSi₆O₁₅ (SNL-A). - *Chemistry of Materials*, 12, 3449-3458.
- [3] ROCHA, J. & ANDERSON, M. W. (2000): Microporous titanosilicates and other novel mixed octahedral-tetrahedral framework oxides. - *European Journal of Inorganic Chemistry*, 2000, 801-818.

**CHEMICAL TRANSPORT REACTION STUDIES OF THE SYSTEM $\text{Sc}_2\text{O}_3\text{-}\text{Al}_2\text{O}_3\text{-}\text{TiO}_2\text{-}\text{SiO}_2$:
GROWTH AND STRUCTURAL STUDIES OF SINGLE CRYSTALS OF MULLITE AND
OTHER PHASES**

U. Kolitsch¹, M. Weil² & E. Tillmanns¹

¹Institut für Mineralogie und Kristallographie

Universität Wien, Geozentrum, Althanstrasse 14, A-1090 Wien, Austria

²Institut für Chemische Technologien und Analytik, Bereich Strukturchemie
Technische Universität Wien, Getreidemarkt 9/164-SC, A-1060 Wien, Austria

The system $\text{Sc}_2\text{O}_3\text{-}\text{Al}_2\text{O}_3\text{-}\text{TiO}_2\text{-}\text{SiO}_2$ contains several important binary ceramic phases, but the complete system is poorly known. Flux growth experiments in this system have yielded high-quality crystals of several oxidic Sc compounds by using various selected solvent mixtures [1-5], and have provided results on the apparent low-temperature instability of several Sc phases previously reported in this system. For comparison purposes, we have started studies of the phases and phase equilibria using the technique of chemical transport reactions [6] which are known to sometimes yield metastable phases. The studies of the system $\text{Sc}_2\text{O}_3\text{-}\text{Al}_2\text{O}_3\text{-}\text{TiO}_2\text{-}\text{SiO}_2$ were conducted in the overall temperature range $1100 \rightarrow 950^\circ\text{C}$ (endothermal transport), and were performed in sealed and evacuated silica glass ampoules which were filled with variable amounts of high-purity powders of the component oxides and the transport media. After run times of 7-10 d and quenching of the ampoules in cold water, runs with Cl_2 (oxidizing conditions, provided from PtCl_2) and HCl (reductive conditions, provided from NH_4Cl) as transport media yielded several phases as small (< 1 mm), often well-formed crystals: synth. rutile, synth. anatase, synth. corundum, synth. mullite, Sc_2O_3 , and synth. thortveitite ($\text{Sc}_2\text{Si}_2\text{O}_7$), whereas experiments with HgCl_2 as transport medium yielded no crystals at all. Studies with TeCl_4 have not been performed yet. The growth of synthetic anatase confirms that metastable compounds can be prepared at high temperatures using this technique.

Chemical transport reactions have not been used so far to produce single crystals of mullite, but only to prepare very thin, microcrystalline protective mullite coatings on SiC ceramic bodies, e.g., [7-10]. Our studies show that mullite single crystals with dimensions suitable for determination of various physico-chemical properties can be prepared using the technique of chemical transport reactions.

The average crystal structures of two colourless, prismatic mullite crystals from different experiments (starting materials: $\text{Sc}_2\text{O}_3 + \text{Al}_2\text{O}_3 + \text{TiO}_2 + \text{SiO}_2$; transport medium: Cl_2 or HCl) were determined from highly redundant single-crystal X-ray diffraction data (Mo-K α radiation, CCD area detector) and refined in space group $Pbam$ to $R1(F)$ values of 2.0 and 1.9 %, respectively. No first- or second-order satellite reflections or any streaking were recognisable on the recorded CCD frames, despite overexposure.

The two crystals have the following, similar unit-cell parameters (first value refers to crystal grown using Cl₂): a = 7.591(2) / 7.600(2), b = 7.709(2) / 7.700(2), c = 2.895(1) / 2.894(1) Å, and V = 169.41(9) / 169.36(9) Å³. The structure of the Cl₂-grown crystal shows a reasonably good agreement with the mullite model (both coordinates and occupancies) proposed by SAALFELD & GUSE [11] or ANGEL & PREWITT [12], whereas the other, HCl-grown crystal has distinctly different occupancies, and appears to be poorer in Si. Largest variations in metal-oxygen bond lengths are shown by the T*-Oc* distances. The unit-cell dimensions of both crystals are anomalously enlarged (especially the b-axes), and can, at present, only be explained by incorporation of impurity cations (Ti and/or Sc?), but not by a simple variation of the Al:Si ratio, or by the additional influence of quenching the grown crystals. Results from chemical analyses are not available yet, but will ultimately provide a more detailed picture of these anomalous mullites.

Financial support by the Austrian Science Foundation (FWF) (Grant P15220-N06) is gratefully acknowledged.

References

- [1] KOLITSCH, U. & TILLMANNS, E. (2003): Sc₂TiO₅, an entropy-stabilized pseudobrookite-type compound. - *Acta Crystallographica*, E59, i36-i39.
- [2] KOLITSCH, U. & TILLMANNS, E. (2003): Bi₃ScMo₂O₁₂: the difference from Bi₃FeMo₂O₁₂. - *Acta Crystallographica*, E59, i43-i46.
- [3] KOLITSCH, U. & TILLMANNS, E. (2003): Li₃Sc(MoO₄)₃: substitutional disorder on three (Li,Sc) sites. - *Acta Crystallographica*, E59, i55-i58.
- [4] KOLITSCH, U. & TILLMANNS, E. (2003): The crystal structure of synthetic Sc₂Si₂O₇ at 100, 200 and 293 K: thermal expansion and behaviour of the Si₂O₇ group. - *Zeitschrift für Kristallographie*, Supplement No. 20, 139.
- [5] KOLITSCH, U. & TILLMANNS, E. (2003): Synthesis and crystal structure of K₂ScFSi₄O₁₀, and its close relation to narsarsukite. (To be submitted).
- [6] GRUEHN, R. & GLAUM, R. (2000): Neues zum chemischen Transport als Methode zur Präparation und thermisch-chemischen Untersuchung von Festkörpern. - *Angewandte Chemie*, 112, 706-731. (in German).
- [7] BASU, S. N. ET AL. (1998): Formation of mullite coatings on silicon-based ceramics by chemical vapor deposition. - *International Journal of Refractory Metals & Hard Materials*, 16, 343-352.
- [8] ARMAS, B. ET AL. (2001): Low-pressure chemical vapor deposition of mullite layers using a cold-wall reactor. *Surface and Coatings Technology*, 141, 88-95.
- [9] HOU, P. ET AL. (2001): Structure and high-temperature stability of compositionally graded CVD mullite coatings. - *International Journal of Refractory Metals & Hard Materials*, 19, 467-477.
- [10] SOTIRCHOS, S. V. & NITODAS, S. F. (2002): Factors influencing the preparation of mullite coatings from metal chloride mixtures in CO₂ and H₂. - *Journal of Crystal Growth*, 234, 569-583.
- [11] SAALFELD, H. & GUSE, W. (1981): Structure refinement of 3:2-mullite (3Al₂O₃,2SiO₂). - *Neues Jahrbuch für Mineralogie, Monatshefte*, 1981, 145-150.
- [12] ANGEL, R. J. & PREWITT, C. T. (1986): Crystal structure of mullite: A re-examination of the average structure. - *American Mineralogist*, 71, 1476-1482.

BAZRSi₂O₇, A NEW MINERAL FROM THE EIFEL VOLCANIC AREA, GERMANY

U. Kolitsch¹, C. L. Lengauer¹, W. Krause², H.-J. Bernhardt³, O. Medenbach⁴ & G. Blaß⁵

¹Institut für Mineralogie und Kristallographie

Universität Wien, Geozentrum, Althanstrasse 14, A-1090 Wien, Austria

²Henriette-Lott-Weg 8, D-50354 Hürth, Germany

³Zentrale Elektronen-Mikrosonde

Ruhr-Universität Bochum, D-44780 Bochum, Germany

⁴Institut für Mineralogie

Ruhr-Universität Bochum, D-44780 Bochum, Germany

⁵Merzbacherstrasse 6, D-52249 Eschweiler, Germany

A new silicate mineral was found in November 1990 in the active leucite-nepheline quarry at Löhley about 1 km NW of Üdersdorf in western Eifel volcanic area, Germany. The locality and mineralogy are described by HENTSCHEL [1, 2]. The locality is known among micromount collectors for aesthetic skeletal perovskite crystals and several rare minerals such as batisite and barytolamprophyllite [1, 2], fersmanite, wöhlerite, volborthite, galenite, willhendersonite, wairakite and natural, unnamed BaCu₂Si₂O₇ [3-5], as well as the new mineral batiferrite [6]. Several late-hydrothermal zeolites cover some of the above early-hydrothermal minerals. The mineralogy of the occurrence is similar to that of the nearby Graulai quarry [3], 16 km NW of the Löhley quarry. The new silicate was formed under hydrothermal conditions in cavities and narrow voids of a melilite- and leucite-nepheline country rock. It is associated with perovskite, götzenite, wöhlerite, dark greenish "clinopyroxene", fluorapatite, leucite, titanite, magnetite and sanidine.

The crystals of the new mineral exhibit a idiomorphic, blocky (i.e. thick tabular {001}) habit with a maximum diameter of about 0.8 mm. Only five crystals on two specimens are currently known. All crystals found so far have crystallised on perovskite crystals or in immediate contact with them. The chemical composition and the optical properties were determined on the same single crystal used earlier for the structure determination. Slight variabilities of the chemical composition are due to substitution of Ba by K, Na and Ca, and of Zr by Ti (and Al?), as indicated by SEM-EDS (EPM analyses are presently underway). This is also suggested by slightly varying optical properties. Ba, Zr and Si are, however, always dominant.

The crystal structure of the new mineral has been solved by direct methods and refined in space group *P4/mbm* (*a* = 8.901(1), *c* = 8.074(1) Å, *V* = 639.7(1) Å³, *Z* = 4) to *R*1 = 1.5 % and *wR*2_{all} = 3.8 % from 800 'observed' reflections with *F*_o > 4σ(*F*_o). The data were collected with a four-circle diffractometer (MoKα X-radiation, CCD area detector, 293 K, 2θ_{max} = 70°). The structure contains one unique Ba, Zr and Si atom, and five unique O atoms. Chains of corner-sharing ZrO₆ octahedra run along [001], and the SiO₄ tetrahedra form Si₄O₁₂ rings arranged approximately parallel to {110}. The chains and rings are corner-linked via common oxygen ligands to form a three-dimensional framework.

The 10-coordinated Ba-atoms are located in the large voids of this framework. The ZrO_6 octahedron is fairly regular, with Zr-O distances ranging between 1.9579(5) and 2.0791(6) Å (average 2.053 Å). The average Si-O bond length, 1.614 Å, is identical to that in $KTaSi_2O_7$ (see below). The average Ba-O bond length is 2.931 Å.

The mineral, ideally $BaZrSi_2O_7$, is isostructural with the synthetic material $KTaSi_2O_7$ (space group $P4/mbm$ [7]) and closely related to the ferro-electric compound $KNbSi_2O_7$ (space group $P4bm$ [8-10]). The non-centrosymmetric structure and ferro-electricity of $KNbSi_2O_7$ is due to a sequence of alternating short and long Nb-O bonds along the tetragonal c-axis. The hypothetical high-temperature paraelectric modification of $KNbSi_2O_7$ would crystallise in the same centrosymmetric space group as $KTaSi_2O_7$ [7]. A close structural relation also exists with $K_4Sc_2(OH)_2[Si_4O_{12}]$ (pseudo-tetragonal, space group $Pbam$ [11]) which can be reformulated as $K_2Sc[Si_2O_6](OH)$. Somewhat surprisingly, the chemically related compounds $SrZrSi_2O_7$, $CaZrSi_2O_7$ (gittinsite), $BaTiSi_2O_7$ and $SrTiSi_2O_7$ all have different crystal structures. A comparison with other minerals containing Si_4O_{12} rings shows that the structure of the new mineral may be compared with that of members of the nendakevichite group (pseudo-tetragonal). In the latter, there exist chains of corner-linked NbO_6 or TiO_6 octahedra extending along the pseudo-tetragonal a-axis, as well as Si_4O_{12} rings, but these rings are oriented parallel to {100}, i.e. turned by 90° with respect to the chain orientation in the new mineral.

Mr. F.-J. Emmerich is thanked for kindly providing the studied samples. Financial support by the Austrian ScienceFoundation (FWF) (Grant P15220-N06) is gratefully acknowledged.

References

- [1] HENTSCHEL, G. (1987): Die Mineralien der Eifelvulkane. - 2nd, extended ed., Chr. Weise Verlag, Munich, Germany, 177 pp. (in German).
- [2] HENTSCHEL, G. (1989): Die Minerale der Üdersdorfer Lava. - Lapis, 14 (11), 14-25. (in German).
- [3] HENTSCHEL, G. (1993): Die Lavaströme der Graulai: eine neue Fundstelle in der Westeifel. - Lapis 12 (9), 11-23. (in German).
- [4] BLAB, G. & GRAF, H. W. (1993): Neufunde von bekannten Fundorten (VIII). - Mineralien-Welt, 4 (5), 41-48. (in German).
- [5] GUTH, G. (2000): Interessante Neufunde für den Basaltbruch Liley bei Üdersdorf in der Westeifel. - Mineralien-Welt, 11 (2), 28-36. (in German).
- [6] LENGAUER, C. L. ET AL. (2001): Batiferrite, $Ba[Ti_2Fe_{10}]O_{19}$, a new ferrimagnetic magnetoplumbite-type mineral from the Quaternary volcanic rocks of the western Eifel area, Germany. - Mineralogy and Petrology, 71, 1-19.
- [7] LEE, J.-G. ET AL. (1996): A potassium tantalum(V) tetrasilicate $KTaSi_2O_7$. - Journal of Solid State Chemistry, 123, 123-128.
- [8] CROSNIER, M. P. ET AL. (1991): Potassium niobate silicate ($K_2(NbO)_2Si_4O_{12}$): a new material for nonlinear optics. - Ferroelectrics, 124, 61-66.
- [9] CROSNIER, M. P. ET AL. (1992): The potassium niobyl cyclotetrasilicate $K_2(NbO)_2Si_4O_{12}$. - Journal of Solid State Chemistry, 98, 128-132.
- [10] FOSTER, M. C. ET AL. (1999): $K_2(NbO)_2Si_4O_{12}$: a new ferroelectric. - Journal of Applied Crystallography, 32, 421-425.
- [11] PYATENKO, YU. A. ET AL. (1979): Crystal structure of $K_4Sc_2(OH)_2[Si_4O_{12}]$. - Doklady Akad. Nauk SSSR, 248, 868-871. (in Russian).

**AKTUELLE UMWELTBELASTUNGEN DURCH LAGERSTÄTTEN UND
HISTORISCHE BERGBAUE IM OBERPINZGAU, SALZBURG**

F. Koller¹, R. Seemann² & P. Englmaier³

¹Institut für Geologische Wissenschaften

Universität Wien, Geozentrum, Althanstrasse 14, A-1090 Wien, Austria

²Mineralogisch-Petrographische Abteilung

Naturhistorisches Museum, Burgring 7, A-1014 Wien, Austria

³Institut für Ökologie und Naturschutz

Universität Wien, Althanstrasse 14, A-1090 Wien, Austria

Im Rahmen des Projektes "Umweltgeochemische Untersuchungen an historischen Bergbauen im Tauernfenster" sind einige charakteristische Lagerstätten im Oberpinzgau für detaillierte Beprobungen ausgewählt worden. Es handelt sich durchwegs um sulfidische und vorwiegend polymetallische Vorkommen in metamorphen Serien des Tauernfensters und der Innsbrucker Quarzphyllite, - alle im Nahbereich des nördlichen "Fensterrandes". Die in Bezug auf Erzparagenesen und Nebengestein stark unterschiedlichen Vorkommen sind durch künstliche - und z.T. durch natürliche Aufschlüsse zugänglich. Dadurch ist auch die für geochemische Umsetzung und Mobilisierung notwendige Wasserwegigkeit bevorzugt gegeben.

Die Beprobungsserien erfolgten zu unterschiedlichen Jahreszeiten an Bergwässern, ausgehend vom Grubengebäude, vom Stollenmund oder von den Halden soweit möglich bis zum Vorfluter. Parallel dazu sind über Tag im Umgriff Probennahmen an geeigneten Pflanzen durchgeführt worden. Um einen Bezug zwischen den verschiedenen Lagerstätten und den korrespondierenden Bergwässern herzustellen, kamen in den Wasserproben – abgesehen von den physikalischen Daten und den Hauptelementen, die Spurenelemente As, Sb, Cd, Cu, Zn, Pb, Co, Ni, Cr zur Bestimmung. Die zur Untersuchung herangezogenen Erzvorkommen bzw. Bergbaue im Oberpinzgau sind:

1. Pb-Zn-Lagerstätte Achselalm und Flecktrogalm, Hollersbachtal:

Stark absätzige, NE-SW-streichende Quarz-Calcit-Gänge in Gesteinsserien der Habach-Gruppe. Die Gänge sind vorwiegend mit Fluorit, Sphalerit und Galenit angereichert, daneben geringere Mengen an Pyrit, Arsenopyrit, Chalkopyrit und Greenockit. Die komplexe Vererzung liegt im Achsel- und Flecktrogrevier. Zugänglich sind einige alte, zum Teil wasserführende und verbrochene Stollen mit vorwiegend Obertag-Entwässerung. Im ehemaligen Bergbaurevier befinden sich etliche Halden.

2. Sulfidlagerstätte Bärnbach, Hollersbachtal:

Komplexe Sulfidlagerstätte in metamorphen Gesteinsserien der Habachformation mit Chloritschiefern, Quarziten und Talk-schiefern. Als Mineralphasen werden u.a. Galenit, Chalkopyrit, Pyrit, Arsenopyrit, Pyrrhotin, Stannin, Tetradymit, Molybdänit, gediegen Bismut, gediegen Gold und Eclarit beschrieben. Bedingt begehbar sind einige z.T. verbrochene Stollen mit teilweiser Wasserführung. Vor Ort finden sich einige Halden.

3. Sulfidische Cu-Lagerstätte Hochfeld, Untersulzbachtal:

Deutlich schichtgebundene Cu-Fe-Vererzung in Biotit-Chloritschiefern der Habachformation ("Knappenwandmulde"); teilweise wechseltlagernd mit Albitgneisen, Quarziten und Epidotamphiboliten, die in genetischem Zusammenhang mit einem altpaläozoischen Inselbogenmagmatismus stehen. Hauptbestandteile der Vererzung sind Chalkopyrit, Pyrit und Pyrrhotin. In geringeren Mengen treten Sphalerit, Galenit, Magnetit, diverse Telluride, Ag- und Bi-Phasen sowie gediegen Gold und Bismut auf. Zugänglich sind ca. 3 km alte Stollen aus dem Anfang des 16. bis ins 20. Jh. Die in mehreren Etagen angelegten Stollen und Schächte sind meist wasserführend. Obertagihalden sind kaum vorhanden.

4. Ag-reiche sulfidische Lagerstätte Peitingalm-Gamskogel, Habachtal:

Pyritdominierte Cu-Ag-Vererzung, die an Quarzmylonite und Phyllite der Habachformation gebunden ist. Hauptmenge ist Pyrit und Chalkopyrit, daneben u.a. Galenit, Sb-Fahlerze, Sphalerit, Bi- und Ag-Phasen sowie gediegen Gold. Die Aufschlüsse des alten Bergbaurevieres am Gamskogel sind relativ weit verstreut; - nur mehr ein geringer Teil ist zugänglich. Im Bereich des Maria-Theresiastollens - mit noch ca. 100 m begehbarer Reststrecken - sind ca. 10 weitere Stollenmundlöcher bekannt. Die meisten Stollen haben Wasserführung oder sind "abgesoffen". Zahlreiche kleinere Halden liegen vor.

5. Pyritlagerstätte Rettenbachtal bei Mittersill:

As-reiche Pyritlagerstätte in Schiefern der Innsbrucker Quarzphyllite. Folgende Erzphasen sind beschrieben: Pyrit, Pyrrhotin, Chalkopyrit, Arsenopyrit, Millerit, Tetraedrit, Galenit, Sphalerit, Bouronit und Antimonit. Viele der tiefer liegenden Strecken sind wasserführend, mit Drainagen ins Kulturland und Siedlungsgebiet.

6. Pyritvererzung Wieseckrinne ("Stinkende Gräben"), Stockeralm, Untersulzbachtal (natürl. Aufschluß):
Pyritreiche, sulfidische Vererzung in Kyanit-Quarziten, Schiefern und Gneisen der Habachgruppe ("Habachmulde"). Neben As-reichen Phasen auch Chalkopyrit, Magnetit, Sphalerit und Galenit. Großflächige z.T. stark und tiefgründig verwitterte Obertag-Aufschlüsse mit natürlichen Halden. Zahlreiche Gerinne und Quellen im Aufschlussbereich an der Ostseite des Untersulzbachtals. Auf der anderen Talseite, in derselben Serie, befindet sich der aus dem 18. und 19.Jh. stammende Finkalmstollen.

Über die Zusammensetzung der vorrätigen oderehemals abgebauten Erze - samt den umgebenden Gesteinen im Anstehenden - weiß man vielfach gut Bescheid. Im Gegensatz dazu gibt es wenige Daten über die Gehalte an Schwermetallen in den jeweiligen Halden und austretenden Bergwässern, samt den durch Verwitterung löslichen Anteilen. Durch Berg- und Oberflächenwässer mobilisiert, gelangen sie meist mitten im Kulturland, ins umgebende Erdreich und in den Grundwasserkörper. Mit zunehmender Entfernung erfolgt dabei allerdings eine Verdünnung. Es bilden sich Kontaminationsfahnen, die ihren Ausgangspunkt in der Lagerstätte oder in den alten Halden haben. Dasselbe gilt aber auch für natürlich aufgeschlossene Vererzungszonen.

Die Wässer der einzelnen Lagerstätten haben nach den Analysen charakteristische Spuren-elementspektren mit jahreszeitlichen bzw. witterungsbedingten Variationen. Die pH-Werte schwanken zwischen 2.5 und 8.5, die elektrische Leitfähigkeit zwischen 65 und 1.250 µS/cm.

Die Schwankungsbreite der Spurenelementgehalte der Erzwässer (in µg/l):

As:	0.5	bis	106
Cd:	0.1	bis	7.3
Co:	0.02	bis	37.2
Ni:	0.1	bis	96.3
Cr:	0.2	bis	32.5
Cu:	4.6	bis	310
Pb:	4.3	bis	165
Sb:	0.1	bis	2.4
Zn:	92	bis	1420

Die Schwankungsbreite der Spurenelementgehalte der Pflanzen (in mg/kg):

As:	0.1	bis	7.6
Cd:	0.04	bis	8.8
Co:	0.3	bis	3.1
Ni:	2.2	bis	16.9
Cr:	0.3	bis	16.0
Cu:	1.8	bis	256
Pb:	1.5	bis	212
Sb:	0.1	bis	1.2

Folgende Pflanzen kamen dabei zur Untersuchung: div. Moose, Pilze (*Suillus sp.*) sowie *Saxifraga aizoides*, *Silene vulgaris*, *Gypsophila repens* und Fichte (Jungwuchs, Nadeln).

**PUMPELLYITE WITHIN THE SCHNEEBERG COMPLEX (EASTERN ALPS):
A RELICT OF PROGRADE METAMORPHISM ?**

K. Krenn, R. Kaindl & G. Hoinkes

Institute of Mineralogy and Petrology
University of Graz, Universitätsplatz 2, A-8010 Graz, Austria

Introduction

Indicators for alpine thrust tectonics are rarely preserved within metapelites of the Eastern Alps. Our study area, the Schneeberg Complex (SC), shows fine grained serizitic garnet mica schists, which are intensely deformed in three dimensional scale. They occur adjacent to paragonite-hornblende metabasites metamorphosed at HP-LT conditions [1].

Textural observations of pumpellyite within recrystallized quartz grains suggest early prograde formation. These minerals are investigated by optical and scanning electron microscopy (SEM) and Raman spectroscopy and compared to a pumpellyite hornfels sample of California and data from literature. Exhumation history of the study area is determined by fluid inclusion data and quartz rheology.

Geological and structural setting

The Schneeberg Complex (SC) and its adjacent Ötztal Basement Complex (ÖC) are part of the Austroalpine tectonic unit and consist of medium to high-grade metamorphic rocks of varying tectonometamorphic history. Peak conditions of the eo-alpine overprint were reached in the Texel group with minimum pressures of ca. 1.2 GPa and 500–550°C, forming staurolite and kyanite up to eclogitic parageneses [2]. There, exclusively eo-Alpine Rb-Sr and K-Ar cooling ages are revealed around 100–80 Ma [3], whereas in central and north-western parts of the ÖC mixed ages and Variscan ages dominate (for overview see [4]).

The incorporated Schneeberg Complex includes Alpine staurolite growth and eo-Alpine pressure dominated metamorphism. At the NW margin of the SC, high pressure low temperature mineral assemblages, presented by paragonite-hornblende schists [4], reflect peak metamorphic conditions for the metabasic units within the central SC around 8–10 kbar and 550–600°C and yield Ar/Ar ages of 84.5 ± 1 Ma [5] for Eoalpine amphibolite facies conditions.

The study area within the Seewertal Valley defines the hanging wall limb of the Schneeberger main syncline that includes various lithologies with garnet-mica schists, amphibolites, quartzites and hornblende-garnet schists and gneisses. Lithologies are intensely prograde mylonitized followed by intense tight folding that occurs predominantly perpendicular to the main direction of stretch. Rims of garnet porphyroblasts, up to cm in scale, overgrow these mylonitic and folded layers that are embedded within a fine grained serizitic matrix. Garnets show rotated quartz inclusion patterns with straight grain boundaries, suggesting low differential stress during growth [6].

Petrography and microstructures of the studied metapelites

Structures are evaluated parallel and perpendicular to foliation (x-z and y-z sections). Within ductile deformed quartz layers (y-z-sections) pumpellyite, always included in biotite, occurs at fold hinge areas. Pumpellyite forms aggregates and lenses up to 0.4 mm in size. Optical properties are very similar to epidote with high relief and anomalous grey-brown birefringence.

By Raman Spectroscopy the pumpellyite is clearly distinguished from epidote and clinozoisite. Pumpellyite within hornfels from California is comparable to the studied crystals but reflects a distinct shift in wavenumber (Figure 1). This may be attributed to chemical differences between pumpellyites in hornfels rocks and metapelites [7].

Chemical analyses with the SEM show higher Mg contents in pumpellyite compared to epidote (around 3 wt.% MgO).

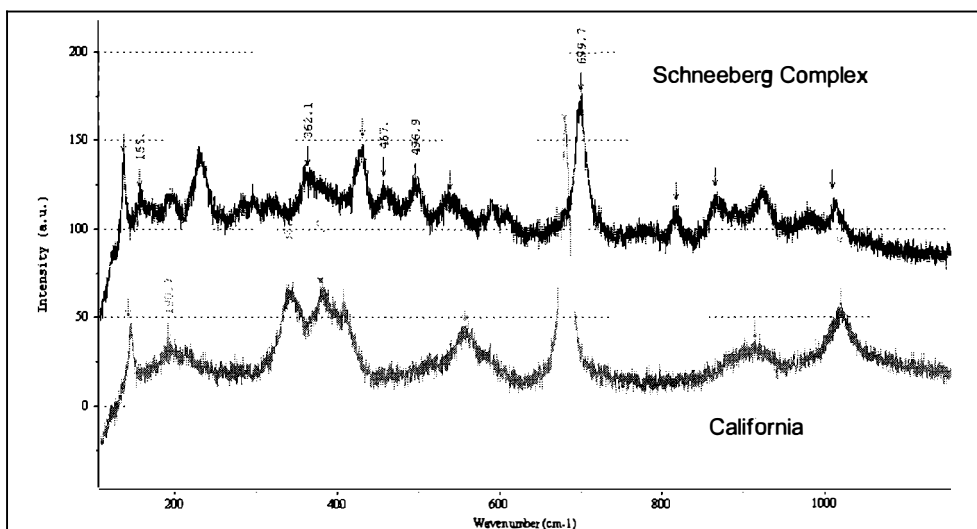


Figure 1

Raman spectra of pumpellyite within metapelite from the SC (black) and metabasite from California (grey).

Interpretation and conclusion

Prograde growth of pumpellyite within fold hinge areas of ductile deformed quartz aggregates is established. Host mineral quartz is recrystallized by grain boundary migration after peak metamorphism. Retrograde isothermal decompression down to low pressure and high temperature conditions, derived from combined fluid inclusions and quartz deformation textures, [8] contradict growth of pumpellyite during uplift within fold hinge areas of tightly deformed quartz layers. Therefore, the timing of formation is related to the crustal thickening of the Ötztal-Stubai Complex during onset of alpine thrust tectonics at ca. 120–100 Ma. [4].

References

- [1] KONZETT, J. & HOINKES, G. (1996): Paragonite-hornblende assemblages and their petrological significance: an example from the Austroalpine Schneeberg Complex, Southern Tyrol, Italy. - Journal of Metamorphic Geology, 14:85-101.

- [2] HOINKES, G. & THÖNI, M. (1983): Neue geochronologische und geobarometrische Daten zum Ablauf und der Verbreitung der kretazischen Metamorphose im Ötztalkristallin. - Jahresbericht, Hochschulschwerpunkt S15, 73-83.
- [3] EXNER, U. ET AL. (2002): Relative chronology and absolute age dating of structures related to eo-Alpine high pressure metamorphism and Oligocene magmatism in the SE Ötztal complex (Texel Group, South Tyrol, Italy). - Mitt. naturw. Ver. Steiermark, 132, 63-82.
- [4] THÖNI, M. (1999): A review of geochronological data from the Eastern Alps. - Schweiz. Mineral. Petrogr. Mitt. 79, 209-230.
- [6] STÖCKHERT, B. ET AL. (1997): Low differential stress during high pressure metamorphism: The microstructural record of a metapelite from the Eclogite Zone, Tauern Window, Eastern Alps. - Lithos, 41, 103-118.
- [7] POTEL, S. ET AL. (2002): Composition of Pumpellyite, epidote and chlorite form New Caledonia - How important are metamorphic grade and whole-rock composition? - Schweiz. Mineral. Petrogr. Mitt., 82, 229-252.
- [8] KRENN, K. ET AL. (2003): Structural evolution of the Schneeberg Complex during onset of extensional tectonics (Eastern Alps, Austria). - Geophysical Research Abstracts, Vol.5, 2003.

STRUKTUR UND EIGENSCHAFTEN VON MINERALIEN

M. Kunz

Naturhistorisches Museum
Augustinergasse 2, Ch-4001 Basel, Schweiz

Mineralogie wird heute oft unter Verweis auf die begrenzte Vielfalt der zu untersuchenden Objekte als eine altmodische und ausgeforschte Wissenschaft bezeichnet. In der Tat lässt sich nicht leugnen, dass die ca. 5000 verschiedenen Mineralarten im Vergleich z.B. zur Vielfalt des Lebens eine äusserst überschaubare Menge an möglichen Studienobjekten darstellen. So ist es auch nicht überraschend, dass die makroskopische qualitative Beschreibung und Klassifizierung der Mineralwelt, abgesehen von exotischen Neuentdeckungen, abgeschlossen ist. Mit der Entdeckung der Röntgenbeugung und der Entwicklung automatischer Diffraktometer machte auch die quantitative mikroskopische Beschreibung der Mineralstrukturen grosse Schritte vorwärts, so dass heute von den allermeisten Mineralien eine detaillierte strukturelle Beschreibung verfügbar ist. Das bedeutet nun aber nicht, dass die Arbeit in der Mineralogie erledigt ist. Vielmehr haben wir damit nun die Grundlagen, um die entscheidenden naturwissenschaftlichen Fragen nach der Ursache von beobachteten Phänomenen zu stellen. Nachdem wir wissen, welche physikalischen und thermodynamischen Eigenschaften die Mineralien aufweisen, geht es darum zu verstehen, warum wir bei verschiedenen äusseren Bedingungen, unterschiedliche Phasen mit verschiedenen physikalischen Eigenschaften beobachten, warum gewisse Zusammensetzungen interessante physikalische Eigenschaften aufweisen, und andere nicht.

Der Schlüssel dazu ist das Verständnis des Zusammenhangs zwischen mikroskopischer Kristallstruktur und makroskopischen, physikalischen Eigenschaften. Um dieses Programm zu verfolgen, stehen uns zwei wichtige Werkzeuge zur Verfügung: Zum Einen sind das die gesammelten Daten mineralogischer Arbeiten der vergangenen Jahrzehnte, welche uns in zunehmend umfangreichen und benutzerfreundlichen Datenbanken zur Verfügung stehen. Zum Andern müssen wir das bekannte Wissen ergänzen durch Untersuchungen von Mineralien unter kontrollierten äusseren Bedingungen. Als kontrollierbare äussere Bedingungen dienen uns dabei Druck, Temperatur, elektrische Felder, aber auch chemische Zusammensetzung. Nicht ausser Acht gelassen werden sollte dabei auch die Notwendigkeit der quantitativen Messung physikalischer Eigenschaften von Mineralien, welche zur Zeit nur von wenigen Forschungsgruppen betrieben wird.

In meinem Vortrag möchte ich anhand zweier Beispiele den möglichen Nutzen vom Gebrauch von Datenbanken einerseits und von Experimenten unter kontrollierten äusseren Bedingungen andererseits, illustrieren. Die ausgewählten Beispiele mögen darauf hinweisen, dass das grundlegende Verständnis der die Erde aufbauenden Materialien trotz umfangreicher beschreibender Datenmenge noch in den Anfängen steckt.

WATER TRACES AND CHEMISTRY OF CASSITERITES

Z. Losos¹ & A. Beran²

¹Institute of Geological Sciences
Masaryk University Brno, Kotlářská, 611 37 Brno, Czech Republic

²Institut für Mineralogie und Kristallographie
University Wien, Geozentrum, Althanstrasse 14, A-1090 Wien, Austria

The presence of water (OH groups) in natural cassiterite was originally established by BERAN & ZEMANN [1] on the basis of IR-spectroscopy. Cassiterites are characterized by absorption bands centered in the 3250 and 3350 cm⁻¹ region.

Our suite of 16 cassiterite samples originate from localities in Czech Republic, Great Britain, Mongolia, Portugal, France, Bolivia, Brazil and Russia. Most of the cassiterites come from greisen (high temperature hydrothermal) deposits (Cínovec, Krupka, Horní Slavkov, Cornwall). A sample from Potosí belongs to the cassiterite-sulphidic deposit of Bolivia type. Cassiterite from Li-pegmatite is represented by a sample from Rožná.

Single-crystal plates cut parallel to the z-axis were used for the IR measurements. Band deconvolution procedure revealed distinct absorption maxima with varying intensities. Generally 2 types of IR absorption spectra were found.

IR spectrum type I is represented by synthetic cassiterites. It is characterized by only one sharp maximum centered at 3255 cm⁻¹, with an additional weak band centered at 3265 cm⁻¹. Chemically these cassiterites are pure SnO₂, suggesting that the absorption band at 3255 cm⁻¹ corresponds to structural OH groups solely coordinated by Sn.

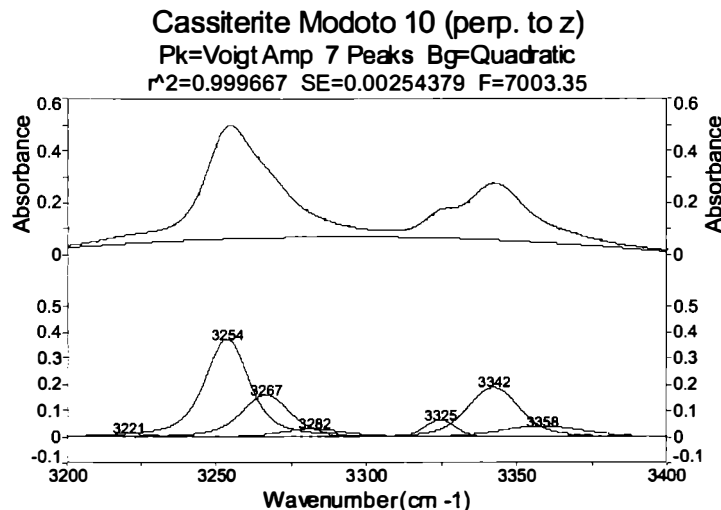


Fig. 1
Typical polarized IR spectrum type II (*E* vector perpendicular to z-axis) of a natural cassiterite crystal from Modoto, Mongolia. The result of band deconvolution by the PeakFit 4 program is shown in the lower part of the diagram.

The IR spectrum type II, represented by a natural cassiterite sample from Modoto, shows a very complex absorption pattern with several absorption bands. Most of these bands can also be observed in the spectra of cassiterite samples from other localities. The spectra are characterized by two band groups with maxima centered around 3250 and 3350 cm⁻¹ (Fig. 1). Each band group can be separated in three peaks with different intensities at individual samples:

- The first sharp band maximum at 3254 cm⁻¹ corresponds to that of synthetic cassiterites. An additional band can be observed in the 3219–3224 cm⁻¹ region and a more intense band in the 3265–3270 cm⁻¹ region.
- The second absorption maximum is centered at 3340–3350 cm⁻¹, two additional bands which are centered at 3324–3327 cm⁻¹ and 3360–3370 cm⁻¹ can be separated.

Most of natural cassiterite crystals, especially from greisens, show under the microscope sharp colour zoning (from colourless over yellow to brown and black-brown with changing intensity). Zoning is often oscillatory, the dark-brown to black zones are typical for marginal parts of the crystals. However, small areas are microscopically homogeneous in colour and were measured by polarized and unpolarized FTIR microspectroscopy. All the measured areas of different colour reveal similar types of absorption spectra (band positions), except the black-brown zone, where the distinct absorption bands differ in intensities.

Extremely strong absorption of the visible light and of the IR-radiation is observed in cassiterite from the Li-pegmatite in Rožná (CZ). Slabs of black-brown colour with a thickness of about 0.5 mm are opaque for visible light, as well as for IR-radiation.

The individual absorption bands of natural cassiterites, especially in the 3320–3370 cm⁻¹ region are probably correlated with OH groups that are coordinated to different trace elements (Ti, Fe, Nb, Ta, W) or cation vacancies. Natural samples are strongly varying in their trace element content. No significant correlation with the striking colour zoning in some of the samples could be observed. Very dark-coloured, nearly opaque cassiterites, rich in Fe, Nb and Ta (several tenths of wt.%) reveal also higher concentrations of OH defects, showing an IR spectrum, characterized by strong absorptions in the 3350 cm⁻¹ region.

Based on the molar OH absorption coefficient for cassiterite, determined to 65 000 l.mol⁻¹ H₂O cm⁻² by MALDENER ET AL. [2] the calculated analytical water content ranges from about 2.7.10⁻⁴ to 1.9.10⁻² wt.%. The synthetic samples prepared from melts contain H₂O concentrations of only about 2.7–9.5.10⁻⁴ wt.%. As a general feature samples from hydrothermal occurrences show enhanced H₂O values, ranging from 3.6.10⁻³ to 1.9.10⁻² wt.%.

Acknowledgements

This work was supported by the EU through the Human Potential Program (Project No RTN1-1999-00353 "HYDROSPEC")

References

- [1] BERAN, A. & ZEMANN, J. (1971): Messung des Ultrarot-Pleochroismus von Mineralen. XI. Der Pleochroismus der OH-Streckfrequenz in Rutil, Anatase, Brookit und Cassiterit. Tschermaks Mineral. Petrogr. Mitt., 15: 71-80.
- [2] MALDENER, J., RAUCH, F., GAVRANIC, M. & BERAN, A. (2001): OH absorption coefficients of rutile and cassiterite deduced from nuclear reaction analysis and FTIR spectroscopy. - Mineral. Petrol., 71: 21-29.

**THE TAUERN WINDOW AND THE OROGENIC STRUCTURE OF THE EASTERN ALPS
FROM TRANSALP DEEP SEISMIC REFLECTION MEASUREMENTS**

E. Lueschen^{1,2} & TRANSALP Working Group²

¹Department of Earth and Environmental Sciences

Geophysics Section, University of Munich, Theresienstrasse 41, D-80333 Munich, Germany

²Universities of Munich, Salzburg, Leoben, Bologna, Milan, Rome, Trieste,

Company ENI-AGIP-Division-Milan, GeoForschungsZentrum Potsdam

The TRANSALP Group, comprising of partner institutions from Italy, Austria and Germany, acquired data on a 340 km long deep seismic reflection line crossing the Eastern Alps between Munich and Venice [1, 2]. Although the field campaign was split into four different parts, between fall 1998 and summer 2001, the project gathered for the first time continuous sections in the Alps using consistent field acquisition and data processing parameters. These sections include the orogen itself, at its broadest width, as well as the two adjacent basins. Vibroseis near-vertical seismic profiling formed the core of the field data acquisition, mainly designed to get a high-resolution image of the upper and middle crust. It was contemporarily complemented by explosive near-vertical seismic profiling for imaging the lower crust, cross-line recording for three-dimensional control, wide-angle recording by a mobile 3-component receiver array for velocity control and seismicity recording by a stationary array for lithospheric tomography and seismicity studies.

The key observations of all these surveys favour north-south compression tectonics by crustal wedging of both the European and Adriatic-African continental margins along transcrustal ramps as the main mountain-building processes. These observations are (Fig. 1): 1) Bi-vergent structure at whole crustal scale beneath the Alpine axis. This bi-vergent pattern is characterised by some asymmetry and culminates in a relatively narrow zone above the crustal root zone. 2) Transcrustal ramp-like structures. The bi-vergent pattern appears to be bounded at depth by a predominant, about 1–2 s (approximately 3–6 km) thick, reflection pattern, the ‘Sub-Tauern-Ramp’, which can be traced from the Inn Valley dipping to the south at an angle of about 30 degree with a length of 80–100 km into the alpine root zone at 55 km depth. A northward dipping structure, the ‘Sub-Dolomites-Ramp’ can be traced to the Valsugana backthrust fault system. Both structures show enhanced seismicity in the brittle upper crust. 3) Crustal root and asymmetric crustal structure of maximum 55 km thickness little south of the Alpine axis. The Adriatic-African middle and lower crust shows higher seismic velocities, higher densities and a thickened reflective lower crust with respect to the European crust.

The Tauern Window – a narrow crystalline metamorphic belt of European origin – appears as a huge wedge in the hanging wall of the ‘Sub-Tauern-Ramp’ (Fig. 2). Except north-dipping reflectors at its northern boundary, which might represent backthrust faults, this wedge is dominated by southward dipping patterns of reflections. The inner parts of the Tauern Window are less clearly characterised by seismic reflections, probably because of complex folding.

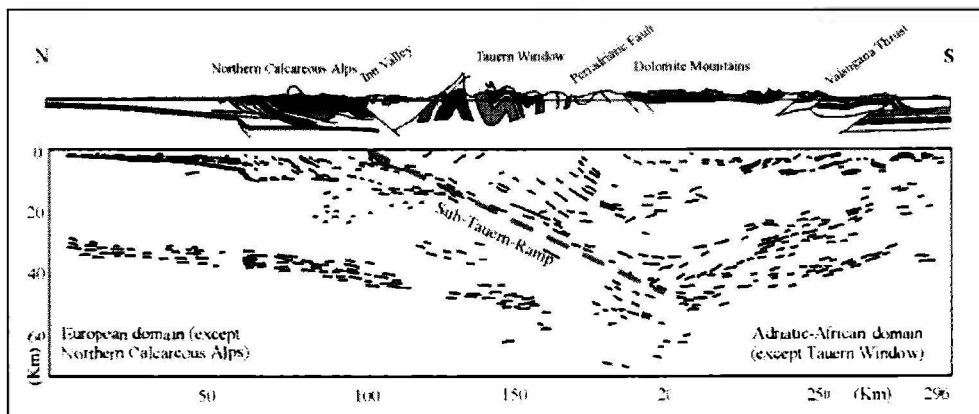


Fig. 1

Summarised reflective structures, compiled from Vibroseis and explosive seismic sections and cross-line recording.

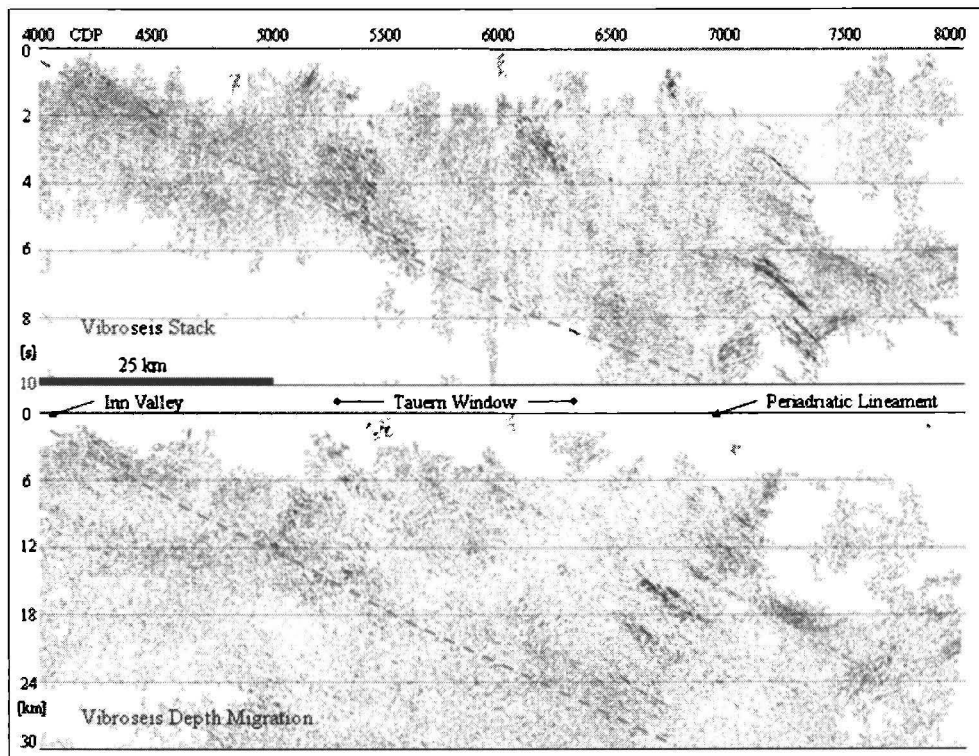


Fig. 2

The Tauern Window within a 100 km long part of the seismic section obtained by the Vibroseis technique, stack section after common-midpoint (CMP) stacking (top) and depth-migrated section (bottom). 'Sub-Tauern-Ramp' is outlined by a dashed line. Additional explosive and cross-line recordings in the CDP-range 6000–7000 have shown that the ramp-reflections are even stronger pronounced than shown here.

The strong sub-parallel reflections beneath the Periadriatic Lineament are interpreted to represent slip surfaces and fracture zones within the deformed wedge of the Tauern Window, as indicated by reduced seismic interval velocities. Uprising fluids from dewatering processes in the Alpine root zone may be responsible for enhancing the reflection strength. Our new evolution model describes the Tauern Window as part of the former European continental margin, exhumed and upthrust along the ‘Sub-Tauern-Ramp’. Alternative views concern the role of the Periadriatic Lineament, which is not directly seen in the seismic sections. Seismic Anisotropy in the Tauern Window, showing preferred orientations in E-W direction, is compatible with N-S compression and E-W stretching seen in the microfabric.

References

- [1] TRANSALP Working Group (2001) : European Orogenic Processes Research Transects the Eastern Alps. - EOS, Transactions, American Geophysical Union, 82, No.40, pages 453, 460-461.
- [2] TRANSALP Working Group (2002): First Deep Seismic Reflection Images of the Eastern Alps Reveal Giant Crustal Wedges and Transcrustal Ramps. Geophysical Research Letters, 29, No. 10, DOI 10.1029/2002GL014911, 92-1 – 92-4.

LONG-TERM EXPERIMENTS ASSESSING HYDROGEN PRODUCTION IN RESIDUES
FROM MUNICIPAL SOLID WASTE INCINERATORS

G. Magel, S. Heuss-Aßbichler & K. T. Fehr

Department of Geo- and Environmental Science, Mineralogical Section
University of Munich, Theresienstrasse 41, D-80333 Munich, Germany

The monofill at Waldering is the oldest monofill in Bavaria for the residues from a municipal solid waste incinerator (MSWI). Bottom ash (BA) and residues of the air pollution control system (APC) from the MSWI in Rosenheim have been deposited there since 1976. After the first section was entirely filled, it was covered with a landfill liner and cap, according to the German law for waste treatment. During final operations on the landfill liner an explosion occurred. The analysis of the landfill gas revealed that hydrogen gas was produced within the landfill body. Due to the sealing, the hydrogen gas could not diffuse to the atmosphere and instead concentrated within the landfill. Above a concentration of 4 %, hydrogen is an explosive gas in the presence of oxygen.

Abiotic hydrogen generation in MSWI-residues has been noted in only a few studies, which conclude that hydrogen production largely terminates after three months and therefore constitutes no long-term problem [1, 2]. However, the prolonged hydrogen production in Waldering contradicts these statements.

In order to investigate long-term hydrogen production, material deposited up to 12 years ago in the monofill in Waldering has been analysed and compared to fresh material from the MSWI in Rosenheim.

The APC-residues contain a large amount of portlandite and therefore generate alkaline conditions in contact with water. As a result of the deposition of BA together with APC-residues, all material in the monofills is buffered at pH-values above 11 for several decades [3].

The pore water in the landfill residues contains a high concentration of chlorine, due to the large amount of chlorine salts such as sylvine, halite and calcium-chloride-hydroxide [3] present in the APC-residues.

Both the alkaline pH-value and the high chlorine concentrations in the aqueous solution influence the hydrogen production in the MSWI-residues:

- Higher pH values lead to greater hydrogen production.
- The hydrogen production is initially high at high chlorine concentrations. During the course of the reaction, the reaction rate slows down.

The hydrogen production rate in MSWI-residues is not constant. Repeated fluctuation were observed during all long-term experiments with BA indicating that several processes influence the production of hydrogen within BA. Due to the recurrent deceleration and acceleration of the hydrogen producing reactions, no mathematical modelling can be applied, but the long-term hydrogen production rate can instead be empirically determined.

For BA a long-term hydrogen production rate of $1 \cdot 10^{-5}$ - $1 \cdot 10^{-4}$ ml H₂/h*g was analysed. At a consistent hydrogen production rate, the hydrogen-generating reaction will take several decades or even centuries to terminate.

The hydrogen production rate is $5.2 \cdot 10^{-3}$ ml H₂/h*g upon first contact of fresh APC-residues with water, and therefore four times higher than the maximum hydrogen production rate of fresh BA. This violent reaction is the result of the small grain size of the aluminium particles in the APC-residues, which provides a large surface area for the reaction. However, despite a low metal content and the large surface area, this material still produces hydrogen years after its deposition. Hydrogen is expected to be produced at a rate of $5 \cdot 10^{-6}$ - $1 \cdot 10^{-5}$ ml H₂/h*g from the APC-residues over several decades.

Owing to a slow hydrogen production rate, a prolonged generation of hydrogen has to be expected in Waldering. Assuming that the production rate is constant, the hydrogen production terminates after 26–355 years in BA and after 4–26 years in APC-residues.

Literature

- [1] JAROS, M. & HUBER, H. (1997): Emissionsverhalten von MVA - Schlacke nach forcierter Alterung. - Waste Reports, Abfallwirtschaft - Waste Management, Universität für Bodenkultur Wien 6, pp. 72.
- [2] FÖRSTNER, U. & HIRSCHMANN, G. (1997): Verbundvorhaben Deponiekörper: Langfristiges Deponieverhalten von Müllverbrennungsschlacken. - pp. 202, Umweltbundesamt, Projektträger Abfallwirtschaft und Altlastensanierung des BMBF.
- [3] MAGEL, G., HEUSS-AßBICHLER, S. & FEHR, K. T. (2001): Abiotic H₂ generating reactions in a MSWI monofill. - in: Eighth International Waste Management and Landfill Symposium , pp. 489-498, Sardinia.

THE METAMORPHIC EVOLUTION OF THE ORTLER CRYSTALLINE

V. Mair¹ & R. Schuster²

¹Amt für Geologie und Baustoffprüfung
Eggentalerstrasse 48, I-39053 Kardaun (BZ), Italy
²Geologische Bundesanstalt
Rasumofskygasse 23, A-1030 Wien, Austria

In the Martell valley (western Südtirol) the Martell granite intrudes into medium-grade micaschists and paragneisses of the Ortler crystalline basement.

The intrusion is situated at the lithological and tectonical contact of three different units: a) the Laaser series, characterized by intensely deformed, mylonitic amphibolites, micaschists, paragneisses and almost pure marbles; b) the Martell Micaschists, which are a more or less homogeneous stack of Grt-Sta-Bt-bearing micaschists; c) The Zebro Schuppenzone: this unit consists mainly of quartzphyllites with small intercalations of greenschists, quartzites and impure marbles. The Martell Granit forms an inhomogenous intrusive body consisting of prevalent coarse grained leucogranitic, pegmatitic and minor fine-grained aplitic rock types, and an extensive surrounding dyke swarm. This study was performed to get information on the age of the Martell granite and its relationship to the different surrounding country rock units.

Sample RS32/01 represents a fine-grained Martell granite with a mineral assemblage of Pl + Kfp+ Qtz + Ms + Grt ± Trm ± Bt. It was collected in the central region of the intrusive body at the road near to St. Johannhütte in the central Martell valley. The whole rock (WR) and two garnet fractions (Grt1, Grt2) were analyzed by the Sm-Nd method. The two garnet separates show quite similar Sm contents (1.50 ppm and 1.76 ppm), but different Nd contents (0.38 ppm and 0.15 ppm). For this reason they show different $^{147}\text{Sm}/^{144}\text{Nd}$ ratios of 2.5 and 6.69 respectively. Most probable the garnet separate with the lower spread Grt1 is contaminated by a Nd-rich, Sm-poor phase. The isochron age calculated with all three data points is 279 ± 24 Ma. Calculations of the individual garnet separates with the whole rock yield 291 ± 3 Ma and 277 ± 3 Ma respectively. The Ar-Ar age determination of the magmatic muscovite from the same sample yielded a plateau type spectra and a value of 250 ± 2 Ma.

From the road along the Zufritt Lake a coarse-grained pegmatite dyke (RS33/01) outcropping at the rim of the Martell granite with a mineral assemblage of Pl + Kfp+ Qtz + Ms + Grt + Trm was sampled. The rock is characterized by a primary magmatic foliation and a slight overprint of mylonitic greenschist-facies deformation. The garnets have low Sm (1.05 ppm) and Nd (0.16 ppm) contents and a $^{147}\text{Sm}/^{144}\text{Nd}$ ratio of 4.08. The Sm-Nd garnet-whole rock age is 274 ± 3 Ma. For the same sample a Ar-Ar plateau type age of 230 ± 3 Ma has been measured on a coarse-grained muscovite.

A fine-grained quartzphyllite (RS35/01) from the Zebru Schuppenzone was collected to the west of the Zufritt Lake, about 10 m to the west of the Zebru line that separates the Zebru Schuppenzone from the Martell Micaschists. It is characterised by a mineral assemblage of Ms + Chl + Qtz + Pl ± Grt. Garnet is scarce and up to 1cm in diameter, whereas biotite or chloritoid has never been found in this unit. The rock shows a S-C deformation or crenulation cleavage respectively, which indicates NNW-directed ductile deformation. The muscovites from this sample yielded a plateau type age spectra of 87 ± 2 Ma.

Three samples from the Martell Micaschists were investigated. The first one, a typical staurolite-garnet micaschist (RS34/01) was collected near the sample described above, less than 10 m to the east of the Zebru fault, not far from the top but outside the small contact aureola of the granite. The rock shows a planar schistosity and extended planar layers of quartz lenses and bands. Staurolite crystals up to 2 cm in length crosscut the schistosity. Muscovite from this sample yielded a total gas age of 170 ± 4 Ma with individual age steps of 154 to 186 Ma. The biotite Rb-Sr age from the same sample is 86 ± 1 Ma.

From the Peder valley ca. 3 km W of the sampling point described above a staurolite-garnet micaschist (RS36/01) was used for dating. It is rich in up to several centimeters large and perfectly crystallized postdeformative staurolite porphyroblasts, which occur in a fine-grained, graphitic white mica matrix. Further up to several millimeters large garnet and biotite porphyroblasts are present. The Ar-Ar muscovite age spectra from this sample is saddle shaped and yielded a total gas age of 196 ± 3 Ma. The individual steps are in the range of 176 to 208 Ma. The Rb-Sr age of the biotite porphyroblasts is 138 ± 2 Ma.

Another staurolite-garnet micaschist from the Laaser Spitz (RS37/01) ca 6 km N of the Zufritt lake is also rich in staurolite. However, the individual crystals are only up to 1 cm in size and form black, elongated batches without sharp crystal edges. Muscovite from this sample yielded also a saddle shape spectra with a total gas age of 195 Ma and individual steps of 177 to 209 Ma.

Based on a Rb-Sr-WR-isochron BOCKEMÜHL [1] postulated a Lower Permian age (271 Ma) for the Martell granite. The new data prove this age and argue for a intrusion at about 275 Ma. The Ar-Ar ages of the muscovites are 250 and 230 Ma in age. However, these age values have to be taken with care, because micas from pegmatitic rocks often contain excess argon. In addition, an eo-Alpine overprint of the rocks has to be considered, which, as implied by the deformation structures of the granite, increases from the center to the border of the intrusion leading to an increasing rejuvenation of the ages.

The medium-grade staurolite-garnet micaschists of the Martell Micaschists yielded pre-Alpine Ar-Ar muscovite ages in the range of 170 to 196 Ma and a Rb-Sr biotite age of 138 Ma (sample RS36/01). These ages might be interpreted as Permo-Triassic cooling ages or Variscan ages partly reset during the eo-Alpine tectonometamorphic event. One argument for the first possibility is that ages of c. 200 Ma are typical for areas, which contain Permian pegmatites [2]. Several arguments though argue for the second possibility: The Variscan amphibolite facies mineral assemblage garnet + staurolite + biotite + plagioclase + quartz is partially replaced and/or overgrown by the eoalpine greenschist facies assemblage of garnet + plagioclase + biotite + musco-

vite ± chloritoid + paragonite ± margarite. In addition the eo-Alpine deformation features such as folds and mylonites are of medium to high greenschist facies with generally decreasing temperatures from NE to SW.

The sample RS34/01, collected from the uppermost part (at the SW-end) of the Martell Micaschist unit near the Zebru fault, indicates some rejuvenation, and shows a typical eo-Alpine Rb-Sr age of 86 Ma. As the blocking temperature for the Rb-Sr system in biotite (c. 300°C) is much lower than that for the Ar-Ar system in muscovite (c. 40°C) it implies eo-Alpine temperatures between 300 and 400°C for this area at the contact with the Zebru Schuppenzone.

The quartzphyllite of the Zebru Schuppenzone sampled a few meters above the Zebru fault shows an eo-Alpine muscovite age of 87 Ma. Since the staurolite micaschists immediately underlying the Zebru fault show Ar-Ar muscovite age of 170 Ma and a typical eo-Alpine Rb-Sr age of 86 Ma, it seems clear that the Zebru fault is eo-Alpine in age. In addition the quartzphyllites of the Zebru Schuppenzone have to be considered as a separate tectonic unit with a slightly higher eo-Alpine overprint than the underlying rocks. This is in strong contrast to previous investigations by [3], [4] and [5] reported also in [6], which argued that the quartzphyllites were the strongly retrogressed pendants of the underlying micaschists.

References

- [1] BOCKEMÜHL, C. (1988): Der Marteller Granit (Südtirol, Italien); Petrographie, Geochemie, Altersbestimmungen. - Unpubl. Diss. Univ. Basel.
- [2] SCHUSTER, R., SCHARBERT, S., ABART, R. & FRANK, W. (2001): Permo-Triassic extension and related HT/LP metamorphism in the Austroalpine - Southalpine realm. - Mitt. Geol. Bergbau Stud. Österr., 44, 111-141.
- [3] ANDREATTA, C. (1952): Polymetamorphose und Tektonik in der Ortlergruppe. - N. Jb. Mineral. Mh. Stuttgart, 1, 13-28.
- [4] GREGNANIN, A. & PICCIRILLO, E. M. (1972): Litostratigrafia, tettonica e petrologia degli scisti austridici di alta e bassa pressione dell'area Passiria-Venosta (Alto Adige). - Mem. Ist. Geol. Min. Univ. Padova, 28, 1-55.
- [5] GREGNANIN, A. & PICCIRILLO, E. M. (1972): Hercynian metamorphism in the Austroalpine crystalline basement of the Passiria and Venosta Alps. - Mem. Soc. Geol. It., 13, 241-255.
- [6] HOINKES, G. & THÖNI, M. (1993): Evolution of the Ötztal-Stubai, Scarl-Campo and Ulten basement units. In: von Raumer, J. F. & Neubauer, F. (Eds.), Pre Mesozoic Geology in the Alps. Springer Verlag, Berlin, 485-494.

THE METAMORPHIC EVOLUTION OF THE ORTLER CRYSTALLINE

V. Mair¹, P. Tropper² & A. Piber²

¹Amt für Geologie und Baustoffprüfung

Eggentalerstrasse 48, I-39053 Kardaun (BZ), Italy

²Institute of Mineralogy and Petrography

University of Innsbruck, Innrain 52, A-6020 Innsbruck, Austria

The Ortler crystalline represents a polymetamorphic Austroalpine crystalline basement which occurs southwest of the Ötztal crystalline between the Vinschgau- and the Ultental Valley. During the Eo-Alpine orogeny, the Ötztal Crystalline was juxtaposed onto the northern part of the Ortler Crystalline and its sedimentary cover [6].

Tectonostratigraphy

Tectonically, the Ortler crystalline represents a stack of three distinct units which can be distinguished by their polymetamorphic P-T evolution:

A): The Laaser Series: It is the lowermost unit and is characterized by intensely deformed, mylonitic amphibolites, micaschists, paragneisses and almost pure marbles (Laas Marble).

B): The Martell Micaschists: It is on top of the Laas Series and is comprised of a more or less homogeneous stack of micaschists (Grt-Sta-Bt-bearing schists) with intercalations of amphibolites, orthogneisses and rarely marbles.

C): The Zebre Schuppenzone: This unit consists mainly of quartzphyllites with small intercalations of greenschists, quartzites and impure marbles. This unit is tectonically emplaced onto the Martell Micaschists and occurs at the base of the overlying sedimentary cover (Ortler Trias).

Deformation history

The Variscan orogeny led to the formation of large-scale (km) folds, directed E-W and a penetrative foliation. Crosscutting relations between the foliation and the pegmatite dike swarms of the Permian Martell Granite [2] clearly indicate a Variscan age of the deformation. During the Eo-Alpine orogeny, the Variscan fold system was re-deformed which led to the formation of mylonites with WNW oriented stretching lineations and ± N-directed fold axes in the crystalline basement and the sedimentary cover. A second Eo-Alpine deformation phase caused the formation of a new fold system with fold axes directed towards WSW and NNW-directed thrusts. This deformation phase re-activated the early Eo-Alpine W-directed thrust systems such as the Zebre Line and the Zumpanell Line and led to the formation of a second penetrative foliation striking 60°- 80° and falling 30°- 40° south.

Metamorphic evolution

The Laas series and the Martell Micaschists clearly show a polymetamorphic evolution with an earlier Variscan and a later Eo-Alpine metamorphic overprint. In contrast to the Martell Micaschists, the Laas Series shows a stronger Eo-Alpine re-equilibration, thus erasing almost all of the Variscan metamorphic history. The Variscan mineral assemblage is in both units comprised of garnet + staurolite + biotite + plagioclase + quartz, the Eo-Alpine mineral assemblage contains garnet + plagioclase + biotite + muscovite ± chloritoid + paragonite ± margarite. While the P-T conditions of the Variscan event have not been constrained yet, the Eo-Alpine metamorphic conditions in both units range from 6.7–8.5 kbar and 480–500°C constrained from paragneisses and quartzphyllites. These data are in accordance with geochronological investigations which clearly indicate an Eo-Alpine metamorphic evolution. Previous investigations by [1], [3] and [4] reported also in [6] suggested that the deformation and metamorphic evolution of the Ortler Crystalline was mainly Variscan of age with a slight Eo-Alpine overprint, while our results clearly show that the Eo-Alpine metamorphic overprint was very strong and pervasive and thus led in the Laas Unit to a complete recrystallization during the Alpine orogeny. The metamorphic overprint decreases towards the W, indicated by the diminishing overprint of the Martell micaschists that in their westernmost part (Upper Peder and Sulden Valley) have almost preserved their variscan mineral assemblage.

Acknowledgements

Financial and logistic support from the projects CARG-PAT and CARG-PAB of the Autonomous Provinces of Trento and Bolzano-Südtirol.

References

- [1] ANDREATTA, C. (1952): Polymetamorphose und Tektonik in der Ortlergruppe. - N. Jb. Mineral. Mh. Stuttgart, 1, 13-28.
- [2] BOCKEMÜHL, C. (1988): Der Marteller Granit (Südtirol, Italien); Petrographie, Geochemie, Altersbestimmungen. - Unpubl. Diss. Univ. Basel.
- [3] REGNANIN, A. & PICCIRILLO, E. M. (1972): Litostratigrafia, tettonica e petrologia degli scisti austridici di alta e bassa pressione dell'area Passiria-Venosta (Alto Adige). - Mem. Ist. Geol. Min. Univ. Padova, 28, 1-55.
- [4] REGNANIN, A. & PICCIRILLO, E. M. (1972): Hercynian metamorphism in the Austridic crystalline basement of the Passiria and Venosta Alps. - Mem. Soc. Geol. It., 13, 241-255.
- [5] HAMMER, W. (1912): Erläuterungen zur geologischen Spezialkarte der Österr.- ungar. Monarchie im Maßstabe 1: 75.000, Blatt Glurns und Ortler.
- [6] HOINKES, G. & THÖNI, M. (1993): Evolution of the Ötztal-Stubai, Scarl-Campo and Ultendorf basement units. - In: von Raumer, J. F. and Neubauer, F. (Eds.), Pre Mesozoic Geology in the Alps. Springer Verlag, Berlin, 485-494.

STRUCTURAL AND CHEMICAL INVESTIGATIONS OF OSUMILITES
FROM THE EIFEL DISTRICT (GERMANY)

A. Malsy & T. Armbruster

Laboratorium für chemische und mineralogische Kristallographie
Universität Bern, Freiestrasse 3, CH-3012 Bern, Switzerland

The group of double-ring silicates can be described by the general crystal-chemical formula $^{VI}A_2^{IX}B_2^{XII}C^{XVIII}D^{IV}(T2)_3^{IV}(T1)_{12}O_{30}$ [1]. Various minerals of this group have been detected relatively late for two reasons: First because they were mistaken for other minerals, second because the light, lithophile elements which play an import role to this group are often overlooked in microprobe analyses [2].

Osumilite (space group $P6/mmc$, $a \approx 10.098(3)\text{\AA}$, $c = 14.312(4)\text{\AA}$) named after the province of Osumi was first recognized as a new mineral by Miyashiro who deduced its crystal structure in 1956 [2]. The structure is based on double-six-membered rings of T1 tetrahedra that are predominantly occupied by Si and secondary by Al, a remarkably consistent Si content at 10.5 Si is reported [3]. The T2 tetrahedra are mainly occupied by Al with little Fe and Mg [3]. Octahedra (A) are mainly occupied by Mg and Fe, together with T2 tetrahedra they build 12-membered T2/A-rings. T1 double rings and T2/A rings are alternately stacked above each other, thus forming continuous channels along the c-axis [4]. Along these channels the C site (0, 0, 1/4) is situated between two sets of double rings and is occupied by large alkali- or alkaline-earth ions (mainly K), whereas the D site (0, 0, 0) in the center of the double-rings is assumed to be empty. An additional atomic position ^{IX}B at $(1/3, 2/3, 0)$ or B' ($(1/3, 2/3, z)$) is well known from osumilite related double-ring silicates (e.g. roedderite and sugilite). B' is slightly shifted from the mirror plane and occurs in space group $P6/mmc$ as a split positions. This site was hitherto not considered for osumilite.

For this study crystal-structures including site occupancies of five natural osumilites from Eifel district were refined from X-ray single-crystal data. Three crystals from Sattelberg were yellow; one from Bellerberg was blue and the other orange in color. Chemical variations and the adjustment of the structure were analyzed and compared with data by ARMBRUSTER & OBERHÄNSLI (1988). The latter authors found significantly more alkalies (Na, K) by electron microprobe-analyses than they could locate in corresponding structure refinements.

In this investigation special care was taken to resolve electron density on low-occupied positions by using a state of the art CCD-equipped diffractometer. With the exception of one crystal, significant electron density above the assumed noise level of $\pm 0.5 \text{ e}/\text{\AA}^3$ at the B' site ($(1/3, 2/3, z)$) was detected. Electron microprobe analyses carried out on the same crystals as used for structure refinements, indicate that mainly Na occupies this B' position up to 22 %. Thus, the sought-after site for excess alkalies is the interstitial B' position.

Although Fe populations were refined on the octahedral A and tetrahedral T2 site, it is striking that microprobe analyses gave significantly higher Fe concentrations than site occupancy refinements. A suggested explanation for this discrepancy is submicroscopic hematite inclusions adulterating microprobe data. Hematite inclusions have no bearing on site-occupancy refinements, but overstate the Fe concentration of microprobe analyses.

Regression analyses indicate a positive correlation between refined Fe population on octahedral and tetrahedral sites for all samples except the yellow ones from Sattelberg. Samples from Sattelberg incorporate Fe almost exclusively on the T2 site (up to 8 %) suggesting ferric iron. This assumption is also confirmed by the observed T2–O bond-lengths and supported by the conspicuous yellow hue.

References

- [1] FORBES, W. C. ET AL. (1972): Crystal chemistry of milarite-type minerals. - American Mineralogist, 57, 463-472.
- [2] HAWTHORNE, F. C. ET AL. (1991): The crystal chemistry of the milarit-group minerals. - American Mineralogist, 76, 1836-1856.
- [3] OLSEN, E. & BUNCH, T. E. (1970): Composition of natural osumilites. - American Mineralogist, 55, 875-879.
- [4] ARMBRUSTER, T. & OBERHÄNSLI, R. (1988): Crystal chemistry of double-ring silicates: Structural, chemical, and optical variation in osumilites. - American Mineralogist, 73, 585-594.

**POLYMETALLIC MINERALIZATION IN SVRATKA DOME (MORAVICUM, CZECH REPUBLIC):
STABLE ISOTOPE AND FLUID INCLUSION STUDY**

K. Malý¹ & Z. Dolníček²

¹Muzeum Vysočiny Jihlava

Masarykovo nám, 55, 586 01 Jihlava, Czech Republic

²Department of Geology

Palacký University, tr. Svobody 26, 771 46 Olomouc, Czech Republic

Polymetallic mineralization is widespread in the Moravicum, the western margin of the Bohemian Massif, Czech Republic. The ore occurrences have been mined since the 13th century and new prospected during 1958–1965. The geological reserves of Pb-Zn, Cu, Ag, and F-Ba ores are small and therefore not significant.

We found three principal types of polymetallic mineralizations:

1) The **Pb-Zn(-Sb) mineralizations** are vein type or metasomatic (in marble). The most common ore minerals are sphalerite (from 0.18 to 4.44 wt. % Fe; 0.00–0.59 wt. % Cd) and galena (up to 1404 ppm Ag, 974 ppm Bi, 2100 ppm Sb). Chalcopyrite, arsenopyrite, pyrite, antimonite, boulangerite, tetrahedrite, freibergite, bournonite, pyrargyrite etc. are not frequent. Gangue minerals are represented by quartz, carbonates (dolomit-ankerite) and (calcite and siderite are rare) barite (sometimes it is missing or rare).

The estimated isotopic composition of total sulfur ($\delta^{34}\text{S}_{\Sigma}$) in the hydrothermal fluids is different in the various localities, it changes from 5 to 11 ‰ CDT (in one locality is $\delta^{34}\text{S}_{\Sigma}$ is from about -1 to +1 ‰ CDT). Temperatures of crystallization of sulfides are between 180 and 220°C (and new calculated for the sphalerite-galena mineral pairs according to [1]). The isotopic composition of oxygen ($\delta^{18}\text{O}$) of the hydrothermal fluids was calculated and is in the range from +3 to +12 ‰ SMOW (according to [2]). Isotopic composition of oxidized carbon ($\delta^{13}\text{C}$) in the hydrothermal fluids was determined in the range -9 to -3 ‰ CDT (according to [3]).

Primary fluid inclusions contain a fluid of the $\text{H}_2\text{O}-\text{NaCl}$ (Ca, K, Mg, Cl) type; inclusions of the $\text{H}_2\text{O}-\text{NaCl}$ (Ca, K, Mg-Cl)- CH_4 type were found only once. The salinity of the entrapped fluids and the temperature of homogenization are different depending on the locality and the mineral. The salinity is between 5.1 (barite) and 11.8 (sphalerite) wt. % NaCl equiv. The temperature of homogenization is about 130°C (barite), 140–240°C (quartz), 175°C (sphalerite). The pressure of formation of the sulfides is assumed to be about 50–60 MPa.

2) The **Cu-Pb(-Zn) mineralization** is of vein type, it is probably younger than the Pb-Zn(-Sb) mineralization. It is composed of galena (up to 107 ppm Ag, 134 ppm Bi and 828 ppm Sb), chalcopyrite (up to 349 ppm Ag, 4138 ppm Zn), quartz, calcite and barite. Other minerals are rare: pyrite, marcasite, tetrahedrite, dolomit-ankerite. The mineralization is typical by numerous secondary minerals such as malachite, azurite, brochantite, posnjakite, langite, copper, silver, djurleite, covellite are common and characteristic.

The estimated isotopic composition of total sulfur ($\delta^{34}\text{S}_{\Sigma}$) in the hydrothermal fluids is between +9 and +11 ‰ CDT. Temperatures of crystallization of sulfides are between 95 and 105°C (minerals pairs sphalerite-galena, sphalerite-chalcopyrite, chalcopyrite-galena). The isotopic composition of oxygen ($\delta^{18}\text{O}$) of the hydrothermal fluids was in the range from -7 to +9 SMOW. Isotopic composition of oxidized carbon ($\delta^{13}\text{C}$) in the hydrothermal fluids was determined -9 to -5 ‰ CDT.

Primary fluid inclusions (in quartz and barite) are $\text{H}_2\text{O}-\text{NaCl}(-\text{Ca, K, Mg-Cl})$ type; their liquid vapour ratio is variable (liquid-only inclusions were found too). The salinity changes between 0.1 and 6.1 wt.% NaCl equiv. (on average about 3 wt.% NaCl equiv.). Temperature of homogenization is between 104 and 170°C (on average about 120°C).

3) The **calcite-barite-fluorite mineralization** is also of vein-type and probably the youngest one (Upper Permian-Lower Triassic paleomagnetically).

A detailed mineralogical study proved polyphase evolution of the mineralization. The oldest is dolomite fill, followed by two generations of calcite, then fluorite and barite, and finally two generations of calcite. Typical is the presence of hematite, goethite and common sulfides, especially chalcopyrite (9–40 ppm Ag, 670–1090 ppm Zn) and galena (330 ppm Ag, 500 ppm Sb, 12 ppm Bi), rarely occurs sphalerite (0.5 % Fe, 0.9–1.6 % Cd), marcasite (770 ppm As), pyrite (0.7–2.2 % As, 7 ppm Mn, 18 ppm Ni, 9 ppm Co), tetrahedrite, bravoite and gersdorffite.

The mineralization is clearly of low-temperature (Th of fluid inclusions < 50–125°C) and originated from highly saline fluids (salinities up to 24 wt. % NaCl equiv.), which locally mixed with meteoric waters, mainly in late stages. The solutions contain especially Na and Ca chlorides. $\delta^{34}\text{S}$ values of sulfide minerals decrease from the dolomite stage (c. +5 ‰ CDT) through fluorite-barite (c. -9 ‰ CDT) to late calcite (-30 ‰ CDT); barite has +11 to +19 ‰ CDT. Neither among coexisting sulfides nor between sulfides and barite the isotopic equilibrium was reached (unrealistic calculated isotopic temperatures from -47 to +1170°C). The calculated $\delta^{13}\text{C}$ values of the parent fluid range between -7 and -13 ‰ PDB and calculated $\delta^{18}\text{O}$ value of the fluid is 0 ± 3 ‰ SMOW.

The calculated values of $\delta^{34}\text{S}_{\Sigma}$ of the Pb-Zn(-Sb) and Cu-Pb(-Zn) types indicate that sulfur of the hydrothermal fluid may be derived from country rocks. The carbon of homogenization of the Earth's crust mixed with carbon from the surrounding marbles, limestones and carbon from graphitic rocks are assumed to be the source of carbon in the hydrothermal fluids. The oxygen of water of the hydrothermal fluids was isotopically equilibrated with the metamorphic rocks at high temperature (metamorphic waters s.l.). Meteoric waters took part in the formation of late stage Cu-Pb(-Zn) mineralization. The genesis of the hydrothermal solutions are probably connected with late (retrograde) phases of Variscan metamorphism. The genetic connection of the mineralization with a magmatic source or with tectonic lineaments [4] is improbable.

The genesis of the fluorite-barite veins was probably connected with post-Variscan migration of the basinal brines along NW-SE fault structures at low temperatures. The sulfate may come from P-Tr marine water. Reduced sulfur may be derived either from an isotopically light external source or originates directly within the hydrothermal system due to some of the sulphate-reducing processes. The formation conditions are well comparable with other occurrences of Mesozoic fluorite-barite mineralization within remaining parts of the Bohemian massif as well as elsewhere in Europe.

References

- [1] OHMOTO, H. & RYE, R. Q. (1979): Isotopes of sulphur and carbon.- In: Barnes, H.I. (ed.): Geochemistry of hydrothermal ore deposits, 2nd ed., J. Wiley and Sons. New York.
- [2] ONEIL, J. R., CLAYTON R. N. & MAYEDA, T. K. (1969): Oxygen isotope fractionation in divalent metal carbonates. - *J. Chem. Phys.*, 51, 5547-5558.
- [3] MATSUHISA, Y., MORISHITA, Y. & SATO, T. (1985): Oxygen and carbon isotope variations in gold-bearing hydrothermal veins in the Kushikino mining area, Southern Kyushu, Japan. - *Economic Geology*, 80, 1985, 283-293.
- [4] BERNARD, J. H. (1991): Empirical types of ore mineralization in the Bohemian Massif. - *Czech geological Survey*. Praha.

**GEOGENIC PLATINUM GROUP ELEMENT (RU, RH, PD, OS, IR AND PT)
AND RE BACKGROUND ABUNDANCES IN THE AUSTRIAN ALPS**

T. Meisel

Institut für Allgemeine und Analytische Chemie
Montan-Universität Leoben, Franz-Josef-Strasse 7. A-8700 Leoben, Austria

The Federal Environment Agency of Austria (Umweltbundesamt, UBA), in cooperation with the General and Analytical Chemistry (University of Leoben, Austria) started an environmental sampling project in soils along major Austrian motorways (from Vienna to Vorarlberg). Emphasis was put on platinum group elements (PGE) since some of these metals are used in automobile catalytic converters. At all sample sites the Rh, Pd, Pt but also Ir and Re significantly exceed natural background values and reach concentrations up to 13 ng/g, 25 ng/g, 134 ng/g, 1.1 ng/g and 9.8 ng/g respectively on the top soil layer adjacent to the motorways.

In this study not only the contaminated soil surface was sampled but also the layer 5–10 cm below the surface and 10 m away from the polluted area. This was done to estimate the natural background level of the sample site. The bedrock below the soil layers is the only PGE source in soils other than automobile catalytic converter. Since motorways are mainly build in valleys, probably on stream sediments, the analysis of soils could give a good average for the geogenic or natural background of the region. It is the aim of this work to compare the regional background level with estimates of continental upper crust based on loess [1], impact melts [2] and European graywackes [3].

The continental upper crust is severely depleted in PGE relative to the Earth's core and mantle and contains < 0.001 % of the terrestrial PGE budget [1]. The extremely low abundance and the analytical difficulties involved in analyzing these elements as well as finding representative samples makes estimations that are essential for geochemical modeling a challenging task. For this study we applied an analytical procedure [4] based on an on-line cation exchange ICP-MS isotope dilution determination after acid attack in a high pressure ashing (HPA-S Anton Paar, Graz).

The variation within one site is similar to the variation amongst localities. Thus an overall average can be taken as being representative for all soils sampled in this study. The PGE average abundances in uncontaminated Austrian soils (average of 11 samples from 8 localities) is presented in table 1 and plotted as mantle normalized values in figure 1. Higher Os and Ir abundances than the upper crustal estimates is the most apparent feature. Whereas for all the other elements a comparison is made difficult due to the high variances in concentrations. If Os and Ir are preferentially enriched in soils or if the PGE abundances in an average bedrock is different to the loess (e.g. due to lesser abundance of higher density PGE bearing minerals such as chromite in loess) cannot be said at this stage of the study.

ng/g	Os	Ir	Ru	Rh	Pt	Pd	Re
this work	0.073	0.105		0.050	0.730	0.800	0.185
Lit. [1]	0.031	0.022	0.210		0.510	0.520	0.198
Lit. [2]	0.030	0.030	0.106	0.380		0.500	0.400
Lit. [3]	0.050	0.050	0.100	0.060	0.400	0.400	0.400

Table 1

PGE abundances in soils and PGE estimates of the continental crust.

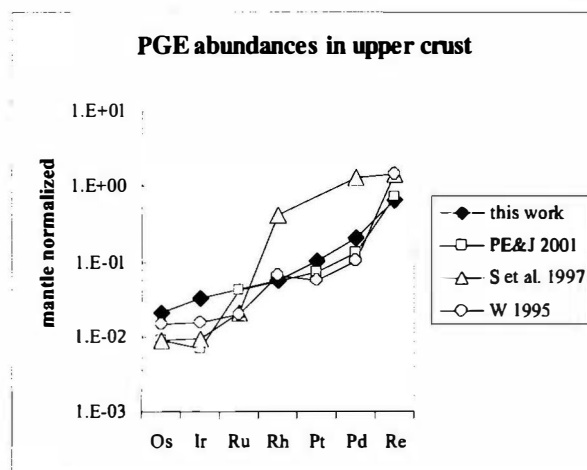


Fig. 1

Mantle normalized abundances in Austrian soils and in estimates for the continental crust. PE & J[1] estimated based on loess, S[2] based on impact melts from the Scandinavian shield [3] based on European graywackes.

References

- [1] PEUCKER-EHRENBRINK, B. ET AL. (2001): Rhenium-osmium isotope systematics and platinum group element constraints: Loess and the upper continental crust. - *g-cubed*, 2, 2001GV000172.
- [2] SCHMIDT, G. ET AL. (1997): Highly siderophile elements (Re, Os, Ir, Ru, Rh, Pd, Au) in impact melts from three European impact craters (Sääksjärvi, Mien, and Dellen): Clues to the nature of the impacting bodies. - *Geochimica et Cosmochimica Acta*, 61, 2977-2987.
- [3] WEDEPOHL, K. H. (1995): The composition of the continental crust. - *Geochimica et Cosmochimica Acta*, 59, 1217-1232.
- [4] MEISEL, T. ET AL. (2003): A simple procedure for the determination of platinum group elements and rhenium (Ru, Rh, Pd, Re, Os, Ir and Pt) using ID-ICP-MS with an inexpensive on-line matrix separation in geological and environmental materials. - *Journal of Analytical Atomic Spectrometry*, 18, 720-726.

A METAMORPHOSED EARLY CAMBRIAN CRUST-MANTLE TRANSITION IN THE
SPEIK COMPLEX, EASTERN ALPS, AUSTRIA

F. Melcher¹ & T. Meisel²

¹Bundesanstalt für Geowissenschaften und Rohstoffe
Stilleweg 2, D-30655 Hannover, Germany

²Institut für Allgemeine und Analytische Chemie
Montan-Universität Leoben, Franz-Josef-Strasse 7, A-8700 Leoben, Austria

In the Austroalpine Speik Complex (Eastern Alps, Austria), highly melt-depleted, metamorphosed harzburgites are interlayered with a suite of metamorphosed orthopyroxenites, clinopyroxenites and gabbros. Small pods and narrow bands of chromitite are abundant in the Kraubath and Hochgrößen massifs. At Kraubath, coarse-grained orthopyroxenites occur as cm- to m-wide veinlets and pods, but also as intrusive plugs several tens of metres wide. Intimately associated meta-clinopyroxenite and metagabbro are present as bodies up to several metres thick at a distinct stratigraphic level within the Kraubath and Pernegg massifs. In the ultramafic rocks, relict magmatic olivine, orthopyroxene, clinopyroxene and spinel are overprinted by a metamorphic assemblage of forsterite, diopside, tremolite, anthophyllite, chlorite, serpentine, talc and Cr-Fe-rich spinel. Calcic amphibole, epidote, zoisite and chlorite dominate the metamorphic paragenesis in metagabbros, besides few relicts of clinopyroxene and garnet. The polymetamorphic evolution of the Speik Complex includes rarely preserved pre-Variscan (> 400 Ma) eclogite facies conditions [1], Variscan (~300 Ma) amphibolite facies (600–700°C, > 5 kb) and Eoalpine (~100 Ma) greenschist- to amphibolite facies conditions reaching 550°C and 7–10 kb.

Orthopyroxenites are characterized by high concentrations of SiO₂, MgO and Cr, and by U-shaped chondrite-normalized rare earth elements (REE) patterns similar to those of their harzburgite hosts [4]. The REE patterns of the clinopyroxenites are flat to slightly enriched in light REE [4]. Metagabbro compositions are variable, but generally characterised by low SiO₂ and high *mg*-numbers (61–78). Their REE patterns all have Gd_N/Yb_N > 1; some samples have large positive Eu anomalies implying the original presence of cumulus plagioclase.

In metaperidotites, two types of chondrite-normalized platinum-group element (PGE) patterns are observed: (1) flat patterns without significant fractionation from Os to Pd; Re_N/Os_N is < 0.5. (2) Positively sloping patterns with low concentrations of the IPGE, but significant fractionation between IPGE and PPGE (Pd_N/Os_N = 10 to 50) are observed in a few peridotites; Re_N/Os_N ranges from 2 to 17. Chromitites have a variety of normalized PGE patterns, and carry up to 4 ppm total PGE [2, 3, 5]. Many have negative slopes typical for ophiolitic-podiform chromitite. Also present are flat patterns, zig-zag patterns with positive peaks of one or more of the PGE, and positive slopes. In the orthopyroxenites and clinopyroxenites, Pt, Pd and Re are distinctly enriched compared to the IPGE.

$^{187}\text{Os}/^{188}\text{Os}_{(i)}$ ratios are chondritic to slightly suprachondritic, ranging from 0.1185 to 0.1288 in most metaperidotites of the Speik Complex, and from 0.123 to 0.127 in most chromitites. In-situ LA-ICPMS analyses of platinum-group minerals (laurite, ruarsite) separated from podiform chromitite reveal a large variation from subchondritic to chondritic $^{187}\text{Os}/^{188}\text{Os}$ (0.1158–0.1244) [3]. Those metaperidotites that have positively sloping chondrite-normalized PGE patterns, have significantly lower Os (< 1 ppb) and/or higher Re concentrations (up to 0.8 ppb); these samples yield radiogenic $^{187}\text{Os}/^{188}\text{Os}$ ratios ranging from 0.17 to 0.77. Radiogenic $^{187}\text{Os}/^{188}\text{Os}$ (0.14 to > 10) and $^{187}\text{Os}/^{188}\text{Os}$ (~0.7 to > 400) are also typical for orthopyroxenite, metaclinopyroxenite and chromitite associated with orthopyroxenite.

The Os isotopic data of the metaperidotites contain no or little age information, because (1) of large scatter in $^{187}\text{Os}/^{188}\text{Os}$, and (2) low Re/Os ratios. On the other hand, the Re-Os isotope compositions of the pyroxenites define an errochron at 550 ± 17 Ma and a supra-chondritic $^{187}\text{Os}/^{188}\text{Os}$ of 0.179 ± 0.003 (Fig. 1A). An isochron age of 554 ± 37 Ma with $\epsilon_{\text{Nd}(i)} +0.7$ is indicated by the Sm-Nd isotope compositions of whole-rock pyroxenites and gabbros from the Kraubath massif (Fig. 1B). The harzburgites of the Speik Complex plot on an errorchron of 745 ± 45 Ma and $\epsilon_{\text{Nd}(i)} +6$; this possibly dates an ancient melt extraction event in the mantle.

The pyroxenites and gabbros represent a cogenetic suite of magmatic dykes intruded into uppermost, highly depleted suboceanic mantle close to the crust-mantle transition zone in an oceanic basin close to the north-western margin of Gondwana. Second-stage melting in a supra-subduction zone setting during the Early Cambrian resulted in formation of highly depleted residual mantle and radiogenic, high-(Si, Mg) mantle melts. From such melts, the intrusive orthopyroxenite/clino-pyroxenite/gabbro suite formed as cumulates under the influence of variable melt-rock reaction. Despite the polymetamorphic history of the Austroalpine basement complex, geochemical data, in combination with Re-Os, Sm-Nd isotope investigations provide constraints for the age, origin and source of melts percolating refractory upper mantle.

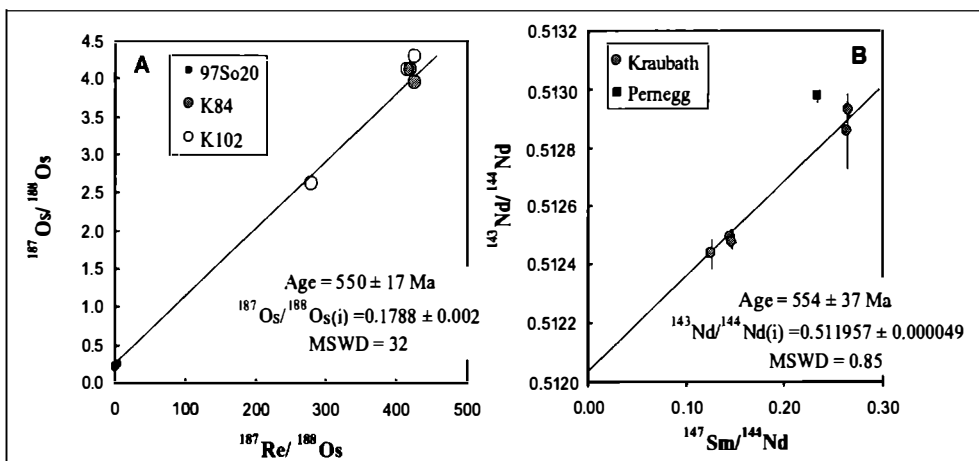


Fig. 1

Radiometric data from the Speik Complex. A) Re-Os errorchron of orthopyroxenites from the Kraubath massif. B) Sm-Nd isochron of orthopyroxenites and metagabbro from the Kraubath massif.

References

- [1] FARYAD, S. W., MELCHER, F., PUHL, J., HOINKES, G. & FRANK, W. (2002): Relics of eclogite-facies metamorphism in the Austroalpine basement, Hochgrößen (Speik Complex), Austria. - Mineralogy and Petrology, 74, 49-73.
- [2] MALITCH, K. N., MELCHER, F. & MÜHLHANS, H. (2001): Palladium and gold mineralization in podiform chromitite at Kraubath, Austria. - Mineralogy and Petrology, 73, 247-277.
- [3] MALITCH, K. N., THALHAMMER, O. A. R., KNAUF, V. V. & MELCHER, F. (2003): Diversity of platinum-group mineral assemblages in banded and podiform chromitites from the Kraubath ultramafic massif, Austria: evidence for an ophiolitic transition zone? - Mineralium Deposita, 38, 282-297.
- [4] MELCHER, F., MEISEL, T., PUHL, J. & KOLLER, F. (2002): Petrogenesis and geotectonic setting of ultramafic rocks in the Eastern Alps: constraints from geochemistry. - Lithos, 65, 143-164.
- [5] MELCHER, F., PUHL, J., MALI, H. & MEISEL, T. (1999): Chromite and platinum-group element mineralization in ultramafic rocks of the Speik Complex, Eastern Alps. - In: Mineral Deposits: Processes to Processing. Balkema Stanley, C.J. (ed.), Rotterdam, pp. 739-742.

PHOSPHIN BEI DER VERBRENNUNG PHOSPHORHALTIGER ABFÄLLE

J. Metschke

Müllkraftwerk Schwandorf Betriebsgesellschaft mbH
Alustrasse 50-52, D-9242 Schwandorf, Germany

Phosphate und sonstige Phosphorverbindungen kommen in sehr unterschiedlichen Größenordnungen in den verschiedenen zur thermischen Verwertung gelangenden Abfällen vor. Nachstehend ein Überblick über den Gehalt an Phosphorverbindungen in den für thermische Abfallbehandlungsanlagen relevanten Abfällen:

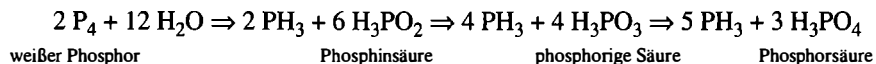
Abfallart	Gramm Phosphor/kg Abfall
Hausmüll	1 – 4
Klärschlamm	2 – 55
Getreide, Stroh	4 – 10
Gras, Heu	1 – 3
Tiermehl	10 – 30
Knochenmehl	70 - 90

Im Zusammenhang mit dem Verarbeitungs- und Verfütterungsverbot von Tier- und Knochenmehl während des Höhepunktes der BSE-Krise wurden auch diese Abfälle in einigen thermischen Abfallbehandlungsanlagen angeliefert und zusammen mit anderen Abfallarten verbrannt. Bei orientierenden Messungen wurden entlang des Weges der Schlacken Phosphorwasserstoffkonzentrationen (Phosphin, PH_3) ermittelt, die zum Teil deutlich über der zulässigen maximalen Arbeitsplatzkonzentration (MAK-Wert) von 0,1 ppm lagen.

Phosphin ist ein selbstentzündliches, explosives Gas und außerdem ein starkes Stoffwechsel- und Nervengift. In der Praxis wird es als Pflanzenschutzmittel verwendet. Acetylen zum Schweißen ist häufig mit Phosphin odorisiert. Daher röhrt der typische "carbidische" Geruch des Gases. Phosphin ist schwerer als Luft und die Geruchsschwelle liegt mit etwa 1 ppm deutlich über dem MAK-Wert.

Es war deshalb für die Anlagenbetreiber von größtem Interesse, die Entstehung von Phosphinen bei der Verbrennung von Hausmüll und hausmüllähnlichen Abfällen aufzuklären.

Die reduzierende Atmosphäre (Reaktion mit Kohlenstoff und/oder mit metallischem Aluminium) im Müllbett des Verbrennungsrostes bei hohen Temperaturen kann zur Freisetzung von elementarem Phosphor aus den im Abfall enthaltenen Phosphor- und Phosphatverbindungen führen. Der so gebildete rote Phosphor kann sich bei der Abkühlung der Schlacke bei etwa 600°C zu weißem Phosphor umwandeln, der mit dem stark alkalischen Wasser des Nassentschlackers unter Disproportionierung zu Phosphin und Phosphorsäure reagiert.



Als potentielle Phosphorträger in den Abfällen kommen mehrere Quellen in Frage.

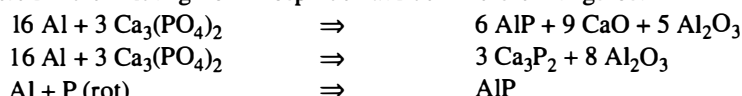
Beim Verbrennungsprozess können sich aus den Phosphorverbindungen und Metallen bestimmte Phosphide bilden.

Elementarer, roter Phosphor kann in sehr fein verteilter Form als Bestandteil von Flamm-schutzmitteln in PVC und Nylon-Erzeugnissen vorkommen.

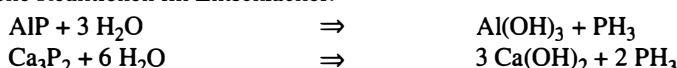
Aber auch der in der Knochensubstanz enthaltene Hydroxylapatit kann mit stets in den Abfällen vorhandenem metallischem Aluminium oder Zink oder auch Alkalien und Erdalkalien zu Calciumphosphiden (Metall-Phosphorverbindungen) reduziert werden.

Diese Phosphide hydrolyseren mit dem Wasser des Entschlackers zu Metallhydroxiden und Phosphin.

Beispiele für die Bildung von Phosphiden auf dem Verbrennungsrost:



Mögliche Reaktionen im Entschlackeraufschluss



Grundsätzlich läuft bei der Bildung von Phosphin unter den Bedingungen einer Müllverbrennungsanlage also ein zweistufiger Prozess ab:

1. Unter reduzierenden Bedingungen bei gleichzeitig hohen Temperaturen kann sich elementarer Phosphor bilden. Dieser reagiert mit Metallen zu Phosphiden. Oder es reagieren Metalle direkt mit Phosphaten unter Bildung von Phosphiden.

2. Mit Wasser zusammen reagieren diese Phosphide oder auch der elementare Phosphor z. B. im Entschlacker unter Freisetzung von Phosphin. Begünstigt wird diese Reaktion u. a. durch alkalische Lösungen. U. U. reicht auch schon die Luftfeuchtigkeit aus, um diese Reaktionen in Gang zu setzen.

Vom gesamten in der Schlacke enthaltenen Phosphor wird im Allgemeinen nur ein sehr geringer Anteil (etwa 0,01–0,02 %) während des Durchlaufs über den Müllverbrennungsrost zu elementarem Phosphor oder zu Phosphin reduziert.

Bei den Untersuchungen wurde auch festgestellt, dass die im Entschlacker freigesetzte Phosphinfracht nicht unbedingt proportional der Menge an "reaktionsfähigem Material" (Phosphide oder elementarer Phosphor) ist. Milieufaktoren wie der pH-Wert, die Temperatur, das Redoxpotential und der Salzgehalt des Wassers bestimmen die Reaktivität und damit die Geschwindigkeit und die Dauer der Phosphinfreisetzung.

Auch die Korngrößenverteilung und die Porosität der Schlacken und damit direkt auch der Heizwert des verbrannten Abfalls sowie bestimmte begleitende Phasen in der Schlacke haben erheblichen Einfluss auf die Freisetzung des Gases. Das mag auch erklären, dass bei der Mitverbrennung von Tier- und/oder Knochenmehl auf Grund des deutlich höheren Brennwertes und der daraus resultierenden stärkeren Versinterung und Verglasung der Schlacke die Phosphinfreisetzung nicht im gleichen Maße zunimmt wie der gesamte Phosphorgehalt in den Schlacken.

Die Phosphide und elementarer Phosphor sind größtenteils fein verteilt in der Matrix des Schlackefeinkorns zu finden. Eine Anreicherung an der Oberfläche konnte nicht festgestellt werden. So erklärt es sich, dass nach der Benetzung der Schlacke der Großteil des Phosphins während der ersten 8–10 Stunden frei gesetzt wird.

Unter Einwirkung von UV-Licht zerfällt Phosphin zusammen mit Luftsauerstoff in Wasserstoff und Phosphorpentoxid. Die Halbwertszeit ist abhängig von der Umgebungstemperatur. Bei den Untersuchungen unter Laborbedingungen wurde eine Halbwertszeit von 10,7 Stunden ermittelt.

Die Mitverbrennung von Tier- und Knochenmehl in den thermischen Abfallbehandlungsanlagen der BRD ist in der Zwischenzeit eingestellt worden. Die heute messbaren Konzentrationen an Phosphin auf dem Weg der Schlacke liegen im Allgemeinen in der Größenordnung des MAK-Wertes. Vor längere Zeit andauernden Arbeiten an Entschlackern werden vorsichtshalber orientierende Messungen durchgeführt.

EXPERIMENTELLE UNTERSUCHUNG DER HYDRISCHEN REAKTION
GIPS - BASSANIT: EINE INDIREKTE METHODE ZUR ERFASSUNG
ANOMALEN PVT-VERHALTENS VON WASSER ?

P. W. Mirwald

Institut für Mineralogie und Petrographie
Universität Innsbruck, Innrain 52, A-6020 Innsbruck, Austria

Wasser ist eine Verbindung von enormer und vielfältiger Bedeutung. Im Bereich der Erdwissenschaften spielt Wasser einerseits die Rolle einer Mineralkomponente andererseits ist es Lösungs- und Transportmedium bei Prozessen in der Erdkruste und Erdmantel.

Die Kenntnis der Eigenschaften von Wasser ist immer noch begrenzt, trotz seiner einfachen chemischen Zusammensetzung. Die gilt insbesonders für seine Eigenschaften bei hohen Drucken und Temperaturen.

Vor kurzen konnten Hinweise gewonnen werden, daß – entgegen der allgemeinen Annahme – Wasser hinsichtlich seiner PVT-Eigenschaften kein kontinuierliches Verhalten aufweist. Es konnte gezeigt werden, daß es bei Wasser unter hohen Drucken und Temperaturen P-T Bereiche verschiedenen PVT-Verhaltens gibt, die durch Anomalien begrenzt sind (vergl. Abb. 1) [1, 2].

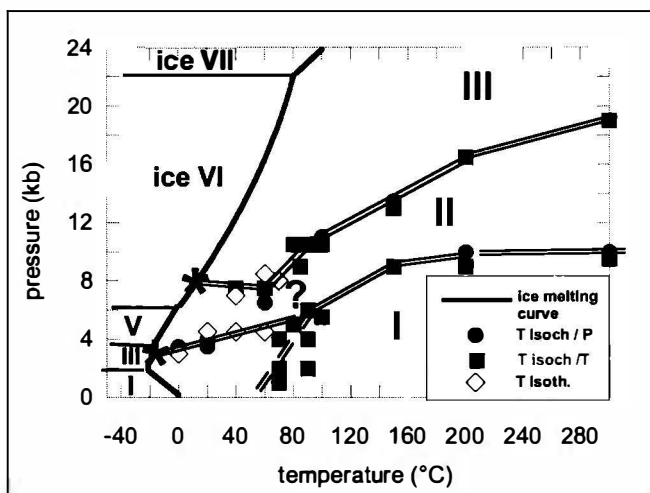


Abb. 1
Phasendiagramm von H_2O mit den Schmelzkurven von Eis I, III, V und VI sowie einer ver- suchweisene Lokalisierung von PVT-Anomalien von Wasser [1]. Die Darstellung beruht auf Daten der Kompressibilität, Thermischen Expansion und des isochoren Koeffizienten von Wasser, die aus den Steam Tables [4] berechnet wurden.

Kompressionsexperimente an Wasser mittels einer konventionellen Kolben-Zylinderapparatur haben den Temperaturbereich bis ca. 50°C – bei Drücken bis zu 12 Kb – erschlossen [2]. Eine Erweiterung dieser Experimente zu höheren Temperaturen gestaltet sich experimentell sehr schwierig. Deshalb wurde eine Methode gesucht die vermuteten PVT-Anomalien von Wasser zu höheren Temperaturbedingungen zu erfassen.

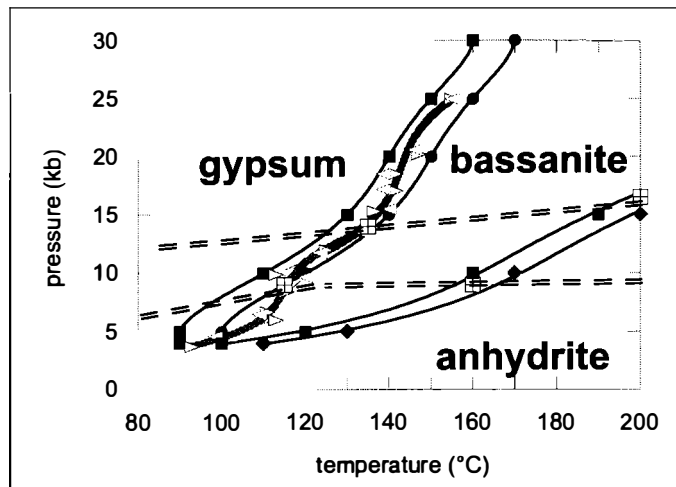
Es wurde eine experimentelle Studie unternommen, in der das P-T-Verhalten der hydratischen Reaktion von Gips Bassanit untersucht wurde, denn es schien wahrscheinlich, daß diskontinuierlich veränderliche Wassereigenschaften sich hierbei bemerkbar machen.

Die Versuche wurden mit einer Kolben Zylinder Apparatur in einem "22mm Druckgefäß" durchgeführt. Als Druckzelle diente eine konventionelle Salzzelle. Die in einer Goldkapsel befindliche Probenmenge betrug ca. 120 mg Gips und ca. 8 mg H₂O. Die erforderlichen kontinuierliche Temperaturänderungen im Bereich von 1–10K/h wurden über ein NiCrNi Thermoelement mittels eines fein regelbaren Kontrollers gesteuert. Der Druck wurde stets zu Versuchsbeginn fixiert und veränderte sich dann während des Experiments nur quasi-isochorisch. Die Dehydratation bzw Hydrationsreaktion wurde mittels differentieller Druckanalyse (DPA) verfolgt, d.h. es wurde der Kolbenweg, die Druckänderung sowie die Temperatur kontinuierlich gemessen. Alle Meßdaten wurden über ein Datenloggersystem für die Auswertung gespeichert.

Abbildung 2 zeigt die Ergebnisse der bis zu 25 kb Druck durchgeführten Versuche. Die bislang einzige Untersuchung von YAMAMOTO & KENNEDY [3] kann in seinem generellen Ergebnis bestätigt werden. Jedoch zeigen die eigenen Versuche, daß die Reaktionsgrenze tatsächlich eine Feinstruktur aufweist. Die in ca 1.5 Kb Druckintervallen vorgenommen Messungen zeigen, daß die Reaktionsgrenze zwei Wendepunkte, bei 8 und 15 kb, aufweist. Ein Vergleich mit der P-T-Lage der bisher bekannten Anomalien von Wasser, die ebenfalls in Abb. 1 dargestellt sind, zeigt eine signifikante Korrelation mit diesen Wendepunkten in der Dehydratations/Hydratationsgrenze. Man kann daraus schließen, daß - trotz der Tatsache, daß die mit Bassanit koexistierende Fluidphase kein reines Wasser sondern eine Lösung darstellt – sich die Anomalieeigenschaften von Wasser auch bei hydratischen Reaktionen bemerkbar machen. Möglicherweise kann indirekte Methode auch bei höheren P-T Bedingungen angewendet werden kann.

Abb.2

Die Gleichgewichtskurve Gips Bassanit bei hohen Drücken anhand der experimentellen Daten von [3] (volle Kreise und Quadrate) und der eigenen DPA-Messungen (Dreiecke mit der Spitze in Richtung des Reaktionspfades). Die teilweise wiedergegebene Reaktion Bassanit-Anhydrit beruht ebenfalls auf Daten von [4].



Literatur

- [1] MIRWALD, P. W. (2001): Mitt. Österr. Miner. Ges. 146, 193-195
- [2] MIRWALD, P. W. (2002): Ber. Dtsche. Mineralog. Ges., No.1, 2002, p.110
- [3] YAMAMOTO, H. & KENNEDY, G. C. (1969): Amer. J. Sci. 267-A, 550-557.
- [4] HAAR, GALLAGHER & KELL (1984): NBS/NRC Steam Tables, Mc-Graw-Hill.

**PLATINUM GROUP MINERALS
FROM THE YUBDO MAFIC-ULTRAMAFIC ROCKS, WESTERN ETHIOPIA**

A. Mogessie

Institute of Mineralogy and Petrology
University of Graz, Universitätsplatz 2, A-8010 Graz, Austria

The Yubdo platinum deposit is located in Western Ethiopia 520 km from Addis Ababa. Platinum has been mined from the Yubdo area since ancient times. MURDOCK [1] suggested that platinum grains of Yubdo were used to decorate objects in Egypt in the 7th century B C. The period of greatest mining activity in the area, involving British and Italian companies, falls in the years between 1926 and 1941. An estimated 2700 kg of platinum has been extracted from the deposit during its mining history and the annual production reached its peak of 233 kg in 1933. After the mine closures in 1941, several attempts were made to study the elluvial-alluvial platinum deposits and other mafic-ultramafic intrusions in the area. In 1972 the Nippon mining Co. estimated 12,060 kg of platinum reserves in the weathered lateritic deposit with an average platinum content of 0.336 g/t of ore on the basis of the investigations of sample material taken from 29 pits. Placer platinum and gold workings are common in the Yubdo area along the Alfe and Birbir rivers in addition to the known elluvial-alluvial lateritic placer deposits on top of the birbirite and dunitic rocks belonging to the ultramafic body. The presence of sperrylite in the dunite and birbirite rocks of Yubdo as well as the growth of the Pt-Fe nuggets under surfacial conditions have been reported by AUGUSTITHIS [2]. CABRI ET AL. [3] studied the Pt-Fe alloys and identified several PGM inclusions with sulphides, arsenides and oxides.

The 9 km long and 4–5 km wide ultramafic intrusion of Yubdo strikes NNE-SSW and is crossed by the Birbir river in the eastern and southern part of the intrusion. The mafic-ultramafic rocks are underlain by Precambrian basement rocks of sedimentary origin consisting mainly of gneisses, quartzites, mica schists, amphibolites and chlorite schists. Acidic intrusive rocks include syntectonic granodiorites, hybrid granites, quartz-diorite and diorite porphyries which intrude the ultramafic rocks.

The central part of the ultramafic body is dominated by a serpentinised dunite with a cumulate texture and a forsterite content of 81–84 mol.%. Due to the serpentinisation, the olivine grains are commonly rimmed by talc, serpentine, carbonate and opaque minerals. Peridotites rich in amphibole and olivine are found with intercalated dunite and pyroxenite at the east and southern parts of the ultramafic body. Apart from common hornblende, the altered parts contain cummingtonite. The olivine grains are serpentinised at the margins and the opaque minerals consist mainly of chromite and martitised magnetite, where the latter occurs as interstitial single and intergranular grains within olivine. Pyroxenites are found at the outer rim of the ultramafic body and consist of diopsidic pyroxenes. The alteration products are serpentine, amphibole and chlorite. Birbirite, which is found at the top of the dunite and pyroxenites in the center of the ultramafic body, consists of diffuse iron oxides located around the margins of olivine grains.

Several Pt-Fe primary grains were identified enclosed in chromite phases and along alteration zones Pt-Fe alloys found in serpentinised zones have variable sizes and shapes. Some are elongate and relatively large (ca. 20–30 μm) compared to the rounded small grains in the chromites. The most abundant platinum-group minerals (PGM) have intermediate compositions between $\text{Pt}_{1.6}\text{Fe}$ and $\text{Pt}_{3.1}\text{Fe}$ with some grains of tulameenite. The PGM in altered rocks have relatively higher values of Pt (69–72 at. %), Cu (1.48–4.97 at. %), Pd (1.39–154 at. %) and lower Fe contents compared to those found in the core of chromite grains.

The nuggets in the pan concentrates have a composition close to Pt_3Fe and some are tulameenite (Pt_2FeCu). Fe content of the Pt_3Fe varies between 23–30 at. % and has up to 3.66 at. % Cu. Tulameenite grains have more than 32 at. % Fe and up to 16 at. % Cu. Most of the grains have Rh contents between 0–2.09 at. %, Pd 0–1.46 at. % and Ir 0–2.99 at. %. Ru values are very low, generally < 0.5 at. %. The average Rh and Ir values in the Pt-Fe nuggets are slightly higher compared to Ru, Os and Pd. PGM occurring as inclusions within the Pt-Fe nuggets consist of alloys, sulphides, sulpharsenides, sulphantimonides, antimonides and telluro-antimonides. They vary widely in shape from laths of osmium-rich phases to equidimensional crystals of laurite. Os-Ir alloys are the most abundant PGM found as inclusions in the Pt-Fe nuggets. The compositions of the Os-Ir alloys are relatively homogeneous with 82–95 at. % Os and 1.18–4.92 at. % Ir. PGM-Sulphide inclusions in the Pt-Fe nuggets include: rhodian-pentlandite ($\text{Rh}(\text{Fe},\text{Ni})_9\text{S}_8$), kashinite ($(\text{Ir},\text{Rh})_2\text{S}_3$), prassoite ($\text{Rh}_{17}\text{S}_{15}$), laurite ($\text{Ru},\text{Os}\text{S}_2$) and an unidentified Rh-Fe-Ni-S phase. Irarsite (IrAsS), platarsite (PtAsS), hollingworthite (RhAsS), genkinitie ($((\text{Pt},\text{Pd})_4\text{Sb}_3)$, iridium-rhodium sulphantimonide ($\text{Ir},\text{Rh}\text{SbS}$) and an unidentified RhSbS phase were also identified in the placer nuggets as inclusions forming euhedral crystals. Possible new PGM from Yubdo are antimoniides ($(\text{Rh},\text{Pt},\text{Pd})\text{Sb}_2$, $(\text{Rh},\text{Pt})\text{Sb}$, and $(\text{Rh},\text{Pt})\text{Sb}_2$); sulpharsenide ($\text{Ru},\text{Rh},\text{Pt}\text{AsS}$), and tellurides ($(\text{Rh},\text{Ir},\text{Pt})\text{SbBiTe}$, $(\text{Pt},\text{Pd},\text{Rh})(\text{SbAsTe})$). In addition placer nuggets of native gold (76.10–94.03 at. % Au) and electrum (46.10 at. % Au) are found associated with the Pt-Fe nuggets. The embayed and sculptured surfaces of the platinum-iron nuggets and their intimate association with fine grained iron oxides in the cavities of the nuggets documented from Yubdo are also features of gold grains considered to have grown in a lateritic environment indicating that the processes of formation of gold in laterites are likely to be paralleled by comparable development of platinum-group minerals (PGM). Based on the investigation made one can conclude that 1) the occurrence of droplets of PGM in chromites from bore hole ultramafic samples at depth suggests a magmatic origin; and 2) a remobilization and transport of the Pt-Fe alloys have taken place from a possible dunitic source and concentrated them in the laterites.

PGE analyses of 130 mafic-ultramafic samples from Yubdo indicate enrichment of Pt, Rh and Pd (PPGE) than Ir, Ru, and Os (IPGE). The absence of Os and Rh in the core analyses and their abundance in the inclusion phases might suggest introduction of these elements with hydrothermal fluids during the serpentinisation and lateritisation stage.

This project was supported by the Austrian Research Fund (FWF) – P13643-GEO.

References

- [1] MURDOCK, T. G. (1944): United States Technical Project in Ethiopia: mineral investigation of platiniferous Yubdo area. - Ethiopian Institute of Geological Survey. Ministry of Mines and Energy, Addis Ababa, Unpubl. Rep., 5p.
- [2] AUGUSTITHIS, S. S. (1965): Mineralogical and geochemical studies of the platiniferous Dunite-Birbirite-Pyroxenite Complex of Yubdo/Birbir, Western Ethiopia. - *Chemie der Erde*, 24, 159-196.
- [3] CABRI, L. J., CRIDDLE, A. J., LAFLAMME, J. H. G., BEARNE, G. S. & HARRIS, D. C. (1981): Mineralogical study of complex Pt-Fe-nuggets from Ethiopia. - *Bull. Mineral.*, 104, 508-525.

**QUATERNARY CLIMATE PLAYING SPRINGBOARD WITH AN
UPLIFTING, YOUNG MOUNTAIN RANGE:
MODEL AND POSSIBLE GEOMORPHOLOGIC CONSEQUENCES IN THE EASTERN ALPS**

F. Neubauer

Institute of Geology and Paleontology
University of Salzburg, Hellbrunnerstrasse 34, A-5020 Salzburg, Austria

As well known from continents at higher latitudes, Pleistocene inland ice glaciers represent a load exerting subsidence of the surface of continental crust during ice build-up and surface uplift during ice decay. The amount of subsidence during ice-loading and isostatic rebound after ice melting mainly depends from three factors: (1) thickness of the ice shield, (2) effective elastic thickness of the lithosphere, which counteracts ice-load, and, subordinately, (3) duration of ice-loading.

The model was seemingly not applied to young mountain belts like Alps where the effective elastic thickness is much lower than in cratons like the Fennoscandian shield with its thick lithosphere and its corresponding high effective elastic thickness. This suggests that the effects of vertical motion in young orogenic belts could be in a similar range like in cratonic areas. However, due to topography and limited thickness of the Alpine ice shield, we calculate a somewhat lower vertical motion in the order of minimum 60 and maximum 180 metres. Five sets of moraines walls in the Alpine foreland suggest a fivefold cycle of ice-loading and unloading during the last ca. one million years. Observations from ice shield and climatic proxies argue for slow ice-shield build-up and rapid ice decay.

The Eastern Alps represent an orogen with surface uplift since Neogene (e. g. [1]). E. g., the Tauern window area cooled below ca. 110–120°C ca. 9–10 Ma ago, suggesting an average uplift rate, assuming an average geothermal gradient, of ca. 3 mm/a (without the additional effect of surface uplift). The present-day, post-glacial surface uplift is estimated at 1.5 mm/a by geodetic measurements (e. g. [2]), which is obviously related to the distribution of the last, Würm, ice shield. Calculation with a similar ice-load for all five Quaternary glaciations, the resulting surface motion is a superposition of the overall surface uplift and cyclic depressions by slow ice-loading and rapid rebound by unloading (Fig. 1). Because of the lower ice thickness, the effect of vertical motion was lower along marginal sectors of the ice shields, yielding an apparent depression in the center of Alps.

The question on possible geomorphic evidences for Pleistocene and Holocene vertical motion now arises. For the Holocene, series of elevated, Holocene river terraces may indicate apparent stepwise surface uplift along rivers. The effect of surface elevation along rivers increases from external Alps towards the Hohe Tauern where a minimum of 60 meters of terrace elevation is observed. The present-day rivers incise into bedrocks, sometimes blanketed by moraines, so that the Holocene uplift is ca. 6 mm/a close to the Hohe Tauern, more than in external sectors of Eastern Alps where the Holocene river terraces are much lower.

Cyclic Pleistocene surface uplift could be monitored by a number of geomorphologic effects: (1) river terraces ("Niederterrassen") external to the area covered by the Alpine ice shield, e. g. along the Mur river east of Judenberg, (2) bedrock terraces along valleys in the centre of the Eastern Alps, (3) gorges along rivers which could have been formed during rapid surface uplift

due to rapid post-glacial river incision, and Pleistocene karst caves relative close to the present-day river levels.

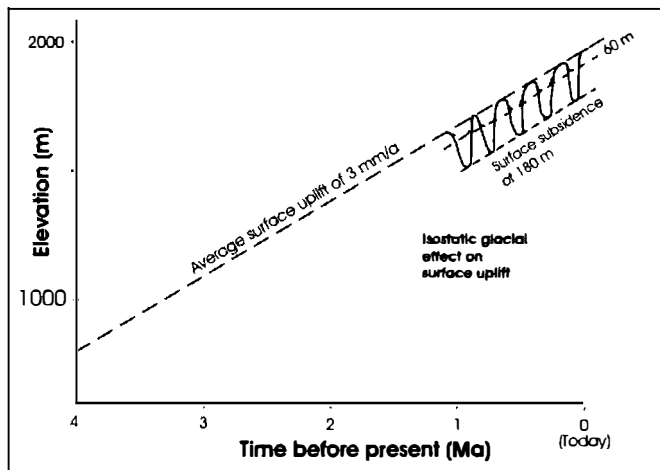


Fig. 1

Schematic graph showing the overall surface uplift and its superposition by isostatic effects by ice loading and unloading.

References

- [1] FRISCH, W., KUHLEMANN, J., DUNKL, I. & BRÜGL, A. (1998): Palinspastic reconstruction and topographic evolution of the Eastern Alps during late Tertiary tectonic extrusion. - *Tectonophysics*, 297: 1-15.
- [2] RUESS, D. & HÖGGERL, N. (2002): Bestimmung rezenten Höhen und Schwereänderungen in Österreich. - In: Pangeo Austria 2002, Programm und Kurzfassungen. University of Salzburg, p. 151.

TECTONIC EVOLUTION OF THE WESTERN MARGIN OF THE
GURKTAL NAPPE COMPLEX, EASTERN ALPS:
CONSTRAINTS FROM STRUCTURAL STUDIES AND $^{40}\text{Ar}/^{39}\text{Ar}$ WHITE MICA AGES

F. Neubauer, J. Genser & R. Handler

Institute of Geology and Paleontology
University of Salzburg, Hellbrunnerstrasse 34, A-5020 Salzburg, Austria

New structural data and $^{40}\text{Ar}/^{39}\text{Ar}$ white mica ages constrain aspects of the pre-Alpine and Cretaceous structural and metamorphic relationships as well as the tectonic evolution of Middle and Upper Austroalpine nappe units along the western margin of the Gurktal nappe complex (Upper Austroalpine units) in the Eastern Alps. There, a strong contrast of metamorphic pressure-temperature conditions of the penetrative Cretaceous overprint exists between the Middle Austroalpine nappe and the Murau and Stolzalpe nappes of the Gurktal nappe complex.

(1) An outcrop displaying the basal angular unconformity between Variscan Bundschuh basement and Triassic Stangalm Mesozoic cover, which are part of the uppermost Middle Austroalpine nappe, has been examined, both overprinted by Cretaceous age upper greenschist facies metamorphic conditions. The outcrop exposes the primary contact between the basement (micaschist) and the transgressively overlying Quartzite (Skythian). The basement micaschist displays ca. E-trending, upright open folds, which are discordantly overlain by quartzites of suggested Skythian age. Hangingwall sectors of the quartzite are well foliated and display an E-dipping foliation. New sericite is grown on the foliation plane. An $^{40}\text{Ar}/^{39}\text{Ar}$ age of a concentrate of a few white mica grains yielded a plateau age of ca. 89.0 ± 0.6 Ma. This age is interpreted to date cooling after throughout recrystallization of the Middle Austroalpine unit, demonstrating the Cretaceous metamorphic overprint in the footwall of the east-directed detachment fault at the western margin of the Gurktal nappe complex. This age is supported by further similar, more variable integrated $^{40}\text{Ar}/^{39}\text{Ar}$ ages from the same level.

(2) The overlying Murau nappe is pervasively overprinted in upper greenschist facies metamorphic conditions, including garnet-bearing siliciclastic rocks. A plateau age of 85.78 ± 0.33 Ma from white mica at Aigen (near Bad Kleinkirchheim) demonstrates for the first time the pervasive Late Cretaceous metamorphic overprint on the Murau nappe in the footwall of regional, ESE-directed detachment fault.

(3) The classical area of the basal tectonic boundaries along the western margin of the Gurktal nappe complex has been examined (Eisentalhöhe – Pfannockscharte/Karlwand). This shows the juxtaposition of Stangalm Mesozoic cover with extremely thinned Murau nappe, as e. g. along the Nockalpen road. The dolomite marbles of the Stangalm Mesozoic sequence are in part strongly foliated and lineated, the lineation plunges E and ESE.

The marbles are overlain by a several tens of metres thick phyllonite, which exhibits a clearly visible extensional crenulation cleavage fabric. The sense of displacement is top to the E/ESE. The phyllonite was interpreted as Carnian Raibl Formation. The inclusion of chlorite phyllite excludes this stratigraphic interpretation and argues rather for an Early Paleozoic age. This level is now interpreted as part of the Murau Nappe of the Gurktal Nappe Complex because lithological composition and continuous exposure to true Murau Nappe along the structural base of the Gurktal Nappe Complex. In the hangingwall, nearly unmetamorphic dark Late Triassic fossil-rich limestones, which belong to the cover of the Pfannock Nappe of the Gurktal Nappe Complex are exposed. In many places along the upper margin of the phyllonite zone, a dense network of east-dipping low-angle normal faults is preserved. These faults were active under pervasive circulation of hydrothermal fluids as the common presence of chlorite along fault surfaces as well as quartz fibres indicate. Fault and striae data collected in these outcrops and their assessment with palaeostress methods proof the ESE-WNW extension, which overprints rare faults of an earlier stage of NW- and N-directed thrusting.

The new age data give for the first time exact time constraints on the age of low angle normal faulting in the Murau nappe complex. The data also proof that the Murau nappe was fully overprinted by Cretaceous metamorphism and the main branch of the normal fault is between the Murau and Stolzalpe nappes. Together, these ages proof that the cooling occurred at the same time as the Krappfeld Gosau basin had their strongest phase of tectonic subsidence during the same time interval.

Acknowledgements

The work has been supported by a grant (FWF P9918-GEO "Collisional orogen") of the Austrian Research Foundation to FN.

TECTONIC MODELS OF EXHUMATION AND UPLIFT OF THE TAUERN METAMORPHIC
CORE COMPLEX TESTED BY THE TRANSALP DEEP SEISMIC LINE

F. Neubauer¹, K. Millahn², G. Grassl² & TRANSALP Working Group

¹Institute of Geology and Paleontology

University of Salzburg, Hellbrunnerstrasse 34, A-5020 Salzburg, Austria

²Department of Geophysics

Mining University of Leoben, A-8700 Leoben, Austria

Many processes have been proposed to contribute to the exhumation and final surface uplift of previously buried continental crust exposed in central sectors of orogens, as e. g. exposed within the Tauern metamorphic core complex. These processes include: (1) early isostatically driven exhumation of high-pressure rocks (forming now the Eclogite Zone and the basal Glockner nappe) along the subduction channel, (2) uplift and exhumation of a duplex complex over underthrusted crust by wedge formation during fore-thrusting opposite to the subduction direction, (3) exhumation due tectonic unroofing due to formation of a transtensional overstep along strike-slip fault system, and exhumation from mid-crustal levels by tectonic and erosional unroofing due to orogen-parallel extension, and finally, (4) exhumation and uplift thickened crust due to late-stage back-thrusting opposite to the subduction direction.

The geological interpretation of the TRANSALP deep seismic line clearly shows a double-vergent orogen with continuous crustal thickening towards the centre of the orogen, with thickest crust beneath the Tauern window (TW). The sub-Tauern ramp is displayed by a reflective zone extending from 15 km, with several breaks, down to ca. 35 km) and appears to delimit the continuous European basement beneath ca. the northern edge of the TW [1]. Two major gently S-dipping reflective zones can be traced from beneath the central TW (ca. 20 resp. 30 km) to beneath the Southalpine unit (SA) (ca. 25 resp. 35 km). These structures together are interpreted to represent a major crustal-scale fore-thrust with several major splays along which basement-cover nappes were stacked towards north.

The TW area does not display many reflective zones in shallow structural levels. The northern shallow gently N-dipping reflective zones can be interpreted to represent cover schists along the upper margins of the window. A central shallow reflective zone may represent a synform. Major portions in shallow southern levels are transparent (Variscan Central Gneiss). Some gently north-dipping reflectors occur in 20 km depth (vibroseis) and coincide there with the orientation of the Periadriatic fault. These are possible buried European sediments. Consequently, the TW Penninic units form a duplex-type structure, which is wedged into the Austroalpine units by ca. northward thrusting.

These data show that all above mentioned processes, except the in two dimensions untestable overstep, can be shown to have worked in sequence during exhumation of the Tauern metamorphic core complex.

References

- [1] TRANSALP Working Group: GEBRANDE, H., LÜSCHEN, E., BOPP, M., BLEIBINHAUS, F., LAMMERER, B., ONCKEN, O., STILLER, M., KUMMEROW, J., KIND, R., MILLAHLN, K., GRASSL, H., NEUBAUER, F., BERTELLI, L., BORRINI, D., FANTONI, R., PESSINA, C., SELLA, M., CASTELLARIN, A., NICOLICH, R., MAZZOTTI, A., BERNABINI, M. (2002): First deep seismic reflection images of the Eastern Alps reveal giant crustal wedges and transcrustal ramps. - Geophys. Res. Lett., 29/10: 92-1 - 92-4.

**MARBLES AS PETROGENETIC INDICATORS OF INCREASING EO-ALPINE
METAMORPHIC GRADE IN THE ORTLER CRYSTALLINE**

C. Nocker¹, P. Tropper¹ & V. Mair²

¹Institute of Mineralogy and Petrography

University of Innsbruck, Innrain 52, A-6020 Innsbruck, Austria

²Amt für Geologie und Baustoffprüfung

Eggentalerstrasse 48, I-39053 Kardaun (BZ), Italy

The Ortler crystalline represents a polymetamorphic Austroalpine crystalline basement which occurs southwest of the Ötztal crystalline between the Vinschgau- and the Ultental Valley. During the Eo-Alpine orogeny, the Ötztal Crystalline was juxtaposed onto the northern part of the Ortler Crystalline and its sedimentary cover [4]. Tectonically, the Ortler crystalline represents a stack of three distinct units which can be distinguished by their polymetamorphic P-T evolution: A): The Laaser Series: It is the lowermost unit and is characterized by intensely deformed, mylonitic amphibolites, micaschists, paragneisses and almost pure marbles (Laas Marble). B): The Martell Micaschists: It is on top of the Laas Series and is comprised of a more or less homogeneous stack of micaschists (Grt-Sta-Bt-bearing schists) with intercalations of amphibolites, orthogneisses and rarely marbles. C): The Zebre Schuppenzone: This unit consists mainly of quartzphyllites with small intercalations of greenschists, quartzites and impure marbles. This unit is tectonically emplaced onto the Marteller Micaschists and occurs at the base of the overlying sedimentary cover (Ortler Trias).

In the course of this study, we collected a suite of marble samples from all three units along a profile from the southernmost, highest, unit (Zebre Schuppenzone) to the northernmost, lowest, unit (Laas Series) in order to provide additional informations about the increasing Eo-Alpine metamorphic grade. The sample from the Zebre Schuppenzone contains the following mineral assemblage: epidote + muscovite + titanite + calcite. Since we up today have no datations on these rocks it is not clear if this mineral assemblage is of variscan or of eoalpine age. However, the structural features of the marbles are perfectly concordant to that of the surrounding quartzphyllites which are dated and yield ages of around 87 Ma. Therefore the perfectly reequilibrated postdeformative mineral assemblage of the marbles may be Eo-alpine in age.

The samples from the Martell Micaschists were collected from the basal area of this unit close to a contact area between marbles and the pegmatitic dikes from the Martell Granite. This Variscan contactmetamorphic overprint led to the formation of a complex mineral assemblage: garnet + idocrase + zoisite + titanite + diopside + calcite + quartz. The Eo-Alpine metamorphic overprint leads to the replacement of diopside by tremolite. In contrast to the samples from the Zebre Schuppenzone and the Martell Micaschist units, Eo-Alpine metamorphism was pervasive in the Laas unit. The marbles from this unit only contain an Eo-Alpine mineral assemblage such as: tremolite + clinzoisite + titanite + calcite + quartz.

The chemical composition of the tremolites shows a slight increase in Na and Al (edenite vector) towards the North, thus indicating possibly a slightly higher Eo-Alpine metamorphic grade in the Laas Series. We also investigated titanites from all three units to possibly correlate titanite zoning with the metamorphic evolution of these rocks. Titanites in all samples except for the samples from the southern Zebrù Schuppenzone, show distinct chemical zoning with respect to Ti, Al and F thus showing an increase in Al + F in the rims indicating a chemical substitution such as: $\text{Al} + \text{F} \leftrightarrow \text{Ti} + \text{O}$. The highest Al and F contents are from titanites from the Martell Micaschist unit with up to 9 wt.% Al_2O_3 and 2 wt.% F.

Although the Laas Series and the Martell Micaschists clearly show a polymetamorphic evolution with an earlier Variscan and a later Eo-Alpine metamorphic overprint, it is not clear yet if titanite zoning corresponds to these distinct metamorphic events. The Eo-Alpine metamorphic conditions in the Martell Micaschists and the Lass Series range from 6.7–8.5 kbar and 480–500°C. These data are in accordance with current investigations in the Ortler Crystalline which clearly show that the Eo-Alpine metamorphic overprint was very strong and pervasive and thus led in the Laas Unit to a complete recrystallization during the Alpine orogeny in contrast to previous ideas ([1], [2], [3]).

Acknowledgements

Financial and logistic support from the projects CARG-PAT and CARG-PAB of the Autonomous Provinces of Trento and Bolzano-Südtirol.

References

- [1] ANDREATTA, C. (1952): Polymetamorphose und Tektonik in der Ortlergruppe. - N. Jb. Mineral. Mh. Stuttgart, 1, 13–28.
- [2] REGNANIN, A. & PICCIRILLO, E. M. (1972): Litostratigrafia, tettonica e petrologia degli scisti austridici di alta e bassa pressione dell'area Passiria-Venosta (Alto Adige). - Mem. Ist. Geol. Min. Univ. Padova, 28, 1–55.
- [3] REGNANIN, A. & PICCIRILLO, E. M. (1972): Hercynian metamorphism in the Austridic crystalline basement of the Passiria and Venosta Alps. - Mem. Soc. Geol. It., 13, 241–255.
- [4] HOINKES, G. & THÖNI, M. (1993): Evolution of the Ötztal-Stubai, Scarl-Campo and Ultental basement units. - In: von Raumer, J. F. and Neubauer, F. (Eds.), Pre Mesozoic Geology in the Alps. Springer Verlag, Berlin, 485–494.

**CHEMICAL COMPOSITION OF TOURMALINE FROM GRANITIC ROCKS;
GEOCHEMICAL VERSUS CRYSTAL-STRUCTURAL CONSTRAINTS**

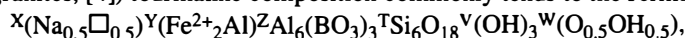
M. Novák

Institute of Geological Sciences
Masaryk University, Kotlářská 2, 611 37 Brno, Czech Republic

Tourmaline is a common accessory mineral in peraluminous granitic rocks such as leucocratic granites, orthogneisses and granitic pegmatites [1]. Its chemical composition is commonly of the schorl-dravite-foitite-(±elbaite) solid solution, with highly variable $X_{Fe} = Fe/(Fe+Mg)$, commonly high $YAl \sim 0.5$ apfu and variable concentrations of F and Li. Degree of geochemical fractionation is generally considered a dominant factor, which controls chemical composition of tourmaline such as X_{Fe} and YAl or concentrations of Li and F. However, crystal-structural study of the tourmaline group minerals suggested a significant role of crystal-structural constraints on tourmaline composition [2] and [3], and significant role of crystal-structural constraints on chemical composition of tourmaline from granitic pegmatites in the Moldanubicum was revealed [4]. Granitic rocks with accessory tourmaline are commonly Na, Al, Si, Fe(Mg) and B saturated with variable activities of Li and F, and they formed at similar PT conditions. Consequently, they represent a suitable example for study of effect of geochemical versus crystal-structural constraints on compositional evolution in tourmaline. In the less evolved granitic systems (less evolved two-mica granites, primitive barren pegmatites; [4]) containing tourmaline with $X_{Fe} < \sim 0.80$, a single compositional trend was recognized showing apparent increase X_{Fe} and YAl during fractionation [5] and [4] and tourmaline composition commonly tends to the formula:

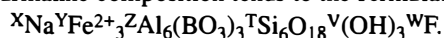


In more evolved granitic systems involving Fe-rich tourmaline with $X_{Fe} > \sim 0.80-0.95$ three distinctive compositional trends were recognized controlled by activities of Li and/or F [6]. In rocks with low activities of F and Li (outer zones of complex pegmatites, muscovite and two-mica granites; [4]) tourmaline composition commonly tends to the formula:



which differs from less evolved rocks in higher X_{Fe} and commonly elevated YAl .

In granitic rocks with high activity of F but low activity of Li (F-rich muscovite granite; [7] and [6]) tourmaline composition tends to the formula:



In granitic rocks characterized by high activity of F and Li (intermediate zones of complex pegmatites with Li-muscovite and lepidolite, highly evolved Li-mica granites; [8], [9] and [10]) tourmaline composition tends to the formula:



These well-defined distinctive trends in tourmaline from granitic rocks with similar chemical composition and PT conditions of their formation strongly suggest significant role of crystal-structural constraints on the tourmaline composition.

In F-, Li-poor rocks with variable X_{Fe} in tourmaline the composition is characterized by high vacancy in the X-site, and significant amount of O in the W-site [4]. The occupation of the Y-site is controlled by short-range requirements [2] and [3] and the configuration $R^{2+} - R^{2+} - Al^{3+}$ in tourmaline is the most suitable; tourmaline differs mostly in X_{Fe} . High amount of F in the W-site controls the X-site (high Na and low vacancy; [11]) and W-site (dominant F, low O) occupancies and configuration in the Y-site commonly tends to $Fe^{2+} - Fe^{2+} - Fe^{2+}$. In rocks with high activities of both F and Li content of F controls the X-site (high Na and low vacancy) and W-site (dominant F, low O), but the configuration in the Y-site is due to incorporation of Li different showing $Li^{+} - Fe^{2+} - Al^{3+}$.

Compositional variation in Fe-rich tourmaline from granitic environments, which are characterized by very similar PT conditions and chemical composition (except activities of Li and F), suggests significant role of Li and F. These elements not only enter their appropriate crystallographic sites (Y-site and W-site, respectively), but significantly control configuration in the Y-site and occupancy in the X-site. Chemical composition of tourmaline from granitic rocks exhibits combination of both geochemical and crystal-structural constraints; the first one is marked by increase of X_{Fe} and concentrations of Li and F. The second one significantly controls occupancies and configurations in the X-site, Y-site and W-site in tourmaline.

This research was supported by Granting Agency of the Czech Republic, Grant No. 205/99/0434 and 205/03/0400 to MN and the research project CEZ: J07/98: 143100003.

References

- [1] LONDON, D. ET AL. (1996): Boron in granitic rocks and their contact aureoles. - In: Boron: Mineralogy, Petrology and Geochemistry (Grew, E. S. & Anovitz, L. M. eds). - Review in Mineralogy., 33, 299-330.
- [2] HAWTHORNE, F. C. (1996): Structural mechanisms for light-element variations in tourmaline. - Canadian Mineralogist, 34, 123-132.
- [3] HAWTHORNE, F. C. (2002): Bond-valence constraints on the chemical composition of tourmaline. - Canadian Mineralogist, 40, 789-797.
- [4] NOVÁK, M. ET AL. (2003): Crystal chemistry, substitution mechanisms and classification of tourmaline in the schorl-oxy-schorl to dravite-oxy-dravite series from granitic pegmatites; examples from the Moldanubicum, Czech Republic. - European Journal of Mineralogy, accepted.
- [5] HENRY, D. J. & GUIDOTTI, C. V. (1985): Tourmaline as a petrogenetic indicator mineral: an example from the staurolite-grade metapelites of NW Maine. - American Mineralogist., 70, 1-15.
- [6] NOVÁK, M. ET AL. (2003): Locality No. 3 Nedvědice - Muscovite-tourmaline orthogneiss, tourmaline-fluorite layer. - In: Novák M. (ed.): Field Trip Guidebook, LERM, Nové Město na Moravě June 2003.
- [7] SINCLAIR, W. D. & RICHARDSON, J. M. (1992): Quartz-tourmaline orbicules in the Seagull batholith, Yukon Territory. - Canadian Mineralogist, 30, 923-935.
- [8] JOLLIFF, B. L. ET AL. (1986): Tourmaline as a recorder of pegmatite evolution: Bob Ingersoll pegmatite, Black Hills, South Dakota. - American Mineralogist, 71, 472-500.
- [9] LONDON, D. & MANNING D. A. C. (1995): Chemical Variation and Significance of Tourmaline from Southwest England. - Economic Geology, 90, 495-519.
- [10] SELWAY, J. B. ET AL. (1999): Compositional evolution of tourmaline in lepidolite-subtype pegmatites. - European Journal of Mineralogy, 11, 569-584.
- [11] ROBERT, J.-L. ET AL. (1997): Crystal-chemical relationships between OH, F and Na in tourmaline. - Tourmaline 1997 International Symposium on Tourmaline, Abstract Volume, Nové Město na Moravě, Czech Republic, 84-85.

KRISTALLE UND KULTUREN

P. Paulitsch

Institut für Mineralogie
Technische Universität Darmstadt, D-64285 Darmstadt, Germany

In dieser Arbeit wird der Einfluß der Kristalllagerstätten auf die Humangeschichte in den Ländern aufgezeigt (1).

Darin werden ausgeführt einundzwanzig Vorkommen der Kristalle in Europa, z.B. Grönland und Kreta, zudem in den Ländern Türkei, Persien, Pakistan, Sibirien, Mongolei, China und Japan. Von afrikanischen Vorkommen wurden ausgewählt Tunesien, Kenia und Namibia.

Hingewiesen wird auf die jeweilige Gestalt der Kristalle, die Kristallstruktur nach H. Strunz (2001), auf die experimentellen und natürlichen Reaktionen bei ihrer Bildung im Druck-, Temperatur- und Konzentrationsfeld (2).

Die Kristallstrukturen können aus ungleichen Tiefenlagen in der Erdkruste stammen. Die unterschiedlichen Gestalten der gleichen Kristallart werden von ungleichen Temperaturen und Lösungsgenossen beeinflusst.

Es folgen Beobachtungen zur bevorzugten Orientierung der Kristalle in Abhängigkeit von der Paragenese. Die Kristalle können Antwort geben auf Fragen nach dem Zusammenhang zwischen Erzführung Mutter- und Lagergestein. Ferner gibt die Gestalt der Lagerstätten Hinweise auf die Entstehung an den Plattengrenzen. Die variablen Formen für die Ausstellung erlesener Kristalle werden behandelt.

Literatur

- [1] PAULITSCH, P. (2003): Kristalle und Kulturen. - im Druck, 170 S.
- [2] PAULITSCH, P. (1990): Kristalle als Geothermo- und barometer. - Zentralbl. Geologie, Stuttgart.

**DIE BESTIMMUNG DER EROSIONSRATE IM ALLCHARGEBIET (MAZEDONIA)
MIT HILFE LANGLEBIGER KOSMOGENER RADIONUKLIDE**

M. K. Pavićević^{1,2}, G. Amthauer¹ & B. Boev³

¹Institut für Mineralogie

Universität Salzburg, Hellbrunnerstrasse 34, A-5020 Salzburg, Austria

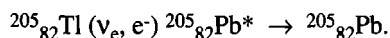
²Fakultät für Bergbau und Geologie

Universität Belgrad, Džusina 7, 11000 Belgrad, Serbia and Montenegro

³Fakultät für Bergbau und Geologie

Goce Delcev 89, MK-32000 Stip, Mazedonia

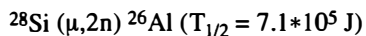
Das Mineral Lorandit ($TlAsS_2$) aus Allchar dient als geochemischer Detektor für den Nachweis der pp-Sonnenneutrinos durch die Kernreaktion



Wegen einer Schwellenenergie von nur 0.052 MeV und der längsten "Integrationszeit" von $4.2 \cdot 10^6$ Jahren sind wir im Prinzip in der Lage, mit Hilfe des Gehaltes von ^{205}Tl im Lorandit Aussagen über die Luminosität der Sonne während die letzten 5 Millionen Jahre zu machen. Dies ist mit keinem anderen "aktuellen" Neutrino-Experiment möglich. Der Nachweis der Sonnen-Neutrinos mit Hilfe von ^{205}Tl erfolgt im multidisziplinären und internationalen Projekt LOREX (Abkürzung von LORandit und Experiment) [1].

Vor der Durchführung von LOREX muss unter anderem der Beitrag des "Untergrundes" bzw. der "Untergrundreaktionen" bestimmt werden. Außer durch Neutrinoreaktionen kann nämlich ^{205}Pb auch durch hochenergetische und gestoppte Myonen der kosmischen Strahlung, durch natürliche Radioaktivität (Zerfallsprodukte von U und Th) und durch mobilisiertes ^{205}Pb aus der Umgebung gebildet werden. Die Summe aller drei Beiträge nennt man in der Kernphysik Untergrund. Die Produktion des ^{205}Pb durch die kosmische Strahlung ist vom geologischen Alter und der Tiefe der Tl-Mineralisation in Allchar abhängig. Um dieses Problem zu lösen, muß die genaue Bestimmung der Erosionsrate während der letzten 5 Ma mit Hilfe langlebiger, durch kosmische Strahlung erzeugter Nuklide, wie z.B. ^{10}Be , ^{26}Al und ^{53}Mn , durchgeführt werden.

Durch die Wechselwirkung von Myonen mit Silikaten in terrestrischen Gesteinen wird in-situ das kosmogene Radionuklid ^{26}Al nach der Reaktion



erzeugt.

Die Halbwertszeit des ^{26}Al bedingt, dass man mit Messungen dieses Elementes in Gesteinen einen Zeitraum von etwa $6 \cdot 10^6$ Jahren untersuchen kann. Quarz ist aufgrund seiner großen Häufigkeit in der Erdkruste und der Tatsache, dass Quarz quasi ein abgeschlossenes System bildet, aus dem die Radionuklide weder entweichen noch von Außen eindringen können, ein ideales Targetmaterial für *in situ* Bestimmungen der kosmogenen Radionuklide ^{10}Be und ^{26}Al .

Zum Problem des Untergrundes durch kosmische Strahlung wurde bei VERA (Vienna Environmental Research Accelerator) an der Universität Wien die ^{26}Al Konzentration in mehreren Quarzproben aus dem Gebiet von Allchar mit AMS (Accelerator Mass Spectrometry) gemessen [2]. Die Proben-Vorbereitung für AMS - Messungen besteht aus zwei Phasen:

- A) Gewinn von reinstem Quarz durch chemische Mineralseparation und
- B) Chemische Trennung von Al aus Quarz und Erzeugung von AMS-Targets.

Über erste Ergebnisse und die Übereinstimmung zwischen geomorphologischer Analyse und unseren Resultaten, d.h. der Bestimmung von ^{26}Al im Quarz aus Allchar, wird berichtet.

Literatur

- [1] PAVICEVIC, M. K. (1994): The "Lorex"- Project, solar neutrino detection with the mineral lorandite. - N. Jb. Miner. Abh. 167, 205-245.
- [2] PAVICEVIC, M. K., WILD, E. M., AMTHAUER, G., BERGER, M., BOEV, B., KUTSCHERA, W., PRILLER, A., PROHASKA, T. & STEFFAN, I.: AMS measurements of ^{26}Al in quartz to assess the cosmic ray background for geochemical solar neutrino Experiment LOREX. - Int. Conf. AMS-9, Nagoya 2002, Japan. Suppl. Nucl. Instr. and Meth. B (in press).

**THERMOBAROMETRIC CONSTRAINTS ON THE EO-ALPINE METAMORPHIC
OVERPRINT IN THE AUSTROALPINE NAPPE STACK
NORTH OF THE TAUERN WINDOW FROM A METAPEGMATITE DIKE
IN THE KELLERJOCHGNEISS (NORTHERN ZILLERTAL, TYROL, AUSTRIA)**

A. Piber & P. Tropper

Institute of Mineralogy and Petrography
University of Innsbruck, Innrain 52, A-6020 Innsbruck, Austria

This investigation is part of the ongoing project on the tectonometamorphic evolution of the Austroalpine nappes in the northern Zillertal area, Eastern Alps. The units studied are the Wildschönau Schists in the tectonically highest position, the Kellerjochgneiss and the underlying Innsbruck Quartzphyllite in the tectonically lowest position. These units show a polymetamorphic evolution with a pre-Alpine metamorphic overprint (Variscan and/or Permian) and a pervasive Eo-Alpine metamorphic overprint under low- to high greenschist facies conditions [1]. Within the Kellerjochgneiss a small strongly deformed meta-pegmatite dike occurs. Field relations indicate that the pegmatite intersects the Kellerjochgneiss discordant and it contains the mineral assemblage of muscovite + biotite + albite + chlorite + quartz + garnet₁ (Alm₆₈Spess₂₇Pyr₃Gro₂) + garnet₂ (Gro₅₂Alm₃₃Spess₁₅) ± stilpnomelane. Textural investigations reveal a protolith assemblage comprised of K-feldspar, quartz and garnet. These garnets (garnet₁) are essentially almandine-spessartine solid solutions, which is comparable to garnet compositions from other pegmatites from the Eastern Alps (e.g. Koralm Crystalline complex; [2]).

Thermobarometry of the metapegmatite was performed by calculating invariant points within the Eo-Alpine assemblage garnet₂ + muscovite + stilpnomelane + albite + chlorite + biotite with the program TWQ v1.02 [3] using the data bases of [3] and [4]. In addition, the empirically calibrated muscovite + chlorite + stilpnomelane + quartz thermobarometer by [5] was applied. Thermobarometry with TWQ v1.02 with the data base of [3] yields pressures ranging from 5.5 to 7.2 kbar and temperatures ranging from 292 to 380°C. Calculations with the data base of [4] including Fe-Stilpnomelane yield pressures of 6.7 to 7.9 kbar and temperatures of 330 to 354°C. These data are in good agreement with the P-T data from the Kellerjochgneiss [1]. Thermobarometric calculations performed with THERMOCALC v2.07 with the data base of [6] yield pressures ranging from 3.8 to 8.5 kbar and temperatures of 284 to 378°C. Application of the empirically calibrated muscovite + chlorite + stilpnomelane + quartz thermobarometer by [5] yields pressures ranging from 6.5 to 7.4 kbar and temperatures ranging from 289 to 314°C.

Thermobarometric data from the northern Zillertal area reveal a wide range of pressures which can be the result of a mixture of two metamorphic stages or a lack of complete reequilibration during the latest Eo-Alpine metamorphic event.

Thermobarometric investigations in this area were mostly performed on samples from the Kellerjochgneiss on synkinematically grown minerals, which constitute the predominant foliation (S2) in these rocks. The P-T results from these lithologies can therefore be directly related to the West-directed thrusting during the Eo-Alpine metamorphic overprint indicating that deformation took place under greenschist-facies conditions. The data also indicate that the Kellerjochgneiss seems to have been metamorphosed under slightly higher pressures (6 ± 2 kbar) than the Innsbruck Quartzphyllite and the Wildschönau Schists (5 ± 1 kbar) [1].

References

- [1] PIBER, A. (2002): Unpubl. MSc Thesis, Univ. Innsbruck, 269 p.
- [2] THÖNI, M. & MILLER, C. (2000): SMPM, 80, 169-186.
- [3] BERMAN, R. G (1992): written comm.
- [4] MASSONNE, H. J. (1998): written comm.
- [5] CURRIE, K. L. & VAN STAAL, C. R. (1999): J. Metam. Geol. 17, 613-620.
- [6] HOLLAND, T. J. B. & POWELL, R. (1998): J. Metam. Geol. 16: 309-343.

**THERMOBAROMETRY IN THE WESTERNMOST INNSBRUCK QUARTZPHYLITE
AND THE PATSCHERKOFEL CRYSTALLINE (EASTERN ALPS, TYROL, AUSTRIA)**

A. Piber & P. Tropper

Institute of Mineralogy and Petrography
University of Innsbruck, Innrain 52, A-6020 Innsbruck, Austria

The area of investigation is located in the South of Innsbruck (Tyrol, Austria) and is adjacent to the northern part of the Brenner Basis Tunnel line. The two lithological units studied are the Innsbruck Quartzphyllite and the overlying Patscherkofel Crystalline. Both units show a poly-metamorphic evolution, whereas the Patscherkofel Crystalline shows clear evidence for a strong Variscan amphibolite-facies overprint, and geochronological evidence points to a possible Permian event in the Innsbruck Quartzphyllite. Both units show a pervasive Eo-Alpine metamorphic overprint under low- to high greenschist-facies conditions.

The Innsbruck Quartzphyllite contains the mineral assemblage muscovite + albite + quartz \pm chlorite \pm biotite \pm garnet. No pre-Alpine relics have been found so far. Within this unit, a metamorphic zonation with increasing grade from the biotite- into the garnet zone has been observed. The overlying Patscherkofel Crystalline is mainly composed of mica schists with the mineral assemblage albite + plagioclase + muscovite + biotite + chlorite + quartz \pm chloritoid \pm garnet₁ \pm garnet₂ \pm ilmenite \pm clinozoisite \pm staurolite \pm kyanite \pm margarite. Pre-Alpine relics are garnet₁ + staurolite + kyanite, all other minerals are part of the Eo-Alpine overprint.

Thermobarometry of the Innsbruck Quartzphyllite and the Patscherkofel Crystalline was performed by calculating invariant points with the program TWQ v1.02 [1] and the data base of [2]. These calculations yield pressures ranging from 5.2 to 6.1 kbar and temperatures ranging from 360°C to 476°C for the area in the south of Innsbruck while for the northern Zillertal area pressures ranging from 2.6 to 4.2 kbar and temperatures ranging from 280 to 390°C for the mineral assemblage muscovite + chlorite + quartz [3]. Application of the garnet-biotite thermometer yields temperatures of 500°C to 524°C at pressures in the range of 5–6 kbar for the biotite- and garnet zone within the Innsbruck Quartzphyllite. Chemically hints for higher metamorphic grade of the Innsbruck Quartzphyllite in the south of Innsbruck are manifested through higher Si contents in phengites, which range from 3.10 to 3.28 apfu, while Si contents in the northern Zillertal area range from 3.06 to 3.18 apfu [3].

The calculations of samples from the Patscherkofel Crystalline with TWQ v1.02 using the data base of Berman [1] yield an invariant point with pressures of 10.6 \pm 0.3 kbar and temperatures of 504.6 \pm 7.6°C for the Eo-Alpine mineral assemblage albite + biotite + muscovite + garnet₂ + chlorite. Application of the garnet-biotite thermometer and the garnet-plagioclase-muscovite - quartz barometer, yields temperatures of 498°C to 580°C and pressures ranging from 8.2 to 12.2 kbar. These data are in good agreement with the results from the other thermobarometer.

The thermobarometric data and the Si contents in phengite of the Innsbruck Quartzphyllite reveal a decrease in metamorphic grade from the west to the east of the westernmost part of the Innsbruck Quartzphyllite during the Eoalpine metamorphic overprint. The obtained PT-data from the Patscherkofel Crystalline indicate higher metamorphic conditions during an Eoalpine event, which suggest that the Patscherkofel Crystalline was subsequent thrusted onto the Innsbruck Quartzphyllite after the peak of Eoalpine metamorphism.

References

- [1] BERMAN, R. G. (1992): written comm.
- [2] PARRA, T., VIDAL, O. & AGARD P. (2002): Contrib. Mineral Petrol, 143, 706-732.
- [3] PIBER, A. (2002): Unpubl. MSc Thesis, Univ. Innsbruck, 269 p.

**MULTIVARIATE ANALYSIS FROM DATA OF THE SYSTEM
CAO - SiO₂ - MGO - Al₂O₃ - TiO₂ - GYPSUM - CLINKER
FOR STANDARD CEMENT PERFORMANCE TESTS**

C. Potocan¹, E. Marte² & R. Tessadri¹

¹Institute of Mineralogy and Petrography

University of Innsbruck, Innrain 52, A-6020 Innsbruck, Austria

²IPOSE AG - Prozessoptimierung und Softwareentwicklung

CH-5303 Würenlingen, Althau 316, Switzerland

Producing spherical particles in the range of 10–100 µm using spray granulation is a well-known technique in metal powder processing. When dealing with mineral melts, blast furnace slags, glasses etc. the high viscosities together with the low surface tensions of these materials give rise to more fibred aggregates (i.e. mineral wool). However, as recently shown using more sophisticated technologies spray granulation producing spherical particles from blast furnace slags is possible [1]. Since these slags are intensively used as an additive in cements spray granulation could be an excellent tool to replace the cost-intensive grinding procedure of the slag. As there is a huge range in slag chemistries and furthermore the various compositions play an important part on the final cement quality it is necessary to understand the relation between slag chemistry and cement properties.

Therefore a multivariate model (comparable to [2]) based on synthetic melts in the system CaO-SiO₂-MgO-TiO₂-Al₂O₃ was established with the following restrictions: CaO/SiO₂ (alkalinity) 0.9–1.2, TiO₂ 0–2, Al₂O₃ 6–12 and fixed MgO-content of 10 wt.%. On one hand this represents commonly produced blast furnace slags in steel industry and on the other hand this gives a model with an acceptable set-up of experiments (16). The melts were made of pure-grade chemicals and in weights of 5 kg for each lot to guarantee a sufficient amount of material for the compressive strength tests. In a second part of the model various mixing ratios (30) with clinker and gypsum (= actual cement) were calculated. With these cements the usual compressive strength tests have been performed. Combining these results with the data of the established system CaO-SiO₂-MgO-TiO₂-Al₂O₃-gypsum-clinker it was possible to create algorithms to predict compressive strengths for 2, 7 and 28 days depending on the slag chemistry and the mixing ratios. Verification tests show a deviation of predicted and measured compressive strengths better than 10 %.

References

- [1] POTOCHAN, C., VAVTAR, F. & TESSADRI, R. (2001): Preliminary results of steam processed slags produced by spray granulation (Pilot-Project DGM-Tribowen/Lorüns): mineralogical and physical parameters. - Mitt. Österr. Miner. Ges. 146, 232.
- [2] DEHUAI W. & ZHAOYUAN C. (1997): On predicting compressive strengths of mortars with ternary blends of cement, GGBFS and fly ash. - Cement and Concrete research, 27, 487-493.

**PETROLOGIC EVALUATION OF HIGH-PRESSURE ROCKS:
STATE OF THE PROBLEM, MEANS OF SOLUTION**

A. Proyer

Institut für Mineralogie und Petrologie
Universität Graz, Universitätsplatz 2, A-8010 Graz, Austria

In the petrologic evaluation of high-pressure rocks we face the problems common to all rocks plus some additional ones that become flagrant at high pressures. It all comes under the heading: "What do we want to know?" – e.g. a P-T path, versus "What can we know?" – What is preserved, and which of the preserved features are diagnostic for a particular stage in the evolution of a rock? The recent years have brought an improved understanding of what preservation means, and we have learned more about the diagnostic values of minerals, textures or mineral chemical peculiarities, particularly in high- and ultrahigh-pressure rocks.

Preservation has little to do with thermodynamics, but everything to do with kinetics. It depends on a variety of factors, the most decisive being definitely the presence of a fluid. It plays a triple role: It is always important as a catalyst of reactions and as a transport medium, and it may also be required as a reactant for further reactions to occur. Its disappearance from the rock due to its mobile character has thus been regarded as the most influential factor to stop reactions and freeze in assemblages that can later be sampled and examined.

Consequently, the main thermodynamic foothold on any preservation discussion is dehydration (devolatilization) reactions. They tell us when – in theory, i.e. under equilibrium conditions – dehydration will occur. In the past, these phenomena have been discussed mainly in the context of (idealized) univariant reactions and their corresponding field isograds.

The new NKFMAH grid for metapelites (PROYER, in press), for example has enabled us to discuss preservation of HP-assemblages in a really large P-T range, with realistic bulk compositions, whereas for metabasites and other rock types the variance is usually too high, and the number of useful univariants or even invariant points too small for such an approach. A much more thorough and detailed method is that of contoured pseudosections for particular samples/bulk compositions. A series of recent papers shows the advantages and drawbacks of this method, but its potential is enormous. In fact, we can now precisely define, what we mean by "peak conditions of metamorphism" along a given P-T path, i.e. those conditions that are preserved by a rock, and it is almost never the T- or P-peak of that path. This tool is currently developed even further to describe fluid-absent conditions, also below the solidus.

The ideal sample records just one set of P-T conditions, at which it was perfectly equilibrated and then frozen in. However, at low to medium metamorphic grades, in the greenschist and amphibolite facies, several minerals can be zoned or vary in composition, either irregularly or depending on their textural position. Garnet, plagioclase, muscovite and amphibole are typical examples for such a behaviour. Furthermore, overprinting relationships, where a peak metamorphic assemblage is replaced along fluid pathways or in certain domains by a younger assemblage and older phases are affected by resorption and zoning, are quite common in rocks. There have been many efforts in the past to utilize such phenomena to derive more than one point for a P-T path (KRUHL, 1993; SCHULZ, 1994; CARSWELL, 1999). These efforts have been quite enlightening, both by their successes and failures. A reasonable interpretation of textures and a flawless application of phase petrologic laws are vital to establish, if it is possible to derive P-T conditions in such cases or not. Even though deriving P-T paths from a single specimen is troublesome, the obvious solution of using several samples from the same outcrop area which differ in equilibration stage or bulk composition, has not found a wide application by petrologists. In this case, problematic overprinting relationships may and in most cases will exist on an outcrop scale.

Facing the problem of preservation of the bulk mineral assemblage, particularly for rocks with a high- and ultrahigh-pressure history, geologists have turned more and more to those traces of early stages that are preserved on a micro-scale: inclusions of index minerals like omphacite, coesite or diamond in refractory hosts (mainly zircon) and diagnostic mineral compositions, either preserved directly (as inclusions) or indirectly (exsolution textures).

Experimental petrology plays a very important role as it provides a lot of hints about which phases can be expected at extreme pressures. At ultrahigh pressures, geothermobarometry in a classical sense is virtually impossible, not only because most phases have reequilibrated at lower P-T conditions, but also because the properties of solid solutions and fluids in complex bulk compositions are basically unknown. Experiments with simplified but also with common pelitic or metabasic bulk compositions can provide important constraints on the range and nature of solid solution in phases like garnet, clinopyroxene and others, which may become useful first-order geothermobarometers (e.g. ONO et al., 1998). However, experimental work with this purpose in mind is still in its very beginnings.

The speed of exhumation of HP and UHP rocks is a major issue in the geological community. The traditional approach of applying a number of isotopic systems to get several constraints on the exhumation path has been refined, but the absolute ages have statistical error which are at least one order of magnitude greater than those of "durations" calculated from diffusion profiles, mostly in garnet, using recently developed "geospeedometry" programs (e.g. PERCHUK et al, 1999; DACHS & PROYER, 2002)

Finally, even the most classical approach of deriving P-T conditions for eclogites is hampered by unforeseen difficulties, when it comes to UHP conditions. Omphacite incorporates significant amounts of a Ca-eskola molecule $\text{Ca}_{0.5}[\cdot]_{0.5}\text{AlSi}_2\text{O}_6$, which introduces vacancies and makes it impossible to calculate Fe^{3+} from the formula. Garnet-omphacite temperatures can be wrong by up to 150°C, if no independent value for Fe^{3+} , e.g. from Mössbauer spectrometry, is known.

References

- CARSWELL, D. A. & ZHANG, R. Y. (1999): Petrographic characteristics and metamorphic evolution of ultra-high-pressure eclogites in plate-collision belts. - *Int. Geol. Review* 41: 781-798.
- DACHS, E. & PROYER, A. (2002): Constraints on the duration of high-pressure metamorphism in the Tauern Window from diffusion modelling of discontinuous growth zones in eclogite garnet. - *J. metamorphic Geol.* 20: 769-780.
- KRUHL, J. (1993): The P-T-d development at the basement-cover boundary in the north-east Tauern Window (Eastern Alps): Alpine continental collision. - *J. Metamorphic Geol.* 11: 31-47.
- ONO, S. (1998): Stability limits of hydrous minerals in sediment and mid-ocean ridge basalt compositions; implications for water transport in subduction zones. - *J Geophys. Res.* B:103/8:18, 253-18, 267.
- PERCHUK, A., PHILIPPOT, P., ERDMER, P. & FIALIN, M. (1999): rates of thermal equilibration at the onset of subduction deduced from diffusion modelling of eclogitic garnets, Yukon-Tanana terrane, Canada. - *Geology*, 27, 531-534.
- PROYER, A. (2003): Metamorphism of pelites in NKFMASH - a new petrogenetic grid with implications for the preservation high-pressure rocks during exhumation. - *J. Metamorphic Geol.* (in press).
- SCHULZ, B. (1993): P-T-deformation paths of Variscan metamorphism in the Austroalpine basement: controls of the geothermobarometry from microstructures in progressively deformed metapelites. - *SMPM* 73: 301-318.

**EPIHERMAL GOLD MINERALIZATION
AT CAPILLITAS, CATAMARCA PROVINCE, ARGENTINA**

H. Putz & W. H. Paar

Institut für Mineralogie
Universität Salzburg, Hellbrunnerstrasse 34, A-5020 Salzburg, Austria

Capillitas ($27^{\circ}21'S$, $66^{\circ}23'W$) is located in the Department of Andalgalá, Catamarca Province, north-western Argentina, at elevations between 2800 and 3400 m above sea level. It is part of the Farallón Negro Volcanic Complex, known for porphyry Cu-Au (e. g. Bajo de la Alumbra, Agua Rica) and epithermal vein-type deposits (Farallón Negro - Alto de la Blenda, Capillitas) [1, 2, 3]. The Capillitas diatreme is located in the Capillitas granite (upper Ordovician - lower Silurian age) and is host of a subvolcanic, polymetallic, epithermal vein-type deposit [4, 5]. It has been the source of gem-type rhodochrosite for more than 50 years. The diatreme is composed of intrusive and volcaniclastic rocks (ignimbrite, rhyolite porphyry, dacite porphyry and tuffs) of Miocene age (~ 5 Ma) and melanocratic and leucocratic dykes are exposed within the granite north and west of the diatreme [4, 5, 6, 7]. During late stages hydrothermal fluids altered the diatreme volcanics and a series of epithermal polymetallic veins were formed in and around the diatreme [6, 7]. Both the dykes and mineralized veins are structurally controlled, following the main joint systems in the Capillitas granite [6, 7].

The epithermal veins, hosted in rhyolite, ignimbrite and granite, generally strike ENE-WSW (e. g. La Rosario, La Grande, La Argentina and Nueva Esperanza veins) or WNW-ESE (e. g. Capillitas, Nieve, Ortiz, Restauradora and Bordon veins) and are associated with silicification, advanced argillic and sericitic alteration [4, 5]. They consist of many smaller veins and veinlets that pinch, swell and anastomose; their average thickness is 50–70 cm and they extend laterally between 100 and 800 m [4, 5]. Open space filling, rhythmic banding and brecciation are common textural features. At the surface, mineralized veins are only observed in the Capillitas granite, where they form silicified outcrops with brown to black color, due to oxidation of sulfides and rhodochrosite. The possible and probable ore reserves are approximately 387.000 tons, the average grades are Au 2.6 g/t, Ag 108 g/t, Cu 2.32 %, Pb 1.62 % and Zn 3.10 % [5].

On the basis of the geologic environment, the alteration and the ore mineralogy both low- and high-sulfidation mineralization can be distinguished. A number of separate mineralization stages were identified [4, 5], showing a complex Cu-Pb-Zn-Fe-As-Sb-Au-Ag paragenesis, with Bi, W, Sn, Te, Ge, Cd, In, V, Ni, Co and Tl in traces [4, 5, 8]. Quartz, rhodochrosite, barite and alunite are the associated gangues. Mineralization of the high-sulfidation style with pyrite, enargite, tennantite, hübnerite, Bi-sulfosalts, Sn-sulfides, bornite and ± native gold in a quartz-alunite gangue is mainly restricted to the diatreme volcanics. The veins hosted in granite and some distance away from the diatreme show typical low-sulfidation features and are composed of galena, iron-poor sphalerite, tennantite-tetrahedrite, chalcopyrite, pyrite and marcasite, associated with rhodochrosite, quartz and barite as gangues. The silver carriers of the ore are native silver, acanthite, proustite, pearceite and argyrodite.

Native gold is a rare constituent of the microparagenesis and associated with different ore types and mineral assemblages. It usually has microscopic dimensions (up to 25 µm) and microprobe analyses show a wide range of compositions from $\text{Au}_{0.88}\text{Ag}_{0.12}$ to $\text{Au}_{0.67}\text{Ag}_{0.33}$.

In ores from the Nueva Esperanza vein gold was observed as fracture-fillings in pyrite, tennantite and sphalerite or as tiny inclusions in tennantite and chalcopyrite (6.8 to 16.8 wt.% Ag, 0 to 0.15 wt.% Cu). Only traces of gold were detected in pyrite-rich mineralization from the Bordon vein, where it occurs in association with hessite and Bi-sulfosalts as inclusions in pyrite and chalcopyrite. In a stockwork-like bornite-digenite-chalcocite mineralization from old dumps near the Rosario vein gold is usually silver-rich (18.2 to 20.2 wt.% Ag) and forms inclusions in Te-tennantite/goldfieldite, associated with hessite, bornite, digenite, covellite and mawsonite.

Within the upper levels of several veins gold is enriched and forms platy aggregates up to 15 millimeters in size, sometimes well crystallized. This gold shows a weak chemical zonation with silver-rich cores (18.6 to 20.9 wt.% Ag) and rims slightly depleted in silver (13.5 to 14.5 wt.% Ag). It is usually associated with quartz, clay minerals and limonite.

Financial support of the Austrian Science Foundation (FWF) through grants P11987 and P13974 to W. H. Paar is gratefully acknowledged.

Literature

- [1] ACEÑOLAZA, F. G., TOSELLI, A. J., DURAND, F. R. & DIAZ TADEI, R. (1982): Geología y estructura de la región norte de Andalgalá, Provincia de Catamarca. - Acta Geológica Lilloana, 16, 121-139.
- [2] SASSO, A. M. (1997): Geological evolution and metallogenetic relationships of the Farallón Negro Volcanic Complex, NW Argentina. - Unpublished Ph.D. thesis, Queen's University, Kingston, Ontario, 841 p.
- [3] SASSO, A. M. & CLARK, A. H. (1998): The Farallón Negro group, northwest Argentina: Magmatic, hydrothermal and tectonic evolution and implications for Cu-Au metallogeny in the Andean back-arc. - SEG Newsletter, 34, 1-18.
- [4] MARQUEZ-ZAVALIA, M. F. (1988): Mineralogía y genesis del yacimiento Capillitas (Catamarca, República Argentina). - Unpublished Ph.D. thesis, University of Salta, Argentina, 258 p.
- [5] MARQUEZ-ZAVALIA, M. F. (1999): El yacimiento Capillitas, Catamarca. - En: Recursos Minerales de la República Argentina (Ed. O. Zappettini), Instituto de Geología y Recursos Minerales SEGEMAR, Anales, 35, 1643-1652.
- [6] BREITENMOSER, T. (1999): Geology and geochemistry of the calc-alkaline Farallón Negro Volcanic Complex at Capillitas, NW-Argentina. - Unpublished M.Sc. thesis, ETH Zürich, 105 p.
- [7] HUG, A. (1999): Petrography and genesis of the Capillitas diatreme, Farallón Negro Volcanic Complex, NW-Argentina. - Unpublished M.Sc. thesis, ETH Zürich, 74 p.
- [8] PUTZ, H., PAAR, W. H., SUREDA, R. J. & ROBERTS, A. J. (2002): Germanium mineralization at Capillitas, Catamarca Province, Argentina. - 18th General Meeting of the IMA, Edinburgh, Scotland, Abstracts, 265.

LUMINESZENZ-UNTERSUCHUNGEN AN SCHEELIT UND RE-Os DATIERUNG
VON MOLYBDÄNIT AUS DER SCHEELITLAGERSTÄTTE FELBERTAL

J. G. Raith¹, H. Stein² & U. Kempe³

¹Institut für Geowissenschaften

Montanuniversität Leoben, A-8700 Leoben, Austria

²AIRIE Program

Colorado State University, Fort Collins, USA

³Institut für Mineralogie

TU Bergakademie Freiberg, Germany

Einleitung

Die im Abbau stehende Wolframlagerstätte Felbertal, Bundesland Salzburg, gilt als Typlagerstätte für schichtgebundene Scheelitlagerstätten und stellt die weltweit wirtschaftlich wichtigste Lagerstätte dieses Typs dar (Jahresproduktion ca. 450000 t Erz mit 0.5 Gew.% WO₃).

Vor allem wegen der ungenügende Kenntnis des Alters der Erzbildung wird ihre Genese immer noch sehr kontrovers gedeutet. Syngeneticisch-exhalativen Modellen stehen solche, in denen intrakrustale magmatisch-metamorphe Prozesse favorisiert werden, gegenüber. Bei letzteren wird entweder ein genetischer Zusammenhang mit subduktionsbezogenem Magmatismus kambrischen Alters oder mit granitischen Intrusionen unterkarbonen Alters postuliert. Jüngste Arbeiten gehen von einer mehrphasigen granitgebundenen Vererzung mit einer ersten Vererzungsphase im Kambrium und einer zweiten im unteren Karbon aus (EICHHORN ET AL., 1999).

In diesem Beitrag werden Re-Os Datierungen von Molybdänit präsentiert, die einen Beitrag zur Diskussion des Alters und damit auch der Genese dieser Lagerstätte liefern. Sie werden ergänzt durch Mikroanalytik und Kathodenlumineszenzuntersuchungen (KL) an Scheelit.

Vererzungen und Scheelitegenerationen

Die Wolframlagerstätte Felbertal tritt in Metabasiten und Orthogneisen des Habach-Komplexes auf, die an der Grenze Jungproterozoikum-Paläozoikum an einem aktiven Kontinentalrand gebildet wurden (HÖLL & EICHHORN, 2000). Sie werden von frühkarbonen granitoiden Gesteinen (Zentralgneise) intrudiert. Scheelit tritt oft gemeinsam mit wenig Molybdänit in quarzreichen Erzkörpern auf, die als metamorphisierte und z.T. stark deformierte Gang- und Stockwerkvererzung magmatisch-hydrothermalen Ursprungs interpretiert werden können.

Im in Abbau befindlichen Westteil der Lagerstätte werden Scheeliterze überwiegend aus der Umgebung eines hochentwickelten Orthogneiskörpers (K1-K3 Gneis) gewonnen, der mit 336 ± 19 Ma datiert ist (HÖLL & EICHHORN, 2000). Im heimgesagten Ostfeld wurden vor allem die sogenannten quarzitischen Reichereze und die sie unterlagernde Stockwerkvererzung abgebaut.

Basierend auf den Arbeiten von Münchner Kollegen (siehe Zusammenfassung in HÖLL & EICHHORN, 2000) wurden die unterschiedlichen Generationen von Scheelit aus der Lagerstätte mit KL und mikroanalytisch untersucht: Scheelit 1, nur vom Ostfeld bekannt, ist feinkörnig und meist gelblich fluoreszierend. Er bildet Relikte mit einer primären Wachstumszonierung, die durch winzige feste und fluide Einschlüsse, sowie hell-dunkle Zonen im KL-Bild definiert sind. Die durchschnittlichen Mo-Gehalte einzelner Scheelitkörner sind zwischen ca. 1.0 bis 1.2 Gew.% MoO_3 . Winzige Einschlüsse opaker Phasen sind eher selten, aber auch in Scheelit 1 nachweisbar.

Scheelit 2, vor allem im Westfeld auftretend, ist meist mittel- bis grobkörnig (z.T. Porphyroblasten bis cm-Größe) und in der Regel ebenfalls gelblich fluoreszierend. Die Mo-Gehalte einer im Detail untersuchten Probe sind mit jenen von Scheelit 1 vergleichbar. Die Kornränder deformierter Scheelit 2 Porphyroblasten führen häufig Einschlüsse von Molybdänit, die als Entmischungen interpretiert wurden. Da Scheelit 2 in deformierten Quarz-Scheelit-Gängen im unterkarbonen K1-K3 Gneis zu finden ist, ist ein prä-karbones Alter dieser Scheelitgeneration auszuschließen.

Scheelit 3: Scheelit 1 und 2 sind fast immer von jüngeren Scheelit-Rekrystallisaten umgeben. Diese sind feinkörnig und zeigen eher blau-weiße Fluoreszenz. Die durchschnittlichen Mo-Gehalte einzelner Körner sind variabel (im Mittel ca. 0.4–0.5 Gew.% MoO_3) aber generell niedriger als in Scheelit 1 und 2. Im KL-Bild zeigt sich, dass diese Rekrystallisate aus Bereichen meist ohne klar sichtbare Internstruktur und ohne deutliche kristallographisch orientierte Begrenzung mit unterschiedlicher KL-Helligkeit aufgebaut werden. Die als metamorph interpretierten Rekrystallisate sind parallel zur dominanten Schieferung eingeregelt, wobei die Kornrekrystallisation aber die Deformation überdauert hat.

Re-Os Altersdatierungen

Drei Gruppen von Re-Os Altern an Molybdänit sind in der Lagerstätte Felbertal zu unterscheiden:
(a) Mehrere Molybdänitseparate, eines aus dem K1, zwei aus dem K2 Erzkörper, geben Re-Os Modellalter zwischen 337.9 ± 1.1 und 344.7 ± 1.1 Ma. Molybdänit der Scheelit-Quarz-Stockwerkvererzung aus dem Liegenden des quarzitischen Reicherzes im Ostfeld, für die ein kambrisches Alter vermutet wurde, ergeben ein ähnliches Alter von 342.4 ± 1.2 Ma. (b) Zwei Molybdänitseparate aus dem K2 Erzkörper lieferten etwas ältere Modellalter von 354.5 ± 1.2 Ma bzw. 358.3 ± 1.2 Ma (c) Zwei Separate einer einzelnen Molybdänitprobe – sie stammt aus stark alpidisch überprägten Metabasiten des Ostfeldes – ergaben Modellalter von 413.6 ± 1.3 bzw. 416.8 ± 1.3 Ma.

Interpretation

Die Modellalter der meisten Molybdänite liegen zwischen ca. 340–360 Ma und innerhalb des 2 Sigma Fehlerbereiches des Protolithalters des K1-K3 Gneises. Die Streuung der Alter von Molybdänitseparaten aus dem K2 Gneis, die signifikant größer ist als die 2 Sigma Abweichung der Einzelanalysen, deutet allerdings an, dass die Bildung der Molybdänite über einen längeren Zeitraum, mit einem Maximum bei ca. 340 Ma, erfolgt sein könnte bzw. dass mehr als eine Molybdänitgeneration, die bei der mechanischen Separation nicht getrennt werden können, vorliegt. Die geologische Bedeutung der beiden silurischen Alter ist unklar. Es könnte sich um Molybdänitbildung im Zusammenhang mit einer aus anderen Teilen des Tauernfensters nachgewiesenen kadomischen Metamorphose handeln (VON QUADT ET AL., 1997).

Die vorliegenden Altersdaten von Molybdänit bekräftigen die wichtige Rolle variszischer Granite für die Bildung der Lagerstätte. Da die Relikte von Scheelit I aus dem quarzitischen Reicherz, für die bisher ein kambrisches Alter postuliert wurde, trotz unserer Versuche bisher nicht datiert werden konnten und sie auch nicht mit datierbarem Molybdänit assoziiert sind, lässt sich eine prä-variszische Vererzungsphase nicht definitiv ausschließen.

Literatur

- [1] EICHORN, R. ET AL. (1999): Implications of U-Pb SHRIMP zircon data on the age and evolution of the Felbertal tungsten deposit (Tauern Window, Austria). - International Journal of Earth Sciences, 88, 496-512.
- [2] HÖLL, R. & EICHORN, R. (2000): Tungsten mineralization and metamorphic remobilization in the Felbertal scheelite deposit, Central Alps, Austria. - Reviews in Economic Geology, 11, 233-264.
- [3] VON QUADT, A. ET AL. (1997): The evolution of pre-Variscan eclogites of the Tauern Window (Eastern Alps): A Sm/Nd-, conventional and ICP-MS zircon U-Pb study. - Schweizer Mineralogische Petrographische Mitteilungen, 77, 265-279.

PHASENÜBERGÄNGE IN MINERALEN: DAS BEISPIEL PYROXENE

G. J. Redhammer^{1, 2}

¹Institut für Mineralogie

Universität Salzburg, Hellbrunnerstrasse 34, A-5020 Salzburg, Austria

²Institut für Kristallographie

RWTH Aachen, Jägerstrasse 17/19, D-52056 Aachen, Germany

Pyroxene, Amphibole und Glimmer gehören zu den wesentlichen Bestandteilen in der Erdkruste, im oberen Mantel und in Meteoriten [1]. Die detaillierte Kenntnis der Kristallstrukturen und deren Verhalten als Funktion von Temperatur und Druck ist deshalb von fundamentaler Bedeutung für das Verständnis des Erdinneren. Drei Typen von Pyroxenen können unterschieden werden: Orthopyroxene, Klinopyroxene und Protopyroxene. Vor allem die Klinopyroxene zeigen eine Vielzahl von Phasenübergängen als Funktion von Druck und/oder Temperatur. Am Beispiel von Modellsystemen werden die verschiedenen möglichen Arten von Phasentransformationen näher diskutiert. Dabei werden neben den Ergebnissen aus Untersuchungen mittels Einkristall-Diffraktion auch solche vorgestellt, die mit spektroskopischen Methoden (Raman, Infrarot) erzielt wurden.

(1) Klinopyroxene mit geringen Gehalten an Natrium und/oder Calcium wie die Vertreter der Mischreihe Klinoenstatit - Klinofersilit ($MgSiO_3$ - $FeSiO_3$), Pigeonit ($Mg,Fe,CaSiO_3$) oder Kanoit ($MnMgSi_2O_6$) zeigen bei Normalbedingungen die Raumgruppe $P2_1/c$. Mit steigender Temperatur durchlaufen diese Pyroxene displazive Phasenübergänge, die mit einem Wechsel von der Raumgruppe $P2_1/c \Rightarrow C2/c$ einhergehen. Gut beschrieben ist dieser Phasenübergang im System (Mg,Fe) SiO_3 [2, 3, 4].

(2) Auch durch Druckerhöhung kann ein $P2_1/c \Rightarrow C2/c$ Übergang erzwungen werden. Die Stabilität dieser $C2/c$ Phase ($HP\text{-}C2/c$) unter den Druckbedingungen des oberen Mantels wurde im Detail an den Zusammensetzungen $MgSiO_3$ (Enstatit) und $FeSiO_3$ (Fersilit) unter anderem von ANGEL und Mitarbeitern [5, 6] untersucht. In beiden Verbindungen ist der Phasenübergang 1. Ordnung, reversibel und displaziv im Charakter, der Übergangsdruck ist allerdings mit 1.7 GPa in $FeSiO_3$ und 6.5 GPa in $MgSiO_3$ sehr unterschiedlich. Der Einbau von Fe^{2+} stabilisiert dabei die $C2/c$ Hochdruck-Modifikation. Ähnliche $P2_1/c \Rightarrow HP\text{-}C2/c$ Phasenübergänge konnten auch noch in den Verbindungen $MnMgSi_2O_6$, $CrMgSi_2O_6$ und $MnMnSi_2O_6$ gefunden werden [7]. Dabei zeigt sich, dass nicht alleine die effektiven Radien der M1 und M2 Kationen die Übergangstemperaturen/-drücke kontrollieren, sondern dass Klinopyroxene mit Übergangselement-Ionen zusätzliche Stabilisierungsenergien aus Kristallfeld-Effekten erhalten. Ein Vergleich zwischen der Hochtemperatur $HT\text{-}C2/c$ und der Hochdruck $HP\text{-}C2/c$ Form offenbart, dass diese zwei unterschiedliche Phasen darstellen, die sich u.a. in der Knickung der Tetraederketten unterscheiden.

(3) Unter den Alkali - Klinopyroxenen sind vor allem die $\text{LiMeSi}_2\text{O}_6$ Verbindungen von besonderer Bedeutung. Diese weisen bei Normaldruck alle oberhalb 100°C $C2/c$ -Symmetrie auf. Jene Vertreter, bei denen die M1 Position mit Cr^{3+} , Ga^{3+} , V^{3+} , Fe^{3+} oder Sc^{3+} besetzt ist, zeigen zu tiefen Temperaturen hin einen $\text{HT-}C2/c \Rightarrow P2_1/c$ Phasenübergang [8, 9], der jenen in den $(\text{Mg},\text{Fe})\text{SiO}_3$ Klinopyroxenen sehr ähnlich ist. Am Beispiel dieser Substanzgruppe können die topologischen Änderungen, die mit der Transformation von der $P2_1/c$ -Tieftemperatur in die $C2/c$ -Hochtemperaturform einhergehen, im Detail besprochen werden. Die wichtigsten strukturellen Änderungen sind die Existenz von zwei unterschiedlich geknickten Tetraederketten und die Reduktion der Koordination von Li^+ von 6-fach auf 5-fach. Wird die M1 Position von sehr großen (In^{3+}) oder sehr kleinen (Al^{3+}) Kationen besetzt, kann zu tiefen Temperaturen hin kein Phasenübergang beobachtet werden. Diese Substanzen zeigen bei Untersuchungen als Funktion der Temperatur immer $C2/c$ - Symmetrie. Wie Untersuchungen von REDHAMMER ET AL. [10] gezeigt haben, verschiebt sich die Übergangstemperatur von $P2_1/c$ nach $C2/c$ in der Verbindung $\text{LiFeSi}_2\text{O}_6$ durch Ersatz von Li^+ durch Na^+ rasch unter 80 K. Dies weist darauf hin, dass die Natur des M2 Kations einen Einfluss auf die Übergangstemperatur zeigt.

(4) Durch eine Erhöhung des Druckes können auch bei den Vertretern der Li-Pyroxene Phasenübergänge induziert werden. Von besonderer Bedeutung ist hier die Verbindung ZnSiO_3 , bei der bei 1.92 GPa Druck ein $C2/c \Rightarrow P2_1/c$ Phasenübergang beobachtet wird [11], der in seiner Charakteristik den $C2/c \Rightarrow P2_1/c$ Übergängen bei tiefen Temperaturen und Atmosphärendruck sehr ähnlich ist. Das besondere an ZnSiO_3 allerdings ist, dass bei höheren Drucken (4.9 GPa), ähnlich den $(\text{Mg},\text{Fe})\text{SiO}_3$ Pyroxenen, ein $P2_1/c \Rightarrow C2/c$ Phasenübergang stattfindet, wobei diese $C2/c$ -Struktur ungleich jener bei Raumtemperatur ist. Eine ähnliche Abfolge von Phasentransformationen existiert auch in den Verbindungen $\text{LiFeSi}_2\text{O}_6$ und $\text{LiCrSi}_2\text{O}_6$, während z.B. $\text{NaFeSi}_2\text{O}_6$ bis zu Drucken von 13.5 GPa keine Änderung der Symmetrie zeigt (B. Downs, G.J. Redhammer, erste unveröffentlichte Ergebnisse).

(5) Neben der bislang beschriebenen $\text{HT-}C2/c \Rightarrow P2_1/c \Rightarrow \text{HP-}C2/c$ Abfolge konnte jüngst für die Verbindung $\text{NaTiSi}_2\text{O}_6$ eine Phasentransformation beschrieben werden, in der die $\text{HT-}C2/c$ ohne Zwischenstufen direkt in die trikline Raumgruppe P-1 fällt [12].

(6) Es existieren aber nicht nur kristallographische Phasenübergänge innerhalb der Gruppe der Pyroxene. Verbindungen mit Übergangselement-Kationen wie $\text{CaFeSi}_2\text{O}_6$, $\text{CaCoSi}_2\text{O}_6$, $\text{CaNiSi}_2\text{O}_6$ oder $\text{LiFeSi}_2\text{O}_6$ zeigen bei tiefen Temperaturen Übergänge in magnetisch geordnete Zustände, die im Rahmen des Vortrags ebenfalls kurz behandelt werden sollen.

References

- [1] YANG, H. & PREWITT, C. T. (2000): Chain and Layer Silicates at High Temperatures and Pressures. - *Reviews in Mineralogy and Geochemistry*, Vol. 41, 211-255, Mineralogical Society of America.
- [2] IISHI, K. & KITAYAMA, K. (1995): Stability of high-clinoenstatite. - *N. Jb. Mineral. Mh.*, 65-74.
- [3] SUENO, S., KIMATA, M. & PREWITT, C. W. (1984): The crystal structure of high-clinoferrositelite. - *American Mineralogist*, 69, 264-269.

- [4] ARLT, T. & ARMBRUSTER, T. (1997): The temperature dependent phase transition in the clinopyroxene kanoite $\text{MnMg}[\text{Si}_2\text{O}_6]$. - European Journal of Mineralogy, 9, 953-964.
- [5] ANGEL, R. J., CHOPELAS, A. & ROSS, N. L. (1992): Stability of high-density clinoenstatite at upper-mantle pressures. - Nature, 358, 322-324.
- [6] HUGH-JONES, D., WOODLAND, A. & ANGEL, R. (1994): The structure of high-pressure $C2/c$ ferrosilite and crystal chemistry of high-pressure $C2/c$ pyroxenes. - American Mineralogist, 79, 1032-1041.
- [7] ARLT, T., ANGEL, R. J., MILETICH, R., ARMBRUSTER, T. & PETERS, T. (1998): High-pressure $P2_1/c$ - $C2/c$ phase transition in clinopyroxenes: Influence of cation size and electronic structure. - American Mineralogist, 83, 1176-1181.
- [8] REDHAMMER, G. J., ROTH, G., PAULUS, W., ANDRE, G., LOTTERMOSER, W., AMTHAUER, G., TREUTMANN, W. & KOPPELHUBER-BITSCHNAU (2001): The crystal and magnetic structure of Li-Aegirine $\text{LiFe}^{3+}\text{Si}_2\text{O}_6$: a temperature dependent study. - Physics and Chemistry of Minerals, 28, 337-346.
- [9] REDHAMMER, G. J. & ROTH, G. (2003): The temperature dependent $C2/c \rightarrow P2_1/c$ phase transition in $\text{Li-Me}^{3+}\text{Si}_2\text{O}_6$ clinopyroxenes with $\text{Me}^{3+} = \text{Ga, Cr, V, Fe, Sc and In}$. - Zeitschrift für Kristallographie (under review).
- [10] REDHAMMER, G. J. & ROTH, G. (2002): Structural variations in the aegirine solid-solution series $(\text{Na,Li})\text{FeSi}_2\text{O}_6$ at 298 K and 80 K. - Zeitschrift für Kristallographie, 217, 63-72.
- [11] ARLT, T. & ANGEL, R. J. (2000): Displacive phase transitions in C-centred clinopyroxenes: Spodumene, $\text{LiScSi}_2\text{O}_6$ and ZnSiO_3 . - Physics and Chemistry of Minerals, 27, 719-731.
- [12] REDHAMMER, G. J., ROTH, G. & OHASHI, H. (2003): Single crystal structure refinement of $\text{NaTiSi}_2\text{O}_6$ clinopyroxene at low temperatures ($100\text{K} < T < 298\text{K}$). - Acta Crystallographica B, (under review).

KRISTALLSTRUKTUR UND $^{57}\text{MÖSSBAUER}$ -SPEKTRUM EINES NEUEN
GEMISCHT-VALENSEN EISENPHOSPHATES $\text{Fe}_7(\text{PO}_4)_6$

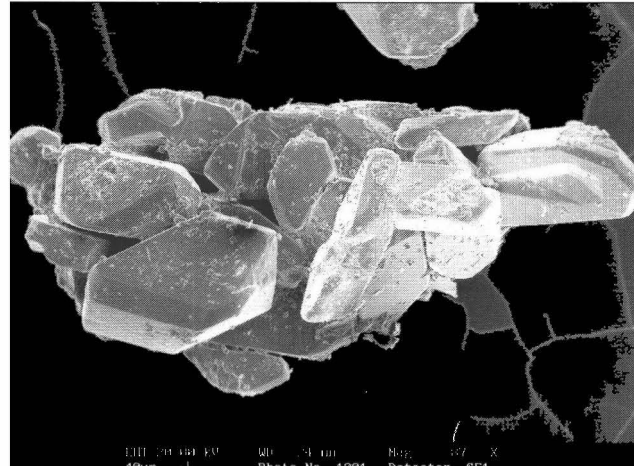
G. J. Redhammer^{1, 2}, G. Roth², G. Amthauer¹, W. Lottermoser¹ & G. Tippelt¹

¹Institut für Mineralogie
Universität Salzburg, Hellbrunnerstrasse 34, A-5020 Salzburg, Austria

²Institut für Kristallographie
RWTH Aachen, Jägerstrasse 17/19, D-52056 Aachen, Germany

ubstanzen, die Eisen sowohl in der 2-wertigen als auch in der 3-wertigen Form enthalten, sind von Interesse, da diese – das Vorhandensein von unendlichen, zumindest über Kanten verknüpfte trukturelle Baueinheiten (Ketten) vorausgesetzt – bei höheren Temperaturen interessante elektronische Eigenschaften ("electron hopping") zeigen können. Eine solche Substanz ist das Mineral Lipscombit, nominell $\text{Fe}^{2+}\text{Fe}^{3+}_2(\text{PO}_4)_2(\text{OH})_2$, das möglicherweise eine leicht oxidierte Hochtemperaturform des Phosphat-Minerals Barbosalit $\text{Fe}^{2+}\text{Fe}^{3+}_2(\text{PO}_4)_2(\text{OH})_2$ darstellt [1].

Bei der hydrothermalen Behandlung von synthetischem, feinkörnigem Pulver von Barbosalit entstanden bei einer Temperatur von 723 K und einem Druck von 0.4 GPa große, schwarze Kristalle mit einer Länge von bis zu 1 mm (Abbildung 1). Dieses Material wurde mit ^{57}Fe Möß-



bauer- Spektroskopie und Röntgenbeugung am Ein-kristall näher charakterisiert.

Abbildung 1
Raster-Elektronenmikroskopisches Bild der Substanz $\text{Na}_{0.18}\text{Fe}_{6.91}(\text{PO}_4)_7$, hergestellt unter hydrothermalen Bedingungen bei 723 K und 0.4 GPa.

Die Substanz kristallisiert in der triklinen Raumgruppe P-1, Gitterparameter $a = 6.3944(9)$ Å, $b = 7.9562(11)$ Å, $c = 9.3643(13)$ Å, $\alpha = 105.13(1)^\circ$, $\beta = 108.35(1)^\circ$, $\gamma = 101.63(1)^\circ$, $Z = 1$. Im Zuge der Strukturlösung mit direkten Methoden ergab sich die generelle chemische Zusammensetzung mit $\text{Fe}_7(\text{PO}_4)_6$. Eine Restelektronendichte von 5.3 eÅ^{-3} auf der speziellen Position $0, 1/2, 1/2$) wurde Natrium zugeordnet, das im Ausgangsmaterial für die Synthese in geringen Mengen als Verunreinigung in der Form $\text{NaH}_2(\text{PO}_4)$ vorlag.

Das Vorhandensein von Na in der Struktur wurde mit EDX-Analyse bestätigt. Die Na-Position ist nur zu etwa 1/5 besetzt. Die Zusammensetzung des untersuchten Materials ergibt sich demnach mit $\text{Na}_{0.18}\text{Fe}_{6.91}(\text{PO}_4)_7$. Der Ladungsausgleich erfolgt über ein geringes Defizit an Fe auf den Eisenpositionen. Die Verifizierung der Zusammensetzung erfolgt noch über eine Mikrosonden-Analyse.

Die Struktur zeigt insgesamt 4 verschiedene Eisenplätze, drei verschiedene Phosphor- und 12 verschiedene Sauerstoff-Positionen. Bindungsvalenz-Rechnungen weisen darauf hin, dass eine Ladungsordnung vorliegt und zwei der Positionen ausschließlich mit Fe^{2+} , die beiden anderen mit Fe^{3+} besetzt sind. Die Position Fe1 liegt genau im Zentrum der Elementarzelle, ist oktaedrisch von Sauerstoff-Atomen koordiniert und wird von Fe^{2+} besetzt. Diese Position zeigt mit $2.179(1)$ Å auch den größten mittleren Fe-O Bindungsabstand aller Fe-Polyeder. Alle Ecken des Fe1-Oktaeders sind zugleich Ecken von PO_4 -Tetraedern. Vier Ecken des Fe1-Oktaeders sind zudem mit weiteren Fe-Polyedern verknüpft. Die Positionen Fe2 und Fe4 sind mit Fe^{3+} besetzt, das in beiden Fällen oktaedrisch koordiniert ist. Die mittleren Fe-O Bindungslängen betragen $2.029(1)$ Å bzw. $2.047(1)$ Å. Eine etwas ungewöhnliche Koordination zeigt die Fe3 Position. Sie ist mit Fe^{2+} besetzt und wird von nur 5 Sauerstoff-Atomen umgeben. Die mittlere Bindungslänge Fe3-O beträgt $2.081(1)$ Å. Die Koordinationspolyeder der Fe2, Fe3 und Fe4 Positionen bilden, jeweils über eine gemeinsame Kante verknüpft, unendliche, stark abgeknickte Ketten, die parallel zur kristallographischen [1 0 1] Richtung verlaufen. Die Abfolge in einer Kette ist $\text{Fe3}-\text{Fe2}-\text{Fe2}-\text{Fe3}-\text{Fe4}-\text{Fe4}-\text{Fe3}-\dots$. Dadurch ergibt sich in einer Kette eine Sequenz: $\text{Fe}^{2+}-\text{Fe}^{3+}-\text{Fe}^{3+}-\text{Fe}^{2+}-\text{Fe}^{3+}-\text{Fe}^{3+}-\text{Fe}^{2+}-\dots$. Insgesamt vier derartige, über den Fe1O_6 -Oktaeder miteinander über Ecken verknüpfte Ketten durchlaufen eine Elementarzelle. Die Phosphat-Tetraeder liegen als voneinander isolierte Einheiten in der Struktur vor.

Das ^{57}Fe Mößbauer-Spektrum der Substanz zeigt bei 298 K die Existenz von 4 verschiedenen Subspektren, die den 4 vorhandenen Fe-Plätzen zugeordnet werden können. Die aus dem Spektrum erhaltenen relativen Flächenanteile weisen - ebenso wie die Einkristalldaten - darauf hin, dass die Fe1-Position (Fe^{2+}) vollständig besetzt ist, während die drei übrigen Plätze ein geringes Fe-Defizit aufweisen (bis zu 0.02 Atome pro Formeleinheit). Die Zuordnung der beiden Fe^{2+} -Dubletten zu den kristallographischen Plätzen gestaltet sich als sehr einfach, da diese ein 2:1 Verhältnis aufweisen, das sich auch im Mößbauer-Spektrum wiederfinden lässt. Auffällig beim oktaedrisch koordinierten Fe^{2+} auf der Fe3-Position ist die relativ hohe Isomerieverziehung von $1.293(4)$ mm/s, jene auf dem 5-fach koordinierten Fe1-Platz beträgt $1.153(8)$ mm/s. Die Zuordnung der beiden Fe^{3+} Dubletten erfolgt nach dem Grad der Verzerrung der Oktaeder, da diese im Fall des $3d^5$ Kations Fe^{3+} direkt mit der Größe der Quadrupolaufspaltung korreliert.

[1] KRAL, E. (1992): Dissertation, Universität Salzburg.

**DER $C2/c \Rightarrow P\bar{1}$ PHASENUBERGANG IN DER KLINOPYROXEN-VERBINDUNG
 $\text{NaTi}^{3+}\text{Si}_2\text{O}_6$**

G. J. Redhammer^{1, 2}, G. Roth² & H. Ohashi³

¹Institut für Mineralogie
Universität Salzburg, Hellbrunnerstrasse 34, A-5020 Salzburg, Österreich
²Institut für Kristallographie
RWTH Aachen, Jägerstrasse 17/19, D-52056 Aachen, Deutschland
³HASHI Institute for Silicate Science
Nishinakanobu 1-9-25, Shinagawa, Tokyo, 142-0054 Japan

Klinopyroxene gehören zu den wichtigen gesteinsbildenden Mineralen und ihre detaillierte Erforschung hat hohe Relevanz sowohl in den Geowissenschaften als auch in der Festkörperforschung. In jüngster Zeit erfreuen sich vor allem die so genannten 1:3 Klinopyroxene großer Beliebtheit, da viele Vertreter sowohl bei tiefen Temperaturen [1, 2] als auch bei hohen Drucken [3] Phasenübergänge von der monoklinen Raumgruppe $C2/c$ nach $P2_1/c$ zeigen, die teilweise mit großen Sprüngen im Volumen der Elementarzelle verbunden sind.

Im Rahmen unserer systematischen Untersuchungen des Tieftemperatur-Verhaltens der Alkali-Klinopyroxene wurde die Verbindung $\text{NaTi}^{3+}\text{Si}_2\text{O}_6$, eine der wenigen bislang bekannten Ti^{3+} -Verbindungen, bei 6 GPa Druck und einer Temperatur von 1873 K in einer Belt-Typ Hochdruck-Anlage synthetisch hergestellt. Einer der tiefblauen prismatischen Kristalle wurde mit Ein-kristallmethoden bei tiefen Temperaturen (300 K bis 100 K) an einem STOE IPDS II Bildplatten-system untersucht.

Die Raumtemperatur-Struktur von $\text{NaTiSi}_2\text{O}_6$ ist isotyp mit anderen $\text{NaMeSi}_2\text{O}_6$ Pyroxenen und zeigt die typische Raumgruppe $C2/c$. Bei 197 K allerdings tritt ein bislang für die Klinopyroxene noch nicht beschriebener $C2/c \Rightarrow P\bar{1}$ Phasenübergang auf. Das Volumen der Einheitszelle in der triklinen Form ist genau die Hälfte jenes der monoklinen Form. Der Phasenübergang ist verbunden mit einer Verzwilligung der Kristalle.

Die wesentlichen strukturellen Änderungen, die mit diesem Übergang einhergehen, betreffen den M1-Oktaeder-Platz. Hier treten in der $P\bar{1}$ Phase zwei unterschiedliche kürzeste $\text{Ti}^{3+}-\text{Ti}^{3+}$ Abstände innerhalb der M1-Oktaederkette auf, die ein sicheres Indiz für die Bildung von Ti-Ti Dimeren sind (Abbildung 1a). Dies ist in Hinblick auf die magnetischen Eigenschaften der Substanz mit einem möglichen Spin-Gap Übergang bei ≈ 200 K von besonderer Bedeutung. Die mittleren $\text{Ti}^{3+}-\text{O}$ Bindungslängen nehmen mit sinkender Temperatur sukzessive ab, wobei am Phasenübergang ein leichter Sprung im Datenverlauf zu beobachten ist. Die Abnahme der Symmetrie von $C2/c$ zu $P\bar{1}$ am Phasenübergang zeigt sich in teils drastischen Änderungen in den individuellen $\text{Ti}^{3+}-\text{O}$ Abständen. Diese Änderungen betreffen vor allem die beiden $\text{Ti}^{3+}-\text{O}$ Abstände, die zu den beiden Spitzen des Oktaeders weisen (i.e. zu den Apex-Sauerstoffen, Abbildung 1b).

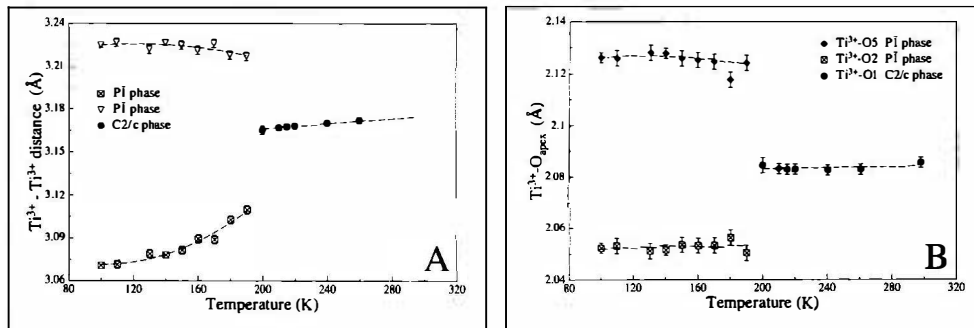


Abbildung 1

Strukturelle Änderungen innerhalb des $Ti^{3+}O_6$ Oktaeders in $NaTiSi_2O_6$ als Funktion der Temperatur. (a) Auftreten zweier kürzester $Ti^{3+}-Ti^{3+}$ Abstände in der M1-Oktaederkette, (b) Änderungen in den $Ti-O$ apex Bindungslängen im Zuge des $C2/c \Rightarrow P-1$ Phasenüberganges.

Aber auch innerhalb der Äquatorialebene zeigen sich sprunghafte Änderungen für die Abstände von Ti^{3+} zu jenen Sauerstoff-Atomen, die Oktaederkette und Tetraederkette lateral verbinden. Die $Ti^{3+}O_6$ -Oktaeder sind in Kettenrichtung gestreckt, wobei die Elongation in der triklinen Tief-temperaturform etwas größer ist als in der monoklinen Hochform. Dennoch sind die Oktaeder in der P-1-Phase im Bezug auf die Bindungslängen-Verzerrung und die quadratische Bindungswinkel-Varianz weniger stark verzerrt als in der C2/c Phase.

Der mittlere Na–O Bindungsabstand nimmt nahezu linear mit sinkender Temperatur ab, die Änderungen in den individuellen Na–O Bindungslängen sind gekennzeichnet durch deutliche Sprünge am Phasenübergang und resultieren aus den Änderungen der Geometrie der $Ti^{3+}O_6$ -Oktaeder. Die SiO_4 -Tetraeder erscheinen als eine sehr rigide Einheit, die weder in den Bindungslängen noch in den Bindungswinkeln deutliche Variationen erkennen lassen. Allerdings treten in der P-1 Phase zwei unterschiedliche Tetraederpositionen auf, wobei der Si1-Tetraeder etwas größer und mehr verzerrt ist als der Si2-Tetraeder. Im Gegensatz zum $C2/c \Rightarrow P2_1/c$ Phasenübergang, der vor allem in den $LiMeSi_2O_6$ Pyroxenen [1, 2] auftritt, zeigen sich bei dem in $NaTiSi_2O_6$ beobachteten Phasenübergang keine deutlichen Änderungen im Brückenzwinkel der SiO_4 -Tetraederkette. Insgesamt wird der Phasenübergang in der Titelverbindung aller Wahrscheinlichkeit nach durch die spezifische Natur des Ti^{3+} und die Tendenz zur Bildung von Ti–Ti Paaren bei tieferen Temperaturen hervorgerufen. Die strukturellen Änderungen auf den M2 und Si-Nachbarplätzen werden vornehmlich durch die Änderungen in der Geometrie des $Ti^{3+}O_6$ -Oktaeders kontrolliert.

References

- [1] REDHAMMER, G. J., ROTH, G., PAULUS, W., ANDRE, G., LOTTERMOSER, W., AMTHAUER, G., TREUTMANN, W. & KOPPELHUBER-BITSCHNAU (2001): The crystal and magnetic structure of Li-Aegirine $LiFe^{3+}Si_2O_6$: a temperature dependent study. - Physics and Chemistry of Minerals, 28, 337-346.
- [2] REDHAMMER, G. J. & ROTH, G. (2003): The temperature dependent $C2/c \rightarrow P2_1/c$ phase transition in $LiMe^{3+}Si_2O_6$ clinopyroxenes with $Me^{3+} = Ga, Cr, V, Fe, Sc$ and In. - Zeitschrift für Kristallographie (under review).
- [3] ARLT, T. & ANGEL, R. J. (2000): Displacive phase transitions in C-centred clinopyroxenes: Spodumene, $LiScSi_2O_6$ and $ZnSiO_3$. - Phys. Chem. Minerals, 27, 719-731.

ORIGIN OF ORTHOGNEISSES OF THE CZECH PART OF THE MOLDANUBIAN ZONE

M. René

Institute of Rock Structure and Mechanics
Academy of Sciences, V Holešovičkách 41, CZ-182 09 Praha 8, Czech Republic

The Moldanubian Zone of the Bohemian Massif contains various types of orthogneisses with distinct and contrasting modal compositions and geochemical characteristics. Although orthogneisses play a key role in unravelling the pre-Variscan evolution of the Moldanubian Zone, only scarce modern data on these rocks are presently available. The occurrence of orthogneisses is typical especially for the Drosendorf group of the Moldanubian Zone. Orthogneisses from the Moldanubian Zone have been attributed to different genetic groups: a) Synmetamorphic intrusives of Precambrian and or Cambro-Ordovician age, b) metamorphosed effusive and volcaniclastic rocks, c) products of Variscan migmatization and anatexis. Based on the few available geochronological data, at least three broad age groups of orthogneisses can be distinguished in the Moldanubian Zone: a) orthogneisses with Precambrian protolith ages (e.g., Dobra gneiss 1.38 Ga [1], Světlík gneiss 2.1 Ga [2]), b) orthogneisses with Cambro-Ordovician protolith ages (e.g., Gföhl gneiss 482 Ma [3], Stráž gneiss 537 Ma [4], c) products of Variscan migmatization and anatexis (e.g., Wolfshof gneiss 338 Ma [5]). However, protolith ages of most orthogneiss bodies are presently unknown. Extensive evidence suggests that the Moldanubian Zone represents a mosaic of tectonic units with a distinct tectonometamorphic history, which were finally assembled in the course of the Palaeozoic collision of Laurasia and Gondwana.

Four types of orthogneisses and orthogneisses-like rocks can be distinguished in the Czech part of the Moldanubian Zone. The probably oldest group is formed by biotite orthogneisses and orbicular metagranitoids in the Světlík area [2, 6]. This rock sequence is a part of the Drosendorf group of the Moldanubian Zone, and metagranitoids have a significant I-signature. The early Proterozoic intrusion of the protolith may be associated with convergence and collisions of island-arc-continent and continent-continent types during the Eburnean orogeny of West Gondwana [6].

The Cambro-Ordovician magmatic activity in the Czech part of the Moldanubian Zone is connected with intrusion of significantly leucocratic tourmaline-bearing alkali feldspar granites and monzogranites [7]. This activity was also accompanied by the origin of muscovite and sillimanite-muscovite metagranites with variable amounts of sillimanite, garnet, tourmaline or cordierite. These orthogneisses are composed of quartz, K-feldspar, plagioclase (An_{8-22}), muscovite, biotite and the above mentioned minerals. Accessory minerals include very plentiful apatite, zircon and ilmenite. Their leucocratic character is emphasized by low to accessory amount of biotite and significantly lower contents of FeO and MgO.

Orthogneisses have peraluminous character with values of aluminium saturation index of 1.1–2.1 and characteristic low content of CaO (0.3–0.8 wt.% CaO), Ba (52–139 ppm) and Sr (33–44 ppm). The content of P₂O₅ is relatively high (0.3–0.5 wt.% P₂O₅). Low amounts of Th (1.1–3.5 ppm) and HFSE are controlled by lower content of accessory minerals. Sillimanite, tourmaline and garnet-bearing orthogneisses show significantly low amounts of REE and exceptionally low LREE/HREE ratios ($\text{La}_N/\text{Yb}_N = 0.6\text{--}1.7$). Some of these orthogneisses are characterized by a significant negative europium anomaly ($\text{Eu}/\text{Eu}^* = 0.05\text{--}0.12$).

Compared to the Austrian part of the Moldanubian Zone, biotite and muscovite orthogneisses with I-type signature in the Czech part are relatively rare. Biotite orthogneisses are composed of K-feldspar, quartz, plagioclase (An_{14–28}) and biotite. Some biotite orthogneisses are characterized by the occurrence of garnet. Accessory minerals are zircon, apatite, magnetite, rare accessory mineral is also cordierite. Biotite orthogneisses are metaluminous to slightly peraluminous with values of aluminium saturation index of 0.9–1.3. These orthogneisses are characterized by a higher content of CaO (1.2–2.5 wt.% CaO), Ba (215–983 ppm) and Sr (113–1146 ppm). Some biotite orthogneisses typically show a higher content of Th (7.1–14.7 ppm) and Ce (25–63 ppm), together with a higher ratio of LREE/HREE ($\text{La}_N/\text{Yb}_N = 2\text{--}18.5$). The behaviour of Eu in biotite orthogneisses is highly variable, with a significant positive europium anomaly in some cases ($\text{Eu}/\text{Eu}^* = 1.95$). The presence of a positive europium anomaly evidences the origin of quartz-feldspar cumulates during partial melting of metasediments, which probably represent source rocks of some of the biotite orthogneisses in the Moldanubian Zone of the Bohemian Massif.

A special position is occupied by muscovite-biotite and biotite orthogneisses of the Gföhl group of the Moldanubian Zone. These orthogneisses are closely connected with the Variscan LP-HT metamorphism and the origin of migmatites in the Moldanubian Zone [8]. The bodies and irregular dykes and sills of orthogneisses occur in two different positions in the Gföhl group. The first group of orthogneisses is formed by a zone of stromatitic migmatites several hundreds of metres thick; these are accompanied by concordant bodies of granites several metres thick. Very plentiful variations of orthogneisses and migmatites are characteristic for the occurrence of these rocks in the Podolsko complex in southern Bohemia. The second group is formed by smaller bodies, dykes and sills of anatetic granites that have a truly intrusive character. They exhibit discordant, sharp boundaries against the surrounding paragneisses. These bodies of anatetic granites are not accompanied by layers of stromatitic migmatites. Anatetic granites consist K-feldspar, plagioclase (An_{8–15}), quartz, biotite and sometimes garnet. Anatetic granites are depleted in HFSE, only garnet-bearing granites are enriched in Y and HREE. The LREE/HREE ratio of these granites is relatively variable ($\text{La}_N/\text{Yb}_N = 6.1\text{--}23.9$). Some samples of anatetic granites are enriched in uranium (8–46 ppm). The origin of cumulates of feldspars is connected with a positive europium anomaly ($\text{Eu}/\text{Eu}^* = 0.49\text{--}1.61$).

This study was supported by the Czech-Austrian scientific program KONTAKT/AKTION (Project No. 4-2002) and by the Ministry of Education, Youth and Sports of the Czech Republic (Project No. ME-555).

References

- [1] GEBAUER, D. & FRIEDL, G. (1994): A 1.38 Ga protolith age from the Dobra orthogneiss (Moldanubian Zone of southern Bohemian Massif, NE Austria): evidence from ion-microprobe (SHRIMP) dating of zircon. - Journal of Czech Geological Society, 39, 34-35.
- [2] WENDT, J. I. ET AL. (1993): Evidence from zircon dating for existence of approximately 2.1 Ga old crystal-line basement in southern Bohemia, Czech Republic. - Geologische Rundschau, 82, 42-50.
- [3] FRIEDL, G. ET AL. (1998): New SHRIMP-zircon ages for orthogneisses from the south-eastern part of the Bohemian Massif (Lower Austria). - Acta Universitatis Carolinae, Geologica, 42, 251-252.
- [4] KOŠLER, J. ET AL. (1996): Early Cambrian granitoid magmatism in the Moldanubian Zone: U-Pb zircon isotopic evidence from the Stráž orthogneiss. - Zprávy o geologických výzkumech v roce 1995, 109-110. (in Czech).
- [5] FRIEDL, G. ET AL. (1994): 340 Ma U/Pb-Monazitalter aus dem niederösterreichischen Moldanubikum und ihre geologische Bedeutung. - Terra Nostra, 3, 43-46.
- [6] PATOČKA, F. ET AL. (2003): Granitoid gneisses with relict orbicular metagranitoids from the Varied group of the southern Bohemian Massif Moldanubicum: protolith derived from melting of Archaean crust? - Journal of Czech Geological Society, (in print).
- [7] VRÁNA, S. & KRÖNER, A. (1995): Pb-Pb zircon age for tourmaline alkali-feldspar orthogneiss from Hluboká nad Vltavou in southern Bohemia. - Journal of Czech Geological Society, 40, 127-131.
- [8] DUDEK, A. ET AL. (1994): Gföhl orthogneiss in the Moldanubicum of Bohemia and Moravia. - Krystalinikum, 10, 67-78.

TREATMENT OF ACID MINE WATER

D. Sager¹, F. Hosner², W. Riepe² & P. Ney¹

¹Institut für Mineralogie

Universität Salzburg, Hellbrunnerstrasse 34, A-5020 Salzburg, Austria

²Institut für Chemie und Biochemie

Universität Salzburg, Hellbrunnerstrasse 34, A-5020 Salzburg, Austria

Bodenmais is a health resort in the Bavarian wood. In the nearby Silberberg there was over a long period mining on pyrite and pyrrhotine for the production of ferric oxide and ferric sulfate and secondary sphalerite, galenite and chalcopyrite for winning of silver, copper and lead.

The problem is that sulfide minerals react under the influence of oxygen to sulfate (oxidation). Maybe some kind of bacteria is able to speed up this process.

In aqueous solutions the pH-value is lowered to a value of 2–3 because of the resulting diluted sulfuric acid. In the same time different metals (e.g. aluminium, cadmium, chrome, copper, iron, lead, manganese, mercury, nickel, zinc) are mobilized.

The resulting solutions have temporary different concentrations of these metals and some of these concentrations are too high relating to effective limiting values and so they are not allowed to be mixed with surface water.

Important parameters for the characterization of water are the pH-value and the conductivity. The pH-value differs between 2.64 and 2.9 and the conductivity between 796 and 1224 µS/cm². The reason therefore depends on the current season, e.g. dilution by melted snow and ice.

Because of this conditions the mine water must be treated. An option is the percolation of the mine water through chalky limestone. This limestone is porous and so shows a very reactive surface which is important to neutralize the mine water to a pH-value of 6–7, so the metals are precipitated as hydroxides.

Because of the high concentrations of iron and aluminium we need an adsorbing material e.g. glass wool which should precipitate those metal-hydroxides too.

The first step to treat the mine water, the neutralization, was no problem. Over a period of six hours the pH-value was constantly 6–7. But the second step, the precipitation of the metals is a problem. With the current test conditions the effective threshold values are not fallen short of but they are drastically reduced.

The following figures show the neutralization (fig. 1) and the measured values (with ICP-OES, fig. 2) of different samples. Probe 1 is taken after half an hour, Probe 5 is taken after two and a half hours and Probe 12 after six hours. In the original mine water the amount of aluminium differs between 15–27 ppm, the amount of copper between 0.29–0.44 ppm, the amount of iron between 21.3–41.6 ppm, the amount of manganese between 1.07–1.77 ppm and the amount of zinc between 4.90–8.49 ppm.

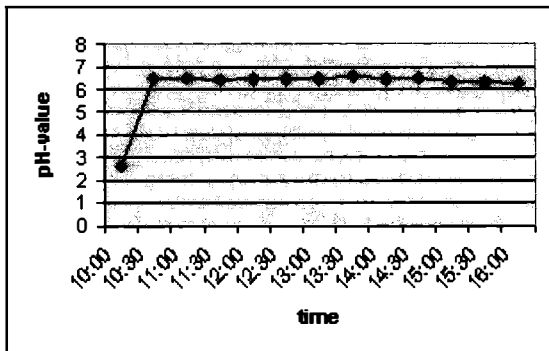


Figure 1
neutralization (pH-value on the y-axis).

The water analysis is carried out by ICP-OES (optical emission spectrometry with inductively coupled plasma), AAS (atom absorption spectrometry) and photometry (UV/VIS spectrometry) for cations and with IC (ion chromatography) for anions. The analysis for the chalky limestone is carried out by XRF (X-ray fluorescence), XRD (X-ray diffraction) and SEM (scanning electron microscope).

element	Probe 1	Probe 5	Probe 12	threshold value
Al	5,89	3,21	3,63	< 3
Cu	0,078	0,063	0,097	< 0,05
Fe	9,62	4,39	3,35	< 2
Mn	1,1	1,25	1,43	
Zn	3,53	4,63	5,68	< 1,5

Figure 2
values of different samples in [ppm]
(time on the x-axis).

**THERMOBAROMETRIC INVESTIGATIONS OF THE PRE-VARISCAN
KLOPAIER MIGMATITE (WESTERN ÖTZTAL CRYSTALLINE, EASTERN ALPS)**

F. Schennach & P. Tropper

Institute of Mineralogy and Petrography
University of Innsbruck, Innrain 52, A-6020 Innsbruck, Austria

The Austroalpine Ötztal Crystalline (ÖC) in the Eastern Alps provides an excellent opportunity to study a metamorphic core complex which underwent several episodes of metamorphic overprints. Although extensive research has been performed on the two predominant orogenic episodes in the Eastern Alps namely the Variscan and Alpine orogenic events, very little attention has been paid to the pre-Variscan (Caledonian) metamorphic history so far [1]. The pre-Variscan events are manifested in localized migmatite occurrences in the central (Winnebach migmatite) and western ÖC (Verpeil migmatite, Klopaijer migmatite). Geochronological investigations by [2] indicate several pre-Variscan metamorphic overprints ranging from 585 to 430 Ma whereas the tonalite gives an age of 490 Ma. The migmatite from the Klopaijer area, western ÖC, is also a nebulitic migmatite containing discrete narrow (0.5–1 cm width) bands of leucosome as well as nebulitic areas with schollen of biotite-plagioclase gneiss and calcsilicates. The observed mineral assemblage is garnet ($\text{Alm}_{66}\text{Prp}_{11}\text{Grs}_5\text{Sps}_{18}$) + biotite + plagioclase ($\text{An}_{21}\text{Ab}_{78}$) + K-feldspar ($\text{Or}_{89}\text{Ab}_{10}\text{An}_1$) + quartz + muscovite ± sillimanite. Textures indicate that the assemblage garnet + biotite + plagioclase + muscovite + quartz is the dominant mineral assemblage. In only one sample, fine grained aluminiumsilicate aggregates were found (presumably sillimanite, but further investigations with microraman spectroscopy are on the way) and garnet appears to have grown during the partial melting event due to the end-member reaction: biotite + aluminiumsilicate + plagioclase + quartz = garnet + K-feldspar + melt. In none of the samples has been any textural and chemical evidence for a polyphase metamorphic evolution (e.g. discontinuous garnet zoning, pseudomorphs etc.) found so far.

Thermobarometry involving the assemblage garnet + biotite + plagioclase + muscovite + quartz and garnet + biotite + plagioclase + sillimanite + quartz was performed using the inverse equilibrium approach of the program WEBINVEQ [3]. Our results yield temperatures of 586–615°C and pressures of 4.5–4.7 kbar. Application of the $\text{Fe}/(\text{Fe} + \text{Mg})$ isopleths of garnet composition from [4] yields pressures of ca. 3–5 kbar at temperatures of 600–700°C for the aluminiumsilicate-bearing sample. The tonalite contains the mineral assemblage: hornblende + biotite + plagioclase + titanite + K-feldspar + quartz. The hornblendes from the Klopaijer tonalite show chemical zoning with Al-rich cores (ca. 12 wt.% Al_2O_3) and Al-poor rims (6–7 wt.% Al_2O_3) and application of the Al-in hornblende barometer by [5] yields pressures of 3–7 kbars for the emplacement of the tonalite. Since the geochronological investigations of KLÖTZLI-CHOWANETZ (2001) indicate that the migmatization took place around 531 Ma and therefore pre-dates the intrusion of the Klopaijer tonalite it is still unclear whether the obtained P-T estimates reflect the later Caledonian- or possibly a Variscan metamorphic overprint (?).

References

- [1] HOINKES, G. ET AL. (1997): SMPM, 77, 299-314.
- [2] KLÖTZLI-CHOWANETZ, E. (2001): Unpubl. PhD Thesis, University Vienna, 155 p.
- [3] GORDON, T. (1992): Geochim. Cosmochim. Acta 56, 1793-1800.
- [5] SCHMIDT, M. W. (1992): Contrib. Mineral. Petrol. 110, 304-310.
- [4] SPEAR, F. S. ET AL. (1999): Contrib. Mineral. Petrol. 134, 17-32.

**DIE GEOLOGISCHE KARTE DES BUNDESLANDES SALZBURG 1:200.000 (GÖH200/S).
KONZEPT UND STAND SEPTEMBER 2003**

G. W. Schnabel¹ & R. Braunstingl²

¹Geologische Bundesanstalt

Rasumofskygasse 23, A-1031 Wien, Austria

²Abteilung 6, Landesbaudirektion - Geologischer Dienst

Amt der Salzburger Landesregierung, Michael Pacer-Strasse 36, A-5020 Salzburg, Austria

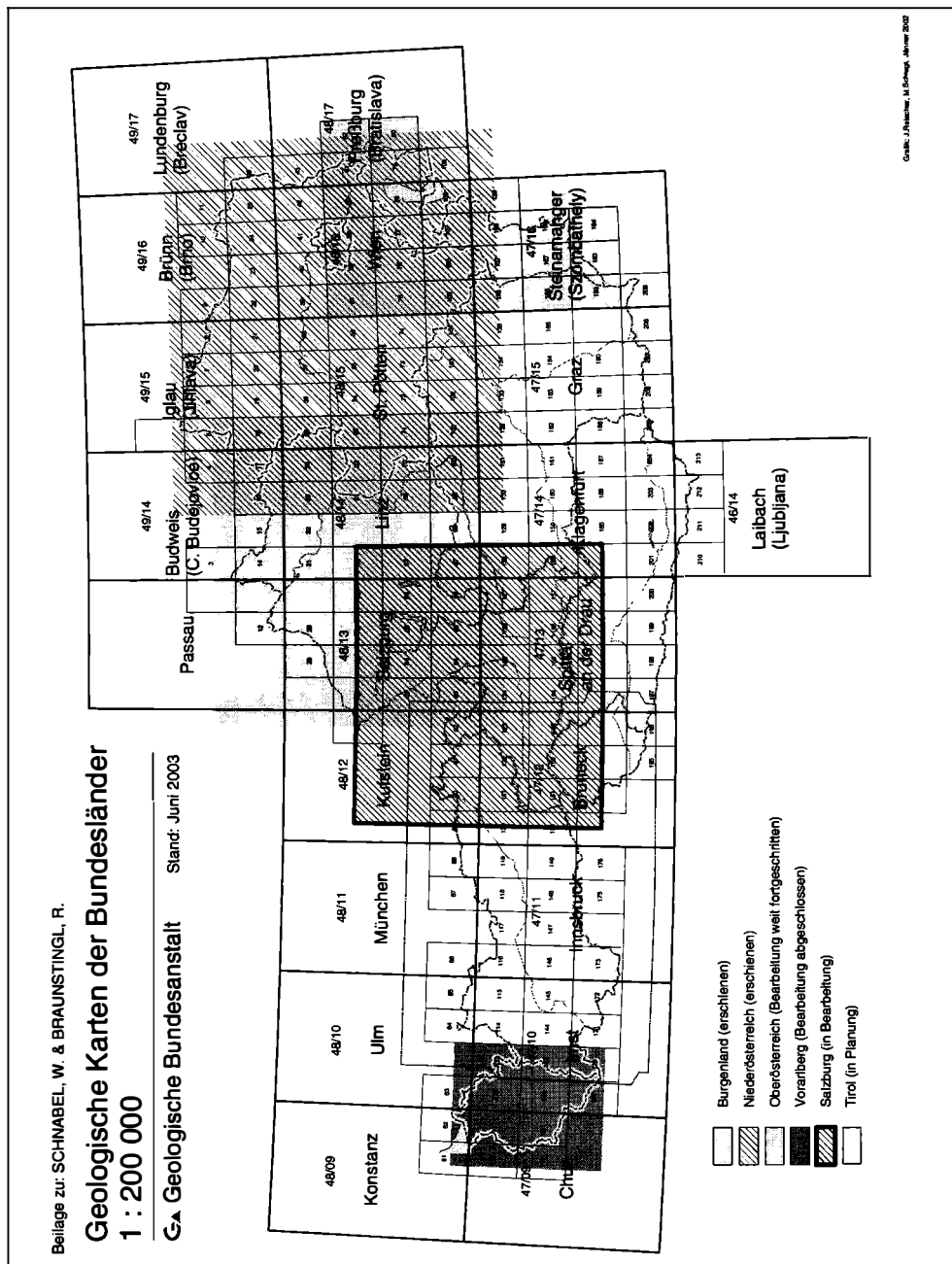
Vorgestellt wird der gegenwärtige Bearbeitungsstand der **Geologischen Karte des Bundeslandes Salzburg im Maßstab 1:200.000**, welche sich nach ihrem voraussichtlichen Erscheinen im Jahr 2004 nahtlos in das Kartenwerk 1:200.000 der Geologischen Karten der Österreichischen Bundesländer einfügen wird. Nach den Karten "Burgenland" (erschienen 2000), Niederösterreich (in 2 Teilen mit dem Bundesland Wien, erschienen 2002) und Oberösterreich (in abschließender Bearbeitung) wird es die vierte Karte dieser Bundesländerreihe sein. Bereits abgeschlossen ist des weiteren die Bearbeitung der Karte "Vorarlberg", wobei es bei dieser vor der Herausgabe noch einer Maßstabsabklärung bedarf.

Die geologische Karte des Bundeslandes Salzburg 1:200.000 ist wie alle anderen Karten der Bundesländerreihe ein Ausschnitt aus der "Geologische Karte der Republik Österreich 1:200.000". Diese ist als **blattschnittsfreie digitale Karte** konzipiert mit allen Voraussetzungen für die Einbindung in ein geologisches Informationssystem, für welches sie die regionale geologische Grundlage im Übersichtsmaßstab darstellt. Als digitale Karte mit individuell zu wählenden Maßstab deckt sie den Maßstabsbereich von Übersichtskarten 1:100.000 bis etwa 1:300.000 ab. Zum Unterschied von herkömmlichen Karten hat die digitale Karte einen "dynamischen" Charakter und wird an der Geologischen Bundesanstalt entsprechend dem Forschungs- und Kartierungsstand laufend ergänzt und damit immer aktuell gehalten werden. Aus ihnen können dem jeweiligen Bedarf der Kunden und Benutzer entsprechend individuelle Ausschnitte und geologische Inhalte ausgewählt und dargestellt werden.

Solche Ausschnitte sind die **Bundesländerkarten**, die als Auflagedrucke gleichsam Momentaufnahmen des gegenwärtigen Wissensstandes und für eine breite Öffentlichkeit bestimmt sind. Demgemäß werden die Erläuterungen in verschiedener Form auch nicht ausschließlich akademisch, sondern allgemein verständlich abgefasst. Sie werden dem Bedarf einzelner Bundesländer entsprechend bearbeitet, die durch namhafte finanzielle und fachliche Beiträge die Bearbeitung des gesamten Kartenwerkes möglich machen.

Bisher sind etwa 70 % der vorgesehenen Fläche des Gesamtkartenwerkes digital bearbeitet, das weit über die Staatsgrenze reicht. Die Verteilung der Bundesländerkarten und deren Lage im Kartenraster der ÖK50 kann aus der Beilage ersehen werden.

Anders als bei den bisherigen Bundesländerkarten hat bei der Geologischen Karte des Bundeslandes Salzburg der Geologische Dienst des Landes auch bei der Manuskripterstellung fachlich mitgewirkt und durch die Einarbeitung der Unterlagen an der Salzburger Landesregierung mit einem Schwerpunkt auf der angewandten Geologie der Entwicklung des gesamten Kartenwerkes bedeutende Impulse verliehen.



LEAD-ZINC DEPOSITS HOSTED BY SEDIMENTARY ROCKS IN THE ALPS
IN THE VIEW OF LEAD ISOTOPES

E. Schroll

Institut für Mineralogie und Kristallographie
Universität Wien, Geozentrum, Althanstrasse 14, A-1090 Wien, Austria

The origin of metals is an essential contribution to understand ore deposits. Lead isotopes are an important tool for it. In the magmatic environment, e.g. volcanogenic massive sulphide (VMS) deposits, the isotopic identity of rock lead and ore lead is evident. Therefore, uranogenic and thorogenic model ages are approximately concordant, and they are evaluated as realistic data. Otherwise, differences between both model ages are common in ore leads from low-temperature sediment-hosted deposits. The uranogenic model range from older than the mineralization (B(leiberg)-type ore lead) to younger (J(oplin)-type ore lead. The uranogenic model ages are older than the thorogenic model ages, e.g. Bleiberg deposit (uranogenic 332 ± 20 my, thorogenic $120 \pm$ my, stratigraphic age 210 to 220 my). Thus, these model ages are an indication for the source of lead. Preferably, the uranogenic lead isotopes ^{235}Pb and ^{238}Pb are only presented and interpreted. Fig. 1 illustrates lead isotope distribution in the Alpine sediment-hosted Pb-Zn deposits using the model age t_2 and the uranogenic environmental parameter μ_2 ($= ^{238}\text{U}/^{204}\text{Pb}$). Model age t_2 and μ_2 -value are parameters of the two stage lead evolution model [2].

Crustal lead has an μ_2 -average at 9.85. This value corresponds to a lead, that is multi-recycled and well-mixed by magmatic and sedimentary processes. Crustal ore lead isotope compositions are present in galena from occurrences in the Northern limestone Alps and in Permian sandstone and carbonates. A peculiarity is a rare galena crystal found in geodes from the Cardita shale at Bleiberg deposit. Its lead isotope composition is identical with the rock lead from Bleiberg deposit [2]. Model ages of ore leads, corresponding approximately with stratigraphic ages, are obtained only from uneconomic occurrences in the Anisian and Carnian stage of the eastern Northern Limestone Alps.

The main trend of the Triassic ore leads contains all important Pb-Zn deposits of the Alps. This main trend includes the Pb-Zn districts hosted by carbonate rocks in the Northern Tyrolian Limestone Alps, in the Drauzug (including Northern Karavancs) and Southern Alps. The field of the main trend is characterized by a positive correlation of t_2 and μ_2 . The μ_2 -values increase from crustal lead to upper crust lead in the following order: Northern Tyrolian Limestone Alps < Drauzug < Southern Alps. Ore leads from deposits hosted by Anisian stage display mostly lower μ_2 -values than ore leads from the Carnian stage. Exceptions are deposits which had economic importance, i.e. Topla in the Northern Karawanks and Auronzo in the Southern Alps. The largest deposits in the Alps, i.e. Bleiberg (3.5×10^6 tons Pb+Zn) and Mežica (2.0×10^6 tons Pb+Zn) are positioned north of the Periadriatic lineament.

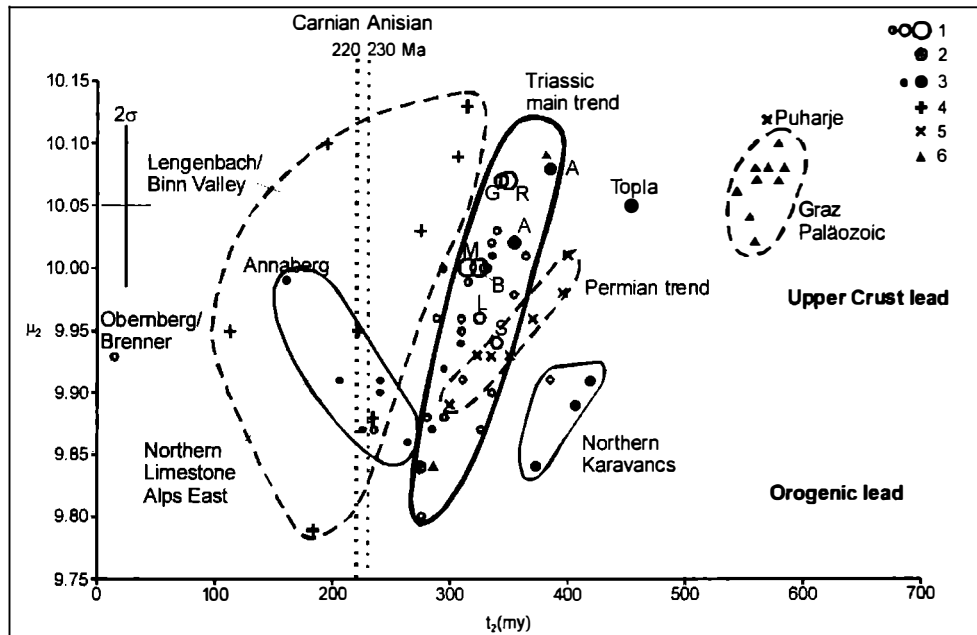


Table 1

Model age t_2 and μ_2 of Alpine deposits. Source of the lead isotope data [3, 4]. Abbreviations: A Auronzo, B Bleiberg, L Lafatsch, M Mezica, G Gorno, R Raibl, S Salafossa; 1 - small, medium and large deposits hosted by Carnian carbonates, 2 - small and medium deposits hosted by Anisian carbonates, 3 - geode (=rock) lead from Bleiberg, 4 - deposits hosted by Permian rocks, 5 - deposits hosted by Devonian rocks

The μ_2 -values of their ore leads are around 10, and their model ages are indistinguishable. The third deposit Raibl (1.5×10^6 tons Pb+Zn tons) situated south of the Periadriatic lineament shows an ore lead with a μ_2 -value of 10.8. Medium deposits, i.e. Lafatsch (Northern Tyrol) and Salafossa (Southern Alps), are characterized by lower μ_2 -values close to 9.9.

The deposits of the Triassic main trend reveal commonly relations between μ_2 -values and trace element geochemistry. High μ_2 -values are overwhelmingly combined with a decrease of Ag and Cu contents and an increase of Ge, Tl and As. In spite of high μ_2 -values, the lead-zinc ores from the Gorno district in the Bergamasco Alps (Italy) deviate significantly from the other districts in regard to geochemical parameters..

Leads from some Occurrences in the Northern Karavancs display higher model ages indicating a change in the source rock. A special trend is suggested for ore leads from deposits hosted by Permian carbonates. B-type ore leads are also typical for the sedimentary massive sulphide (SMS) deposits in the Graz Paleozoic hosted by Devonian sediments.

Obernberg (Brenner Triassic) and Lengenbach /Binn Valley (Switzerland) are carbonate-hosted Pb-Zn mineralizations in areas of amphibolite facies. The ore leads of these occurrences are characterized by radiogenic ore leads. The lead isotope data from the Lengenbach mineralization scatter widely. This deposit was originally a synsedimentary mineralization hosted by Anisian rocks [4].

Thus, the ore leads of the Alpine Triassic indicate relations to stratigraphy, basement and its clastica and - last not least - to regionally and temporally different paleohydrothermal systems. Homogeneity of lead isotope composition is an important constraint regarding for paleohydrogeological modelling. For instances, the Drauzug district hosted by Carnian stage presumes a basin that enables leaching of metals up to 10×10^6 tons by fluid rock reactions. The high homogeneity of the lead isotopes of these deposits excludes a paleohydrogeological model that assumes convective fluid events penetrating deeply into the basement.

Literatur

- [1] STACEY, J. S. & KRAMERS, J. K. (1975): Approximation of terrestrial lead isotopes by two stage model. - *Earth and Planetary Sciences*, 26, 207-221.
- [2] KÖPPEL, V. & SCHROLL, E. (1988): Pb-isotope evidence for the origin of lead in strata-bound Pb-Zn deposits in Triassic carbonates of the Eastern and Southern Alps. - *Mineralium Deposita*, 23, 96-103.
- [3] WEBER, L. (ed.): *Handbuch der Lagerstätten der Erze und Industriemineralen und Energierohstoffe Österreichs*. - *Archiv für Lagerstättenforschung.*, 18, 395-538.
- [4] KNILL, M. D. (1996): The Pb-Zn-As-Tl-Ba deposit at Lengenbach, Binn Valley, Switzerland. - *Beiträge zur Geologie der Schweiz. Geotechnische Serie*, 90, 1-74.

**DATING (PB-PB-TIMS) AND TRACE ELEMENT SIGNATURES (LA-ICPMS)
OF SINGLE ZIRCONS FROM METABASITES IN THE
AUSTROALPINE BASEMENT TO THE SOUTH OF THE TAUERN WINDOW**

B. Schulz¹, K. Bombach², H. Brätz¹ & R. Klemd¹

¹Institut für Mineralogie

Universität Würzburg, Am Hubland, D-97074 Würzburg, Germany

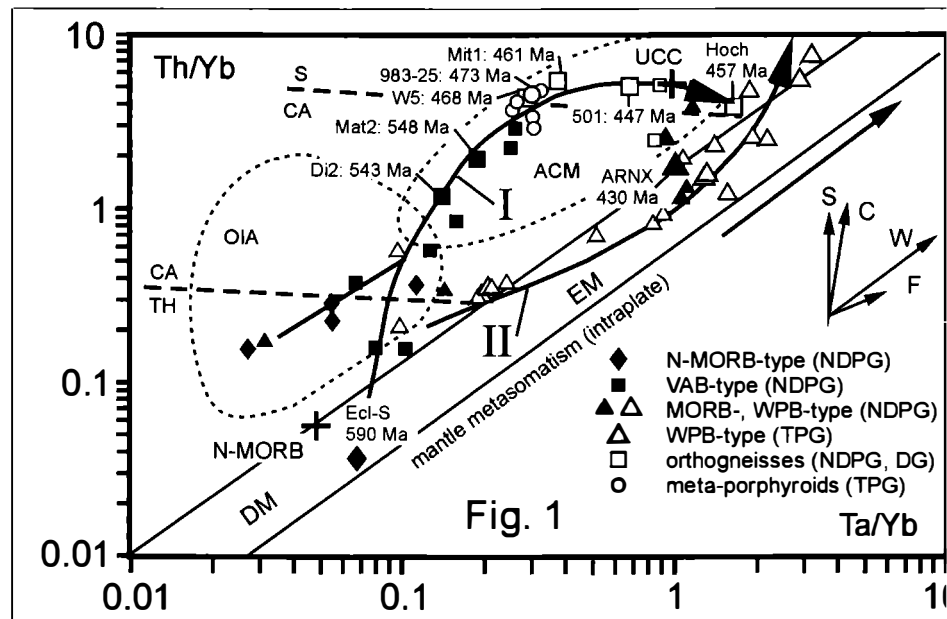
²Institut für Mineralogie, Isotopenlabor

TU Bergakademie Freiberg, Brennhausgasse 14, D-09596 Freiberg/Sachsen, Germany

The Variscan and partly Alpine metamorphic Austroalpine basement to the south of the central Tauern Window is subdivided into four lithological units: (1) the Northern-Deferegggen-Petzeck Group (NDPG) with the metabasic Rotenkogel, Torkogel, Michelbach and Prijakt Subgroups; (2) the Durreck (Cima Dura) Muscoviteschist Group; (3) the Deferegggen Group (DG), all of pre-Upper-Ordovician age, and (4) the Palaeozoic Thurntaler Phyllite Group (TPG). In units 1-3, N-MORB-type eclogitic amphibolites, VAB-type hornblende-plagioclase-gneisses, MORB- and WPB-type amphibolites occur with CAG- and CCG-type orthogneisses. Tholeiitic and alkaline WPB-type metabasites are associated with acid meta-porphyroids in the Thurntaler Phyllite Group.

Whole-rock Ta/Yb-Th/Yb and oxygen, Sr, Nd isotope data define two principal magmatic evolution lines (Fig. 1). An older evolution (I) involved magmatic suites with elevated whole-rock Th/Yb typical of subduction-related magmatism. Protolith ages of defined members in these suites were dated by TIMS with the Pb-Pb single zircon evaporation method [1]. N-MORB-type eclogitic amphibolites of the Prijakt Subgroup in the Schobergruppe with magmatic LIL and LREE enrichment and $(\text{Th}/\text{Ta})_N$ of 1.38–2.5 which can be interpreted as a sign of backarc magmatism display a protolith age of 590 ± 4 Ma. Hornblende-plagioclase-gneisses of the Rotenkogel and Prijakt Subgroups have basic to intermediate compositions. They display Ti/Zr, Ti/V and Cr/Y ratios typical of calk-alkaline volcanic arc magmatites. Their protolith ages range between 550 ± 5.9 and 533 ± 3.8 Ma. Orthogneisses with compositions ranging from metaluminous dioritic to peraluminous granitic are closely associated with the arc magmatic suite, but occur as well widespread in the Deferegggen Group. Protoliths of orthogneisses with compositions matching the continental arc granites discriminant field appear as slightly older (471 to 461 Ma) as those of orthogneisses ranging in the continental collision field (457 to 448 Ma). Geochemical signatures and REE patterns of these orthogneisses and the meta-porphyroids in the Thurntaler Phyllite Group are very similar. The meta-porphyroid protolith ages are 473 ± 6.7 and 469 ± 6.2 Ma. However, when corresponding single zircon ages are compared, the porphyroid volcanism appears slightly older as the granitoid plutonism. Both acid rock groups bear many inherited zircons with ages up to 1930 Ma. A younger evolution (II) in both pre- and post-Ordovician units is characterized by an intraplate mantle metasomatism or mantle-enrichment trend (Fig. 1).

The corresponding amphibolites in the Northern-Defereggen-Petzeck and in the Thurn Phyllite Groups have Zr-Ti-Y contents ranging from MORB tholeiites to within-plate all basalts. A highly differentiated sample from the alkalibasalt-like suite in the Torkogel Subgroup yielded a 430 ± 1.6 Ma Pb-Pb zircon age.



Occurrence of zircon in magmatites poses the question whether this mineral crystallized in magma which can be defined by its actual host rock, or has been assimilated during magma formation, fractionation and ascent. Trace and rare earth elements in zircon populations of these rocks have been extracted in-situ by a 266 nm Merchantek LUV laser and analysed quadrupole AGILENT 7500i ICP-MS. The zircon U, Th, Ti, Ce vs Y allow to distinguish compositional fields and trends. Zircons of N-MORB-type metabasite give a mantle-trend endmember at low Y, Ce, U, but high Ti, whereas zircons with elevated Y, Ce and U from highly differentiated WPB-type amphibolite define an opposite crustal trend. When Yb/Gd and Yb (normal to the primitive mantle) are chosen as proxies for an interplay between magma composition and zircon crystal chemistry, the mantle-trend zircons show low degree of HREE enrichment and very variable HREE fractionation, whereas the crustal-trend zircons have considerable HREE enrichment at low and constant fractionation. The well-defined and limited compositional fields of N-MORB-, VAB- and WPB-type metabasite zircon populations are matched by their homogeneous Neoproterozoic, Cambrian and Early Silurian crystallization ages. Zircons with elevated common Pb and apparently disturbed Pb systematics display deviations from ideal REE patterns. It is concluded that each Austroalpine metabasite zircon population crystallized from a specific magma which is represented by the geochemical characteristics of the actual host rock. Compositional fields of acid metagranite zircon populations show large variations but exclude the extreme mantle-trend compositions. This is explained by a considerable share of inherited and/or assimilated zircons.

These principal magmatic evolution lines are related to a progressively mature Austroalpine active margin which lasted from Neoproterozoic through Cambrian to Early Silurian times along the north-Gondwanan periphery. The subduction-driven magmatism culminated in the formation of an Early-Cambrian magmatic arc. Ordovician acid volcanism and plutonism appear as a mature stage of this evolution. Early-Silurian alkalibasaltic magmatism then signalizes a subsequent and partly simultaneously starting passive margin evolution, which was probably related to the opening of the Palaeo-Tethys. Subduction could still have been the cause of mantle-source enrichment recorded in the corresponding alkaline WPB-type magmatites.

References

- [1] SCHULZ, B. & BOMBACH, K. (2003): Single zircon Pb-Pb geochronology of the Early-Palaeozoic magmatic evolution in the Austroalpine basement to the south of the Tauern Window. - Jahrbuch der Geologischen Bundesanstalt, 143/2, 303-321.

**FT-IR-SPEKTROSKOPISCHE QUANTIFIZIERUNGEN AM GIPS/ANHYDRIT-ROHSTEIN
DES BERGBAUS PUCHBERG AM SCHNEEBERG**

K. Schwendtner¹, E. Libowitzky¹, M. A. Götzinger¹ & S. Koss²

¹Institut für Mineralogie und Kristallographie
Universität Wien, Geozentrum, Althanstrasse 14, A-1090 Wien, Austria
²RIGIPS Austria GmbH
Wr. Neustädter Strasse 63, A-2734 Puchberg am Schneeberg, Austria

Qualitätssicherung zählt zu den wichtigsten Aufgaben eines modernen Industriebetriebes um auf dem Markt wettbewerbsfähig zu bleiben. Durch eine genaue Kenntnis des Rohmaterials gelingt es, die Qualität eines Produktes dauerhaft auf hohem Niveau zu halten. Zu diesem Zweck wurde eine FT-IR-spektroskopische Methode entwickelt, die schnell und benutzerfreundlich die Quantifizierung von Gips, Anhydrit, Magnesit und Cölestin im Rohstein ermöglicht.

Die Vorteile der FT-IR Spektroskopie im Vergleich zu herkömmlichen Methoden wie XRD oder Thermogravimetrie (TG) liegen auf der Hand: Ein Spektrum kann binnen Minuten ohne komplizierte Probenvorbereitung ausgewertet werden, was einen direkten, raschen Eingriff in die Prozesssteuerung ermöglicht.

Der Einfluss von Korngröße und Verdünnung in KBr wurde sowohl in diffuser Reflexion (DRIFT) als auch in Transmission verglichen. Korngrößeneffekte führen in Transmission zu enormen Intensitätsschwankungen im Spektrum, während DRIFT relativ unsensibel darauf reagiert. Transmissionsmessungen erfordern eine sehr große Probenverdünnung in KBr (2 mg Probe auf 500 mg KBr), was bereits beim Einwiegen zu großen Fehlern führen kann.

DRIFT Messungen ergeben auch unverdünnnt Spektren, die qualitativ ausgewertet werden können. Zur quantitativen Analyse erwies sich eine Mischung von 27 mg Probe in 270 mg KBr als optimal, bei Verdünnungen von 1:5 zeigen stark absorbierende Banden noch beträchtlichen Einfluss von gerichteter Reflexion. Mischungsverhältnisse von 1:20 verbessern die Qualität der Spektren nur geringfügig, was nicht im Verhältnis zur wesentlich geringeren Probeneinwaage steht.

DRIFT Spektren liefern wesentlich mehr Daten, die zur Auswertung herangezogen werden können, besonders stark absorbierende Banden werden schwächer, während sehr schwache Banden, wie Oberton- oder Kombinationsschwingungen noch detektiert werden können.

Zur Erstellung der Standardreihe wurden natürliche hochreine Proben (> 98 % rein) verwendet und in definierten Verhältnissen gemischt und dann gemahlen.

Die Standardmaterialien wurden so gewählt, dass auch die physikalischen Eigenschaften dem in Puchberg abgebauten Material möglichst ähnlich sind. Versuche mit reinem Gelmagnesit führten aufgrund der Zähigkeit und Härte zu nicht reproduzierbaren und mit dem abgebauten Material nicht vergleichbaren Korngrößen.

Aus hochreinem Gips (durch brennen bei 600°C für 48h) hergestellter Anhydrit erwies sich als anfälliger auf Luftfeuchtigkeit als natürliches Material.

Großer Wert muss auf den Mahlvorgang gelegt werden: Innerhalb der Standardreihe darf sich die Korngrößenverteilung nicht wesentlich ändern. Dieses Problem könnte zwar im Prozess durch Normierung auf einen internen Standard umgangen werden, aber TG Messungen zeigen, dass sich sowohl Gips als auch Anhydrit durch den Mahlvorgang verändern.

Gips, welcher in einer Schlagkugelmühle für 5 min gemahlen wurde, zeigte in der TG statt des erwarteten Gewichtsverlusts von 20.92 %, welcher im Einkristall derselben Probe gemessen wurde, einen Gewichtsverlust von nur noch 19.86 % (vorsichtig per Hand gemahlener Gips zeigte einen Verlust von 20.45 %). Das entspricht einem Wasserverlust von beinahe 5 % bereits während des Mahlens.

Natürlicher Anhydrit nimmt hingegen durch den Mahlvorgang - wenn auch nur geringfügig - Wasser auf (bei nach oben geschilderter Methode künstlich produziertem Anhydrit verstärkt sich dieser Effekt). Die FT-IR-Methode reagiert auf Wassergehalte sehr sensibel, der Mahlvorgang muss daher für genaue Ergebnisse immer reproduzierbar sein.

Messungen von 5 gleichen Probenmischungen, die mit einer modernen Planetenkugelmühle aufbereitet wurden, zeigten Abweichungen vom Mittelwert der Bandenfläche von etwa 2–3 %.

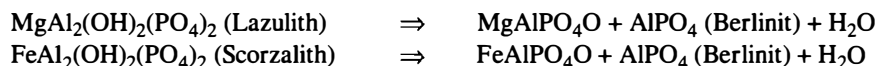
Ein Vergleich der Vor- und Nachteile der FT-IR, XRD-Rietveld und TG/DSC Verfahren bestätigt die Anwendbarkeit der FT-IR Methode. Als problematisch erweist sich bei der Rietveld-Methode die starke Textur der gut spaltbaren Minerale, die eine quantitative Auswertung sehr erschwert. Die Vorteile chemometrischer Software, basierend auf multivariaten statistischen Methoden im Vergleich zu herkömmlichen Peakfitting Methoden werden noch untersucht werden.

**IN-SITU-UNTERSUCHUNGEN DER DRUCK- UND TEMPERATURABHÄNGIGKEIT
DES MOLVOLUMENS VON LAZULITH, SCORZALITH UND DEREN
ENTWÄSSERUNGSPRODUKTEN MGALPO₄O UND FEALPO₄O**

R. Selke¹, P. Schmid-Beurmann¹, L. Cemic¹ & C. Lathe²

¹Institut für Geowissenschaften
Universität Kiel, Olsenhausenstrasse 40, D-24098 Kiel, Germany
²DESY/HASYLAB
Notkestrasse 85, D-22603 Hamburg, Germany

Lazulith kommt in der Natur in Sedimenten, alterierten Vulkaniten, Pegmatiten und Meta-morpheniten der Grünschiefer- und Amphibolitfazies vor. Die Endglieder Lazulith, MgAl₂(PO₄)₂(OH)₂, und Scorzalith, FeAl₂(PO₄)₂(OH)₂, bilden eine vollständige Mischkristallreihe [1, 2]. Ihre p-T-Stabilitätsgrenzen werden durch folgende Entwässerungsreaktionen beschrieben:



Um das Stabilitätsfeld von Lazulith und Scorzalith zu berechnen, ist es von großer Bedeutung, Druck- und Temperaturabhängigkeit der Molvolumina der beteiligten Phasen zu kennen.

Zu ihrer Bestimmung eignet sich insbesondere die energiedispersive Röntgenbeugung, mit der Gitterkonstantenmessungen unter währenden p-T-Bedingungen möglich sind. Am Hamburger Synchrotron Labor (HASYLAB, MAX80) wurde daher die Temperatur- bzw Druckabhängigkeit des Molvolumens von folgenden Phasen gemessen: Lazulith, Scorzalith, MgAlPO₄O und FeAlPO₄O.

Lazulith und Scorzalith wurden bei 0.3 GPa und 500°C unter den Bedingungen des QFI-Puffers synthetisiert. MgAlPO₄O wurde bei 1300°C im Ofen in einem Pt-Tiegel und FeAl-PO₄O bei 950°C in einer evakuierten SiO₂-Glasampulle unter den Bedingungen des WI-Puffers hergestellt. Die Charakterisierung der Syntheseprodukte erfolgte durch Röntgendiffraktometrie (Rietveld-verfeinerung). Bei eisenhaltigen Proben wurde zusätzlich Mößbauerspektroskopie eingesetzt. Die Druckkalibrierung erfolgte über die Messung des (200)-Reflexes von NaCl, dessen Lage als Funktion des Drucks und der Temperatur genau bekannt ist.

Die Pulverspektren der Proben wurden bei Drücken von 0.1 MPa bis 6.0 GPa und bei Temperaturen von 25 bis 900°C aufgenommen.

Sowohl Scorzalith als auch Lazulith zeigen über den untersuchten p-T-Bereich eine lineare Änderung der Molvolumina mit dem Druck bzw. der Temperatur. Bei Drücken größer als 4.4 GPa und Temperaturen größer als 900°C wurde ein Abbau von Scorzalith beobachtet. Im Gegensatz dazu konnte bei Lazulith kein Zerfall bei Drücken bis zu 6.0 GPa und Temperaturen bis zu 600°C festgestellt werden.

Bei FeAlPO_4O findet oberhalb von 1.0 GPa und 25°C eine Transformation in eine strukturell bislang unbekannte Hochdruckphase (α' - FeAlPO_4O) statt, die nicht mit der Hochdruckmodifikation des MgAlPO_4O [3] isotyp ist.

References

- [1] SCHMID-BEURMANN, P., KNITTER, ST. & CEMIĆ, L. (1999): Crystal chemical properties of synthetic lazulite-scorzalite solid-solution series. - Phys. Chem. Minerals, 26, 496-505.
- [2] SELKE, R., SCHMID-BEURMANN, P. & CEMIĆ, L. (2003): Cation and valence distribution in Fe-phosphates of the lazulite type. - Eur.J.Mineral., 15, 127-136.
- [3] SCHMID-BEURMANN, P., BRUNET, F. & LATHE, C. (2003): Thermodynamic properties of Mg-Al-phosphates: Polymorphism and stability of MgAlPO_2O , a key phase in the $\text{MgO}\text{-}\text{Al}_2\text{O}_3\text{-}\text{P}_2\text{O}_5\text{-H}_2\text{O}$ lazulite system. - EMPG IX, Zürich.

**PETROLOGIC STUDIES ON CARBONATE CONE IN THE SOUTH VÉRTES MTS.
(W-HUNGARY)**

Z. Siklósy¹, K. Gál-Sólymos¹, L. Korpás²& Cs. Szabó¹

¹Lithosphere Fluid Research Lab. - Department of Petrology and Geochemistry
Eötvös University, Budapest, Hungary

²Geological Institute of Hungary
Budapest, Hungary

Spectacular reddish brown carbonate cone was found in the southern part of Vértes Mts. (Transdanubian Central Range), close to NW of village Gánt (PEREGI & KORPAS, 2002). Some red calcite dikes were already described from other parts of the Transdanubian Central Range (HAAS ET AL., 1984; DEMÉNY ET AL., 1997). These dikes are mostly situated in Upper Triassic carbonates and never cut Tertiary rocks. There are two localities where their Upper Cretaceous age could be stratigraphically determined. The origin of these red calcite formations is different from the other calcite veins that can be found in almost all Mesozoic and Tertiary carbonates. A detailed stable isotope and fluid inclusion study of DEMÉNY ET AL. (1997) suggested that percolation of magmatic fluids played a significant role during the formation of the red calcite dikes. PEREGI & KORPAS (2002) postulated a travertine spring cone origin for the Gánt occurrence and we have carried out a careful petrographic and geochemical study to determine its relation to the red calcite dikes.

The isometric and elliptical carbonate cone is 40 to 50 m long and 7 to 8 m high. It has a ring structure likened to a willow-tree that differs totally from the surrounding Upper Triassic Hauptdolomite. The middle part of the cone is vertically bedded, whereas at the rim the beddings turn to less steep: 10–50°. The carbonate material itself has a typical travertine fabric and consists of alternating massive, layered and porous calcite.

Samples are composed of mostly calcite crystals that can grow up to 0.5 mm. The calcite crystals mostly banded due to the zonation of Fe-oxide layers. Based on petrographic study, the carbonate cone can be described as a travertine deposit. Electron microprobe and scanning electron microscope techniques and neutron activation analyses were also used to determine the accessories minerals of sitting in the carbonate material. Xenomorphic zircon, xenotime and monazite were found as small grains (up to 10 µm). Based on the textural features, only monazite and xenotime can be considered as autochthon minerals. The carbonate cone is relatively enriched in light rare earth elements (La, Ce, etc.) particularly sample collected close to the hypothetical vent facies. Also, each sample has a positive U anomaly (up to 3.73 ppm). The presented geochemical data are partially characteristic and similar to the Quaternary thermal Buda travertine as indicated by KORPAS ET AL. (2003). In our case a generic relation to the Late Cretaceous lamprophyres occurring in the northern part of the Transdanubian Central Range (SZABO ET AL., 1993) can be considered.

References

- DEMÉNY, A., GATTER, I. & KÁZMÉR, M. (1997): *Geologica Carpathica*, 48, 315-323.
- HAAS, J., JOCHÁNÉ EDELÉNYI, E., GIDAI, L., KAISER, M., KRETZOI, M. & ORAVECZ, J. (1984): *Geologica Hungarica Series Geologica*, 20, 353 p.
- KORPÁS, L., KOVÁCS-PÁLFFY, P., LANTOS, M., FÖLDVÁRI, M., KORDOS, L., KROLOPP, E., STÜBEN, D. & BERNER, ZS. (2003): *Quaternary Research*, (submitted).
- PEREGI, ZS. & KORPÁS, L. (2002): *Földtani Közlöny*, 132(3-4), 477-480.
- SZABÓ, CS., KUBOVICS, I. & MOLNÁR, ZS. (1993): *Mineralogy and Petrology*, 47, 127-148.

OLISTOLITHS AND OLISTOSTROMES IN FLYSCH CARPATHIANS

A. Ślęzka

Institute of Geological Sciences
Jagiellonian University, Oleandry 2a, 30-063 Kraków, Poland

The olistotromes developed during all stages of the Flysch Carpathians development. They consist of muddy matrix with different amount of boulder and blocks up to several metres in diameter (olistolithes). Sporadically blocks up to hundreds metres occur. The thickness of individual beds can vary from few metres up to tens of metres or even more. Resedimentation processes involved slumping, debris flow and sporadically rockfall.

The olistolithes, during the development of the Carpathian basin, similar to other orogenic basins, were derived both from extrabasinal, interbasinal and from basinal sources, and at the time of the final, compressional stage of the Northern Carpathians development, from the frontal part of the advancing nappes [1]. Extra- and interbasinal sources supplied igneous, metamorphic [2] and sedimentary olistolithes of different age, generally well rounded. The basinal sources provided penecontemporaneous and/or also older sediments. A special type of olistostromes was connected with volcanic activity (Bachowice, [3]). The extrabasinal sources were the southern part of the North European Platform, situated along the northern margin of the Carpathian flysch basin and areas flanking this basin from south. Internal ridges situated between the Carpathians basins [4], e.g. the Silesian Cordillera and its SE prolongation, the Andychów Ridge and the Marmaros Massif, were represented mainly by remnants of a carbonate platform or folded cordilleras. The basinal olistolithes were derived from the slope of the basins and/or from uplifted part of those basins. In many cases an olistostrome can contain both, extrabasinal and basinal material.

The first appearance of olistostromes within the Carpathian flysch basin was already connected with the initial rifting stage when basinal and extrabasinal sediments slid and slumped from uplifted and tilted blocks into newly created basins. During later stages heterogeneous material from extra- and interbasinal sources predominated. The olistolithes bound to the final compressional stage were connected with the successive emplacement of the Flysch Carpathians nappes towards the north. The displacing nappes covered the internal ridges and olistolithes mainly represented the frontal part of the advancing nappes, slid down to still existing basins, sometimes of piggyback basin type, in the inner part of more external units. In the lower part of the Early Miocene the advancing Magura Nappe covered a part of the Dukla Nappe, its western prolongation and the Silesian Cordillera and reached the southern part of the Silesian basin. From its frontal part huge olistolithes [5] slid locally down to the southern, still preserved part of this basin. Penecontemporaneously the northern part of the Silesian and SubSilesian units have been uplifted and started to be overthrust onto the Skole basin and olistolithes were detached from the uplifted margin of the SubSilesian unit and deposited to the inner part of the Skole basin.

Subsequent olistolithes were derived from the northern margin of the advanced Carpathian stack of nappes and deposited in the Miocene Foredeep Basin [1, 6]. Simultaneously with the over-thrusting of the Carpathians, the NE directed migration of the Foredeep Basin depocentre took place. This process was accompanied periodically by the development of olistolithes, which was derived from the moving uplifted Carpathian front. For many years the olistostromes, which developed in front of the advancing nappes, were regarded as separate tectonic units and their age was based on the age of olistolithes and only when the muddy matrix and the structures were investigated in detail their real age and character was defined.

References

- [1] SLĄCZKA, A. & OSZCZYPKO, N. (1987): Olistostromes and overthrusting in the Polish Carpathians. - Ann. Inst. Geol. Publ. Hungarici, 70: 287-292.
- [2] WIESER T. (ed.) (1985): Researches in the Western part of the Polish Carpathians. Guide to Excursion 1. - Carpath.-Balkan Geol. Assoc. XIII Congrss, Kraków, Poland 1985. Geological Institute. 1-102.
- [3] WIESER, T. (1954): The igneous rocks of Bachowice. - Ann. Soc. Geol. Pologne, 22: 223-275.
- [4] KSIĄŻKIEWICZ, M. (1960): Pre-orogenic sedimentation in the Carpathian geosyncline. - Geologische Rundshau 50: 8-31.
- [5] SZYMAKOWSKA, F. (1976): Olistotromes in the Krosno Beds (Polish Middle Carpathians). - Ann. Soc. Geol. Poloniae 46: 39-54.
- [6] SLĄCZKA, A. & KOLASA, K. (1997): Resedimented salt in the Northern Carpathian Foredeep. - Slovak Geological Magazine 3: 135-155.

**EDELMETALLE: KOMPLEXE MINERALOGIE, UNVERZICHTBARE ROHSTOFFE,
UND DOCH WASSERLÖSLICH ?**

E. Stumpf

Institut für Mineralogie und Petrologie
Montanuniversität Leoben, Franz-Josef-Strasse 18, A-8700 Leoben, Austria

Edelmetalle sind heute weltweit von grösstem wirtschaftlichem und wissenschaftlichem Interesse. Diese kurze Übersicht befasst sich vorwiegend mit den Elementen der Platin-Gruppe (Pt, Ir, Os, Pd, Rh, Ru), die unter der Abkürzung "PGE" zusammengefasst sind, und nur am Rande mit Gold. Angesichts weltweit Gesetzeskraft erlangender Abgas-Kontrollvorschriften sind die PGE als Katalysatoren untrennbar mit dem wichtigsten Indikator wirtschaftlichen Wohlstandes, dem Automobil, verbunden. Auch erfreuen sie sich in den wachsenden Märkten Ost- und Südostasiens zunehmender Beliebtheit als Schmuck-Metalle. In der pharmazeutischen Forschung spielen sie eine wichtige Rolle; ein Grossteil der in der Chemotherapie verwendeten Verbindungen basieren auf PGE.

Geopolitisch relevant ist die Tatsache, dass Südafrika und Russland die wichtigsten Produzenten, die EU, USA und Japan die Haupt-Konsumenten der PGE sind. Der Gesamtwert der Jahresproduktion liegt in der Grössenordnung von sechs Milliarden Euro. So ergibt sich ein spannendes Szenario, das von den Fluktuationen an der London Metals Exchange (LME) ebenso geprägt wird wie von wissenschaftlichem Fortschritt und von politischen Entwicklungen in Russland und im südlichen Afrika.

Die Entstehung von PGE-Lagerstätten und selbst das chemische Verhalten von PGE sind nach wie vor Gegenstand lebhafter wissenschaftlicher Debatte. Einzelne experimentelle Daten zur Löslichkeit von PGE in Fluiden bei hydrothermalen Temperaturen sind erst in den letzten Jahren verfügbar geworden (z.B. [1]). Bis dahin galt weithin das Diktum mineralogischer Lehrbücher: "Platin: löslich nur in heissem Königswasser (aqua regia; HCl/HNO₃)", und der unorthodoxe Versuch, daran zu rütteln (z.B. [2]; [3]), führte zu heftigen Reaktionen. Die komplexe Mineralogie der PGE hat die ersten Hinweise darauf geliefert, dass die oft geforderte Entstehung von Platin-Mineralen (PGM) aus sulfidischen Schmelzen nicht die Regel ist. Die Zahl der bekannten PGM ist inzwischen auf mehr als 150 angewachsen. Darunter sind nicht nur Sulfide, sondern auch eine Vielzahl von Verbindungen mit Sb, Bi, Te, Sn, Cu, Hg, und Pb, die sich häufig aus hydrothermalen Lösungen bilden.

Die Frage, warum in der grössten PGE-Lagerstätte der Welt, dem südafrikanischen Bushveld, die Gesamtgehalte an PGE über hunderte von Kilometern nur geringe Schwankungen zeigen, die Mineralogie der Erze aber radikalen Änderungen unterliegt, ist noch nicht geklärt. Erze der Union-Mine im nordwestlichen Bushveld führen mehr als 80 % Pt-Fe-Legierungen. In Rustenburg, im Südwesten, sind es 40 % Pt-Pd Telluride, 30 % Pt-Pd-Sulfide, und 10 % Laurit (RuS₂). In der Atok-Mine (Lebowa) im östlichen Bushveld liegen die betreffenden Werte bei 75 % Pt-Pd-Sulfide und 15 % Pt-Pd-Telluride ([4]).

Die PGM werden häufig von wasserführenden Silikaten (Amphibole, Glimmer) und von Quarz begleitet, der NaCl-reiche Flüssigkeitseinschlüsse (FI) führen kann. PGE können als Chlorid-Komplexe in wässrigen Lösungen transportiert werden. FI wurden auch in platinführenden Chromititen der Ophiolite des südlichen Ural nachgewiesen. [5] und [6] konnten zeigen, dass podiforme Chromitite ihre Entstehung Flotations-ähnlichen Prozessen in wasserhaltigen Olivin-Chromit-gesättigten Mantel-Schmelzen von Supra-Subduktionszonen verdanken.

Bis vor kurzem haben Mineralogen und Lagerstättenforscher daran gezweifelt, dass Platin-Körner in Seifen, d.h. Konzentrationen von PGM in Fluss-Sanden, ebenso wie Gold-Nuggets, aus Edelmetall-haltigen Oberflächen-Wässern entstehen können. Schon vor fast dreißig Jahren hat der Autor gezeigt, dass PGM in Seifen von Oxydationsrändern umgeben sind (sie "rosten"). Wohin gehen die dabei frei werdenden PGE? Sie werden zur Bildung neuer PGM verwendet ("neoformations"; [7]). "Säurefest" und "nicht oxydierend" sind die PGE nicht einmal immer im Labor, und sicher nicht in der Natur und in geologischen Zeiträumen. Unverzichtbar sind sie trotzdem.

Literatur

- [1] XIONG, Y. & WOOD, S. (2000): Experimental quantification of hydrothermal solubility of platinum group elements with special reference to porphyry copper mineralization. - *Mineral. Petrol.* 68, 1-28.
- [2] STUMPFL, E. F. (1974): The genesis of platinum deposits: further thoughts. - *Minerals Sc. Engineering*, 6, 120-141.
- [3] BALLHAUS, C. G. & STUMPFL, E. F. (1986): Sulfide and Platinum mineralization in the Merensky Reef: Evidence from hydrous silicates and fluid inclusions. - *Contrib. Mineral. Petrol.* 94, 193-204.
- [4] CAWTHORN, R. G., LEE, C. A., SCHOUWSTRA, R. P. & MELLOWSHIP, P. (2002). Relationship between PGE and PGM in the Bushveld Complex. - *Canad. Mineral.* 40, 311-328.
- [5] MELCHER, F., GRUM, W., SIMON, G., THALHAMMER, T. V., & STUMPFL, E. F. (1997). Petrogenesis of the ophiolitic giant chromite deposits of Kempirsai, Kazakhstan: a study of solid and fluid inclusions in chromite. - *J. Petrology*, 38, 1419-1458.
- [6] MATVEEV, S. & BALLHAUS, C. (2000). Role of water in the origin of podiform chromitite deposits. - *Earth Planet. Sc. Letters*, 203, 235-243.
- [7] OBERTHÜR, T., WEISER, T. W., & GAST, L. (2003). Geochemistry and mineralogy of platinum-group elements at Hartley Platinum Mine, Zimbabwe, Part 2. - *Mineral. Dep.* 38 (Stumpfl Issue), 344-355.

**OPHIOLITE-TYPE AND ZONED CLINO PYROXENITE-DUNITE COMPLEXES:
GENETIC CONSTRAINTS FROM PGE MINERALOGY AND OS-ISOTOPES**

O. A. R. Thalhammer & K. N. Malitch

Institute of Mineralogy and Petrology
Department of Geological Sciences, University of Leoben, A-8700 Leoben, Austria

The use of special separation and concentration techniques enabled us to separate and investigate numerous primary Os-rich platinum group minerals (PGM, e.g. predominantly phases of the laurite-erlichmanite series and Os-Ir-Ru alloys) from massive chromitites of ophiolite and clinopyroxenite-dunite complexes. The samples have been taken from the Kraubath and Hochgrößen massifs (Austria), exemplifying ophiolite-type complexes, and from the Guli, Kondyor and Inagli clinopyroxenite-dunite massifs (Siberian Craton, Russia).

In this contribution we particularly present an extensive data set of Os-isotope compositions of Os-rich PGM. The fact that Os-rich PGM contain Os as a main trace element and almost lack Re, permits the determination of accurate initial Os isotope ratios, assuming that the Os-isotope composition of the PGM has not changed after their formation. Therefore, the Os-isotope composition reflects that of the source and primary Os-rich PGM, frequently the earliest precipitates in ultramafic rocks, are considered the best tracers of i) mantle melting events, and ii) different mantle environments. The Os-isotopic composition of PGM has been measured by i) negative thermal ionization mass-spectrometry (NTI-MS), and ii) laser ablation multiple collector inductively coupled plasma mass-spectrometry (LA-MC-ICP-MS).

The range of $^{187}\text{Os}/^{188}\text{Os}$ ratios in PGM derived from the Guli, Kondyor and Inagli clinopyroxenite-dunite complexes (Siberian Craton, Russia) show a narrow range of 'unradiogenic' $^{187}\text{Os}/^{188}\text{Os}$ values, indicative of a sub-chondritic mantle source of platinum group elements (PGE, i.e. 0.12432–0.12520, $n = 30$; MALITCH ET AL. 2002). In contrast, Ru-Os sulfides from podiform chromitites of the mantle section of the Kraubath and Hochgrößen massifs (Eastern Alps, Austria) revealed a wide range of chondritic to sub-chondritic $^{187}\text{Os}/^{188}\text{Os}$ values (i.e. 0.1158 ± 0.0015 to 0.1244 ± 0.0005 , $n = 18$; MALITCH ET AL. 2003). These $^{187}\text{Os}/^{188}\text{Os}$ ratios of PGM from the residual oceanic mantle of ophiolites demonstrate a prolonged melting history of parent ultramafic protoliths, which did obviously not result in a significant concentration of PGE. In contrast, we propose a highly productive single stage melting event in clinopyroxenite-dunite complexes resulting in a significant metallogenic potential.

References

- MALITCH, K. N., AUGE, T, BADANINA, IYU, GONCHAROV, M. M., JUNK, S. A. & PERNICKA, E. (2002): Mineral. Petrol. 76, 121-148.
MALITCH, K. N., JUNK, S. A. , THALHAMMER, O. A. R. , MELCHER, F., KNAUF, V. V., PERNICKA, E. & STUMPFEL, E. F. (2003): Canad. Mineral. 41, 331-352.

**MINERAL REACTIONS WITHIN THE BIOTITE-PLAGIOCLASE GNEISS SCHOLLEN
OF THE POLYMETAMORPHIC WINNEBACH MIGMATITE
FROM THE ÖTZTAL CRYSTALLINE, EASTERN ALPS:
ADDITIONAL CLUES TO UNRAVELING THE COMPLEX METAMORPHIC HISTORY ?**

W. Thöny & P. Tropper

Institute of Mineralogy and Petrography
University of Innsbruck, Innrain 52, A-6020 Innsbruck, Austria

The Austroalpine Ötztal Crystalline (ÖC) in the Eastern Alps provides an excellent opportunity to study a metamorphic core complex which underwent several episodes of metamorphic overprints. Although extensive research has been performed on the two predominant orogenic episodes in the Eastern Alps namely the Variscan and Alpine orogenic events, very little attention has been paid to the pre-Variscan (Caledonian) metamorphic history so far [1]. The pre-Variscan events are manifested in localized migmatite occurrences in the central (Winnebach migmatite) and western ÖC (Verpeil migmatite, Nauderer migmatite).

The Winnebach migmatite is built up by granodioritic neosome containing remnants of biotite-plagioclase gneiss and schollen of biotite-plagioclase gneiss and calc-silicate lenses thus indicating a higher degree of melting [2]. Petrological investigations of [3] indicate partial melting at pressures of ca. 8 kbar and at least 750°C during the Caledonian orogeny. The Variscan metamorphic overprint lead to the formation of Ca-rich garnet overgrowths and locally staurolite.

The Eo-Alpine event is characterized by the possible formation of chloritoid. The biotite-plagioclase gneiss lenses contain the assemblage biotite + muscovite + garnet (1) + plagioclase + quartz and seem to preserve important informations about the metamorphic history following the Caledonian migmatic event. Thin section traverses through the gneiss schollen reveal the progression of a reaction front, leading to complete replacement of the protolith assemblage over a distance of few centimeters by the secondary assemblage garnet (2) + clinozoisite + diopside + K-feldspar. Garnet (1) has a chemical composition of $\text{Alm}_{72}\text{Pyr}_5\text{Grs}_5\text{Sps}_{18}$ and garnet (2) has a composition of $\text{Alm}_{60}\text{Pyr}_2\text{Grs}_{22}\text{Sps}_{16}$.

These petrographic changes can be ascribed to the progression of two end-member reactions such as: plagioclase + biotite + garnet (1) + $\text{H}_2\text{O} \rightleftharpoons$ clinozoisite/zoisite + K-feldspar + diopside and plagioclase + muscovite + garnet (1) + $\text{H}_2\text{O} \rightleftharpoons$ clinozoisite/zoisite + K-feldspar. Both reactions require the influx of an H_2O -rich fluid phase which results in the stabilization of Fe-poor clinozoisite/zoisite.

In addition, mineral chemical investigations reveal features such as complex chemical zoning in garnet porphyroblasts and titanites (core: 2.31 wt.% Al₂O₃; rim 3.24 wt.% Al₂O₃) and zoisite/clinozoisites (core: 8.33 wt.% Fe₂O₃; rim: 1.89 wt.% Fe₂O₃). Discontinuous chemical zoning, indicating a strong increase in the Ca-component was also observed in garnets from leucosome samples. These data indicate a possible later metamorphic overprint accompanied by an influx of a fluid phase, but it is still unclear whether these reactions can be attributed to the Variscan or the Eo-Alpine metamorphic overprint.

References

- [1] HOINKES, G. ET AL. (1997): SMPM, 77, 299-314.
- [2] HOINKES, G. ET AL. (1972): TMPM, 18, 292-311.
- [3] KLÖTZLI-CHOWANETZ, E. (2001): Unpubl. PhD Thesis, University Vienna, 155 p.

**RECENT STATE OF KNOWLEDGE OF THE DEEP STRUCTURE OF THE EASTERN ALPS:
A REVIEW**

C. Tomek¹, E. Brückl² & V. Höck¹

¹Institute of Geology and Paleontology

University of Salzburg, Hellbrunnstrasse 34, A-5020 Salzburg, Austria

²Institut für Geodäsie und Geophysik

Technische Universität Wien, Gusshausstrasse 27-29, A-1040 Wien, Austria

The eastern Alps are traditionally thought to be a elongated belt of mountains between the Rhine valley in the W and the Vienna Forest in the E situated North of the Insubric line. All this area in Austria, Switzerland, Germany and Italy is covered by high quality potential field maps.

The gravity map shows the East Alpine gravity minimum. This gravity low is divided into three parts. The W part between the Rhine and the Brenner fault is the most pronounced gravity low in the Alps at all. The second part of minimum accompanies the Tauern window and is of different character than the W anomaly. An important, circa 40 mGal part of the minimum is characterized by a relatively low wavenumber, its source must be present in the upper 10 km of the crust. The third part E of the Tauern window is lower in amplitude. The amplitude decreases eastwards and is becoming very small in the Semmering area. This decreasing amplitude is accompanied by the narrowing of the Alpine foredeep. From the point of view of the diminishing minimum and narrow foredeep, the Alps E of the Bohemian Massif promontory around St. Pölten posses already the Carpathian deep characteristics.

The aeromagnetic map of the Eastern Alps is characterized by a very pronounced Berchtesgaden anomaly that continues to the East, beneath the Carpathians we are able to trace it until the Cracow area in Poland. The anomaly undoubtedly mirrors the basement rocks of the Bohemian Massif s.l. Refraction seismic experiments in the seventies of the last century revealed basic characteristics of the plunging Moho boundary beneath the Eastern Alps. Depths more than 50 km were discovered beneath the central parts of the Alps between the Rhine valley and the Tauern window. Farther to the east the Moho is shallower and reaches the depth of some 28 km beneath the Pannonian basin at the eastern boundary of the Alps.

Reflection seismics has been done along the Transalp line five and four years ago. The main results were presented several times and lastly in Trieste during the final Transalp Conference in February 2003. Excellent results were achieved and will be presented also during this conference. Receiver function studies and refraction experiment helped to the success of the Transalp project. New refraction studies were done during the projects of CELEBRATION 2000 and ALP 2002. Also these results will be presented during the MinPet 2003 conference.

All data confirm the model where the Eastern Alps were built during the final Late Oligocene and Early Miocene continental subduction that stopped during the Ottangian (18 Ma ago) and following continental collision, which continues until recent. The Alpine crust is deepest in the W and subsequently is becoming thinner towards the E. The easternmost portion of the Eastern Alps posses already Carpathian characteristics, not only expressed by geophysical data but also by the type of Miocene volcanism in Styria.

MINERALOGICAL ASPECTS OF FLUE GAS DESULFURIZATION

J. Troby¹, R. Abart² & K. Bärnthaler³

¹Institute of Mineralogy and Petrology

Karl-Franzens-Universität Graz, Universitätsplatz 2/II, A-8010 Graz, Austria

²Mineralogical-Petrographical Institute

Basel University, Bernoullistrasse 32, CH-4056 Basel, Suisse

³E Energietechnik

Waagner-Biro Strasse 105, A-8021 Graz, Austria

In the late seventies and early eighties of the twentieth century SO₂ emissions reached a maximum with about 90000 tons of SO₂ in Austria in the year 1980 [1]. The prime emittants being oil and coal fired power plants. Since then the SO₂ emissions have been successively reduced at constant or increasing productivity of the power plants. The annual SO₂ emissions in Austria have now levelled out at about 5000 tons [1]. The reduction of SO₂ emissions by more than 90 % was achieved by the installation of desulfurization systems which is now mandatory in calorific power plants. The most efficient means of removing sulphur dioxide is the so called "wet" process in which an aqueous slurry of finely grained limestone is contacted with the flue gas. The slurry is dispersed into the exhaust gas stream of a power plant as fine droplets through a series of nozzles. SO₂ is adsorbed onto the droplets of the spray and via a number of elemental reactions this leads to the conversion of calcite to gypsum. The bulk reaction may be written as [2]:



Provided that conversion is complete, that is the fraction of residual carbonate in the solid reaction product is less than 5 % per volume, the gypsum produced may be used as construction material and has an economic value. Process engineers therefore try to tune the desulfurization plants so that they can meet the two basic requirements: (1) a desulfurization grade of > 95 % and (2) residual carbonate content in the produced gypsum of < 5 %.

In many desulfurization plants the quality goals can be reached, but some plants are problematic with respect to the purity of the produced gypsum even after thorough process optimisation. Unsatisfactory product quality despite of optimised plant and process design may be due to low quality of the limestone that is used for preparation of the limestone slurry. Manufacturers of desulfurization plants usually have rather crude quality criteria. Regarding the limestone slurry 90 % of the limestone powder must have a particle size of less than 44 µm. It must contain more than 90 % CaCO₃ and less than 3 % MgCO₃. So far no further specifications of quality standards for the limestone raw material were considered. This motivated mineralogical and petrographical studies on limestones used, on intermediate solid-liquid and liquid-liquid reaction products and on the product gypsum in order to identify potential additional quality criteria that would allow to better select appropriate raw materials.

Experiments were done on a producing power plant in Vojany (eastern Slovakia). The most important process parameters, pH and density (i.e. solid particle content) of the intermediate product in the spray reactor, were varied systematically. In addition the natural variation of the sulphur content of the coal and the exhaust gas was monitored and two sorts of limestones were used for the slurry. It was found that the standard process parameters of pH = 5.6 at a density of 1090 g/l slurry resulted in the lowest possible residual carbonate content of the produced gypsum. This indicates that the standard parameters indeed guarantee an optimised process. A change from a limestone with a MgCO₃ content of about 3 wt.% to a limestone with a MgCO₃ content of 6 wt.% caused an increase in the residual carbonate fraction in the product gypsum from about 1.5 to 3 vol.%. This may be due to the fact that the kinetics of dolomite dissolution in acidic environments is slow compared to the kinetics of calcite dissolution. This allows dolomite particles to be carried through the process without significant reaction. An additional effect is that high MgCO₃ contents of the limestone entail high magnesium concentrations in the liquid of the reactor. Magnesium concentrations in the liquid phase of the slurry in the spray reactor may get as high as 3000 ppm. This may lead to partial or complete conversion of calcite to dolomite in the reactor. Above a pH-value of 5.8 of the liquid phase of the slurry the precipitation of dolomite is possible. This secondary dolomite formation may withdraw a significant fraction of the originally available CaCO₃ from the desulfurization process and lead to an elevated residual carbonate content in the form of dolomite in product gypsum.

Another effect may be due to physical interactions among solid particles. A large fraction (up to 80 % per volume) of the residual carbonate in product gypsum is represented by agglomerates, which are comprised of small (< 10 µm) particles of calcite and sheet silicates such as muscovite. In the range of 4 < pH < 8, calcite has a positive surface charge and muscovite has a negative surface charge. The pH conditions in a desulfurization reactor is such that carbonates and sheet silicates have opposite surface charges and thus tend to form aggregates. In such agglomerates calcite appears to be sheltered from the acid attack and it may be carried through the process without reaction.

The mineralogical and chemical composition of the limestone to be used as raw material for limestone slurry in desulfurization systems has a measurable effect on the quality of the product gypsum. On the one hand, the MgCO₃ content of the raw material should be as low as possible to minimize introduction of primary and secondary dolomite particles, which may be carried through the desulfurization process without reaction. On the other hand chemically nominal inert particles such as sheet silicates may lead to elevated residual carbonate contents in the product gypsum by physical particle-particle interactions. We recommend further specification of the quality criteria for limestone raw materials. In particular we propose reduction of the maximum allowed MgCO₃ content and addition of a mineralogical criterion that specifies a maximum tolerable sheet silicate content of the raw material.

References

- [1] NEUBARTH & KALTSCHMIDT (2000): Erneuerbare Energien in Österreich. - Springer Verlag.
- [2] BROGREN & KARLSSON (1997): A Model for Prediction of Limestone Dissolution in Wet Flue Gas Desulfurization Applications. - Ind. Eng. Chem. Res. 1997, 36, 3889-3897.

**THE FORMATION OF COEXISTING MUSCOVITE + PARAGONITE + MARGARITE
DURING EO-ALPINE REPLACEMENT OF STAUROLITE
IN MARTELL MICASCHISTS FROM THE ORTLER CRYSTALLINE**

P. Tropper¹ & V. Mair²

¹Institute of Mineralogy and Petrography
University of Innsbruck, Innrain 52, A-6020 Innsbruck, Austria
²Amt für Geologie und Baustoffprüfung
Eggentalerstrasse 48, I-39053 Kardaun (BZ), Italy

Observations of metamorphic assemblages and experimental studies on white micas indicate the presence of a wide solvus between muscovite and paragonite (see [1]). While coexisting Na-K white micas have been described from low- to medium-grade metamorphic rocks throughout the world and they are widespread in blueschist- and eclogite-facies assemblages ([2] and references therein), the occurrence of coexisting muscovite + paragonite + margarite is very rare and has been described by [3] and [4]. Margarite and paragonite are known to replace Al-rich phases such as staurolite [5]. Staurolite replacement by the assemblage paragonite + chlorite according to the reaction: staurolite + albite + H₂O ⇌ paragonite + chlorite + quartz has been reported from the southern Ötztal Crystalline by [5]. In this study, we report an occurrence of coexisting muscovite + paragonite + margarite pseudomorphing staurolite.

The Ortler crystalline represents a polymetamorphic Austroalpine crystalline basement which occurs south of the Ötztal crystalline between the Vinschgau- and the Ulten Valley. During the Eo-Alpine orogeny, the Ötztal Crystalline was juxtaposed onto the northern part of the Ortler Crystalline and its sedimentary cover [6]. The Laas Series and the Martell Micaschists clearly show a polymetamorphic evolution with an earlier Variscan and a later Eo-Alpine metamorphic overprint. In contrast to the Martell Micaschists, the Laas Series shows a stronger Eo-Alpine re-equilibration, thus erasing almost all of the Variscan metamorphic history. The Eo-Alpine metamorphic conditions were determined in a sample from the Martell Micaschists (RS 34-1) and yield 6.7 ± 0.7 kbar and $480 \pm 44^\circ\text{C}$.

In the course of the investigation of the metamorphic evolution of the Ortler Crystalline, we discovered two samples (RS 34-1, VM 144) from the Martell Micaschist unit, which contain muscovite + paragonite + margarite. The Variscan mineral assemblage in the metapelitic samples is comprised of relict garnet (1) + staurolite + plagioclase (1) + quartz. The Eo-Alpine metamorphic overprint led to the formation of the mineral assemblage garnet (2) + plagioclase (2) + biotite + muscovite + chloritoid + paragonite + margarite + chlorite. The prominent feature in both samples is the replacement of staurolite either by the assemblage muscovite + chloritoid + paragonite + margarite + chlorite as in sample RS 34-1 or by chloritoid + paragonite + margarite + chlorite as in sample VM 144. In sample VM 144, paragonite is mainly a ternary solid solution $\text{Ms}_{8-13}\text{Pg}_{73-76}\text{Mrg}_{14-16}$, whereas margarite is a binary solid solution with paragonite ($\text{Mrg}_{70-72}\text{Pg}_{28-30}$). Muscovite contains no margarite component ($\text{Ms}_{74-76}\text{Pg}_{24-26}$).

These data are very similar to the compositional data from sample RS 34-1. Textural data indicate a reaction similar to the staurolite breakdown from the southern Ötztal Crystalline as proposed by [5], but in our case the anorthite component of plagioclase and the coexisting biotite also play an important role, thus enabling the reactions $\text{staurolite} + \text{anorthite} + \text{biotite} + \text{H}_2\text{O} \rightleftharpoons \text{chloritoid} + \text{margarite} + \text{muscovite}$ and $\text{staurolite} + \text{albite} + \text{biotite} + \text{H}_2\text{O} \rightleftharpoons \text{chloritoid} + \text{paragonite} + \text{muscovite}$ and thus the formation of coexisting muscovite + paragonite + margarite.

Acknowledgements

Financial and logistic support from the projects CARG-PAT and CARG-PAB of the Autonomous Provinces of Trento and Bolzano-Südtirol.

References

- [1] ROUX, J. & HOVIS, G. L. (1996): Thermodynamic mixing models for muscovite-paragonite solutions based on solution calorimetric and phase equilibrium data. - *J. Petrol.* 37:1241-1254.
- [2] GUIDOTTI, C. V., SASSI, F. P., BLENCOE, J. G. & SELVERSTONE, J. (1994): The paragonite-muscovite solvus: I. P-T-X limits derived from the Na-K compositions of natural, quasibinary paragonite-muscovite pairs. - *Geochim. Cosmochim. Acta* 58:2269-2275.
- [3] HÖCK, V. (1974): Coexisting phengite, paragonite and margarite in the metasediments of the mittlere Hohe Tauern, Austria. - *Contrib. Mineral. Petrol.*, 43, 261-273.
- [4] OKUYAMA-KUSUNOSE, Y. (1985): Margarite-paragonite-muscovite assemblages from the low-grade metapelites of the Tono metamorphic aureole, Kitakami Mountains, Northeast Japan. - *J. Japan. Assoc. Min. Petrol. Econ. Geol.*, 80, 515-525.
- [5] HOINKES, G. (1981): Mineralreaktionen und Metamorphosebedingungen in Metapeliten des westlichen Schnebergerzges und des angrenzenden Altkristallins. - *TMPM*, 28, 31-54.

**HERKUNFTSANALYSE RÖMISCHER MARMORARTEFAKTE
DER AUSGRABUNG IM SCHRÖTTELHOFER FELD BEI OBERDRAUBURG (KÄRNTEN)**

M. Unterwurzacher¹, H. Stadler², C. Franzen¹ & P. W. Mirwald¹

¹Institut für Mineralogie und Petrographie

Universität Innsbruck, Innrain 52, A-6020 Innsbruck, Austria

²Institut für Ur- und Frühgeschichte, Mittelalter- und Neuzeitarchäologie

Universität Innsbruck, Innrain 52, A-6020 Innsbruck, Austria

Die Fundstelle im Schröttelhofer Feld bei Oberdrauburg, Kärnten ist seit dem 19. Jh. bekannt. Die historische Bedeutung ist vor allem in verkehrsgeographischer Hinsicht wegen ihrer Lage an der Kreuzung zweier wichtiger Verkehrsverbindungen zwischen Italien, Noricum und Pannonien gegeben. Seit 1995 wird die Siedlungsstelle durch ein internationales Projekt archäologisch erforscht. Die ergrabenen Baustrukturen aus Holz und Mauerwerk deuten auf eine römische Villa des 2. - 4. Jh. n. Chr. hin, die sich durch seltene Buntmetallfunde und reichhaltige Marmorverwendung, Gesimsleisten, Delphinköpfe, Schalen, in Ausstattung und steinernem Inventar von den anderen römischen Stationen der Region deutlich abhebt. Die Marmorartefakte waren das Objekt einer interdisziplinären archäologisch-mineralogischen Studie.

Marmore wurden zu Römischer Zeit häufig verwendet; ihre Herkunft, insbesondere in den Römischen Provinzen, ist jedoch vielfach unklar. Eine Kenntnis der Herkunft ist jedoch von großem Interesse für den historischen Kontext. Wichtige, bereits römerzeitlich genutzte, alpine Marmore kommen aus Laas/Südtirol und aus Gummern/Kärnten. Diese zwei alpinen Marmore waren bereits Forschungsobjekt einiger Studien (z.B. CORTECCI, G.; DINELLI, E.; D'AMICO, C.; TURI, B., 2000 [1]; MÜLLER & SCHWAIGHOFER, 1999 [2]).

Die Marmorobjekte aus Oberdrauburg wurden insbesondere mit folgenden Methoden untersucht: Korngrößenanalyse, Kathodolumineszenzmikroskopie und chemische Analysen.

Besonders hilfreich erwies sich die Unterscheidung verschiedener Marmore mittels der C- und O-Isotope sowie dem Mn-Gehalt. Die erhobenen Daten erlauben eine gute Charakterisierung der unterschiedlichen Marmore. Carrara Marmor kann bereits aufgrund der Isotopensignatur eindeutig ausgeschlossen werden. Aus dem regionalen Vergleich zwischen verschiedenen Marmoren aus Südtirol sowie Westkärnten ergeben die Daten, dass der Marmor aus den Brüchen von Gummern in Kärnten stammen dürfte.

Aus kulturhistorischer Sicht belegt diese Studie, dass selbst bei sehr bedeutenden römischen Siedlungen vielfach hochwertiges Werkmaterial aus dem regionalen Umfeld bevorzugt wurde.

Literatur

- [1] CORTECCI, G., DINELLI, E., D'AMICO, C. & TURI, B. (2000): ¹⁸O-depleted marbles from Val Venosta (Alto Adige, Italy). - Miner. Petrogr. Acta, Vol. 18, p. 87-100.
- [2] MÜLLER, H. & SCHWAIGHOFER, B. (1999): Die römischen Marmorsteinbrüche in Kärnten. - Carinthia II/2, p. 549-572.

BERNSTEIN AUS ÖSTERREICH

N. Vávra

Institut für Paläontologie
Universität Wien, Geozentrum, Althanstrasse 14, A-1090 Wien, Austria

Beim Thema "Bernstein aus Österreich" wird ein Mineraloge zunächst wohl an die verschiedenen Einzelfunde fossiler Harze unterschiedlichen geologischen Alters denken, die aus den einzelnen Bundesländern vorliegen [1]; er wird aber wohl auch an die Problematik erinnert, ob es sich bei dem einen oder anderen Fund tatsächlich um Bernstein im Sinne von "Succinit" handelt. Über derlei Einzelprobleme soll hier aber nur untergeordnet berichtet werden, es soll vielmehr versucht werden, einige der meist mengenmäßig recht unbedeutenden Funde herauszugreifen, die interessante Informationen mehr allgemeiner Art geliefert haben.

Als erstes stellt sich wohl die Frage, ob es sich bei allen aus Österreich bekannt gewordenen Funden tatsächlich um fossile Harze handelt. Dies trifft für eine ganze Reihe dieser organischen Minerale sicher nicht zu: Jaulingit, Ixolith und Köflachit bestehen – zumindest überwiegend – aus einem Gemisch von Kohlenwasserstoffen, bei denen Phyllocladan als Hauptbestandteil festgestellt werden konnte [2, sowie unveröff. Daten]. Phyllocladan liegt unter dem Mineralnamen "Hartit" [3] nicht nur von seiner Typuslokalität vor (Hart bei Gloggnitz, N.Ö.), sondern auch aus dem Köflacher-Voitsberger Kohlerevier. Solche Kohlenwasserstoffe als auch deren Gemische bieten recht interessante Aspekte hinsichtlich der Genese fossiler Harze bzw. der Diagenese von fossilen Terpenen; anaerobe Bedingungen dürften ganz entscheidend dafür verantwortlich sein, daß es zu keiner Polymerisation und damit zu einer "Verharzung" kommt, sondern daß Terpene durch Decarboxylierung, Dealkylierung und Aromatisierung die eben erwähnten Kohlenwasserstoffgemische bilden. Vergleichbares Material ist aus Böhmen unter der Bezeichnung Duxit bekannt [4]. Die Vielfalt der aus Österreich bekannten – mengenmäßig meist relativ unbedeutenden - Einzelfunde fossiler Harze ist recht erstaunlich; sowohl bezüglich ihres geologischen Alters (Trias, Unterkreide, Paläogen, Neogen) als auch bezüglich ihres Chemismus und ihrer pflanzlichen Herkunft (z.B. Rosthornit als Angiospermenharz [2]) bieten sie verschiedene interessante Aspekte. Mengenmäßig der bedeutendste Harzfund Österreichs ist zweifellos das Material aus der Weitenau bei Golling. Hier wurden in den Jahren 1979 – 1982 "einige Zentner" eines fossilen Harzes ergraben, das einige Besonderheiten aufweist – hier sei nur auf das hohe geologische Alter (Unterkreide, 120–130 Mill. Jahre) sowie auf interessante Mineraleinschlüsse (Chalcedon, Achat) in ehemaligen Hohlräumen mancher Harzstücke verwiesen [5]. Versucht man – mangels einer wissenschaftlich befriedigenden Systematik – wenigstens einigermaßen brauchbare Arbeitsbegriffe einzuführen, so könnte man eine Reihe von Funden als "Flyschharze" andere wiederum als "Gosauharze" zusammenfassen; letztere waren bereits REUSS bekannt, der 1851 unter dem Titel "Bernstein in Österreich" – neben Harzfunden aus der Gegend von Lemberg, aus Böhmen und Galizien auch zwei Vorkommen in den Gosauschichten (St. Wolfgang und die Eisenau am Traunsee) erwähnte [6].

Äußerst bescheiden sind die bisher aus Österreich bekannt gewordenen Funde von Inklusen; neben drei Arbeiten, die sich auf das Copalin aus Gablitz beziehen [7], wäre hier einerseits auf die spärlichen Angaben bezüglich des Harzes aus Golling [8] sowie auf den Einzelfund einer Tanzfliege aus einem untermiözänen Harz im Glaukonitsandstein von Herzogbirbaum zu verweisen [9].

Als letztes sei hier noch ein Kapitel zur Verarbeitung des Bernsteins erwähnt, das zwar nichts mit österreichischem Harzmaterial zu tun hat, aber von Wien seinen Ausgang nahm. Am 25. März 1879 erhielten Trebitsch und v. Wehrenbach ein österreichisches Patent für die Herstellung von Preßbernstein ("Ambroid"). Dieses erste, einschlägige Patent schuf die Voraussetzung für die Steigerung der Massenfabrikation von Bernsteinwaren und muß auch im Zusammenhang mit der damals in Wien sehr bedeutenden Fabrikation von Rauchrequisiten in mehr als 100 Kleinbetrieben gesehen und beurteilt werden [10].

Literatur

- [1] VÁVRA, N. (1984): "Reich an armen Fundstellen": Übersicht über die fossilen Harze Österreichs. - Bernstein-Neuigkeiten. Stuttgarter Beiträge zur Naturkunde, Serie C, 18, 9 – 14.
- [2] VÁVRA, N. (1999): Fossil resins from Austria: biomarkers detected in rosthornite (Eocene, Carinthia), köflachite (Miocene, Styria) and a resin from the Lower Cretaceous of Salzburg. - 219-230. In: Kosmowska-Ceranowicz, B. & Paner, H. [Hrsgb.]: Investigations into amber. Proceedings of the International Interdisciplinary Symposium: Baltic Amber and Other Fossil Resins, 2-6 September 1997, Gdansk. - 285 S., Archaeol.Mus.Gdansk & Museum of the Earth, Polish Academy of Sciences, Gdansk.
- [3] HAIDINGER, W. (1841): Ueber den Hartit, eine neue Species aus der Ordnung der Erdharze. - Poggendorfs Annalen der Physik und Chemie, 54, 261-265.
- [3] BOUSKA, V. ET AL. (1998): Hartite from Bílina. - American Mineralogist, 83, 1340-1346.
- [4] VÁVRA, N., BOUSKA, V. & DVORAK, Z. (1997): Duxite and its geochemical biomarkers ("chemofossils") from Bílina open-cast mine in the North Bohemian Basin (Miocene, Czech Republic). - Neues Jahrbuch für Geologie und Paläontologie, Monatshefte, 1997(4), 223-243.
- [5] SCHLEE, D. (1990): Das Bernstein-Kabinett. Begleitheft zur Bernsteinausstellung im Museum am Löwentor, Stuttgart. - Stuttgarter Beiträge zur Naturkunde, Serie C, 28, 100 S.
- [6] REUSS, A. E. (1851): Bernstein in Oesterreich. - Lotos, 1: 199-202, Prag.
- [7] BACHMAYER, F. (1962): Fossile Pilzhyphen im Flyschharz des Steinbruches im Höbersbachtal bei Gablitz in Niederösterreich. - Annalen des Naturhistorischen Museums, 65, 47-49.
- [7] BACHMAYER, F. (1968): Ein bemerkenswerter Fund: Myrica-Früchte im Flyschharz. - Annalen des Naturhistorischen Museums, 72, 639-643.
- [7] BACHMAYER, F. (1973): Ein Myrica (?)-Blatt im Flyschharz. - Annalen des Naturhistorischen Museums, 77, 59-62.
- [8] SCHLEE, D. (1985): Der Österreichische Bernstein von Golling. - Goldschmiede Zeitung 8/85, 70-73.
- [9] BACHMAYER, F. ET AL. (1978): Ein bemerkenswerter Insektenrest im fossilen Harz des Glaukonitsandsteines (Eggenburgien) der Aufschlußbohrung "Herzogbirbaum 1" (Niederösterreich). - Annalen des Naturhistorischen Museums 81, 113-120.
- [10] LUDWIG, G. (o. J.): Sonnensteine. Eine Geschichte des Bernsteins. - 192 S., Die Wirtschaft, Berlin.
- [10] CSILLAG, S. (1999): Bernstein in Medizin, Gewerbe und Industrie. - Diplomarbeit, unveröff., Universität Wien.

**INFRAROTSPEKTROSKOPISCHE UNTERSUCHUNGEN AN BORALUMINATEN
MIT MULLITSTRUKTUR**

D. Voll¹, A. Beran¹ & H. Schneider²

¹Institut für Mineralogie und Kristallographie

Universität Wien, Geozentrum, Althanstrasse 14, A-1090 Wien, Austria

²Institut für Werkstoff-Forschung

Deutsches Zentrum für Luft- und Raumfahrt (DLR), D-51147 Köln, Germany

Mullit ($3\text{Al}_2\text{O}_3 \cdot 2\text{SiO}_2$) ist aufgrund seiner exzellenten thermomechanischen Eigenschaften (u. a. geringe thermische Dehnung, hohe Kriechbeständigkeit) ein sehr wichtiges Material für die Herstellung von oxidischen Hochleistungskeramiken [1]. Mullit-isotype Verbindungen sind in den Systemen $\text{Al}_2\text{O}_3\text{-GeO}_2$, $\text{Ga}_2\text{O}_3\text{-GeO}_2$, $\text{M}_2\text{O}\text{-Al}_2\text{O}_3$ mit $\text{M} = \text{Na}, \text{K}, \text{Rb}$ und $\text{M}_2\text{O}\text{-Ga}_2\text{O}_3$ mit $\text{M} = \text{K}, \text{Rb}$ bekannt. Boraluminat mit Mullitstruktur wurden erstmals 1992 von MAZZA ET AL. [2] im Stabilitätsfeld $\text{Al}_{6-x}\text{B}_x\text{O}_9$, ($1 \leq x \leq 2$), beschrieben. Diese metastabilen Verbindungen entstehen aus chemisch synthetisierten Boraluminat-Precursoren im Temperaturbereich zwischen 900 und 1000°C und gehen bei höheren Temperaturen in die Phase $9\text{Al}_2\text{O}_3 \cdot 2\text{B}_2\text{O}_3$ über.

Die Boraluminat-Mullite wurden synthetisiert durch thermische Zersetzung von Mischungen aus Aluminiumnitrat und Borsäure mit Glyzerin als Reduktionsmittel. Die pauschale Zusammensetzung wurde variiert zwischen $\text{Al}/\text{B} = 5$ und $\text{Al}/\text{B} = 2$.

FTIR Pulverspektren der B-Al-Mullite zeigen Absorptionen im Bereich zwischen 1500 bis 400 cm^{-1} . Das Spektrum der Al-reichsten Verbindung ist charakterisiert durch eine starke und breite Absorptionsbande bei 1300 cm^{-1} und ein Bandensystem im Bereich zwischen 1100 und 450 cm^{-1} . Die Bande bei 1300 cm^{-1} kann den B–O-Streckschwingungen planarer BO_3 -Gruppen zugeordnet werden. Die Bandengruppe im niederenergetischen Bereich wird durch Al–O-Streck- und Al–O–Al-Deformationsschwingungen von tetraedrisch koordiniertem Al bestimmt. Weiter treten Deformationsschwingungen der BO_3 -Gruppen und Streckschwingungen der (AlO_6) -Oktaeder auf. In borreichenen Zusammensetzungen erscheinen im IR-Spektrum zwei zusätzliche Banden bei 1100 und 1000 cm^{-1} , die an Intensität mit dem Borgehalt zunehmen und B–O-Streckschwingungen von vierfach koordiniertem Bor zugeordnet werden. Die FTIR-Spektren der Boraluminat werden für die borreichen Proben zunehmend komplex und feinstrukturiert.

Literatur

- [1] SCHNEIDER, H., OKADA, K. & PASK, J. A. (1994): *Mullite and mullite ceramics*. - John Wiley & Sons, Chichester, pp. 251.
- [2] MAZZA, D., VALLINO, M. & BUSCA, G. (1992): Mullite-type structures in the systems $\text{Al}_2\text{O}_3\text{-Me}_2\text{O}$ ($\text{Me} = \text{Na}, \text{K}$) and $\text{Al}_2\text{O}_3\text{-B}_2\text{O}_3$. - *J. Am. Ceram. Soc.*, 75, 1929-1934.

**TIEFENREFLEXIONSEISMISCHE ERGEBNISSE
AUS DEM ABSCHNITT RECHNITZER SCHIEFERINSEL BIS ZUR MÜRZFURCHE**

F. Weber & H. Grassl

Institut für Geophysik
Montanuniversität Leoben, A-8700 Leoben, Austria

In mehreren Messkampagnen wurden im Zeitraum von 1992 bis 2002 84 km tiefenreflexionsseismische Profile vom Raum Rechnitz beginnend bis ins Mürztal bei Krieglach in der Weise gemessen, dass nur mehr eine Lücke im Messnetz bei Friedberg besteht. Ziel war es, vor allem die Struktur der tieferen Oberkruste, der Unterkruste und die Lage der Mohorovicic-Diskontinuität zu erfassen. Für die höhere Oberkruste war die Aufnahmegeometrie wenig geeignet. Mit den Messungen wurde aus logistischen Gründen im ostalpin - pannonischen Übergangsbereich begonnen, wofür auch die Ergebnisse von früheren Versuchen im Raum Maltern und von Weitwinkel - Reflexionseismik auf dem Alpenlängsprofil 1975 sprachen. Das zunächst knapp südlich des anstehenden Pennins im Tertiär verlaufende E-W Profil Rechnitz – Oberwart – Oberrohr weist eine mit dem Pannonbecken vergleichbare Reflexionscharakteristik auf: relativ geringe Tiefenlage der Moho, die durch ein Reflexionsband oder durch das Ende der Reflexionen am Zeitprofil charakterisiert ist, gut reflektierende Unterkruste, eine durch einen Geschwindigkeitssprung gekennzeichnete Grenze Ober/Unterkruste (Conrad Diskontinuität); ein reflexionsarmer Bereich im Hangenden, in ca. 9 km Tiefe durch sporadische Reflexionen begrenzt, könnte einem Niedriggeschwindigkeitskanal entsprechen (Vergleich mit Weitwinkelmessungen im S). Für eine auffallend reflexionsleere Zone in ca. 4–9 km Tiefe gibt es mehrere Erklärungen, wobei die Annahme von massigen Gneisen als wahrscheinlich erachtet wird. Im Zeitbereich von 0.5–1.3 s treten flach bis mäßig steil W-fallende Reflexionselemente auf, die für eine Reflektivität des Rechnitzer Pennins sprechen. Hinweise für eine aus geologischen Gründen postulierte Subduktionszone konnten bisher nicht gefunden werden.

Aufschluss über den Internbau des Rechnitz - Bernsteiner Pennins und die Tiefenstruktur gibt ein im Jahre 2001 mit moderner Methodik (reflexionseismische Telemetrieapparatur, 100 kg Sprengladungen/Schuss, aufgeteilt auf zwei je 40 m tiefe Schussbohrungen) gemessenes N-S Profil. In der Oberkruste sind bei Bernstein zwei 1–1.5 km dicke, in 3 bzw. 6 km liegende südfallende Reflexionspakete charakteristisch. Das untere Reflexionsband könnte der Basis des Südpennins entsprechen, das dann allerdings wesentlich mächtiger als im Raum Rechnitz wäre. Im oberen Zeitbereich sprechen Reflexionen bis 1.3 s mit mäßigem und variablen Einfallen für die grundsätzliche Reflektivität auch der oberen Kruste und ermutigen zu einem eigenen Messprogramm zur Korrelation mit der Oberflächengeologie. Die Grenze Ober-/Unterkruste wird in ca. 18 km Tiefe angenommen, wo die Reflexionshäufigkeit deutlich zunimmt, wenngleich unter Einschaltung reflexionsärmerer Zonen.

Ab einer am Profil nahezu konstanten Grenze von 24 km Tiefe liegt der Beginn einer stark reflektierenden Unterkruste, die im Liegenden von der Moho begrenzt wird. Diese bildet teilweise ein kräftiges Reflexionsband bei ca. 10.4 s (Tiefe 33 km) und steigt nach Süden mäßig auf ca. 30.5 km bei Stadtschlaining an.

Für den Übergang von der pannonischen zur ostalpinen Tiefenstruktur am wichtigsten ist ein 39 km langes NW-SE Profil, das vom Lassnitztal bei Rohrbach bis ins Mürztal bei Krieglach verläuft. Die Reflektivität weist lateral und vertikal größere Variationen auf. Im westlichen Drittel des Profils ist der Typ der "stark reflektierenden Unterkruste" ausgebildet, mit dem Top in ca. 25–26 km Tiefe, einer nahezu flachliegenden Basis (Moho) in ca. 32.5 km Tiefe. Im östlichen Profilabschnitt liegt die Moho höher, nämlich in ca. 30.5 km Tiefe und wird durch das zeitliche Aufhören der Reflexionen definiert. Eine Modellierung aus einer gravimetrischen Traverse bestätigt diesen generellen Moho-Verlauf. Im W scheint auf ca. 6 km Längserstreckung in ca. 39 km Tiefe eine Submoho-Reflexion auf. Im östlichen Profildrittel sind drei km-dicke Reflexionsbänder charakteristisch, deren Top bei 5 km, 10.5 km und 16 km Tiefe liegt; diesen gemeinsam ist ein mittelsteiles scheinbares (in Profilrichtung) westliches Einfallen. Das obere und mittlere Reflexionsband könnte auf Grund der starken Reflektivität von penninischen Schiefern verursacht sein, welche Annahme beim untersten Reflexionsband wegen der dann zu großen Mächtigkeit für das Pennin zu Schwierigkeiten führt. Das reflexionsarme Intervall zwischen oberem und mittlerem Band könnte analog wie im Raum Schlaining als Auftreten von massigen Gneisen erklärt werden. Das eine dreieckförmige Reflexionskonfiguration aufweisende untere Reflexionspaket setzt sich nach W weiter fort und könnte teilweise von einer Scherfläche verursacht sein. Dieselbe Erklärung kann im mittleren Krustenabschnitt für ein flach muldenförmiges bedeutendes Reflexionselement herangezogen werden. Für manche linsenförmige Reflexionskonfigurationen fehlt derzeit noch eine sichere Erklärung. Durch die Beteiligung beim Lithosphärenprojekt ALP-02 konnte ein Schusspunkt NW vom Mürztal verwendet werden, sodass eine reflexionsseismische Information aus der Unterkruste bis zu Mitte des Mürztals vorliegt. In diesem seismisch und seismotektonisch kritischen Bereich konnten bisher keine Hinweise auf größere vertikale Versetzungen oder eine Subduktionszone gefunden werden.

DIE VERWITTERUNG EINER ERZSTRUKTUR ALS URSAUCE FÜR DEN EINSTURZ DES
EHEMALS 15. ACHTTAUSENDERS IM HOHEN HIMALAYA NEPAL

J. T. Weidinger^{1,2}

¹Institut für Geologie und Paläontologie

Universität Salzburg, Hellbrunnerstrasse 34, A-5020 Salzburg, Austria

²Erkudok[©] Institut

Kammerhofgasse 8, A-4810 Gmunden, Austria

Geländedaten belegen die Existenz eines Sulfiderzkörpers im zentralen Langthangtal von Nepal, etwa 20 km SW der Shisha Pangma (8027 m) auf tibetisch/chinesischem Gebiet [1]. Diese Vererzung mit einer Mächtigkeit von ≤ 50 m markiert auf einer Seehöhe von 5500–6950 m über 3 km im Streichen und ca. 2 km im Fallen die Abbruchsnische der 40000 Jahre alten, größten Massenbewegung der Erde (ursprünglich bewegtes Volumen 10–15 km³) im Kristallin [2]. Die Mineralisation konnte aber auch im Aufschluss in Form von Erzbrekzien bzw. durch die elektrische Leitfähigkeit austretender Bergwässer unter den abgelagerten Bergsturzmassen nachgewiesen werden [3]. Beide Vorkommen legen den Schluss nahe, dass die Vererzung in ursächlichem Zusammenhang mit dem gigantischen Bergsturz steht.

Die Mineralisation in quarzitischer Gangart ist an gangförmige Leukogranite gebunden, die als Erzbringer fungierten. Diese intrudierten vor 17–20 Mill. Jahren im Zuge der Orogenese des Himalaya entlang von aufgerissenen Großstrukturen diskordant in präkambrische Metasedimente, wie Migmatite und Sillimanit-Gneise des Hohen Himalaya Kristallins [4]. Die strukturell kontrollierte Vererzung wird von mikroskopisch feinen Riedel Scherflächen durchsetzt, die sich während syngenetischer Scherung bildeten und mit markasitisierter Pyrrhotin verheilt sind. Untergeordnet treten Sphalerit, Chalcopyrit und Galenit auf.

Laboruntersuchungen, wie eine Strukturanalyse des Erzkörpers und seiner Gangart, Erzmikroskopie, einachsiale Druckversuche an orientiert entnommenen Erzproben, Untersuchungen der dabei mechanisch versagenden erzgefüllten Riedel Scherflächen mit dem Rasterelektronenmikroskop und die Bestimmung der dreiachsisalen Druckfestigkeit an Proben aus dem Nebengestein haben gezeigt, dass diese vererzten Mikro-Scherflächen bei mechanischer Beanspruchung sehr instabil reagieren [5]. Dies legt den Schluss nahe, dass sich diese Flächen durch ihr unterschiedliches chemisches und physikalisches Verhalten zum Umgebungsgestein zu mechanischen Schwächezonen entwickelt haben. Während der Hebung, Abtragung und Verwitterung des Langthang Himalaya [6] übertrug sich dieses schwache mechanische Verhalten auf die gesamte Erzstruktur und destabilisierte die ehemalige Bergflanke. Frostspaltung, Monsunniederschläge und Schmelzwässer der nahen Gletscher begünstigten diese Verwitterungsbedingungen im Zuge der spät- und postglazialen Klimaschwankungen, während die Gletschererosion die Täler übersteilte und damit einen Flankenbruch begünstigte.

Neben weiteren, allerdings untergeordnet in Erscheinung tretenden präexistierenden Strukturen, wie massenhaft auftretenden (Ultra-)mylonit- und Pseudotachylithhorizonten, neotektonischen Klüften und Störungen, die gemeinsam mit der Erzstruktur die Raumlage der Gleitfläche (Fallen: 20° nach WSW) des gigant-schen Bergsturzes nachzeichnen, gibt es keine andere plausible Erklärung für das mechanische Versagen der untersuchten Bergflanke entlang diskordanter Bewegungsflächen.

Die strukturelle und morphologische Analyse des gesamten Abrissbereichs des Bergsturzes [7], die Neigung der rudimentären Flanken sowie der Bau eines Geländemodells im Maßstab 1:5000 (zu besichtigen im Stadtmuseum Gmunden) ermöglichen die Rekonstruktion der dreiseitigen Pyramide des ehemaligen Bergmassivs mit einer absoluten Seehöhe von 7500 bis 8500 m [5], das heißt, des ehemals 15. Achtausenders der Erde im Nepal Himalaya (Abb. 1).

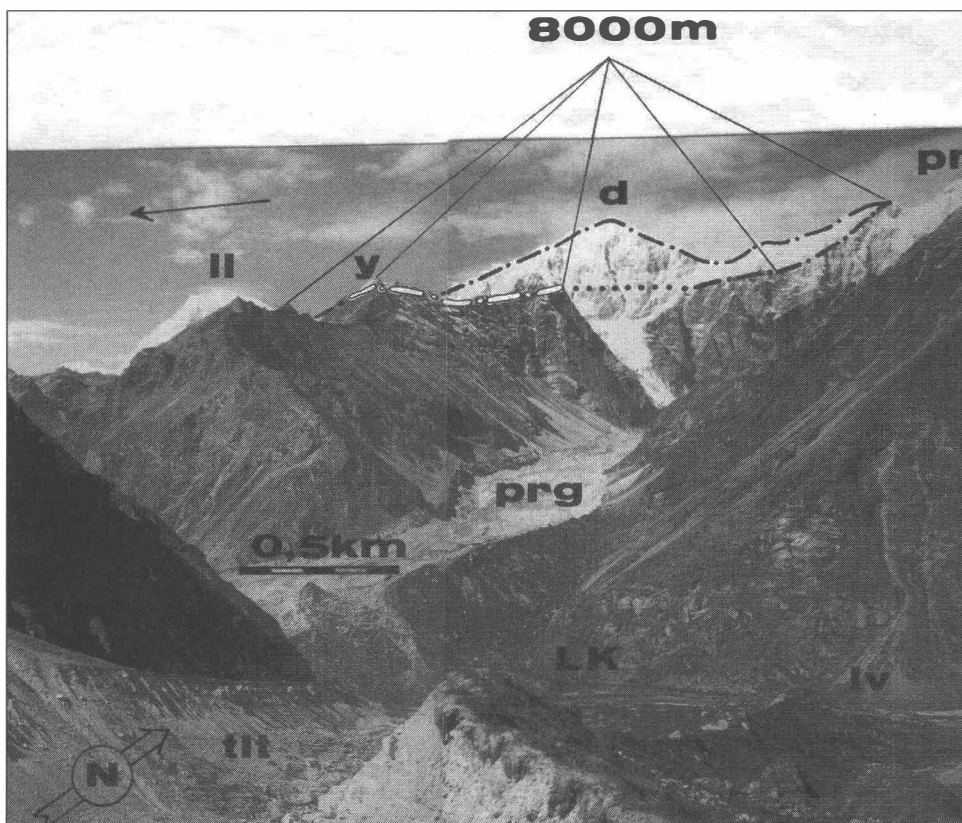


Abb. 1

Blick vom rechten Ufer des Trupaiku-Langshisa-Gletschers (tit, Sh. 4500 m) in Richtung NW, auf den Abrissbereich der Großmassenbewegung im Langthangtal; (-.-.) = Abrisskamm, der zwischen Yala Gipfel (y, 5520 m) und seinem höchsten erhaltenen Punkt, dem Phrul Rangshan Ri - Gipfel (pr, 6950 m), als vererzte Struktur ausgebildet ist; darüber die rekonstruierte, dreiseitige Pyramide des ehemaligen 15. Achtausenders; II = Langhang Lirung Gipfel (7234 m), d = Dragpoche Gipfel (6554 m), prg = Phrul Rangshan Gletscher, LK = Langshisa Kharka Alm (4120 m) im Iv = Langhangtal, ← = Abgleitrichtung der Massenbewegung nach WSW (Foto: J.T. Weidinger 1993).

Literatur

- [1] WEIDINGER, J. T., SCHRAMM, J.-M. & SURENIAN, R. (1995): Disseminated sulfidic ore mineralization at Yala Peak (Langtang Himal, Nepal) - an assisting factor for the Tsergo Ri landslide event? - Mitt. Geol. Inst. ETH Zürich, 298, 294-297.
- [2] WEIDINGER, J. T. & SCHRAMM, J.-M. (1995): Tsergo Ri (Langtang Himal, Nepal) - Rekonstruktion der "Paläogeographie" eines gigantischen Bergsturzes. - Geol. Paläont. Mitt. Innsbruck, 20, 231-243.
- [3] SCHRAMM, J.-M. & WEIDINGER, J. T. (1996): Distribution of electrical conductivity at Tsergo Ri landslide, central-north Nepal. - In: Proc. 7th Int. Symp. Landslides, Balkema, Rotterdam, 889-894.
- [4] WEIDINGER, J. T., SCHRAMM, J.-M., & SURENIAN, R. (1996): On preparatory causal factors, initiating the prehistoric Tsergo Ri landslide (Langtang Himal, Nepal). - Tectonophysics, 260, 95-107.
- [5] WEIDINGER, J. T., SCHRAMM, J.-M. & NUSCHEJ, F. (2002): Ore mineralization causing slope failure in a high-altitude mountain crest – on the collapse of an 8000 m peak in Nepal. - Journal of Asian Earth Sciences, 21, 295-306.
- [6] HEJL, E., SCHRAMM, J.-M. & WEIDINGER, J. T. (1997): Long term exhumation at the Tsergo Ri landslide area (Langtang Himal, Nepal): information fromapatite fission track data. - 12th Himalaya-Karakorum-Tibet Workshop, Abstract Volume, 149-150.
- [7] SCHRAMM, J.-M., WEIDINGER, J. T. & IBETSBERGER, H. J. (1996): Predesign and morphologic evolution of the prehistoric large-scale Tsergo Ri landslide (Langtang Himal, Nepal). - Geomorphology, 26, 107-121.